UNIVERSIDADE FEDERAL DO RIO DE JANEIRO

Centro de Ciências da Saúde

Instituto de Bioquímica Médica Leopoldo de Meis

KARINA MARTINS CARDOSO

Redes extracelulares de neutrófilos (NETs) induzem fenótipo pró-metastático em carcinoma mamário humano

Orientador: Robson de Queiroz Monteiro

Rio de Janeiro

2020

KARINA MARTINS CARDOSO

Redes extracelulares de neutrófilos (NETs) induzem fenótipo pró-metastático em carcinoma mamário humano

Tese de Doutorado apresentada ao Programa de Pós-Graduação em Química Biológica do Instituto de Bioquímica Médica Leopoldo de Meis da Universidade Federal do Rio de Janeiro, como parte dos requisitos necessários a obtenção do título de Doutora em Química Biológica. Sob orientação de Robson de Queiroz Monteiro

Rio de Janeiro

2020

FICHA CATALOGRÁFICA

Martins-Cardoso, Karina

Redes extracelulares de neutrófilos (NETs) induzem fenótipo pró-metastático em carcinoma mamário humano. Rio de Janeiro: UFRJ/IBqMLdM, 2020.

107 f.

Tese de doutorado – Universidade Federal do Rio de Janeiro, Instituto de Bioquímica Média Leopoldo de Meis, Programa de Pós-graduação em Química Biológica, 2020.

Orientador: Robson de Queiroz Monteiro

1. Transição epitélio-mesenquimal 2. Redes extracelulares de neutrófilos 3. Câncer de mama 4. Metástase I. Robson de Queiroz Monteiro II. Universidade Federal do Rio de Janeiro, IBqM, Programa de Pós-graduação em Química Biológica. III. Tese de Doutorado

FOLHA DE APROVAÇÃO

Karina Martins Cardoso

Redes extracelulares de neutrófilos (NETs) induzem fenótipo pró-metastático em carcinoma mamário humano

Aprovada em _____/_____/_____

Orientador: Robson de Queiroz Monteiro
Professor Associado do Instituto de Bioquímica Médica Leopoldo de Meis da UFRJ

Membro da banca: Andreia Cristina de Melo
Chefe da Divisão de Pesquisa Clínica do Instituto Nacional de Câncer, INCA

Membro da banca: Gabriela Nestal de Moraes
Pesquisadora Visitante do Instituto Nacional de Câncer, INCA

Membro da banca: Vanessa Morais Freitas
Professora Associada do Instituto de Ciências Biomédicas da USP

Revisor: Juliana Camacho Pereira
Professora adjunta A do Instituto de Bioquímica Médica da UFRJ

Suplente Interno: Julio Alberto Mignaco
Professor Associado II do Instituto de Bioquímica Médica Leopoldo de Meis da UFRJ

Suplente externo: Julio Cesar Madureira de Freitas Junior
Pesquisador Visitante do Instituto Nacional de Câncer, INCA

Agradecimentos

Enfim, é chegada a hora. Foram dias de lutas e dias de glória. Dias de lágrimas e de vitórias. E depois de tanto, não poderia deixar de agradecer ao grandioso Deus que me acompanhou durante a jornada. Minha fé foi muito pequena diante de tantas maravilhas, mas a Ele toda honra e glória.

À mulher mais incrível da minha vida, que me gerou, me criou, me fez forte e batalhadora. À minha mãe que me aconselhou, me sustentou, me apoiou nas minhas escolhas e me acolheu em meio às crises. Não me permitiu desistir, vibrou com cada conquista e me amou apesar de tudo. Te amo!

À minha amada família que fez parte de toda minha trajetória: minha avó que já se foi, minha mana, minha tia, minha sobrinha, meu cunhado e mesmo meu pai Edson que imprimiu em mim características que fazem parte do que sou.

Ao meu amado marido que me apoia, me faz sorrir todos os dias e compartilha momentos incríveis da vida comigo. Agradeço por cada palavra de apoio e paciência nesta retal final.

Aos meus grandes amigos que me acompanham desde a era pré-histórica: Diego, Maria, Priscilla, Idalina e Clóvis. E os que fiz durante a jornada: Ciro e Gabriela. Aos que vieram durante a minha passagem pela Rural: Viviane, Soraya e Leo, André e Nat. E os que a Minerva me trouxe: Natalia (fortalecendo os laços ruralinos), Isabel, Gabriela, Daniel, Anna, Aquiles, Bárbara, Taissa, Vanessa, Victor David. Vocês são igualmente valiosos na minha vida e na minha conquista. Quero leva-los pra sempre na minha vida.

À Taissa e Ana por me levarem para yoga, e ao Victor e Bárbara pela companhia nas corridas pela UFRJ durante as longas incubações dos meus experimentos.

À minha querida orientadora da graduação e amiga Patrícia Fampa. Um presente que a Rural me deu. Sem ela, talvez eu não fosse uma doutora em Bioquímica. Obrigada pela parceria e pela amizade que perpetua.

Ao meu orientador do mestrado, Mario Alberto, o homem que acreditava na beleza do mundo. Que fazia ciência com paixão e amava a família na mesma intensidade. Sou grata pelos ensinamentos.

Ao meu orientador do doutorado, Robson Monteiro, por ter me aceitado como aluna e ter me dado a oportunidade de trabalhar com um grande pesquisador. Foram quatro anos de aprendizagem e que venham mais anos frutíferos.

À minha grande professora e parceira de bancada, Sandra König. Obrigada pelas trocas, pelas experiências e pelas conversas. Que a vida permita mais dessa parceria. E aos meus excelentes colaboradores Vitor Luna, Kayo Bagri, professora Cláudia Mermelstein e à professora Maria Isabel. Ao Dr Julio Madureira pela sua disponibilidade em me apresentar novas ferramentas de bioinformática.

Às minhas queridas colaboradoras do Laboratório de Parasitas e Vetores, Dayana, Rafaela e Melissa.

Aos meus amigos do laboratório de Sinalização celular: Ana, Carlucio, Fillipe, Carlos, Priscilla, Stephanie que também fizeram parte da minha trajetória. Sou grata por todos os momentos.

Aos meus amigos do laboratório de Trombose e câncer, aos que já se foram (André, Fausto, Araci, Tainá, Bárbara, Sâmara, Andreia Mariano, Andreia Oliveira e Tatiana) e aos que ainda estão (Aquiles, Alex, Carol, Dani, Vitor, Juliana e Sandra), agradeço pela parceria dentro e fora da bancada, pelos momentos de interação intelectual e interação pessoal. Ao pessoal do Laboratório de Hemostase e venenos: professora Lina, Taissa, Victor, Ana, Augusto, Marjory e Dário. O doutorado foi bem mais divertido com vocês.

À minha primeira aluna de graduação, Camila, agradeço por fazer parte da minha trajetória profissional.

Agradeço aos professores e funcionários maravilhosos que conheci no IBqM. Aos órgãos de fomento que tornaram possível minha pesquisa e minha formação acadêmica. Quero agradecer à revisora do meu trabalho e aos membros da banca.

A todos que passaram pela minha vida e que deixaram suas marcas. Certamente foi essencial para meu crescimento pessoal e profissional.

Agradeço a todos que torceram por mim até aqui. Pareceram 20 anos ouvindo “Já acabou o seu doutorado?” Ano que vem me perguntem novamente.

RESUMO

O câncer de mama é a neoplasia mais comum em mulheres em todo o mundo. Embora este tipo de câncer tenha bom prognostico na maior dos casos, altas taxas de mortalidade têm sido associadas à metástase, um processo no qual as células cancerosas se espalham do tumor primário para órgãos distantes e iniciam novos tumores. A metástase pode ser ativada por meio de sinais provenientes do microambiente tumoral que abrange uma variedade de células hospedeiras interagindo com células tumorais. Os neutrófilos infiltrados no tumor, sob condições específicas, liberam armadilhas extracelulares de neutrófilos (NETs), uma estrutura semelhante a uma teia composta por DNA de fita dupla e proteínas como elastase neutrofílica, histonas e mieloperoxidase. As NETs têm sido propostas como possíveis efetoras na progressão tumoral. Neste estudo, buscou-se avaliar a capacidade das NETs isoladas em promover a progressão do tumor através da ativação do programa de transição epitelial-mesenquimal (TEM) em linhagem de células de carcinoma mamário humano. Os neutrófilos foram isolados do sangue de doadores saudáveis e posteriormente estimulados com PMA (Forbol 12-Miristato 13-Acetato), indutor clássico de NETose, para gerar NETs. Células MCF7 foram privadas de soro fetal bovino por 10 horas e então estimuladas com NETs por 16 horas. Após o tratamento, foram geradas amostras para análise de PCR em tempo real, análises de citometria de fluxo, ensaios de migração e imunocitoquímica. Dados de RNAseq de pacientes com câncer de mama depositados no banco de dados do Atlas do Genoma do Câncer (TCGA) também foram avaliados. O tratamento nas células MCF7 com NETs purificadas promoveu mudanças morfológicas marcantes nas células tumorais. Além disso, a incubação das células MCF7 com NETs aumentou dramaticamente as propriedades migratórias das células tumorais. Em seguida, os fatores de transcrição relacionados à TEM foram modulados por NETs juntamente com marcadores de TEM, como E-caderina, Fibronectina, N-caderina e β-catenina. NETs foram capazes de modular os marcadores de células-tronco tumorais CD24 e CD44. Além disso, a expressão de mRNA de genes pró-tumorais e pró-inflamatórios foi aumentada por NETs. A análise do TCGA revelou uma correlação positiva significativa entre a expressão de genes de assinatura de neutrófilos e genes relacionados à TEM, bem como genes pró-inflamatórios. Coletivamente, nossos dados sugerem as NETs como um importante agente pró-tumoral e, desta forma, a interação entre NETs e células tumorais emerge como um potencial alvo terapêutico para reduzir a progressão tumoral.

ABSTRACT

Breast cancer is the most common malignancy in women around the world. High death rates have been associated with metastasis, a process in which cancer cells spread from the primary tumor achieving distant organs and initiating new tumors. Metastasis can be activated through signals from the tumor microenvironment that encompasses a variety of host cells interacting with tumor cells. Infiltrated neutrophils in the tumor, under specific conditions, release Neutrophils extracellular traps (NETs), a web-like structure composed by double strand DNA and proteins, such as neutrophil elastase, histones and myeloperoxidase. NETs have been proposed as possible effectors in the tumor progression. In this study, we sought to evaluate the capacity of isolated NETs to promote tumor progression through activation of the epithelial-mesenchymal transition (EMT) program in human breast carcinoma cell lines. Neutrophils were isolated from blood of health donors and further stimulated with PMA (Phorbol 12-myristate 13-acetate), a classic NETosis inducer, to generate NETs. MCF7 cells were starved in serum-free medium for 10 hours followed by stimulation with NETs for 16 hours. After the treatment, samples were generated for real time PCR analysis, flow cytometry analyses, migration assays and immunocytochemistry. RNA-seq data from breast cancer patients deposited in The Cancer Genome Atlas (TCGA) database were assessed. The treatment of MCF7 cells with purified NETs promoted remarkable morphological changes in the tumor cells. In addition, incubation of MCF7 cells with NETs dramatically increased the migratory properties of the tumor cells. In order, EMT-related transcription factors were modulated by NETs along with EMT markers such as, E-cadherin, Fibronectin, N-cadherin and β-catenin. NETs were capable to modulate cancer stem cells markers CD24 and CD44. Furthermore, mRNA expression of pro-tumoral and pro-inflammatory genes was increased by NETs. TCGA analysis revealed a significant positive correlation between neutrophil signature gene expression and EMT-related genes as well as pro-inflammatory genes in breast cancer patients. Collectively our data demonstrate that NETs increase the pro-tumoral properties of the human carcinoma cells.

LISTA DE ILUSTRAÇÕES

Figura 1. Anatomia da mama. 3
Figura 2. Microambiente tumoral e o estabelecimento da metástase. 8
Figura 3. Polarização de neutrófilos N1/N2 associados ao câncer.....14
Figura 4. Microscopia das Redes extracelulares de neutrófilos.....15
Figura 5. Processo de NETose.....17
Figura 6. NETs e câncer.....22
Figura 7. Processo de transição epitélio-mesenquimal 25
Figura 8. Características morfológicas em diferentes subtipos moleculares. 28
Figura 9. Modelos propostos para heterogeneidade intratumoral. 31
Figura 10. NETs alteram a morfologia celular. 45
Figura 11. Ensaio de migração.....47
Figura 12. Análise da expressão gênica de fatores de transcrição de TEM. 49
Figura 13. Análise da expressão de E-caderina (*CDH1)* em células MCF7 51
Figura 14. Análise da expressão de E-caderina em células HCC 1954. 52
Figura 15. Análise de Fibronectina em células tratadas com NETs 53
Figura 16. Análise de N-caderina 54
Figura 17. Western Blotting de vimentina.....55
Figura 18. Análise de β-catenina por imunocitoquímica.....56
Figura 19. Análise comparativa de marcadores CSCs entre os subtipos de câncer de mama 58
Figura 20. Análise de marcadores de células-tronco tumorais. 59
Figura 21. Analise da expressão de genes pró-tumorais em MCF7.....61
Figura 22. Analise da expressão de genes pró-tumorais em células MDA-MB-231 e HCC1954.....62
Figura 23. Análise das NETs degradas por DNase I 64
Figura 24. Análise de genes de assinatura relacionados a neutrófilos nos diferentes subtipos de câncer de mama. 66

LISTA DE TABELAS

Tabela 1. Correlação entre a classificação clínico-patológica e os marcadores moleculares 4

Tabela 2. Clássicas diferenças entre células epiteliais e mesenquimais 24

Tabela 3. Típicos marcadores de células-tronco tumorais em diferentes tipos de tumor. 33

Tabela 4. Análise de correlação entre genes de assinatura neutrofílica e genes pró-tumorais.....66

Tabela 5. Análise de correlação entre genes de assinatura neutrofílica e genes relacionados à TEM 67

Tabela 6. Análise de correlação entre genes de assinatura neutrofílica em amostras de pacientes com câncer de mama através do GEPIA 2 69

LISTA DE ABREVIATURAS E SIGLAS

ALDH1	Aldeido desidrogenase 1
COX2	Ciclooxigenase 2
CSC	Células-tronco tumoral
DAMPs	Padrões moleculares associados à danos
DNA	Ácido desoxirribonucleotídeo
EGFR	Receptor do fator de crescimento epidérmico
ER	Receptor de estrogênio
GCSF	Fator estimulador de colônias granulocitárias
GM-CSF	F*ator estimulador* de colônias de granulócitos e macrófagos
HER2	Receptor do tipo 2 do fato de crescimento epidermal
HBV	Vírus da hepatite B
HCV	Vírus da hepatite C
HPV	Papiloma virus
IFN	Interferon
IL-1β	Interleucina 1 beta
IL-6	Interleucina 6
LPS	lipopolissacarídeo
MEK/ERK	Proteína quinase ativada por mitógeno
MMP	Metaloproteinase
MPO	Mieloperoxidase
NE	Elastase neutrofílica
NETs	Redes extracelulares de neutrófilos
NFκB	Fator nuclear Kappa B
NLR	Receptor do tipo NOD
PAMPs	Padrões moleculares associados à patógenos
PARP1	Poli ADP-ribose polimerase 1
PD-L1	Proteina de morte programada 1
PMA	Phorbol-12-miristato-13-acetato
PR	Receptor de progesterone

RNA	Ácidos ribonucleotídeos
ROS	Espécies reativas de oxigênio
STAT3	*Proteína* transdutora de sinal e ativadora de transcrição 3
TCGA	The Cancer Genome Atlas
TEM	Transição epitélio-mesenquimal
TGFβ	Fator de transformação do crescimento beta
TLR	Receptor do tipo Toll
TNF	Fator de necrose tumoral
VEGF	Fator de crescimento endotelial vascular

SUMÁRIO

1 Introdução 1
1.1 Câncer 1
1.2 Câncer de mama 2
1.3 Microambiente tumoral 6
1.4 Inflamação 9
1.5 Neutrófilos associados ao câncer 11
1.6 Redes extracelulares de neutrófilos (NETs) 15
1.7 Redes extracelulares de neutrófilos e câncer 19
1.8 Transição epitélio-mesenquimal (TEM) 23
1.9 Células-tronco tumorais 29
2 Objetivos 36
2.1 Objetivo geral 36
2.2 Objetivos específicos 36
3 Materiais e Métodos 37
3.1 Cultura de células 37
3.2 Obtenção de neutrófilos 37
3.3 Geração e isolamento de NETs 38
3.4 Análise de expressão gênica por PCR em tempo real 39
3.4.1 Obtenção da amostra 39
3.4.2 Extração de RNA e síntese de cDNA 39
3.4.3 PCR em tempo real 40
3.5 Citometria de fluxo 40
3.6 Ensaio de migração 41
3.7 Análise por imunocitoquímica 41
3.8 Western Blotting 42
3.9 Análise de expressão gênica de pacientes com câncer de mama 43
3.10 Análise estatística 43
4 Resultados 44
4.1 Alteração da morfologia celular induzida pelas NETs em células MCF7 45
4.2 NETs induzem aumento de migração celular em células MCF7 46
4.3 NETs aumentam a expressão gênica dos fatores transcricionais de TEM em células MCF7 48

4.4 O tratamento com NETs modifica os marcadores de TEM em linhagens tumorais de mama 50

4.5 Expressão de marcadores de células-tronco tumorais é modulada pelas NETs 57

4.6 Análise de expressão gênica de fatores pró-tumorais 60

4.7 A integridade das NETs não altera seus efeitos pró-tumorais 62

4.8 Análise *in silico* de marcadores gênicos de neutrófilos, TEM e genes pró-tumorais 65

5 Discussão.....71

6 Conclusão 79

7 Referências 80

8 Anexos.....94

1. INTRODUÇÃO

1.1 Câncer

De acordo com a Organização Mundial da Saúde (OMS), o câncer é a segunda principal doença que leva à óbito adultos precoces entre 30-69 anos na maior parte do mundo (WINTERS et al., 2017). A cada 8 mortes, 1 é devido à doença. A estimativa mais recente do número de casos de câncer foi de aproximadamente 18 milhões ao redor do mundo, e o número de mortes causado pelo câncer foi de 9,6 milhões em 2018, com expectativa de aumento significativo no número de óbitos anuais (BRAY et al., 2018). Acredita-se que em algumas décadas, o número de mortes por câncer deve superar o de mortes causadas por cardiopatia isquêmica, a principal causa de morte em todo mundo nos dias atuais (MATTIUZZI & LIPPI, 2019). A justificativa para o aumento da incidência do câncer deve-se ao aumento da expectativa de vida da população e ao crescimento demográfico mundial (BRAY et al., 2018).

A incidência do câncer é maior entre países mais socioeconomicamente desenvolvidos (JAYASEKERA & MANDELBLATT, 2020). O estilo de vida da população mais rica tem grande influência sobre os números. Dentre os fatores de risco que favorecem ao desenvolvimento da doença destacam-se o sedentarismo, obesidade, alimentos industrializados, consumo de álcool e tabaco. Além disso, doenças infecciosas como, hepatites virais e papilomavírus humano, e também exposição à radiação solar são fatores de risco incluídos na estatística (WINTERS et al., 2017; BERNARD & CHRISTOPHER, 2020). No entanto cerca de 70% das mortes se concentram em países com baixa e média renda, podendo justificar-se pelo baixo investimento em medicina preventiva, diagnóstico realizado no estágio tardio da doença, custo e acesso ao tratamento e baixo investimento em pesquisa científica na área.

As altas taxas de pessoas afetadas pelo câncer não apenas sugere um problema prioritário de saúde pública mundial, mas também, um problema que afeta a economia global, haja visto o custo médio anual investido, gerando um forte impacto econômico. O custo estimado com pacientes em tratamento é de 1 trilhão de dólares anuais. Além dos investimentos feitos em programas indiretos para reduzir a

incidência de câncer na população, como programa de redução de álcool e tabaco (BERNARD & CHRISTOPHER, 2020). A prevenção e o controle do câncer estão entre os mais importantes desafios da humanidade deste século.

1.2 Câncer de mama

O Câncer de mama está entre os três mais incidentes no mundo, junto com câncer de pulmão e colorretal, com uma taxa de incidência de 10,4 % dentre todos os tipos de câncer (IACOVIELLO et al., 2020). Entre as mulheres, o câncer de mama é o mais incidente (representando 24,2% de todos os novos casos). Anualmente, são diagnosticados aproximadamente 2,1 milhões de novos casos. No Brasil, estima-se mais de 198 mil novos casos de câncer de mama entre 2020-2022 (INCA, 2019).

O câncer de mama não é apenas o mais incidente entre as mulheres, como também representa a principal causa mundial de morte feminina. Essa estimativa independe da condição socioeconômica do país. Na América latina, a taxa de incidência do Brasil e do México, mostram que os números de casos só vêm aumentando, 2,9% e 5,9% por ano, respectivamente. Um aumento observado de maneira semelhante na África e na Ásia. Isso provavelmente pode ser atribuído à implementação dos programas de rastreamento do câncer de mama nos últimos anos (HARBECK & GNANT, 2017; BERNARD & CHRISTOPHER, 2020).

A taxa de mortalidade por câncer de mama ajustada pela população mundial foi de 13,84 óbitos a cada 100.000 mulheres no mundo em 2018 (INCA, 2019). Por outro lado, nos Estados Unidos e na União Europeia a taxa de mortalidade do câncer de mama tem diminuído a cada ano. Isso ocorre devido aos programas de prevenção e detecção precoce do tumor, aumentando as chances de eficácia dos tratamentos. Além de outra parte ser atribuída à diminuição do protocolo de tratamento de reposição hormonal em mulheres após a menopausa (BRAY et al., 2018; FERLAY et al., 2019). Apesar dos números não serem animadores no Brasil, nos países mais desenvolvidos as estimativas de sobrevida de pacientes com câncer de mama têm sido favoráveis, apresentando uma tendência de aumento médio de 5 anos. Pode-se atribuir estes resultados ao melhoramento das técnicas de diagnóstico, qualidade do tratamento local e sistêmico e conhecimento aprimorado sobre a doença e suas características para decisão terapêutica

adequada (INCA, 2019). E quanto mais precocemente detectado, maiores são suas chances de cura. No entanto, a mortalidade por câncer de mama ainda continua alta e deve ser tratada como um problema de saúde pública.

O tumor de mama apresenta dezenas de tipos histológicos e moleculares de carcinomas mamários *in situ* e/ou invasivo **(Figura 1)**. O tipo histológico mais comum é o carcinoma ductal infiltrante, que representa 70-80% dos casos de câncer de mama. O carcinoma lobular infiltrante é o segundo mais frequente, com cerca de 5-15% de incidência (INCA, 2019).

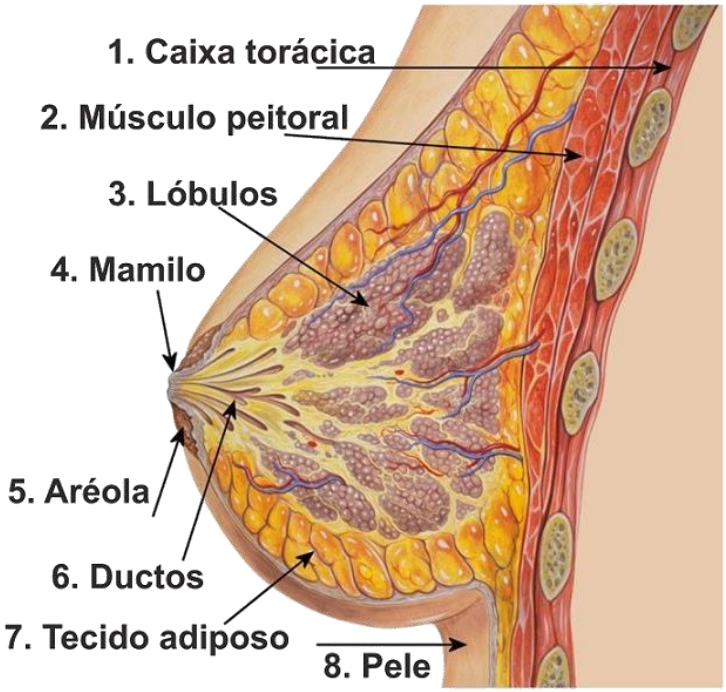

FIGURA 1. Anatomia da mama. Ilustração adaptada de Patrick J. Lynch.

No câncer de mama, há uma classificação molecular na qual os tipos tumorais são divididos de acordo com padrões de expressão molecular capazes de diferenciar no desenvolvimento tumoral (DAI et al., 2015). Os subtipos são classicamente identificados pela expressão de marcadores moleculares: receptor de estrogênio (ER), receptor de progesterona (PR) e receptor do tipo 2 do fator de crescimento epidérmico humano (HER2). Para diagnóstico clínico utiliza-se a imuno-histoquímica como técnica principal **(Tabela 1)**.

Tabela 1: Classificação molecular dos subtipos de câncer de mama. Adaptado de DAI et al, 2015.

SUBTIPOS TUMORAIS	MARCADORES IMUNOHISTOQUÍMICOS AVALIADOS NA CLÍNICA			
LUMINAL A	ER+ e/ou PR+		HER2-	< 14% Ki 67
LUMINAL B	ER+ e/ou PR+		HER2 + HER2 -	≥ 14% Ki 67
HER2	ER-	PR-	HER2+	
BASAL-LIKE/ TRIPLO NEGATIVO	ER-	PR-	HER2-	

Os subtipos luminal A e luminal B, que são positivos para os receptores ER e PR, possuem menor potencial metastático e, geralmente, respondem bem às terapias disponíveis, sendo considerados de melhor prognóstico (ADES et al., 2014). São os mais incidentes entre as mulheres afetadas pelo câncer de mama, representando 75% dos casos diagnosticados. O subtipo luminal B pode ser enriquecido de HER2+ ou não, podendo alterar o comportamento do tumor e, consequentemente, a terapia de escolha. Os subtipos que expressam HER2, independente de expressarem ER e/ou PR, têm um prognóstico intermediário. Entre 15-25% dos tumores de mama expressam HER2.

Por fim, o subtipo negativo para os três receptores ER, PR e HER2, também chamado de triplo-negativo ou subtipo basal, é considerado de pior prognóstico, mais agressivos e com maior potencial metastático (GARRIDO-CASTRO; LIN; POLYAK, 2019). Estes, representam 10% de todos os tumores de mama. Na prática clínica, também há o uso do marcador de proliferação celular, Ki-67, onde a sua quantificação auxilia na avaliação do grau de risco e prognóstico do tumor. A marcação de no mínimo 14% nas células tumorais para Ki-67 determina risco médio, e acima de 30% de marcação, indica um pior prognóstico (HARBECK & GNANT, 2017).

Essa variedade tumoral se dá pela sua heterogeneidade morfológica, genética e à resposta diferencial às terapias. Esse conjunto de alterações podem representar diferentes prognósticos da doença. A heterogeneidade tumoral representa mais um desafio para a eficácia do tratamento da doença. Nos últimos 10 a 15 anos, o sucesso de abordagens terapêuticas têm levado em consideração a heterogeneidade do tumor visando melhorar o desfecho clínico dos pacientes com câncer de mama (HARBECK et al., 2019; BERNARD & CHRISTOPHER, 2020).

A modulação da expressão desses receptores hormonais podem resultar na alteração de expressão de genes envolvidos no crescimento tumoral, migração, invasão, angiogênese e outras etapas do ciclo celular (MASOUD & PAGÈS, 2017). A decisão para o tratamento clínico vem sendo tomada com base na expressão desses marcadores, visto que a maioria das terapias tem como alvo um dos receptores descritos. Por exemplo, para pacientes positivos para ER, o uso de tamoxifeno como terapia hormonal e inibidores de aromatases é capaz de reduzir o tamanho do tumor local, sua recorrência e a mortalidade. Ainda, tumores também positivos para PR costumam apresentar boa sensibilidade ao tratamento hormonal (FRAGOMENI, 2018). A redução da expressão desses receptores pode dificultar o tratamento da doença, bem como seu prognóstico e a sobrevida do paciente (LURIE et al., 2020).

Já para tumores que expressam HER2, o tratamento geralmente é feito com trastuzumabe e lapatinibe que atuam na interrupção da sinalização do receptor HER2 (YEO & GUAN, 2018; HARBECK et al., 2019). HER2 é um receptor de tirosina quinase que regula a capacidade de proliferação e sobrevivência através da ativação da via MEK/ERK. Tumores enriquecidos de HER2 comumente apresentam uma proliferação alta e determinam um pior prognóstico (DAI et al., 2015).

O subtipo triplo negativo, que não expressa nenhum dos receptores descritos acima, pode responder a inibidores de PARP1 (poli ADP ribose polimerase), enzima responsável pelo reparo de danos ao DNA. Também pode ter HER1 como um potencial alvo terapêutico (MASOUD & PAGÈS, 2017). Terapias não adjuvantes são altamente aceitas nesse tipo de tumor, seguido por cirurgia, irradiação e quimioterapia (LOIBL et al., 2021). 40% dos tumores de mama invasivos expressam

EGFR (receptor do fator de crescimento epidérmico), fator responsável pelo comportamento agressivo do tumor e pior prognóstico (MASOUD & PAGÈS, 2017).

Portanto, os subtipos do tumor indicam combinações terapêuticas não apenas através de quimioterapia, mas também radioterapia, ressecção cirúrgica e imunoterapia (YIN et al., 2020). Atualmente, terapias utilizando anticorpos contra inibidores de pontos de controle de morte celular (PD-1 e PD-L1) têm se mostrado eficazes no tratamento para câncer de mama metastático (ESTEVA et al., 2019) Muito embora a heterogeneidade intratumoral possa representar um desafio para a resposta terapêutica (HARBECK & GNANT, 2017), avanços tecnológicos estão cada vez mais identificando marcadores moleculares e caracterizando-os como alvos terapêuticos em tumores de mama, estratégias essas que utilizam linhagens celulares de câncer de mama humano *in vitro* como modelo experimental.

1.3 Microambiente tumoral

Até o início do século XX, o tumor sólido era visto como uma massa homogênea formada apenas por células tumorais exibindo mutações aberrantes. No entanto, seu papel na progressão tumoral foi realmente reconhecido no final dos anos 80 (BIZZARRI & CUCINA, 2014). Nos dias atuais, sabe-se que o tumor é um tecido heterogêneo complexo que abrange uma vasta quantidade de tipos celulares, incluindo vasos sanguíneos, que influenciam o comportamento do tumor (HANAHAN & WEINBERG, 2011). O microambiente tumoral engloba também células endoteliais, fibroblastos, células do sistema imune e adipócitos **(Figura 2)**. A interação entre células malignas e não malignas, cria um ambiente propício para alteração do comportamento tumoral e a malignidade da doença (MAO et al., 2013; MITTAL, BROWN, HOLEN, 2018). Em carcinomas de mama, estômago e pâncreas, as células do estroma podem contabilizar até 90% de toda a massa tumoral (DVORAK, 1986). Esta enorme variação da composição do microambiente tumoral contribui para a heterogeneidade do tumor, complexidade e diferentes respostas à quimioterapia.

Além dos diversos tipos celulares que integram o microambiente tumoral, componentes da matriz extracelular, como glicoproteínas, colágeno e enzimas,

assim como moléculas solúveis, como fatores de crescimento, hormônios, citocinas também são encontrados. Esses fatores acelulares secretados no microambiente permitem a interação entre as células do microambiente, desenvolvendo uma resposta parácrina nas células periféricas (MITTAL, BROWN, HOLEN, 2018).

HANAHAN & COUSSENS (2012) revisaram as possíveis contribuições funcionais que o microambiente poderia exercer sobre o perfil da célula cancerosa e diversas etapas para o desenvolvimento tumoral. São elas: a sinalização proliferativa das células, repressão dos fatores supressores de crescimento, resistência à morte celular, imortalidade replicativa, angiogênese, inflamação, invasão e metástase, reprogramação do metabolismo energético e evasão da resposta imunológica. Essa visão permitiu compreender que não são apenas as mutações genéticas acumuladas nas células malignas, mas também as células do estroma que atuam no desenvolvimento da doença.

As pesquisas científicas vêm enfatizando o papel de células do estroma no crescimento do tumor primário, aumento da migração e invasão de células tumorais, resistência à quimioterapia e pior prognóstico do paciente. Devido essa influência do microambiente tumoral na progressão do tumor, diversos estudos sugerem que ele também é um parâmetro a ser considerado na escolha terapêutica (SOYSAL, TZANKOV, MUENST, 2015).

Diante desta complexidade, é imprescindível o estudo aprofundado do microambiente tumoral, sua composição e suas funções sobre a biologia do tumor, a fim de se obter maiores êxitos no tratamento do paciente com câncer. Em particular, a atenção da comunidade científica às células do sistema imune têm sido cada vez maiores para entender melhor sua contribuição na progressão tumoral bem como o papel da inflamação neste contexto.

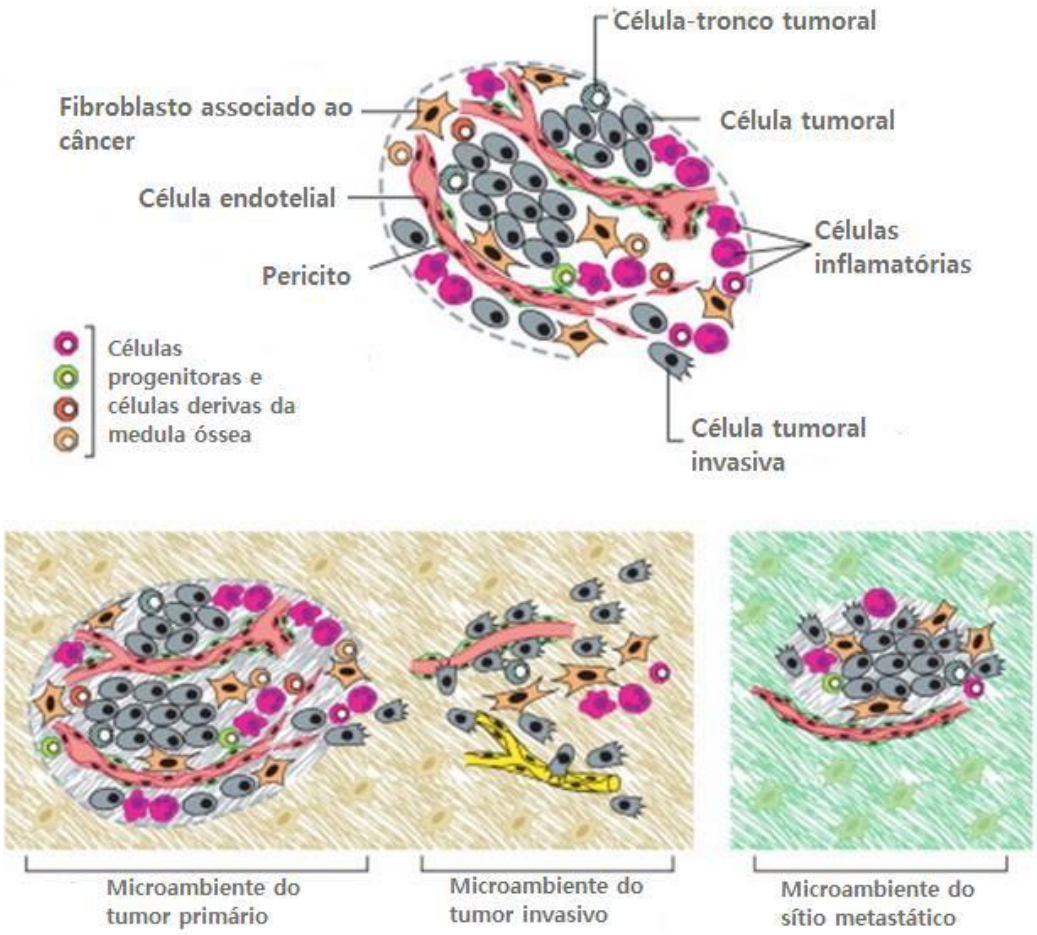

FIGURA 2. Microambiente tumoral e o estabelecimento da metástase. (HANAHAN & WEINBERG, 2011). Um conjunto de diferentes tipos celulares constituem os tumores sólidos, sejam neoplásicas ou não. Essa variedade celular tanto do parênquima, que exercem função, quanto do estroma, que só permite a sustentação, é importante e atuante na progressão tumoral. Além da presença das células inflamatórias no tumor. À medida que o tumor vai progredindo, sucessivos microambientes são formados e alterados conforme o tumor invade um novo tecido. Acredita-se que as células normais do tecido onde o tumor metastático se instala, também pode exercer uma pressão o tumor, podendo alterar seu comportamento.

1.4 Inflamação

O processo inflamatório é exaustivamente descrito como estratégia de defesa do hospedeiro contra patógenos, envolvendo a ativação, recrutamento e ação de células do sistema imune. Além de contribuir para homeostase, no reparo tecidual, remodelamento e regeneração (GRETEN & GRIVENNIKOV, 2019).

No século XIX, o patologista Rudolf Virchow foi o primeiro a observar células do sistema imune infiltradas nos tumores sólidos (SINGH *et al.*, 2019). O processo inflamatório crônico só foi de fato associado ao câncer décadas após a descrição de Virchow. Desta forma, os sítios de inflamação onde o tumor se desenvolve foram definidos como "feridas que nunca curam" (DVORAK, 1986). Diversos trabalhos têm revelado a participação do sistema imune e inflamação na progressão tumoral, participando de todos os estágios da tumorigênese (GRETEN & GRIVENNIKOV, 2019). A partir de estudos epidemiológicos, estima-se que 15 a 20% das mortes associadas ao câncer estejam ligadas às consequências da resposta inflamatória crônica (MANTOVANI et al., 2008; TANIGUCHI & KARIN, 2018).

Entretanto, a participação dessas células inflamatórias tem apresentado funções paradoxais no microambiente tumoral. De um lado, o sistema imune apresenta papel antitumoral, desenvolvendo uma resposta inflamatória clássica, enquanto as células imunes buscam responder ativamente contra a doença. Em contrapartida, a inflamação pode ter função pró-tumoral, impedindo a ação do sistema imune para combate do tumor (GRETEN & GRIVENNIKOV, 2019). Neste último contexto é que os pesquisadores têm se debruçado para compreender o envolvimento das células inflamatórias no desenvolvimento tumoral.

A inflamação ligada ao câncer está geralmente ligada a um estado crônico de inflamação tecidual. Esse estado inflamatório crônico pode ocorrer devido a infecções persistentes como, vírus da Hepatite B (HBV) e Hepatite C (HCV), Papiloma Vírus (HPV) e *Helicobacter pylori*, ou por inflamação estéril, ou seja, livre de qualquer infecção, como exposição ao tabaco e a inalação de amianto (MARELLI et al., 2017), além de doenças autoimunes como lúpus ou diabetes (TANIGUCHI & KARIN, 2018). Essas doenças inflamatórias aumentam significativamente o risco de desenvolver diferentes tipos de tumor como, câncer gástrico, hepático, intestinal, esofágico, ovariano e de próstata. A inflamação crônica pode contribuir para a

instabilidade genômica, levando a formação do tumor, seu desenvolvimento, angiogênese e disseminação da metástase (GRIVENNIKOV, GRETEN, KARIN, 2010).

O efeito da inflamação relacionado à progressão da malignidade está ligado à ativação das células inflamatórias no microambiente tumoral, secretando citocinas como, IL-1β, TNF, IL-6, quimiocinas, fatores de crescimento e enzimas que amplificam mais ainda o processo inflamatório e recrutam ainda mais células imunes para o microambiente tumoral. Geralmente esses fatores mediadores são regulados por dois fatores transcricionais regulatórios principais: NFκB e STAT3 (MARELLI et al., 2017). Com uma contínua ativação de cascata inflamatória se retroalimentando, as células ficam expostas a diversos outros fatores como, espécies reativas de oxigênio e nitrogênio, induzindo alterações epigenéticas nas células adjacentes ao tumor, inibindo mecanismos de reparo de replicação de DNA, que favorece o acúmulo de mutações genômicas, além de favorecer a capacidade das células transformadas de inibir a morte por apoptose e de proliferarem ilimitadamente (TANIGUCHI & KARIN, 2018). A ativação dos fatores transcricionais NFκB e STAT3 podem se dar através do reconhecimento de padrões moleculares associados à patógenos (PAMPs) ou associados a danos (DAMPs). Esses padrões são reconhecidos por uma família de receptores do tipo Toll (TLRs) ou do tipo NOD (NLRs). Pode-se citar uma lista de clássicos genes alvos do fator transcricional NFκB previamente reconhecidos como atuantes na progressão tumoral. São eles: as citocinas pró-inflamatórias TNF, IL-1, IL-6; fatores estimuladores de colônias de granulócitos macrófagos (GM-CSF) e neutrófilos (GCSF); diversas quimiocinas como CXCL8, CXCL2 e CCL5; metaloproteinases de matriz extracelular (MMP2 e MMP9); proteínas pró-proliferativas (ciclina e MYC); proteínas anti-apoptóticas como BCL2 e FLIP); enzimas pró-inflamatórias (como Ciclooxigenase 2); e fatores angiogênicos como o fator de crescimento endotelial vascular (VEGF).

Para a comunidade médica, essas descobertas alteraram consideravelmente a escolha terapêutica para tratamento contra o câncer. Estudos mostraram que o uso diário de anti-inflamatórios não esteroidais pode reduzir significativamente o risco de desenvolvimento de câncer, especialmente câncer colorretal. Além disso, alguns estudos mostram que o uso de anti-inflamatórios em pacientes com tumores já estabelecidos reduz a mortalidade de forma significativa (ROTHWELL et al., 2012;

ROTHWELL et al., 2012; ALGRA & ROTHWELL, 2012). Um resultado mais sutil também foi encontrado em pacientes com câncer de mama com expressão dos receptores hormonais. Anti-inflamatórios não esteroidais inibem a atividade da enzima COX2, levando à redução da síntese de prostaglandinas. As prostaglandinas são lipídeos bioativos que atuam como mediadores da resposta inflamatória e no câncer, aumentando a sobrevivência das células tumorais e a angiogênese (XU, 2002).

As terapias mais modernas para tratamento do câncer têm identificado a inflamação como mais um alvo potencial, buscando não só inibir a progressão do tumor, como também impedir ou reverter a supressão da resposta anti-tumoral (MARELLI et al., 2017). Fármacos desenvolvidos para inibição de citocinas pró-inflamatórias ou atuando diretamente nas células imunes têm se mostrado eficazes nos ensaios clínicos para determinados pacientes. Antagonistas de receptor de IL-6, CCL2, CCR4 e CXCR4 estão em pesquisa clínica para uma variedade de neoplasias epiteliais e hematopoiéticas. (MANTOVANI et al., 2008).

1.5 Neutrófilos associados ao câncer

Neutrófilos são as células inflamatórias mais abundantes no sistema circulatório, representando 50-70% dos leucócitos circulantes. De origem mielóide e contendo núcleo polimórfico, são os primeiros leucócitos a responder e migrar para um sítio de infecção ou injúria. Os neutrófilos possuem 3 mecanismos distintos para mediar uma resposta imunológica: 1) fagocitose de patógenos 2) secreção de grânulos contendo peptídeos antimicrobianos 3) liberação de redes extracelulares de neutrófilos (TREFFERS et al., 2016). Os neutrófilos não só possuem um papel na imunidade inata como também participam da resposta imune adaptativa através da secreção de citocinas e quimiocinas e através da apresentação de antígenos. Pacientes com neutropenia, ou seja, baixa quantidade de neutrófilos circulantes, sofrem de grave imunossupressão, podendo morrer precocemente, vítimas de infecções bacterianas ou fúngicas (ERPENBECK & SCHÖN, 2017). Apesar de ser uma célula de defesa natural do organismo, a ativação exacerbada do neutrófilo pode levar a uma inflamação crônica e dano tecidual, o papel oposto do que lhe foi proposto anteriormente (POWELL & HUTTENLOCHER, 2016).

Nas últimas décadas, diversos estudos têm buscado o entendimento do papel dos neutrófilos no microambiente tumoral. Os neutrófilos representam uma parcela substancial dentre os leucócitos infiltrados no microambiente tumoral de diversos tipos de câncer como câncer de pulmão, gástrico, renal, mama, melanoma, células escamosas de cabeça e pescoço, entre outros. Os neutrófilos expressam os receptores de quimiocinas CXCR1 e CXCR2, sendo estes receptores muito importantes para o seu recrutamento. Algumas células tumorais secretam citocinas e quimiocinas que executam o papel de recrutar os neutrófilos como CXCL8, CXCL5 e CXCL6 (POWELL & HUTTENLOCHER, 2016). GCSF também é um fator imprescindível na mobilização de neutrófilos da medula óssea para a circulação (SENGUPTA, SUBRAMANIAN, PARENT, 2019).

Após se infiltrar no tumor, os neutrófilos assumem diferentes perfis, podendo apresentar ação anti- ou pró-tumoral (COFFELT, WELLENSTEI, DE VISSER, 2016). Evidências têm mostrado que as ideias sobre a função dos neutrófilos tem conflitado porque existem subpopulação de neutrófilos no microambiente tumoral (SHAUL & FRIDLENDER, 2019). Pesquisadores já demonstraram que altas quantidades de neutrófilos infiltrados em câncer de pulmão se correlacionam com maior sobrevida dos pacientes (TREFFERS et al., 2016). No entanto, a relevância no prognóstico vai depender do tipo do câncer e seu estágio de desenvolvimento (SHAUL & FRIDLENDER, 2019). GRANOT et al *(*2011) observou que neutrófilos infiltrados em câncer de pulmão inibem a formação do nicho pré-metastático pela liberação de espécies reativas de oxigênio (do inglês, *reactive oxygen species* - ROS) e secreção de CCL2 pelas células tumorais. LÓPEZ-LAGO et al (2013) também mostrou que quimiocinas secretadas pelas células de câncer renal geravam uma resposta anti-metastástica mediada por neutrófilos.

Em contrapartida, em muitos outros estudos, a presença de neutrófilos no microambiente tumoral está relacionada com pior prognóstico do paciente. Um estudo histopatológico em amostras de câncer de mama mostrou que os tumores do subtipo basal possuem maior infiltrado de neutrófilos. Estes são classificados como tumores mais agressivos e com pior prognóstico. Neutrófilos associados ao tumor também já foram descritos como promotores da angiogênese, e indutores de proliferação, migração e invasão de células tumorais (POWELL & HUTTENLOCHER, 2016; MASUCCI, MINOPOLI, CARRIERO, 2019). Além de

modular outras células imunes, interrompendo a resposta inflamatória contra o desenvolvimento do tumor (SHAUL et al., 2016).

Atualmente, entende-se que essa divergência de atuação sobre o microambiente tumoral depende da polarização de neutrófilos diferenciados em N1 e N2 **(Figura 3)**. O fenótipo que define seu perfil N1/N2 é baseado na sua atuação sobre as células tumorais, além dos marcadores de superfície diferencialmente expressos entre os fenótipos, bem como as proteínas tipicamente secretadas por eles (OHMS, MÖLLER, LASKAY, 2020). Os neutrófilos N1 tem papel anti-tumoral, apresentando um aumento citotóxico sobre as células tumorais e uma capacidade de resposta imunológica. Já os neutrófilos N2 são característicos por expressar diversos fatores pró-tumorais e suprimir a resposta imunológica.

Propõe-se que essa polarização dos neutrófilos, distinguindo-se em dois tipos de comportamento opostos são regulados a partir de sinais advindos do microambiente tumoral (COFFELT, WELLENSTEIN, DE VISSER, 2016). TGFβ e G-CSF são fatores clássicos que promovem metástase. TGFβ disponível em altas concentrações no microambiente tumoral leva a um acúmulo de neutrófilos polarizados em N2. Já a quimiocina Interferon β (IFNβatua como regulador negativo do fenótipo pró-tumorigênico. Com o bloqueio de TGFβ no tumor primário e o aumento de IFN, ocorre um balanceamento, aumentando a quantidade de neutrófilos antitumorais N1 (SHAUL et al., 2016). Camundongos deficientes de IFNβ apresentaram maior crescimento tumoral, angiogênese e metástase associada a neutrófilos do fenótipo N2. Enquanto que a presença de IFNs reverteu o fenótipo N2 para N1, aumentando a citotoxicidade tumoral (SHAUL & FRIDLENDER, 2017). Essa mudança de fenótipos está acompanhada com a alteração de expressão gênica e secreção de diferentes citocinas e quimiocinas. Os neutrófilos N1/N2 apresentam assinaturas gênicas bem distintas. Infiltração de neutrófilos N1 no tumor apresentam maior expressão de TNFs, CCL3, molécula de adesão intracelular (ICAM-1) e baixos níveis de arginase 1 (GALDIERO, MARON, MANTOVANI, 2018). Já os neutrófilos de perfil N2 são caracterizados por expressarem maior quantidade de fatores imunossupressores como, CCL2 e CCL5, além de fatores pró-tumorais como CXCR4, VEGF e metaloproteinases. Além disso, neutrófilos com perfil N2 exibem maior expressão de elastase neutrofílica e catepsina G. Também

apresentam elevados níveis de arginase 1, contrastando com o perfil N1 (WU et al., 2019).

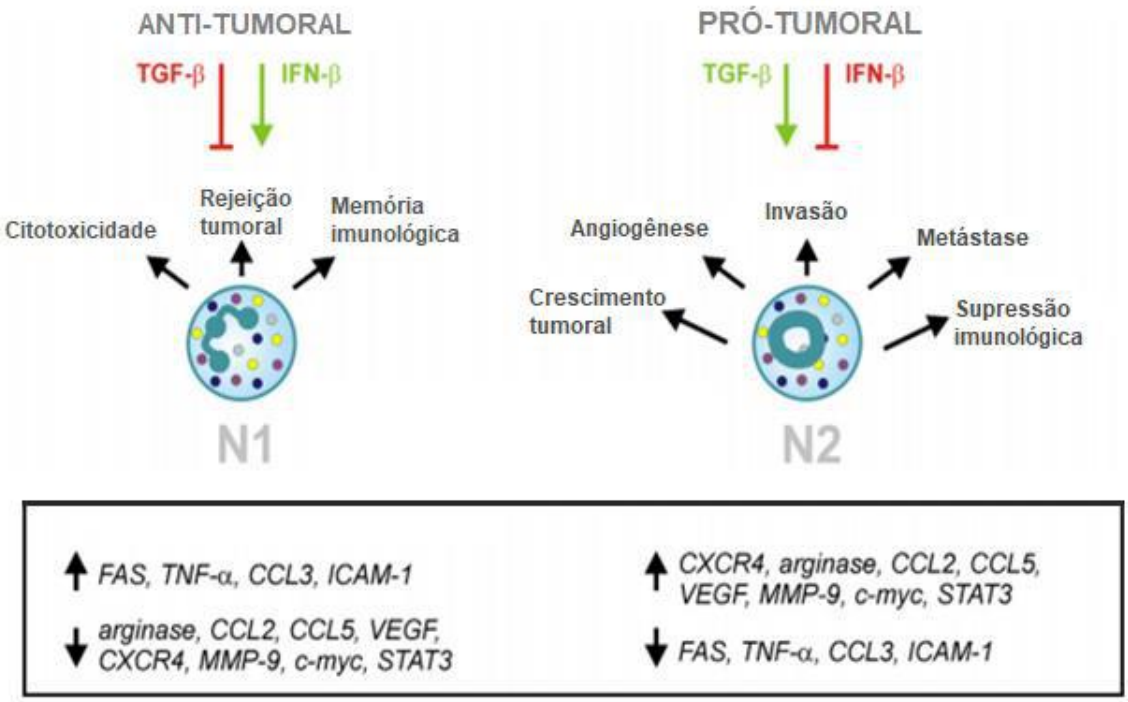

FIGURA 3. Polarização de neutrófilos N1/N2 associados ao câncer. Os neutrófilos quando estimulados pelo o ambiente, são capazes de adquirir um fenótipo com diferentes funcionalidades, expressando genes distintos e secretando proteínas que podem destruir ou coabitar com células tumorais. Adaptado de (PICCARD, MUSCHEL, OPDENAKKER, 2011).

A imunoterapia vem conquistando espaço nas possibilidades de tratamento do câncer. O bloqueio farmacológico de fatores provenientes do tumor que atuam sobre recrutamento e polarização de neutrófilos é apresentado como uma nova abordagem terapêutica. Essa estratégia somada a drogas anticâncer já usuais pode obter um efeito sinérgico e mais eficaz para alguns tipos de tumor (MASUCCI et al., 2020).

1.6 Redes Extracelulares de Neutrófilos (NETs)

Há quase duas décadas, BRINKMANN *et al.* (2004) descreveu um novo mecanismo de resposta imunológica atribuída aos neutrófilos **(Figura 4)**. Denominada como redes extracelulares de neutrófilos, as NETs consistem na liberação de cromatina descondensada decorada por diversas proteínas citosólicas, granulares e nucleares como peptídeos microbianos, mieloperoxidase, elastase neutrofílica, catepsina G, histonas entre outras. Na época, a função descrita para as NETs envolvia um mecanismo de defesa contra invasão de patógenos, onde eles permaneciam presos a esta “armadilha” de redes de DNA, impedindo que se dissemine para além do local de entrada. Além disso, conduzindo-os à morte através de sua atividade microbiana.

Com o passar do tempo, tornou-se claro que as NETs possuem poder de atuação muito mais ampla, desde inflamação crônica estéril, cuja causa não é de origem infecciosa, até trombose e câncer (BRINKMANN, 2018). Atualmente sabe-se que outros granulócitos, como macrófagos, mastócitos e eosinófilos, também são capazes de secretar redes extracelulares, participando da resposta inflamatória local (DANIEL et al., 2019).

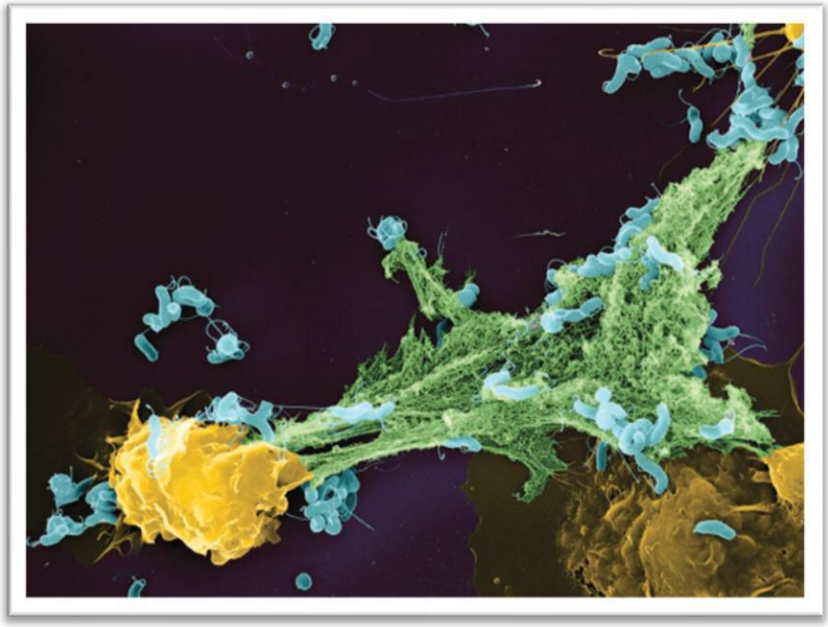

FIGURA 4. Microscopia eletrônica artificialmente colorida das redes extracelulares de neutrófilos. Os neutrófilos (amarelo) foram cocultivados com bactérias *Helicobacter pylori* (azul) por 2 horas, liberando fibras de DNA (verde). Imagem retirada de (THÅLIN et al., 2019).

A formação das NETs foi considerada primeiramente como um tipo de morte celular. Este foi denominado como NETose. No entanto, hoje já se sabe que existem ao menos dois tipos de formação e liberação das NETs. No primeiro, os neutrófilos se mobilizam para um “suicídio” lítico, onde sua membrana plasmática é completamente rompida, liberando seu conteúdo nuclear e citoplasmático. Esta, denomina-se NETose clássica. No outro mecanismo, não há ruptura da membrana plasmática, não levando à morte do neutrófilo (ERPENBECK & SCHÖN, 2017). A este processo dá-se o nome de NETose vital.

Diversos estímulos já foram descritos como indutores de NETose, dentre eles, uma longa lista de espécies de microorganismos como, vírus, fungos, parasitas e bactérias, interação física com plaquetas ativadas e quimiocinas como Interleucina-8 e fator de necrose tumoral (TNFα). Nos ensaios controlados *in vitro* utilizam-se outros tipos de componentes artificiais para indução da NETose: phorbol-12-miristato-13-acetato (PMA), lipopolissacarídeos provenientes de bactérias (LPS) e ionóforos de cálcio e potássio (PAPAYANNOPOULOS, 2018). Outros fatores físico-químicos podem modular a ativação da NETose em tecidos periféricos como níveis de CO_2 e HCO_3^- e pH (CAHILOG et al., 2020).

Durante o processo de formação clássica das NETs, picos de Ca^{2+} desencadeiam a ativação das deaminases e as histonas nucleares então são citrulinadas pela enzima peptidil-arginina-deaminase 4 (PAD4), ou seja, um resíduo de arginina é convertido em citrulina. A citrulinização leva a uma mudança de carga positiva das histonas, diminuindo a força de ligação entre elas e o DNA e consequentemente levando à descondensação da cromatina. **(Figura 5)**. Apesar de recentes estudos *in vitro* mostrarem alguns mecanismos de NETose independentes da citrulinização, a inibição de PAD4 é suficiente para interromper a formação das NETs em diversas condições *in vitro* e *in vivo* (DEMERS et al., 2016; PAPAYANNOPOULOS, 2018).

Na formação de NETs por via lítica, as espécies reativas de oxigênio (ROS) são essenciais no processo. O Ca2+ liberado no citosol, paralelamente a ativação de PAD4, gera uma cascata de sinalização intracelular que leva à ativação da proteína quinase C (PKC), da via Raf-MEK-ERK, ativando NADPH oxidase, gerando ROS intracelular. A mieloperoxidase (MPO) é ativada por ROS e recruta a elastase

neutrofílica (NE) contida no grânulo citoplasmático do neutrófilo. Este, se liga aos filamentos de F-actina no citoplasma e degrada-os para adentrar no núcleo. Assim, a NE exerce atividade proteolítica sobre as histonas, clivando-as e facilitando o rompimento dos nucleossomos (estruturas formadas pela ligação da cromatina (SØRENSEN & BORREGAARD, 2016; PAPAYANNOPOULOS, 2018; BRINKMANN, 2018; BOELTZ et al., 2019). A membrana nuclear se rompe juntamente com as membranas granulares, permitindo a ligação da cromatina com conteúdo dos grânulos citoplasmáticos. Assim, as NETs são liberadas para o meio extracelular.

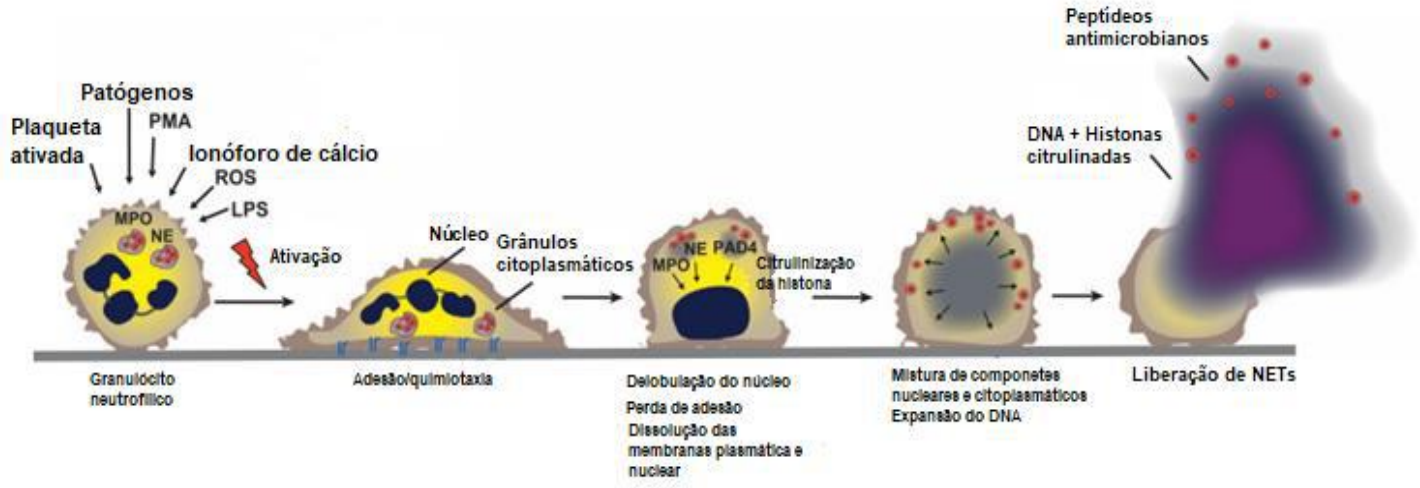

FIGURA 5. Processo de NETose clássica através de diferentes estímulos. Adaptado de Erpenbeck & Shön, 2017.

Dependendo do estímulo de ativação à NETose e das condições experimentais, muitas dessas proteínas descritas como essenciais para a geração de NETs podem ser dispensáveis (ERPENBECK & SCHÖN, 2017). Apesar de estudos utilizando camundongos deficientes de NE demonstrarem a sua importância para geração de NETs em modelos de sepse e câncer (VAN AVONDT & HARTL, 2018), a NETose pode ser independente de ROS e não requerer a atividade de NE. A indução por *Streptomyces hygroscopicus , por exemplo,* não depende de NADPH oxidase e mieloperoxidase (SOLLBERGER, TILLEY, ZYCHLINSKY, 2018). Além disso, alguns indutores, como *Trypanosoma cruzi,* podem depender de receptores do tipo Toll ou de integrinas para geração de NETose e neste caso, a ativação da

via de PCK se torna dispensável (BRINKMANN, 2018). Recentemente, observou-se o envolvimento de quinases dependentes de ciclina (CDKs) no processo de formação de NETs. Quando CDK4 e CDK6 foram silenciadas, o processo de NETose ficou comprometido, mas os mecanismos de fagocitose e degranulação não foram afetados (AMULIC et al., 2017).

Alguns estudos demonstram a participação do DNA mitocondrial no processo de formação das NETs. Neutrófilos sensibilizados primariamente com GCSF (fator estimulante de colônias granulocíticas) e em seguida por LPS ou fator Va, liberariam NETs que seriam formadas a partir de DNA mitocondrial ao invés de DNA nuclear, como descrito classicamente (YOUSEFI et al., 2009). Esse estudo foi corroborado por outro grupo mostrando que NETs enriquecidas de DNA mitocondrial oxidado contribuem para doenças autoimunes semelhantes ao lúpus (LOOD et al., 2016). Ainda não há mecanismo proposto para esse processo a partir do DNA mitocondrial, haja visto que as histonas nucleares, uma das principais proteínas das NETs, são ausentes nesse caso (BRINKMANN, 2018)

Em alguns casos, a NETose pode não levar à morte celular. Em um estudo utilizando neutrófilos cultivados com *Staphylococcus aureus,* os neutrófilos em pouco tempo de contato sofreram uma forte dilatação do núcleo então, formaram-se vesículas contendo DNA que se fusionaram com a membrana citoplasmática e foram posteriormente secretadas pela célula, porém, os neutrófilos continuaram apresentando sinais vitais (BRINKMANN, 2018). Este processo ocorre através de produtos bacterianos ou proteínas ligantes de TRL2, que estimulam os neutrófilos a liberarem microvesículas contendo parte da cromatina (ou possivelmente DNA mitocondrial) e proteínas granulares através de brotamento a partir do envelope nuclear, sem promover o rompimento da membrana celular (VAN AVONDT & HARTL, 2018). A NETose vital ainda permite que os neutrófilos exerçam suas funções locais, como fagocitose e migração celular.

Mais de 20 indutores de NETose já foram reportados na literatura. A partir de uma análise de proteômica em que os neutrófilos foram estimulados com PMA, ionóforos de cálcio A23187 ou lipopolissacarídeos de *Escherichia coli,* observou-se uma intensa heterogeneidade na composição das NETs, além de diferentes modificações pós-traducionais (PETRETTO et al., 2019). Diante disso, sabe-se que

não só as vias de ativação de NETose são diferentes, mas também a composição das NETs geradas e suas modificações pós-traducionais. Esta observação prova a complexidade do fenômeno, sugerindo que NETs podem ter diferentes efeitos biológicos. Ainda há muitas lacunas para serem preenchidas em relação às NETs, seus mecanismos e atuações fisiológicas e patológicas.

1.7 Redes extracelulares de neutrófilos e câncer

O processo de NETose vem sendo amplamente estudado por diferentes vertentes. Sabe-se que DNA liberado em tecidos necróticos pode levar a um exacerbado dano tecidual. Em órgãos lesionados como cérebro, fígado, pulmão, rim, coração, entre outros, já foram observados envolvimento das NETs. Em doenças não-infecciosas como lúpus eritematoso, artrite reumatoide, fibrose cística, aterosclerose, diabetes, periodontite, entre outras, as NETs apresentam um papel relevante em seu desenvolvimento (SØRENSEN & BORREGAARD, 2016; MARTÍNEZ-ALEMÁN et al., 2017; APEL, ZYCHLINSKY, KENNY, 2018; WANG et al., 2019; THÅLIN et al., 2019; GRANGER et al., 2019; SALEMME et al., 2019; MAGÁN-FERNÁNDEZ et al.; GERCHEVA, 2020; HUANG et al., 2020). Em 2020, um estudo mostrou que as NETs contribuem para formação de microtrombos através da interação entre plaquetas e neutrófilos em pacientes com síndrome respiratória aguda grave causada pela COVID-19 (MIDDLETON et al., 2020). Portanto, busca-se compreender melhor a contribuição das NETs em diferentes patogêneses e as implicações terapêuticas para conter a resposta imune exacerbada (LEE et al., 2017; CAHILOG et al., 2020).

No contexto tumoral, a primeira proposta de atuação das NETs no câncer humano foi publicada em 2013, por BERGER-ACHITUV e colaboradores. Utilizando algumas amostras de sarcoma de Ewing observou-se a presença de neutrófilos infiltrados no microambiente tumoral, além do depósito de NETs em 25% das amostras. Esses mesmos pacientes, apresentaram recidiva precoce do tumor após ressecção do tumor e quimioterapia. O estudo sugeriu que pacientes contendo NETs no tumor apresentavam um pior prognóstico. A partir daí, passou-se a correlacionar

a agressividade da doença com o infiltrado de neutrófilos no tumor (ERPENBECK & SCHÖN, 2017). Em um estudo com camundongos xenotransplantados com carcinoma pulmonar de Lewis foi evidenciado um acúmulo de neutrófilos no tumor, além de cromatina extracelular e histonas citrulinadas em (HO-TIN-NOÉ et al., 2009).

A partir daí, surgiram inúmeros trabalhos associando NETs e seus componentes à progressão tumoral, utilizando-se diferentes modelos e tipos tumorais (COOLS-LARTIGUE et al., 2014) As NETs são capazes de sequestrar células tumorais circulantes dando origem a um novo foco metastático. COOLS-LARTIGUE e colaboradores (2013) combinaram um modelo de sepse em camundongos com a injeção de células tumorais. Após 14 dias, observaram a presença dessas células no fígado e no pulmão dos animais, apresentando um número exacerbado de focos metastáticos. A administração intravascular de DNase ou inibidor de elastase impediu drasticamente a adesão das células tumorais circulantes nos capilares do pulmão e fígado. Posteriormente, este grupo demonstrou que a interação entre as células tumorais e as NETs é, em parte, mediada via integrina β1 (NAJMEH et al., 2017).

As NETs também participam do estabelecimento do tumor e seu microambiente. Em camundongos que sofreram indução de esteatose hepática não alcoólica foi observada uma infiltração precoce de neutrófilos, levando à formação de NETs e subsequente montagem de uma resposta inflamatória através do recrutamento de macrófagos e secreção de citocinas pró-tumorais (VAN DER WINDT et al., 2018).

Diversas evidências apontam para a atuação das NETs no crescimento do tumor primário. Utilizando camundongos previamente tratados com GCSF, neutrófilos foram sensibilizados e induzidos à NETose intratumoral, apresentando uma vantagem significativa no crescimento do tumor (DEMERS et al., 2016). O efeito das NETs no crescimento do tumor já foi observado em diversos modelos tumorais (VAN DER WINDT et al., 2018; YAZDANI, 2019; MILLER-OCUIN et al., 2019).

As NETs também são capazes de ativar células dormentes em estágios da inflamação pulmonar. Um elegante estudo em camundongos mostrou que a

exposição à fumaça do cigarro ou inalação de lipopolissacarídeos induziu a formação de NETs que remodelaram proteoliticamente a matriz extracelular, através da clivagem de laminina, e induziram a proliferação de células tumorais dormentes formando sítios metastáticos agressivos (ALBRENGUES et al., 2018).

Células tumorais com maior potencial metastático também induzem a formação de NETs que servem de arcabouço para o estabelecimento da metástase. Células tumorais de mama 4T1, do subtipo triplo-negativo, secretam a quimiocina CXCL1 recrutadora de neutrófilo. O silenciamento gênico da quimiocina, reduziu o infiltrado de neutrófilos no tumor. Além disso, o tratamento com anti-GCSF reduziu a formação das NETs. A aplicação de injeção de nanopartículas cobertas de DNase I, reduziu significativamente a metástase espontânea pulmonar em camundongos inoculados com células 4T1 de mama (PARK et al., 2016).

Pacientes com câncer são frequentemente afetados por eventos de tromboembolismo venoso pela capacidade da célula tumoral ativar plaquetas e a cascata de coagulação. Com o avanço da ciência, foi possível traçar uma nova associação entre trombose e câncer a partir da alta da capacidade trombogênica das NETs. Isso ocorre porque o estabelecimento de um processo inflamatório pode ativar neutrófilos e liberar NETs que sequestram e ativam as plaquetas, e funcionam como uma plataforma de adesão de plaquetas ativadas e das hemácias, contribuindo para a formação do trombo (DEMERS et al., 2012). Além disso, as histonas que compõem as NETs são capazes de aumentar a hipercoagulabilidade através da geração de trombina no plasma (JUNG et al., 2019; LI et al., 2019). A ativação de neutrófilos pode ser sinalizada pelo próprio tumor. Exosomos derivados de células metastáticas de câncer de mama foram capazes de acelerar a trombose venosa em camundongos pré-tratados com GCSF (LEAL et al., 2017). Outro fator preponderante na associação de NETs e trombose no câncer é o papel da Interleucina 1β. O tratamento farmacológico com bloqueador do receptor de IL1β foi capaz de abolir a trombose em modelo de camundongos inoculados com células tumorais de mama (GOMES et al., 2019) (**Figura 6).**

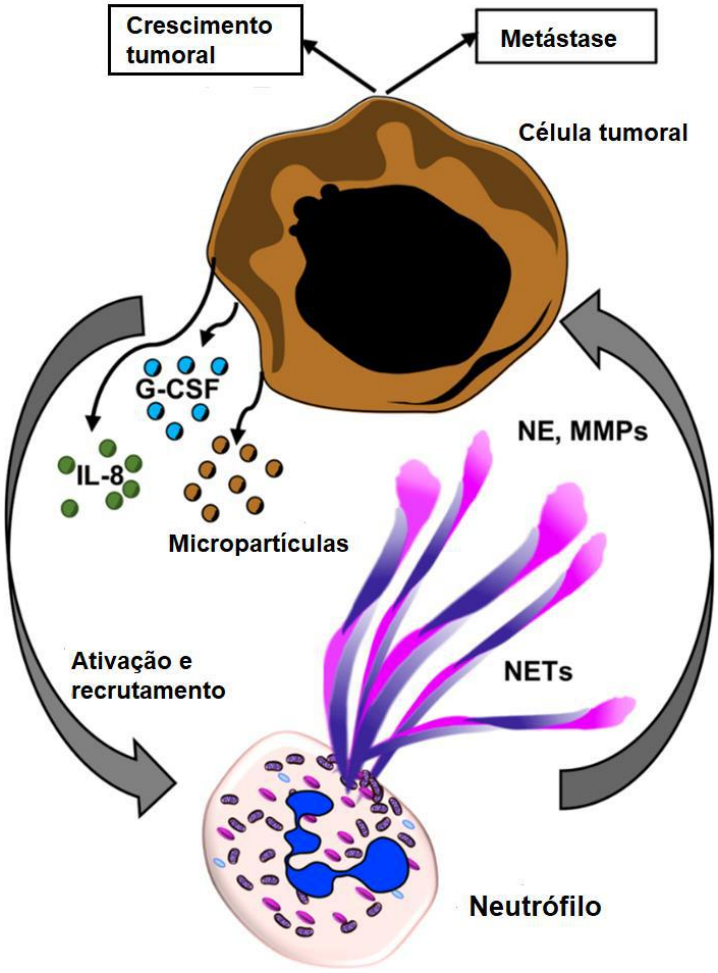

FIGURA 6. Papel das NETs no câncer. Células tumorais podem interagir com os neutrófilos através de fatores mediadores inflamatórios (IL-8), fator de recrutamento e diferenciação de neutrófilos (GCSF) e microvesículas, induzindo a NETose. Os componentes das NETs são capazes de contribuir com a progressão tumoral e amplificação da resposta inflamatória. Adaptado de YOUSEFI et al., 2020.

Pouco ainda se sabe sobre os mecanismos moleculares de ativação das células tumorais induzida por NETs. TOHME e colaboradores (2016) buscaram entender as vias relacionadas à resposta pró-tumoral. Utilizando um modelo de isquemia e reperfusão hepática, observou-se que NETs eram capazes de formar metástases após estresse cirúrgico por meio da ativação do receptor Toll-like 9 (TLR9) causada pela proteína nuclear HMGB1 contida nas NETs. Outro estudo demonstrou que a progressão de linfoma difuso de grandes células B induzida por NETs através da via de TLR9, ativando NFκB, STAT3 e p38 (NIE et al., 2019). TLR4

também foi ativado pela elastase neutrofílica (NE) contida nas NETs em células tumorais de câncer colorretal. Sua ativação levou ao aumento da biogênese mitocondrial, atuando diretamente no metabolismo celular através de maior produção de energia e consequentemente aumento do tumor primário (YAZDANI, 2019)

NETs também induziram a resistência à morte celular em hepatocarcinoma através da ativação de receptores TLR 4/9 e expressão de COX2. A combinação de DNAse I com anti-inflamatórios aspirina ou hidroxicloroquina reduziu drasticamente a metástase em camundongos com hepatocarcinoma (YANG, Lu-Yu *et al.*, 2020).

1.8 Transição epitélio-mesenquimal (TEM)

Descrito primeiramente como um processo fisiológico essencial no desenvolvimento embrionário (Hay, 1995), a transição epitélio-mesenquimal possui um importante papel na diferenciação e na migração celular, responsável pela estrutura morfológica celular e reorganização dos folhetos embrionários. Durante o processo de TEM, as células diferenciadas perdem suas características epiteliais e adquirem um perfil mesenquimal. Atualmente, sabe-se que esse fenômeno não ocorre apenas na embriogênese, mas também em processos patológicos, como fibrose, cicatrização e câncer (YEUNG & YANG, 2017; MITTAL, 2018). O papel funcional desse processo no câncer é complexo e inclui o aumento de motilidade das células tumorais e da habilidade de invadir tecidos adjacentes, facilitando a disseminação da célula tumoral e com isso, contribuindo para a metástase (BURGER, DANEN, BELTMAN, 2017). Além da metástase, o processo de TEM promove outras características nas células tumorais como aquisição de perfil tronco, resistência à quimioterapia, habilidade de evadir à resposta imunológica e bloqueio da senescência da célula (LU & KANG, 2019). As células induzidas por TEM também sofrem alteração metabólica, aumentando a glicólise aeróbica, a glutaminólise, o catabolismo de pirimidinas e reduz a geração de ROS (LU & KANG, 2019)

Durante a transição, as células perdem suas propriedades epiteliais, como a perda das junções célula-célula e de adesão à membrana basal juntamente com sua

polaridade apical-basal, adotando uma morfologia difusa, semelhante ao fenótipo mesenquimal **(Tabela 2)**. As células adquirem um comportamento mais migratório, podendo invadir novos tecidos. A principal proteína de junção que tem sua expressão reprimida, é a E-caderina. Quando a célula perde essa proteína de superfície, a estrutura celular é abruptamente afetada, justificando a alteração morfológica (DONGRE & WEINBERG, 2019). Ocludinas, claudinas, desmossomos e citoqueratinas são outras classes de proteínas de adesão celular epitelial que também têm sua expressão reprimida durante a transição epitélio-mesenquimal (YEUNG & YANG, 2017).

Simultaneamente à essas perdas, a célula aumenta a expressão dos genes N-caderina, Vimentina e Fibronectina, conhecidos como marcadores mesenquimais **(Figura 7)**. Essa alteração molecular induz a formação de protusões na membrana celular que facilitam a invasão das células tumorais em outros tecidos. Além disso, a expressão de metaloproteinases (MMPs) é aumentada. As MMPs são secretadas pelas células e são capazes de degradar a matriz extracelular (YEUNG & YANG, 2017).

Tabela 2. Clássicas diferenças entre células epiteliais e mesenquimais. Adaptado de Ye & Weinberg *Cell Press*, 2015.

CARACTERÍSTICAS	CÉLULAS EPITELIAIS	CÉLULAS MESENQUIMAIS
Morfologia em cultura 2D	Formato poligonal	Formato alongado
Polaridade celular	Apical-basal	Ântero-posterior
Motilidade	sem motilidade	Móvel e invasiva
Citoesqueleto	Expressa citoqueratinas	Expressa Vimentina
Adesão célula-célula	Forma junções aderentes e junções *tight*	Não forma junções aderentes e junções *tight;* forma adesões focais com a matriz extracelular

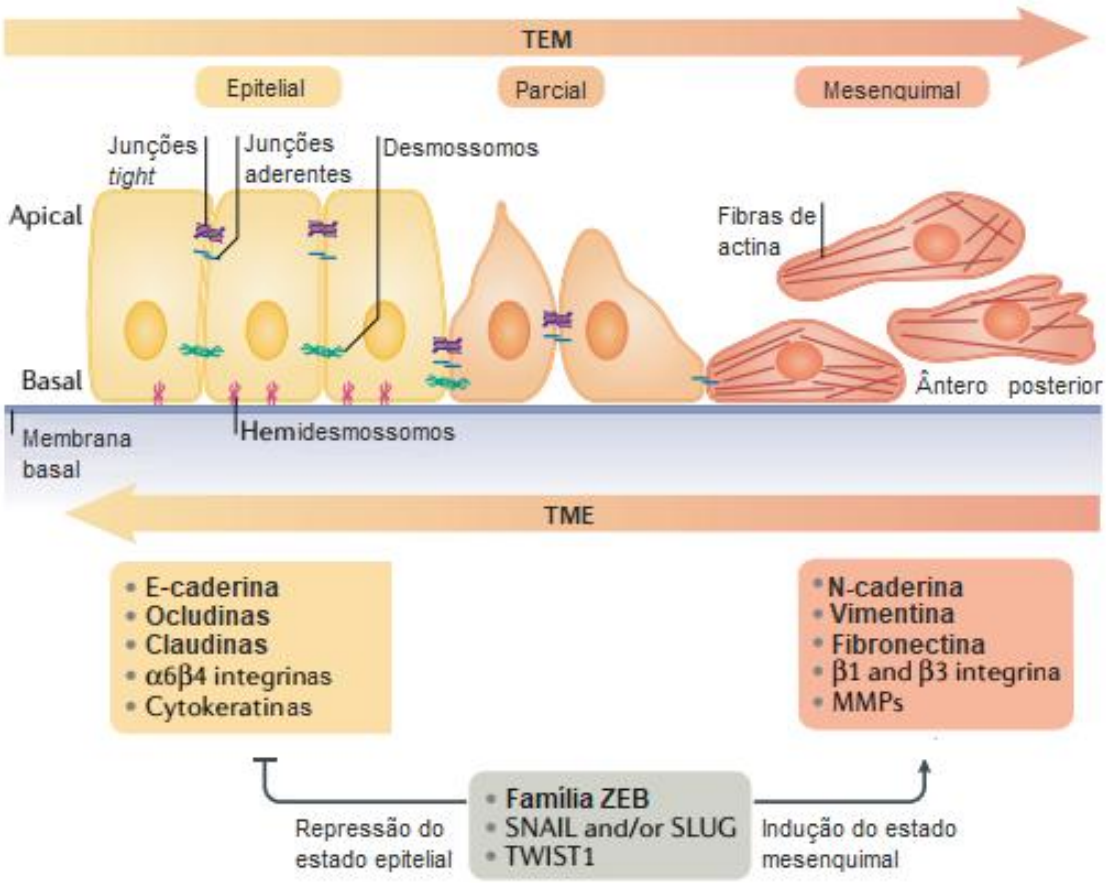

FIGURA 7. Representação do processo de transição epitélio-mesenquimal com os estágios da transição e as proteínas moduladas pelos fatores transcricionais. O processo de TEM é marcado pela perda de caraterísticas epiteliais, como a perda de junções aderentes e o ganho de características mesenquimais. A célula em transição também passa por um remodelamento do citoesqueleto, apresentando uma morfologia diferenciada. Essas características são moduladas por famílias de fatores transcricionais relacionados ao processo. Adaptado de DONGRE & WEINBERG, 2019).

No entanto, este processo é dinâmico e transiente, o que dificulta a visualização dessa alteração fenotípica em amostras clínicas fixadas. Isso ocorre porque nem todas as células passam pelo processo clássico de TEM. Mediante esse dinamismo, estudos mais recentes têm tratado o processo de transição não somente com dois fenótipos, mas também apresentando estágios intermediários com modulação de diferentes mecanismos (VAN STAALDUINEN et al., 2018). Essas

células híbridas costumam apresentar perda de marcadores epiteliais, mas sem ganho aparente de marcadores mesenquimais. Alguns estudos já identificaram células tumorais circulantes co-expressando marcadores epiteliais e mesenquimais (LU et al., 2013; ZHANG et al., 2014; JIA et al., 2015; DONGRE & WEINBERG, 2019). Esses achados levaram à proposta de existência de uma transição epitélio-mesenquimal parcial. No entanto, o papel funcional das células que sofrem TEM parcial ainda não é bem compreendido na progressão do tumor.

A transição epitélio-mesenquimal é regulada por diferentes superfamílias de fatores transcricionais (Twist, Snail e Zeb). Quando ativados em resposta a algum sinal, os fatores transcricionais são capazes de alterar a programação celular, reprimindo ou expressando genes de TEM. Sabendo que este processo é dinâmico, em estágios intermediários do processo de transição as células podem apresentar características híbridas entre fenótipo epitelial e mesenquimal (NIETO et al., 2016).

A ativação de determinado fator transcricional modula diferentes efeitos no processo de TEM. Um estudo mostrou que a deleção de Snail e Twist1 em câncer pancreático não afetou a metástase, mas foi capaz de gerar quimiorresistência. Utilizando o mesmo modelo, mas deletando o fator Zeb 1, a metástase foi afetada (KREBS et al., 2017). Isso mostra que as funções dos fatores transcricionais se complementam no programa de TEM e fortalece a hipótese de subprogramas ou estágios intermediários de TEM. As famílias Zeb e Snail são capazes de se ligar às sequências promotoras do gene E-caderina e impedir sua transcrição. Snail 1 e Zeb 2 regulam positivamente a expressão de MMPs. A ativação de Twist tem sido observada durante o processo de formação de protusões especializadas enriquecidas de actina na membrana plasmática da célula tumoral (conhecidas como invadopodias), levando à degradação da matriz extracelular (NIETO et al., 2016).

Sinais morfogênicos e ambientais já foram determinados como reguladores iniciais do processo de TEM. TGFβ é um clássico indutor de TEM comumente utilizado nos estudos envolvendo a transformação celular através da TEM. Sensores intracelulares de oxigênio, os fatores indutores de hipóxia HIF-1 e HIF-2 também ativam o programa de TEM. Além da via de Wnt, fatores de crescimento epidérmicos (como o EGFR), fator de crescimento derivados de plaquetas (PDGF), receptores de

integrinas (VAN STAALDUINEN et al., 2018). O processo inflamatório crônico também está intimamente associado à TEM, determinando uma maior agressividade ao tumor (SUAREZ-CARMONA et al., 2017). Através de citocinas inflamatórias (IL-6 e IL-8) também liberadas no ambiente tumoral proveniente das células inflamatórias infiltradas.

No câncer de mama, marcadores envolvidos no processo de TEM também têm sido utilizados para distinguir o grau de malignidade do tumor e seu impacto no prognóstico do paciente de acordo com o subtipo tumoral (FELIPE LIMA et al., 2016) **(Figura 8).** Por exemplo, tumores com baixa marcação para proteína de junção oclusiva, claudina, geralmente não expressam nenhum dos receptores ER, PR ou HER2 e possuem uma alta atividade de células-tronco tumoral (HENNESSY et al., 2009). Esses tumores são classificados pelo subtipo triplo-negativo e frequentemente expressam o fator transcricional Slug enquanto os subtipos luminais não expressam (POMP et al., 2015). Por outro lado, os subtipos luminais apresentam maior diferenciação celular e melhor prognóstico. A expressão do receptor de estrogênio no câncer de mama é capaz de inibir a TEM (SINGH & CHAKRABARTI, 2019). Em linhagem MCF7 do subtipo luminal, o silenciamento de ER resultou na alteração da morfologia celular, perda de citoqueratinas e expressão de vimentina (AL SALEH, AL MULLA, LUQMANI, 2011)

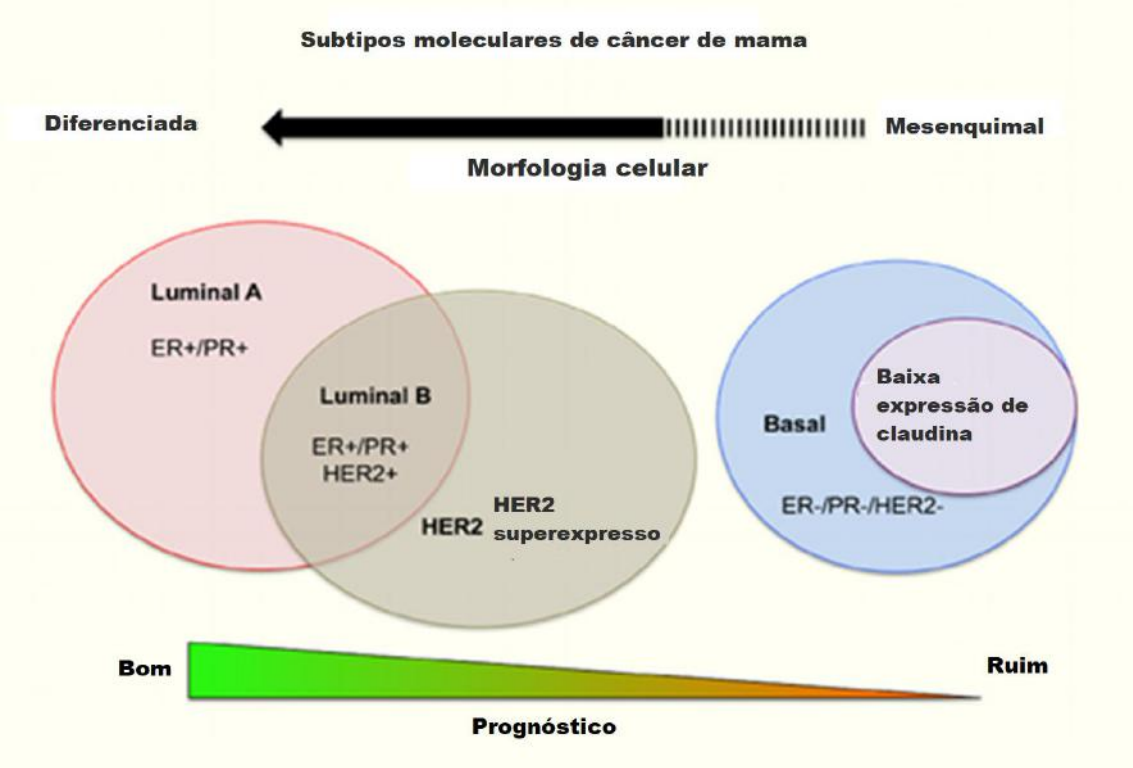

FIGURA 8. Características morfológicas em diferentes subtipos moleculares. Os subtipos luminais frequentemente apresentam um perfil de células mais diferenciadas e com melhor resposta à terapia, apresentando bom prognóstico. Em subtipos HER2 e basal, a TEM geralmente encontra-se ativa e as células tumorais são menos diferenciadas e maior potencial metastático, apresentando pior prognóstico. Adaptado de (HENG et al., 2016).

Portanto, a aquisição do fenótipo mesenquimal através da TEM, pode associar-se a agressividade tumoral. Marcadores da TEM podem predizer o prognóstico do paciente, sendo um relevante fator a ser considerados em futura abordagem terapêutica (YEUNG; YANG, 2017).

1.9 Células-tronco tumorais

O tecido tumoral não é formado apenas por variados tipos celulares como também é formado por subpopulações de células tumorais com diferentes graus de diferenciação e malignidade. O que em parte justifica sua heterogeneidade intratumoral e diferentes respostas terapêuticas. Dentre as células contidas no microambiente tumoral, há a presença de uma subpopulação minoritária de células que tem sido denominadas células-tronco tumorais (do inglês, cancer stem cells - CSC). As CSC são uma subpopulação indiferenciada com capacidade regenerativa e de proliferação ilimitada, semelhante às células-tronco normais, mas com potencial maligno (BATLLE & CLEVERS, 2017; PRAGER et al., 2019). CSCs possuem alta resistência à estresse gerado no microambiente tumoral, como hipóxia, resistência a quimioterapia e à radiação, além de alta durabilidade, e são capazes de permanecer em dormência por longos períodos (APONTE & CAICEDO, 2017).

Apesar dos desafios e limitações técnicas para purificação de subpopulações celulares, o conceito da existência dessas células foi proposta a partir de ensaios experimentais isolando células-tronco (subpopulação CD34+/CD38-) de pacientes com leucemia mieloide aguda que foram posteriormente enxertadas em camundongos imunodeficientes, iniciando a formação de um tumor (LAPIDOT et al., 1994). Conforme o desenvolvimento do tumor, as células-tronco tumorais sofrem pressões do microambiente tumoral, gerando instabilidades genéticas que estimulam sua expansão, gerando novos clones de células-tronco ou células progenitoras de células tumorais diferenciadas. Entretanto, estudos já mostraram em alguns tipos de tumor, que o acúmulo de alterações (epi)genéticas na inicialização de um câncer pode também ocorrer em células já diferenciadas (PEITZSCH et al., 2017). Por conta desses diferentes achados científicos, traçou-se duas diferentes teorias para explicá-los (**Figura 9)**.

A primeira hipótese para explicar a heterogeneidade intratumoral é a evolução clonal descrita por NOWELL (1976). Neste modelo, acredita-se que uma única célula sofra alterações aleatórias gerando uma célula neoplásica, adquirindo capacidade proliferativa superior à de células normais. Ao longo do desenvolvimento tumoral, essas células neoplásicas sofrerão novas mutações gerando novos clones. Outras evidências comprovam que diferentes determinantes não genéticos também podem

contribuir para a heterogeneidade intratumoral, como modificações epigenéticas (metilação de DNA, modificação de histonas, microRNA (KRESO & DICK, 2014). E de acordo com a teoria Darwinista, os clones com mais vantagens proliferativas, como por exemplo, estarem em regiões nutricionalmente abastadas, seriam naturalmente selecionados, enquanto os clones com desvantagens à pressão do microambiente tumoral seriam eventualmente extintos (PRASETYANTI & MEDEMA, 2017).

A segunda hipótese propõe que apenas uma pequena subpopulação de células possuiria a capacidade infinita de auto renovação para iniciar e manter o crescimento tumoral. Semelhantemente ao comportamento das células-tronco saudáveis em tecidos normais, as células-tronco tumorais estariam no topo de uma organização hierárquica, onde a subpopulação de CSC daria origem a novas células com fenótipos diferenciados, gerando heterogeneidade intratumoral (PRASETYANTI & MEDEMA, 2017). Esse processo não é irreversível, haja visto que células já diferenciadas podem por algum sinal proveniente do microambiente tumoral ou mutação se desdiferenciar e retornar ao seu estado primitivo, adquirindo propriedades de células-tronco e estabelecendo novos clones de CSCs, contribuindo para a heterogeneidade do tumor.

Similarmente, evidências vêm comprovando que subpopulações celulares intratumorais se desdiferenciam em CSCs através da TEM. A plasticidade celular das CSCs e o processo de TEM, estão juntamente associados com a agressividade tumoral, haja visto que mutações ou sinais do microambiente tumoral podem sinalizar para ativação de ambos os processos (MANI et al., 2008; APONTE & CAICEDO, 2017). Comumente, em cânceres as vias associadas à auto renovação se encontram ativas continuamente, promovendo a progressão do tumor à metástase.

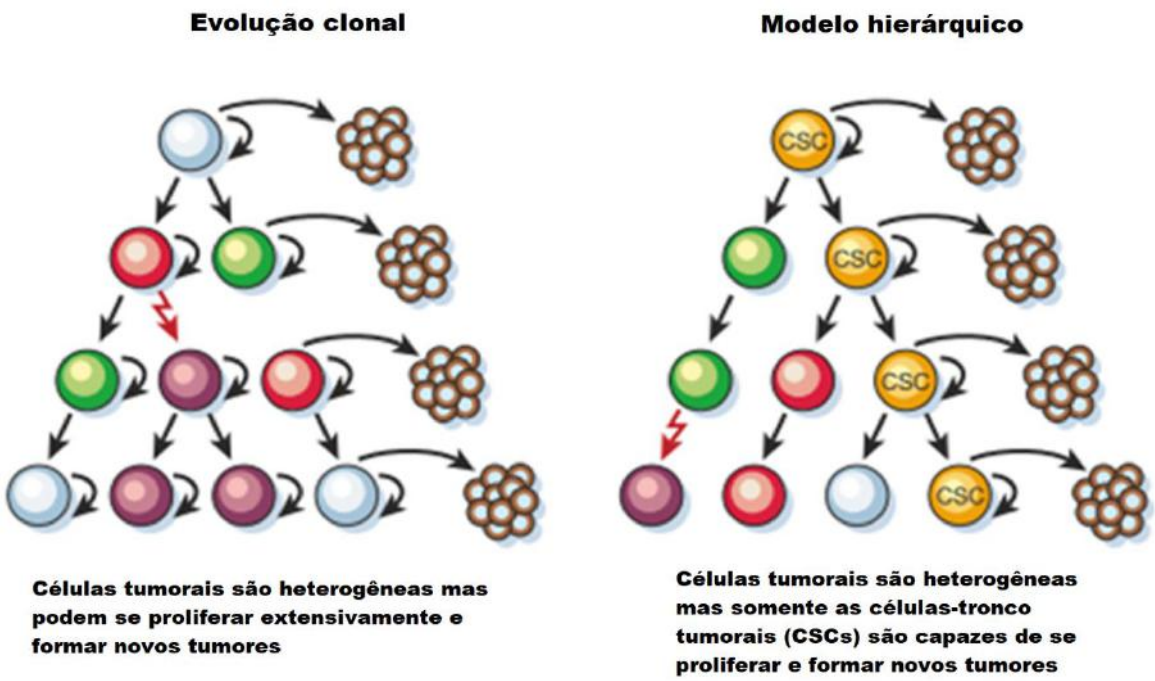

FIGURA 9. Comparativo entre modelos propostos para heterogeneidade intratumoral. A primeira hipótese de evolução clonal suporta a ideia de que a célula-tronco pode surgir a partir de células com acúmulo de mutações, adquirindo a capacidade de auto renovação. A segunda hipótese afirma que apenas as células-tronco tumorais sejam capazes de originar as demais células. Adaptado de (BAUMANN, KRAUSE, HILL, 2008).

Com o avanço das pesquisas com células-tronco, muitas vias de sinalização celular já foram descritas pela sua capacidade de regulação e manutenção. No entanto, os efeitos pro-tumorais da ativação desregulada dessas vias em CSCs em diferentes tipos tumorais podem ser decisivos no desenvolvimento do tumor (NUNES et al., 2018). Dentre elas se encontram: **1)** A via JAK/STAT está envolvida no processo de progressão tumoral em vários tipos de câncer. Sua ativação está relacionada com tumorigênese, capacidade metastática, diferenciação de CSCs e quimiorresistência através da ativação de TEM (JIN, 2020). **2)** A via Hedgehog participa no processo embrionário e da homeostase tecidual, mas sua ativação aberrante leva à transformações neoplásicas, tendo papel essencial na iniciação da leucemia mieloide através das CSCs (SARI et al., 2018). **3)** A sinalização de Wnt/β-

catenina está associada com metástase mediada por CSCs. Em câncer de colorretal e leucemia, esta via costuma estar aberrante desregulando sua capacidade proliferativa (REYA & CLEVERS, 2005). **4)** A via de Notch, quando superativada, sustenta a tumorigênese, aumentando o número de CSCs. Em câncer de mama, sua ativação pode ser um diferencial na agressividade tumoral (MEISEL, PORCHERI, MITSIADIS, 2020). **5)** A via de sinalização de PTEN (proteína homóloga de tensina e fosfatase) / AKT / PI3K (fosfatidilinositol 3-quinase) tem um papel importante no surgimento de CSCs no câncer de próstata. A via PI3K/AKT induz migração e invasão celular de células de câncer de mama através da secreção de Interleucinas 6 e 8 (YANG et al., 2020). **6)** O fator transcricional NFκB exerce um papel central para a sobrevivência das células, inibindo a morte celular por apoptose. Sua inibição impede o desenvolvimento de CSCs no câncer de mama e aumenta sensibilidade à quimioterapia. (KALTSCHMIDT et al., 2019). **7)** O eixo MAPK (Proteínas-quinases ativadas por mitógenos) / ERK, quando bloqueado, observou-se inibição no crescimento do tumor de mama, levando à morte celular por apoptose, aumentando a eficácia de radioterapia e quimioterapia (YIP et al., 2011). **8)** A ativação exacerbada de TGF-β, levou à ativação de SMAD, cuja resposta foi a alteração da plasticidade das células-tronco, levando à sua diferenciação celular e formação de CSCs. (YANG et al., 2020).

Essas diferentes vias podem contribuir para progressão tumoral de forma conjunta. Por exemplo, no hepatocarcinoma agressivo, é comum encontrar as vias de TGF-β, Notch e Wnt desreguladas, alterando seu perfil de auto renovação, diferenciação e sobrevivência (APONTE & CAICEDO, 2017). O processo de regulação de CSCs, assim como muitos outros processos no microambiente tumoral, é bastante complexo, não linear e extremamente dinâmico. Essas vias interagem entre si promovendo a manutenção da população de CSCs (YANG et al., 2020).

Células tumorais e células-tronco tumorais baseiam-se na expressão diferenciada de marcadores **(Tabela 3)**. Estudos demonstraram ser bastante consistente o perfil de marcadores entre os pacientes, apesar de existir grande variação de biomarcadores entre os diferentes tipos tumorais. Isto facilita a identificação e o isolamento de CSCs para realização de estudos (CLARKE & HASS, 2004; WALCHER et al., 2020). Para uso clínico, há uma limitação de biomarcadores além do uso do CEA (antígeno carcinoembrionário), YFRA 21-1 (fragmentos de

citoqueratinas 19) e AFP (alfa-fetoproteína que são expressos por CSCs, pois esses biomarcadores também podem ser expressos por células-tronco de tecidos embrionários ou tecidos adultos. Portanto, é imprescindível a combinação de vários marcadores de superfície e intracelulares para identificar e isolar células que promovem a tumorigênese, resistência à terapia e recidiva do tumor (WALCHER et al., 2020).

Tabela 3: Típicos marcadores de células-tronco tumorais em diferentes tipos de tumor. Adaptado de TURDO et al., 2019.

Tipo tumoral	Marcador de célula-tronco tumoral
Câncer de mama	$CD133^+$, $CD44^+$, $CD24^+$, $EpCAM^+$, $ALDH^{high}$
Câncer colorretal	$CD133^+$, $CD44^+$, $CD24^+$, $CD166^+$, $EpCAM^+$, $ALDH^{high}$, ESA^+
Câncer gástrico	$CD133^+$, $CD44^+$, $CD24^+$
Glioblastoma	$CD133^+$
Câncer de cabeça e pescoço	SSEA-1^+, $CD44^+$, $CD133^+$
Leucemia (LMA)	$CD34^+$, $CD38^-$, $CD123^+$
Hepatocarcinoma	$CD133^+$, $CD44^+$, $CD49f^+$, $CD90^+$, $ALDH^{high}$, $ABCG2^+$, $CD24^+$, ESA^+
Câncer de pulmão	$CD133^+$, $CD44^+$, $ABCG2^+$, $ALDH^{high}$, $CD87^+$, $CD90^+$
Melanoma	$ABCB5^+$, $CD20^+$
Câncer de ovário	$CD133^+$, $CD44^+$
Câncer pancreático	$CD133^+$, $CD44^+$, $CD24^+$, $ABCG2^+$, $ALDH^{high}$, $EpCAM^+$, ESA^+
Câncer de próstrata	$CD133^+$, $CD44^+$, $\alpha2\beta1^+$, $ABCG2^+$, $ALDH^{high}$

Nas células-tronco tumorais provenientes do câncer de mama, os marcadores $CD44^{+}/CD24^{low/-}$ foram os primeiros a serem utilizados. CD44 é uma glicoproteína de membrana que reconhece e se liga ao ácido hialurônico. Este receptor desempenha atividades biológicas relacionadas a migração e invasão das células, além de renovação da subpopulação de CSCs (DITTMER, 2018). Células com potencial tumorigênico enquanto expressam altos níveis de CD44, há ausência ou baixa expressão do marcador CD24. A expressão deste marcador está associada com características de células epiteliais (RICARDO et al., 2011). Adiante, a alta atividade enzimática de aldeído desidrogenase – ALDH1 também passou a ser um marcador de CSCs, devido à capacidade tumorigênica das células $ALDH1^{high}$ (PARK, CHOI, NAM, 2019). ALDH1 é uma enzima intracelular com função metabólica, cuja reação envolve oxidação de aldeídos e retinóis (WALCHER et al., 2020). No entanto, células-tronco hematopoiéticas e células-tronco neurais também expressam e possuem alta atividade de ALDH1, não sendo um marcador exclusivo de CSCs. Portanto, a combinação desses três marcadores se tornou o padrão ouro para seleção de células-tronco tumorais de mama (PARK, CHOI, NAM, 2019).

Novos marcadores vêm sendo associados a CSCs, como a glicoproteína CD133, marcador expresso em CSCs derivados de tumores deficientes para gene BRCA1 (ZHOU et al., 2019). Resultados pré-clínicos utilizando as CSCs CD133 positivas como alvo têm sido promissores (WALCHER et al., 2020). Estudos utilizando células de câncer de mama humano mostrou que CSCs $CD44^{+}/CD24^{low/-}$ e positivas para EpCAM, molécula de adesão celular epitelial, possuíam alto potencial metastático. (DITTMER, 2018). CSCs também possuem alta capacidade de resistência à quimioterapia. Isso porque expressam transportadores transmembrana do tipo ABC (como ABCG2 e ABCC1) são capazes de expulsar algumas drogas do meio intracelular (DITTMER, 2018). Os fatores transcricionais Oct4, Sox2, c-Myc, Nanog e Klf4, relacionados ao ganho de atividades de células-tronco, também já foram avaliados no câncer de mama (SCIOLI et al., 2019).

O isolamento dessas células ainda se apresenta como um desafio dada a quantidade de marcadores necessários para identificar e selecionar uma pequena população celular no universo tumoral (BATLLE & CLEVERS, 2017; SCIOLI et al., 2019). No entanto, a resistência aos tratamentos e a reincidência do tumor tem sido

fator crítico para compreender a complexidade dos mecanismos de atuação e auto renovação dessas células (PRAGER et al., 2019). Estratégias terapêuticas baseadas neste nicho de CSCs têm sido propostas com o avanço da nanotecnologia associada a estratégia de gene-alvo (NUNES et al., 2018).

Baseado na literatura, as NETs são capazes de modificar o perfil das células tumorais, levando à metástase. No entanto, os mecanismos pelos quais este efeito ocorre ainda permanecem desconhecidos. Neste trabalho, propomos avaliar a habilidade das NETs em alterar o fenótipo das células luminais MCF7, adquirindo um comportamento de maior agressividade tumoral e pró-metastático através da ativação do programa de TEM.

2. OBJETIVOS

2.1 Objetivo geral

Determinar o papel das redes extracelulares de neutrófilos sobre a aquisição do fenótipo pró-metastático em células de câncer de mama através da transição epitélio-mesenquimal.

2.2 Objetivos específicos

- Compreender o efeito das NETs sobre a morfologia celular e o comportamento migratório das células tumorais de mama;

- Investigar a atuação das NETs sobre o processo de transição epitélio-mesenquimal;

- Avaliar os efeitos das NETs na expressão dos marcadores de células-tronco tumorais;

- Avaliar a expressão gênica de fatores pró-tumorais em células tratadas com ou sem NETs;

- Analisar a relação entre os genes de assinatura neutrofílica e genes pró-tumorais e associados à TEM através de dados de RNAseq de pacientes com câncer de mama.

3. MATERIAIS E MÉTODOS

3.1 Cultura de células

Foram utilizadas as linhagens de células de câncer de mama MCF7, HCC1954 e MDA-MB-231. As linhagens MCF7 e MDA-MB-231 foram cultivadas em meio de cultura DMEM (Dulbecco's Modified Eagle Medium, Thermo Fisher Scientific) suplementado com HEPES (Sigma), 10% de soro fetal bovino - SFB (Cultilab) e 1% de penicilina/estreptomicina (Thermo Fisher Scientific). Já as células HCC1954 foram cultivadas em RPMI (Thermo Fisher Scientific), com 10% de SFB e 1% de penicilina/estreptomicina. As culturas foram mantidas à 37º C com 5% de CO_2. Para manutenção das culturas, após atingirem 80% de confluência, as células eram dissociadas com tripsina.

3.2 Obtenção de neutrófilos

Para utilização de amostras de sangue, o projeto primeiramente foi submetido e aprovado pelo comitê de ética e pesquisa do Hospital Clementino Fraga Filho/UFRJ sob número de registro 82933518.0.0000.525. Amostras de sangue venoso obtidas de doadores saudáveis foram coletadas em tubos e/ou seringas contento 100 mM citrato de sódio numa diluição de 1:10.

Todo o procedimento foi realizado em ambiente estéril para evitar contaminação externa. Sangue total obtido foi cuidadosamente transferido para tubos cônicos contendo Ficoll Histopaque (Sigma Aldrich) na proporção de 2:1, formando um gradiente de densidade. Os tubos foram centrifugados a 400 g por 30 minutos à temperatura ambiente. As células mononucleares do sangue periférico foram desprezados juntamente com o plasma sanguíneo.

Os neutrófilos coletados foram submetidos à lise hipotônica a adição da solução ACK (155 mM NH4Cl, 10 mM KHCO3, 0.1 mM EDTA, pH 7.4) para remoção das hemácias por pelo menos 5 minutos sob suave homogeneização. Os tubos cônicos contendo neutrófilos foram centrifugados a 400 g, por 10 minutos, à 4 ºC e mantidos no gelo desde então. O processo de lise foi realizado mais uma vez e novamente o tubo foi centrifugado. Então, as células foram lavadas em PBS,

centrifugadas e cuidadosamente ressuspendidas em meio RPMI 1640 sem adição de soro fetal. Os neutrófilos foram contados em câmara de neubauer e a suspensão foi ajustada para 1 x 10^7 neutrófilos/mL. O grau de pureza e viabilidade dos neutrófilos obtidos foram mensurados através da coloração com Azul de metileno e Azul de Trypan, respectivamente.

3.3 Geração e isolamento de NETs

Neutrófilos (1 x 10^7 células/mL) foram transferidos para placa de petri estéril e incubados por 3 horas, à 37 ºC e 5% CO_2, com 500 nM de PMA - Phorbol 12-myristate 13-acetate (Sigma Aldrich). Após incubação, o meio foi cuidadosamente removido e a camada formada no fundo da placa foi recuperada com adição de PBS estéril gelado e tranferida para novos tubos cônicos. Os tubos foram centrifugados a 400 g, por 10 minutos, à 4 ºC para remover o debri celular. O sobrenadante foi transferido para tubos de 1,5 mL e centrifugados novamente a 18.000 g, por 10 minutos, à 4 ºC. Então, o sobrenadente foi descartado e o pellet ressuspendido em PBS estéril (50 µL – 100 µL dependendo do tamanho do pellet). As NETs isoladas foram dosadas a partir da quantificação de DNA utilizando espectrofotômetro NanoDrop Lite (Thermo Fisher Scientific). Após, as NETs ainda frescas, ou armazenadas à 4 ºC por no máximo 24 horas, foram utilizadas para os experimentos posteriores.

Para ensaios utilizando NETs digeridas por DNAse, 500 ng de NETs foram aliquotadas em microtubos de 1,5 mL e incubadas com 5U de DNAse I (Pulmozyme®, Roche, Basel, Switzerland) por 5, 15 ou 30 minutos a 37º C. Para testar a atividade e eficiência da DNAse sobre as NETs, aplicou-se as amostras em gel de Agarose 0,9%, ajustando-as para volume final de 20 µL com 1 µL de GelRed (GelRed™ Nucleic Acid Gel Stain, 10.000x, Biotium) e *q.s.q.* de tampão de amostra (Thermo Fisher). Para o tratamento das células MCF7, foram utilizadas NETs isoladas previamente digeridas conforme descrito acima.

3.4 Análise de expressão gênica por PCR em tempo real

3.4.1 Obtenção da amostra

Em placas de cultura de 6 poços, 5 x 10^5 células de carcinoma mamário foram semeadas por condição e incubadas por 24 horas, à 37 ºC e 5% CO_2, em 1 mL de meio de cultura contendo 10% de soro fetal bovino. Após o período de incubação, as células foram lavadas duas vezes com PBS estéril e à 37º C, em seguida mantidas em 1 mL de meio DMEM sem soro por 8 a 10 horas. Após o período de *starving*, o meio foi renovado e 500 ng/mL de NETs foram adicionadas. Após o tratamento com NETs por 16 horas, à 37 ºC em 5% CO_2, as células foram cuidadosamente lavadas com PBS por duas vezes e 500 µL de TRIzol (Thermo Fisher Scientific) foi adicionado e homogeneizado diversas vezes para garantir a eficiência da extração de RNA.

3.4.2 Extração de RNA e síntese de cDNA

As amostras suspensas em TRIZol foram transferidas para tubos estéreis de 1,5 mL livres de RNA. Foram adicionados 100 µL de clorofórmio (Vetec), avidamente agitados e incubados por 3 minutos à temperatura ambiente. Então, os tubos foram centrifugados a 12000 g, por 15 minutos, à 4 ºC. A fase aquosa (fase superior) foi transferida para um novo tubo e 250 µL de isopropanol (Vetec) foi adicionado. Após leve homogeneização e incubação por 10 minutos à temperatura ambiente, os tubos foram novamente centrifugados a 12000 g, por 10 minutos, à 4 ºC. O sobrenadante foi descartado cuidadosamente e 1 mL de etanol 75% foi adicionado sobre a amostra. Novamente, os tubos foram centrifugados a 9000 g, por 7 minutos, à 4 ºC. O sobrenadante foi retirado ao máximo com a pipeta e os tubos foram deixados abertos, por pelo menos 15 minutos, para secagem total das amostras. Então, 20 µL de água DEPC (Life Invitrogen) foi utilizada para ressuspender as amostras de RNA. Os tubos foram alocados no termobloco por 10 minutos à 56 ºC. O RNA foi quantificado no espectrofotômetro Nanodrop Lite (ThermoFisher).

Em microtubos de 0,2 mL, 1µg de RNA por amostra foi adicionado juntamente com 1µL de DNAse I, 1 µL de Tampão DNAse I µL (ThermoFisher) e água DEPC *q.s.p*. 10 µL. E então incubados no termociclador por 30 minutos à 37 ºC. Após, 1 µL de EDTA (50 mM ThermoFisher) foi adicionado por microtubo e incubado por 10

minutos à 65 ºC. A partir daí, foi adicionado o kit de transcrição reversa seguindo a recomendação do fabricante AppliedBiosystems para síntese de cDNA.

3.4.3 PCR em tempo real

Após a obtenção do cDNA, utilizou-se mix de reação com volume final de 10 µl composto por tampão (tris 20 mM, cloreto de potássio 50 mM, cloreto de magnésio 5 mM; pH 8,0), SYBR® Green I 1x (Sigma), Reference dye for quantitative PCR1x (Sigma), dNTPs (200 nM cada) e 5 U/µl da enzima JumpStart™ Taq DNA Polymerase (Sigma). Ao mix de reação também foi adcionado cDNA diluido 10 vezes e 400 nM de oligonucleotídeos. As reações foram realizadas no equipamento StepOnePlus Real Time PCR (Applied Biosystems) e analisadas no programa StepOne (Applied Biosystems). Para normalização da expressão gênica, utilizou-se GAPDH como gene endógeno e aplicou-se a fórmula $2^{-\Delta\Delta C}$ para calcular a expressão relativa do grupo tratado com NETs em relação ao grupo controle.

3.5 Citometria de fluxo

1 x 10^6 células foram semeadas em garrafas de cultura de 25 cm^2 e incubadas por 24 horas. Após o periodo, foram lavadas duas vezes e incubadas por mais 8 a 10 horas com meio de cultura sem soro. O meio foi trocado e as células tratadas com 500 ng/mL de NETs por 16 horas. As células então foram cuidadosamente lavadas com PBS, dissociadas com tripsina, contadas na câmara de neubauer e ressuspendidas em 1 x 10^6 células/mL. 5 x 10^5 células por condição foram lavadas duas vezes com tampão de FACS (PBS, 0,01% Azida sódica e 3% SFB). As células foram centrifugadas e o sobrenadante foi descartado. As células então foram incubadas no gelo com ou sem anticorpos conjugados 1:40 anti-CD24 conjugado com Phycoerythrin – PE (Clone ML5; Thermo Fisher Scientific) e 1:40 anti-CD44 com allophycocyanin – APC (Clone IM7; Thermo Fisher Scientific). Após a incubação, as células foram novamente lavadas com tampão FACS e a aquisição do sinal foi feita através do equipamento FACSCanto II com o software FACSDiva (BD Biosciences). Controles sem marcação e com marcação individual foram realizados para calibração de cores. Para análise dos resultados, foi usado o software FlowJo (BD Biosciences) e a média da fluorescência foi mensurada.

3.6 Ensaio de migração

Células MCF7 (1 x 10^6) mantidas por 24 horas em meio com soro e em seguida tratadas por 16 horas com NETs (500 ng/mL) à 37 ºC em 5% CO_2. Então, foram lavadas duas vezes com PBS, tripsinizadas, centrifugadas, ressuspendidas e contadas em câmara de Neubauer. Para o ensaio de migração, utilizou-se a câmara de Boyden de 48 poços e membranas de policarbonato com poros de 8 µm (Neuro Probe). No poço inferior da câmara, foi adicionado meio DMEM com diferentes concentrações de SFB (0%, 2% e 10%) como quimioatraente. Células tratadas ou não previamente com NETs foram ressuspendidas em meio sem soro (1 x 10^6 células/mL) e 50 µL desta suspensão foram adicionados em cada poço superior da câmara de Boyden. Cada condição foi realizada em triplicata. O ensaio foi performado por 20 horas à 37 ºC em 5% CO_2. Após o período de incubação, a membrana foi cuidadosamente retirada e a face superior foi raspada para remoção das células que não migraram. A membrana foi fixada e corada utilizando o kit rápido Panótico (Laborclin) e montada sobre uma lâmina de vidro. Fotografias foram obtidas com 200 x de magnificação em microscópio de campo claro. 10 campos por condição foram contados e a média das células migradas por campo foi calculada.

3.7 Análise por imunocitoquímica

2,5 x 10^5 células MCF7 foram plaqueadas em placas de cultura de 35 mm de diâmetro cobertas com lamínulas de Aclar de 22 mm (Pro-Plastics Inc) previamente tratadas com colágeno I proveniente da cauda de rato. Após 24 horas de incubação, período para adesão das células, estas foram lavadas duas vezes com PBS e, em seguida incubadas por aproximadamente 10 horas em DMEM sem soro. Então, as células foram tratadas por 16 horas com NETs (500ng/mL). Após o tratamento, as células foram lavadas cuidadosamente duas vezes com PBS e fixadas com 4% de paraformaldeído diluído em 0,1 M de PBS. As células tratadas com NETs perdem significativamente a adesão à placa, portanto, a troca das soluções foi realizada com bastante cautela para não desprender as células do plástico. Após fixadas, as células foram lavadas mais duas vezes com PBS contendo 0,5% Triton e incubadas

por 1 hora à 37 ºC os seguintes anticorpos primários: β-catenina (#C-2206, Sigma Chemical, USA), E-caderina (#04-1103, Millipore Sigma, USA), Fibronectina (#F-6140, Sigma Chemical, USA) e N-caderina (#C-3865, Sigma Chemical, USA). Novamente, as células foram lavadas com PBS-Triton e incubadas com os anticorpos secundários por mais 1 hora, à 37 ºC, e lavadas com PBS-Triton. Os anticorpos secundários utilizados foram Alexa Fluor 546 (#A-11010, #A11030), Alexa Fluor 488 (#A-11008, #11001). Todos fabricados por Molecular Probes (USA). Ao final, os núcleos foram marcados com DAPI (0,1 µg/mL em solução salina 0,9% de NaCl) ou NucSpot (fabricados por Molecular Probes e Biotium Inc, USA, respectivamente) por 5 minutos. Lâminas foram montadas utilizando Prolong Gold (Molecular Probes) e examinadas no microscópio invertido Axiovert 100 (Carl Zeiss, Germany) ou microscópio confocal Spinning Disk (DSU, Olympus, Japan).

3.8 Western Blotting

NETs (500 ng/mL) foram incubadas com células MCF7 (1 x 10^6) em garrafas de cultura de 25 cm2, previamente mantidas em meio sem soro. Após o tratamento, as células foram cuidadosamente lavadas duas vezes com PBS gelado. Então, 80 – 100 uL de tampão de lise (Tris-HCl 100mM pH 8,0, NaCl 3,04 M, Triton X-100 2%, 2% de deoxicolato, SDS 0,2%, EDTA 10 mM) foi adicionado em cada garrafa e com auxílio do scraper para raspagem da garrafa, as amostras foram coletadas e transferidas para tubos de 1,5 mL. As amostras foram mantidas no gelo por 20 minutos e centrifugadas por 15 minutos a 15000 g, à 4ºC. O pellet foi descartado e a quantidade de proteína por amostra foi dosada pelo método de Lowry, utilizando o kit DC Protein Assay (BioRad), seguindo as recomendações do fabricante.

Na corrida de eletroforese SDS-PAGE (6 – 12% de acrilamida), foram utilizadas 30 – 60 µg de proteína/amostra. Após a corrida, as proteínas foram transferidas para membrana de PVDF (GE Healthcare) por transferência molhada a 200 mA constantes por 2 horas. A membrana foi incubada 2 horas, a 4ºC, com solução de bloqueio (PBS, 0,05% NP40, 5% de leite Molico) e incubadas overnight com os seguintes anticorpos primários: E-caderina (1:10,000; #61082; BD Biosciences, San Jose, CA, USA), Fibronectina (1:750; #F3648; Merck, Darmstadt, Germany) , Vimentina (1:500; #M0725; DakoCytomation, Glostrup, Denmark) e β-

actina (1:1000; #8457; Cell Signaling Technology, Danvers, MA, USA). Após o periodo, as membranas foram incubadas por 1 hora a temperatura ambiente com anticorpos secundários conjugados com HRP (DakoCytomation) e revelados utilizando reagentes de detecção de Western Blotting ECL® (GE Healthcare, São Paulo, Brazil).

3.9 Análise de expressão gênica de pacientes com câncer de mama

Para realizar análise de expressão de genes relacionados à neutrófilos, utilizou-se dados de RNAseq de 1100 pacientes com câncer de mama depositados no repositório The Human Genome Atlas (TCGA). Valores dos transcritos (FPKM = Fragments Per Kilobase Million) de cada gene de relacionado a neutrófilo foram estratificados em diferentes subtipos de câncer de mama: Luminal A (lumA), Luminal B (lumB), HER2+ (HER2) e subtipo Basal. Para análise de correlação entre os genes de assinatura neutrofílica e os genes pro-tumorais, utilizou-se a plataforma cBioPortal (https://www.cbioportal.org/), cujos gráficos e os coeficientes de Spearman juntamente com o valor estatísticos são fornecidos pela plataforma (CERAMI et al., 2012; GAO et al., 2013). Para refinar a análise de co-expressão gênica, utilizou-se a ferramenta GEPIA 2 (http://gepia2.cancer-pku.cn/) a fim de gerar análises de correlação entre os genes alvo e um *subset* de genes de assinatura neutrofílica (*DEFA4, DEFA1B, MMP8, CEACAM6, CEACAM8, LTF,* MPO e *ARG1*). A partir da análise destes dados, gerou-se as tabelas das correlações gênicas apresentadas nos resultados.

3.10 Análise estatística

O software de análise utilizado foi GraphPad Prism 5 (GraphPad Software, San Diego, CA, EUA). Os dados representados nos gráficos informam a média de pelo menos três experimentos independentes ± desvio padrão. Nos ensaios de RT-PCR quantitativo, citometria de fluxo e ensaio de migração, o teste t não pareado foi aplicado para determinar a diferença estatística entre células MCF7 tratadas ou não

com NETs. No ensaio de RT-PCR quantitativo e migração testando o efeito da DNAse nas células MCF7, utilizou-se o teste ANOVA Tukey. Para análise da expressão dos genes de assinatura neutrofílica em diferentes subtipos de tumor de mama, foi aplicado o teste U de Mann-Whitney. As correlações dos valores de RNA-seq (FPKM) obtidos pelo TCGA foram analisadas estatisticamente pelo método Teste de Spearman não paramétrico. Os resultados foram considerados estatisticamente significativos quando o valor de $p \leq 0,05$.

4. RESULTADOS

4.1 Alteração da morfologia celular induzida pelas NETs em células MCF7

De acordo com a classificação dos subtipos de câncer de mama, a linhagem celular MCF7 é classificada como subtipo luminal (NEVE et al., 2006). Seu perfil epitelial apresenta um formato poliédrico, capaz de formar ilhotas em cultura celular. Durante o estímulo prolongado das células MCF7 com NETs, a partir de 8 horas de tratamento, foi observado ao microscópio uma aparente alteração morfológica (dados não apresentados). As células passaram a apresentar um formato mais alongado, do tipo fibroblasto, apresentando uma quantidade expressiva de prolongamentos. Um efeito de perda de adesão dessas células à garrafa de cultura após 16 horas de tratamento com NETs também foi notado **(Figura 10).**

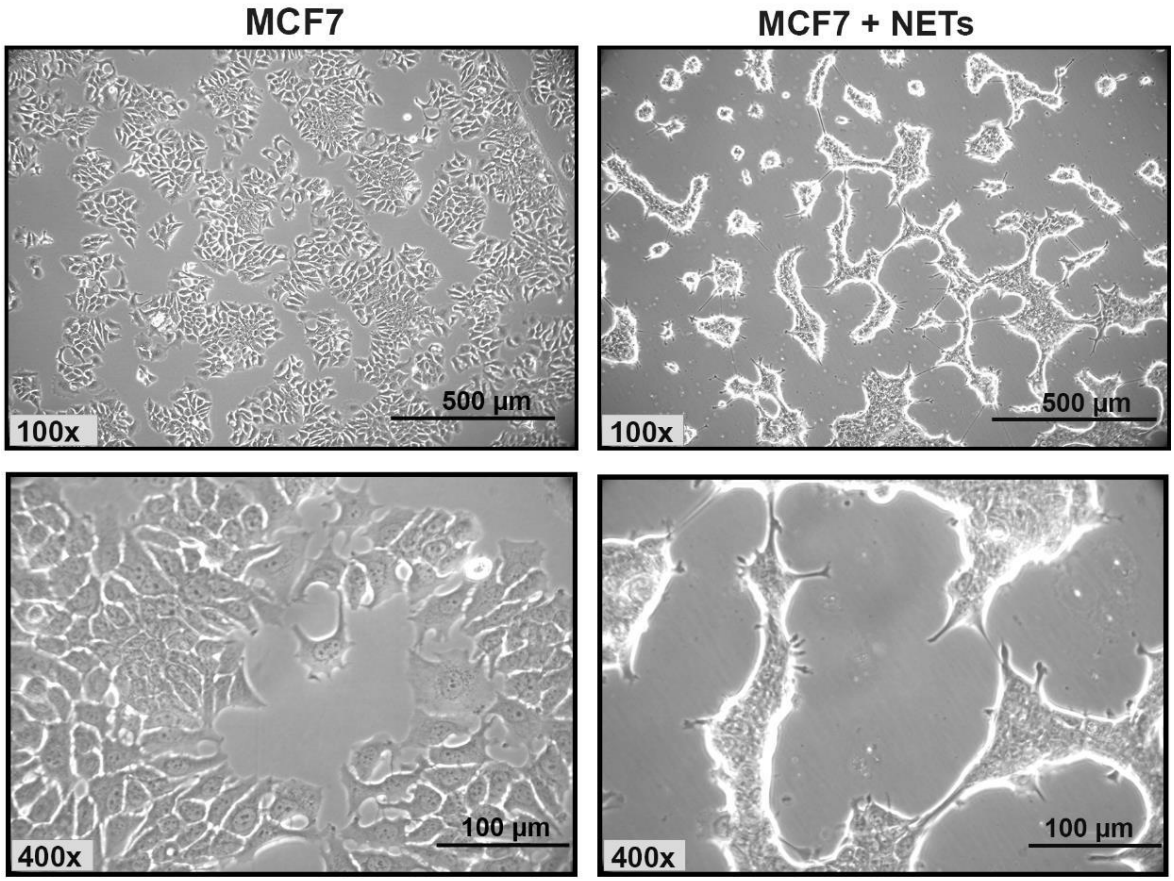

FIGURA 10. NETs altera a morfologia das células MCF7. Imagens representativas de células MCF7 que foram cultivadas por 16 horas na ausência (painéis à esquerda) ou a presença (painéis à direita) de NETs (500 ng/mL). Ampliação da imagem: 100× e 400×. Barra de escala de 500 µm e 100 µm, respectivamente.

4.2 NETs induzem aumento de migração celular em células MCF7

No avanço da malignidade do câncer, uma das etapas de transição epitélio-mesenquimal e metástase envolve a habilidade da célula tumoral em migrar do sítio primário, invadir um tecido adjacente para então se instalar num sítio distante ao tumor primário. A dinâmica do citoesqueleto levando à alteração morfológica é um forte indício dessa nova habilidade da célula em migrar. Portanto, o comportamento migratório das células MCF7 também foi avaliado.

Através do ensaio de migração feito na câmara de Boyden, utilizou-se diferentes concentrações de soro fetal bovino como quimioatraente **(Figura 11).** Nas condições sem soro fetal, as células MCF7 tratadas com NETs (48,9 ± 4,5 células por campo) migraram quase 7 vezes mais do que as células mantidas apenas com meio de cultura sem soro (7,39 ± 5,0). Na presença de 2% de soro fetal bovino na porção inferior da câmara, as células tratadas com NETs (94,9 ± 20,3 células por campo) migraram aproximadamente 3 vezes mais do que as células MCF7 sem tratamento (34,9 ± 16,2). Ao utilizar 10% de soro fetal, observou-se um aumento da migração de células tratadas com NETs (174,6 ± 49,4) duas vezes maior do que as células MCF7 não tratadas (88,1 ± 13,4).

Estes resultados apontam o efeito significativo das NETs sob a motilidade celular, alterando o comportamento migratório das células epiteliais de câncer de mama.

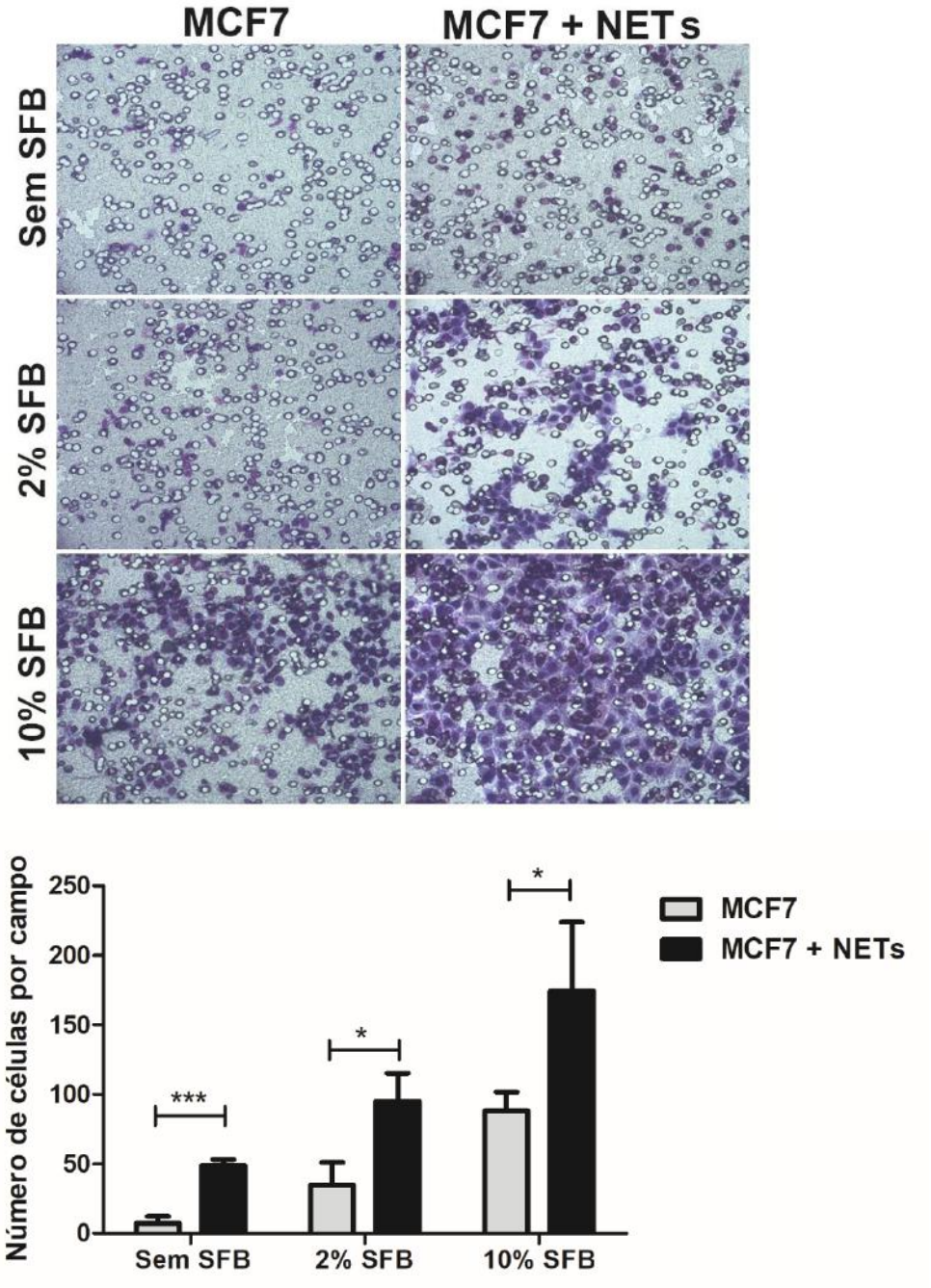

FIGURA 11. NETs modula o padrão migratório das células MCF7. O ensaio de migração foi performado através da câmara de Boyden. Células MCF7 que foram cultivadas por 16 h, na ausência ou na presença de NETs (500 ng/mL), foram semeadas na parte superior câmara (5 × 10^4 células / poço) e a migração avaliada após 20 horas. Como quimioatraente, meio de cultura suplementado com soro fetal bovino nas concentrações de 2% ou 10% foi utilizado nas câmaras inferiores. Imagens representativas do ensaio de migração são mostradas acima (ampliação de 200×). Contagem das células que migraram foram representadas no gráfico. Os dados são a média ± desvio padrão de três experimentos independentes. A análise estatística de cada condição foi avaliada por teste t não pareado. A significância foi assumida para * p <0,05, *** p <0,001.

4.3 NETs aumentam a expressão gênica dos fatores transcricionais de TEM em células MCF7

O padrão de alteração morfológica observado nas células MCF7 foi similar ao que é relatado em diversos estudos envolvendo transição epitélio-mesenquimal (TEM). A partir daí, investigou-se a possível ativação do processo de TEM induzido pelas NETs nas células de câncer de mama não metastáticas, MCF7. Por meio de RT-PCR quantitativo, avaliou-se a expressão de fatores transcricionais reguladores de TEM. Nas células tratadas por 16 horas com NETs, observou-se um aumento significativo na expressão gênica de Zeb1 (*ZEB1)* e Snail (*SNAI1).* Os níveis de mRNA de *ZEB1* foram aproximadamente 4 vezes maiores nas células MCF7 tratadas com NETs do que nas células não tratadas. Adicionalmente, o transcrito *SNAI1,* foi 1,5 vezes aumentado nas células com NETs do que as células MCF7 **(Figura 12).** Sob a mesma análise, os demais fatores analisados, *Slug (SNAI2)* Sip1 (*ZEB2) e Twist (TWIST1* não sofreram modulação gênica induzida pelas NETs.

De acordo estes resultados, as NETs parecem ter um efeito significativo sobre a ativação da transição epitélio-mesenquimal em células MCF7.

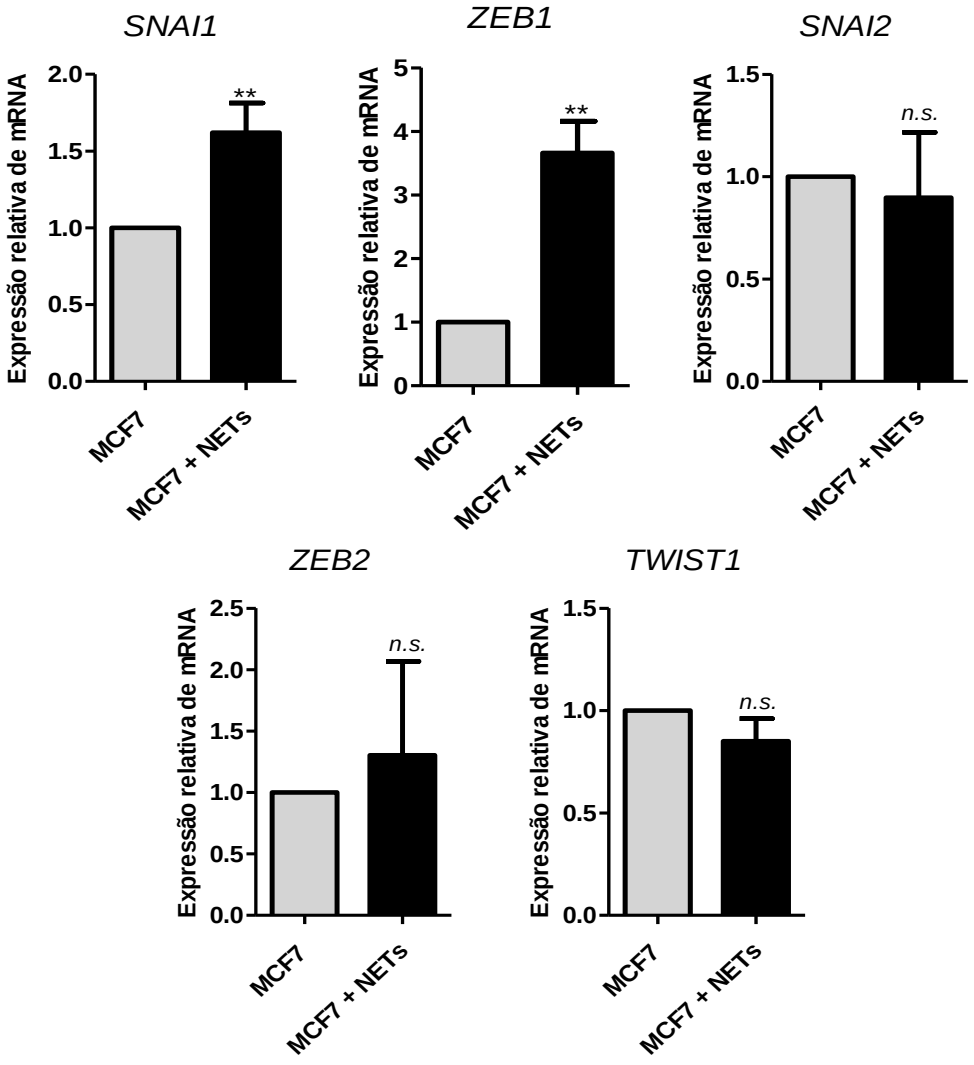

FIGURA 12. NETs induz a expressão de fatores transcricionais associados à TEM. Análise da expressão gênica foi analisada por RT-PCR quantitativo. GAPDH foi usado como o gene de referência. A expressão relativa do mRNA foi calculada usando o método ΔΔCT. As colunas representam médias ± desvio padrão de um mínimo de três experimentos independentes. O teste t não pareado foi aplicado para análise estatística. ** p <0,01 e n.s., sem significância.

4.4 O tratamento com NETs modifica os marcadores de TEM em linhagens tumorais de mama

Na transição epitélio-mesenquimal, as células perdem características epiteliais e adquirem fenótipo de células mesenquimais (LEGGETT et al., 2016). Ocorre uma modificação na expressão de proteínas de adesão célula-célula, como por exemplo, a E-caderina, que é um marcador clássico de TEM, tendo seus níveis reduzidos à medida em que o processo de TEM progride (NIETO et al., 2016; YANG et al., 2020). No contexto deste trabalho, ocorreu a redução de cerca de 35% da expressão gênica de E-caderina (*CDH1*) nas células tratadas com NETs por 16 horas (**Figura 13a**). Os níveis proteicos, avaliados através de Western Blotting, também apresentaram queda no decorrer do tempo de tratamento com NETs (**Figura 13b**), com uma perda de 30% do sinal de E-caderina após 3 horas, 40% após 6 horas, 50% após 12 horas, chegando a 60% de perda após 24 horas. O resultado foi corroborado com ensaio de imunocitoquímica, cuja intensidade do sinal de fluorescência para E-caderina foi notoriamente menor nas células tratadas com NETs por 16 horas (**Figura 13c**).

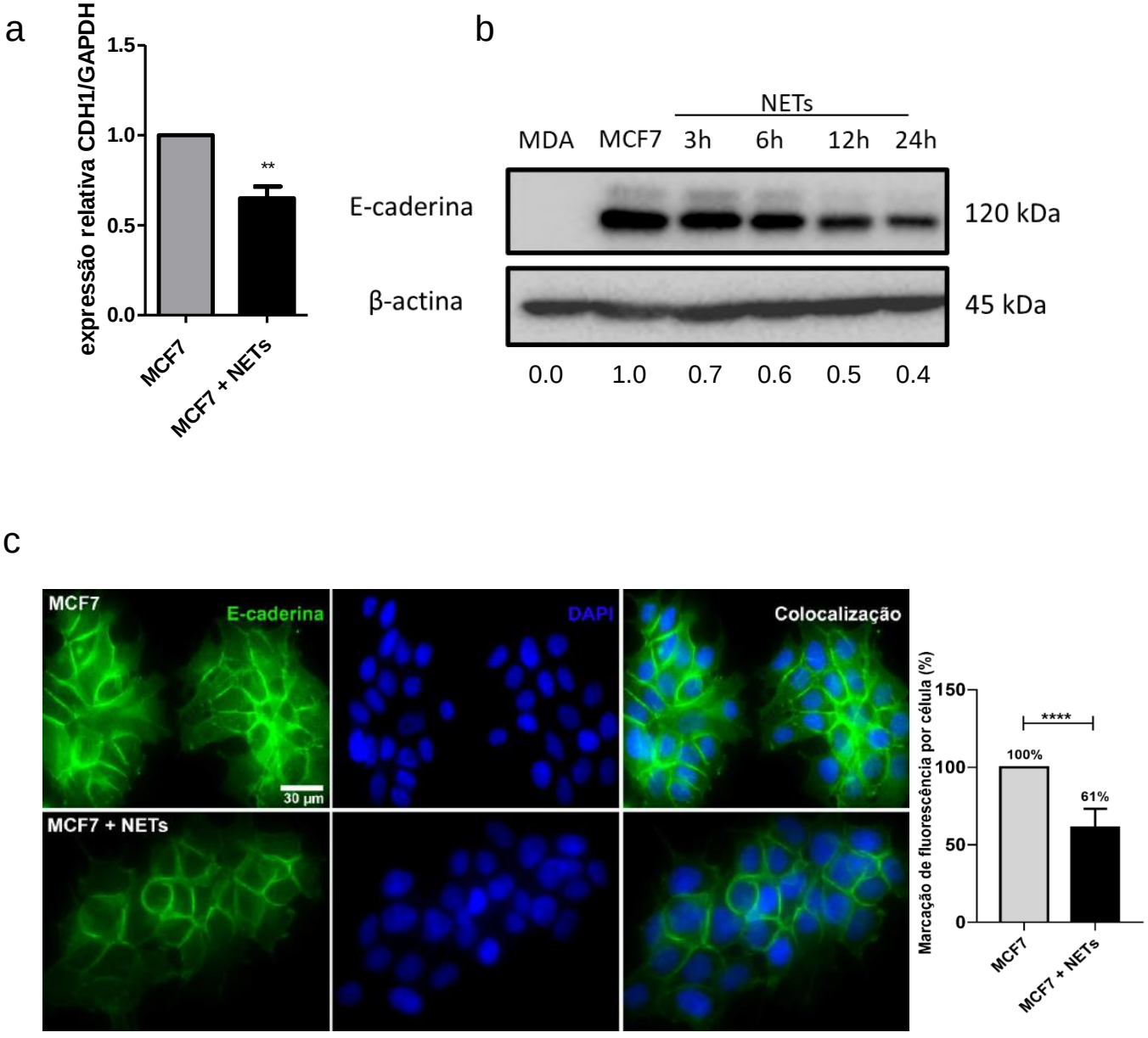

FIGURA 13. NETs modifica o padrão de expressão de E-caderina em células MCF7. A. Análise da expressão gênica de E-caderina (*CDH1)* realizada por por RT-PCR quantitativo. B. Imagem representativa do blotting dos níveis de proteína epitelial E-caderina em 1 × 10^6 células MCF7 tratadas com NETs (500 ng / mL) por uma cinética de 3 a 24 horas (n=2). β-actina foi usada como um controle de carregamento e células MDA-MB-231 (MDA) foi usado como modelo de célula mesenquimal. A densitometria analisada por ImageJ e representada abaixo do blot. (C) Análise de imunocitoquímica de E-caderina (verde, ampliação 630 ×, barras da escala 30 µm); em células MCF7 que foram cultivadas por 16 horas na ausência (acima) ou a presença (abaixo) de NETs (500 ng / mL). Os núcleos foram corados com 4', 6-diamidino-2-fenilindol (DAPI) (azul). O gráfico ao lado mostra a quantificação da imunocitoquímica. Test T foi aplicado para análise estatística. *** $p < 0.001$.

Devido ao efeito tão expressivo das NETs sobre a redução de E-caderina nas células MCF7, decidimos avaliar se em outro tipo celular o mesmo efeito seria encontrado. Utilizamos a linhagem celular HCC 1954, classificada como subtipo HER2+ (NEVE et al., 2006). Em geral, esta linhagem apresenta um fenótipo intermediário entre os subtipos luminais e basal, possuindo uma caraterística híbrida epitelial e mesenquimal. A partir da análise de expressão gênica por RT-PCR, observamos uma redução de cerca de 28% do transcrito que codifica para proteína E-caderina (*CDH1*) nas células tratadas com NETs por 24 horas (**Figura 14a**). Um padrão similar nos níveis proteicos de E-caderina foi observado nas células tratadas por NETs, pela análise de Western Blotting. O nível proteico de E-caderina foi cerca de 50% menor nas células tratadas com NETs em relação às células sem tratamento **(Figura 14b)**. Os resultados obtidos nas células MCF7 foram reproduzidos na linhagem celular HCC 1954, sugerindo o papel das NETs na indução da transição epitélio mesenquimal a partir da perda de características epiteliais.

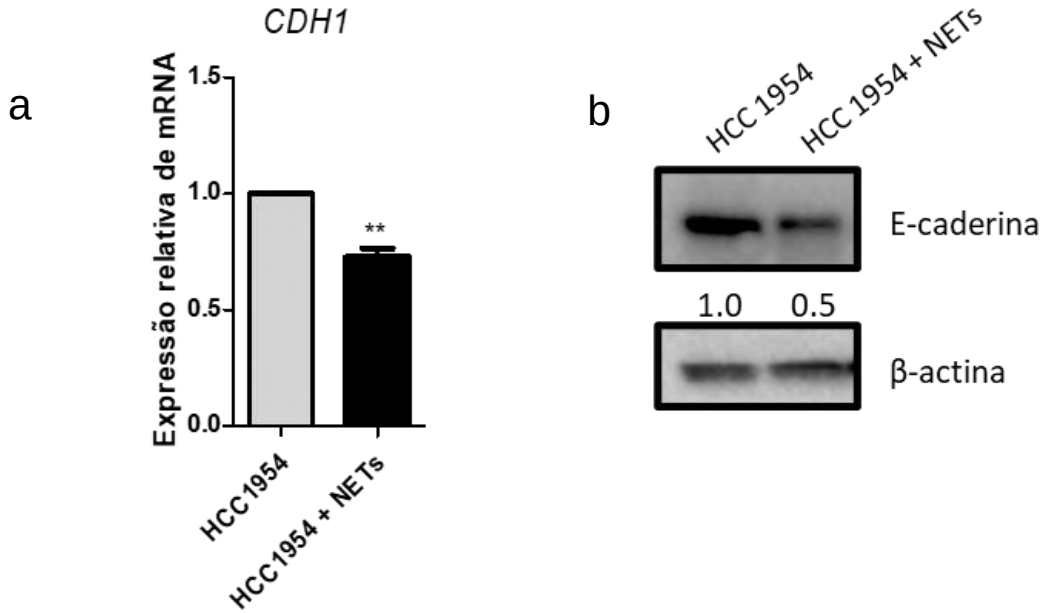

FIGURA 14. NETs modifica o padrão de expressão de E-caderina em células HCC1954. Análise da expressão de E-caderina em células HER2 + subtipo de câncer de mama. 5 x 10^5 células HCC 1954 foram tratadas com NETs (500 ng / mL) durante 24 horas. A. O gráfico à esquerda representa RT-PCR quantitativo do gene E-caderina (*CDH1*). As colunas representam as médias ± DP de três experimentos independentes. Análise estatística Teste t não pareado. ** $p < 0,01$. B. À direita, imagem representativa de Western Blotting de E-caderina (n=2). β-actina foi usada como controle de carregamento. A densitometria analisada por ImageJ abaixo. Os valores foram normalizados por β-actina.

Dentre os marcadores de fenótipo mesenquimal, foi analisado o nível de fibronectina. Uma glicoproteína solúvel no plasma que auxilia as células a aderirem à matriz extracelular, participando da migração e invasão de células tumorais **(Figura 15a)**. Através da análise por Western Blotting, observou-se um aumento dos níveis proteicos nas células tratadas com NETs por 3 horas (4,8 vezes), 6 horas (2,6 vezes), 12 horas (6,1 vezes) e 24 horas (10 vezes). Similarmente, observou-se através da imunocitoquímica um sinal significativamente maior (cerca de 50% de aumento) nas células tratadas por 16 horas com NETs em relação às células sem tratamento **(Figura 15)**.

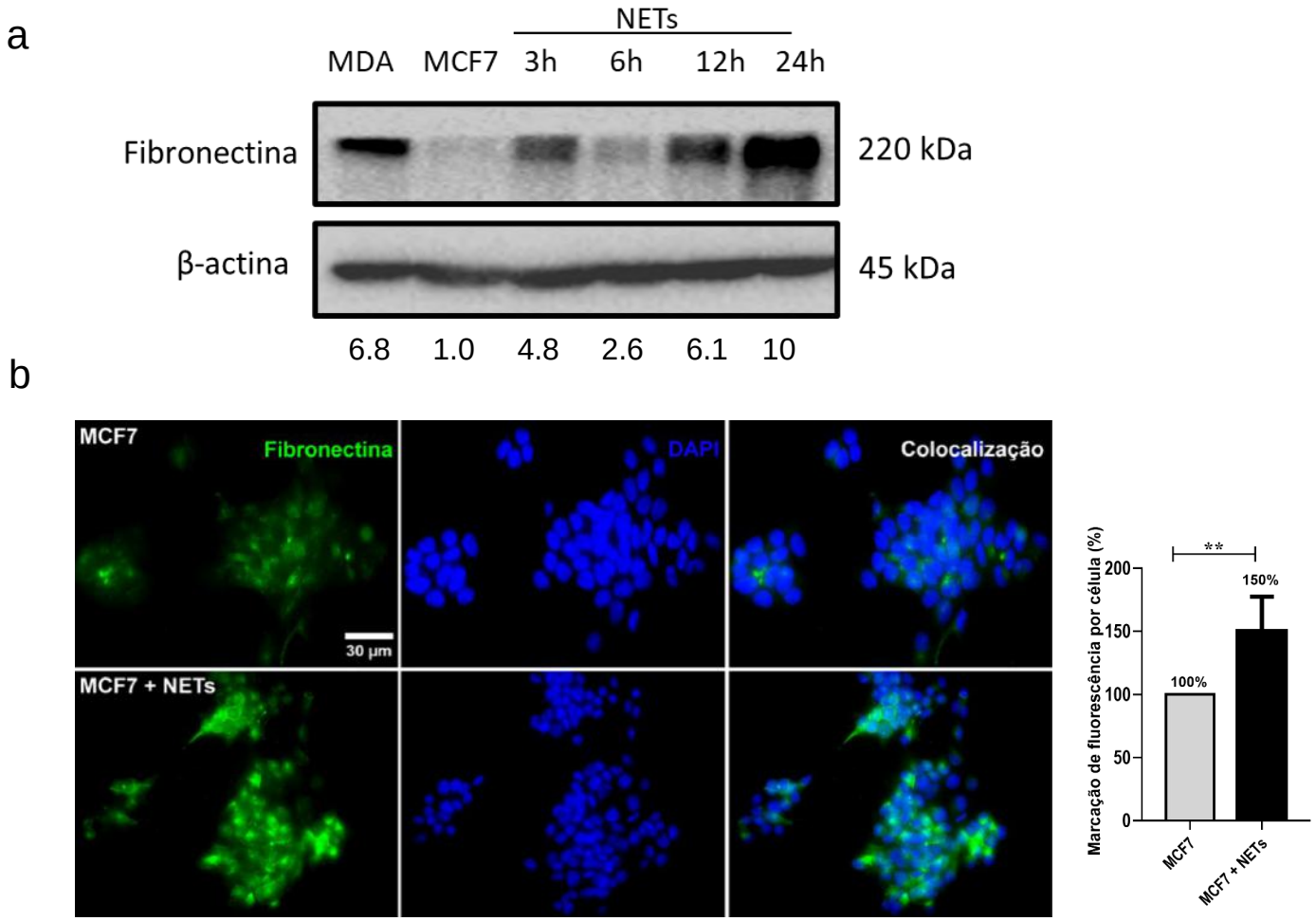

Em seguida, foi analisado também o marcador mesenquimal típico, N-caderina. Através da técnica de imunocitoquímica, constatou-se maior intensidade de sinal de N-caderina nas células cultivadas na presença de NETs por 16 horas (**Figura 16**). Com um

FIGURA 15. NETs modifica o padrão de expressão de fibronectina em células MCF7. A. Western blotting dos níveis de proteína mesenquimal fibronectina em células MCF7 tratadas com NETs entre 3 e 24 horas (n=2). β-actina foi usada como um controle de carregamento e MDA-MB-231 (MDA) foi usada como modelo de célula mesenquimal. Densitometria do blotting foi analisada por ImageJ B. Imunocitoquímica de Fibronectina (verde). Os núcleos foram corados com 4', 6-diamidino-2-fenilindol (DAPI) (azul). Ampliação 630 ×, barra da escala 30 µm. Quantificação da imunocitoquímica é representada à direita da imagem (n=2). Test *T* foi aplicado para análise estatística. ** $p < 0.01$.

aumento de cerca de 30% no sinal fluorescente em relação às células MCF7 sem tratamento com NETs.

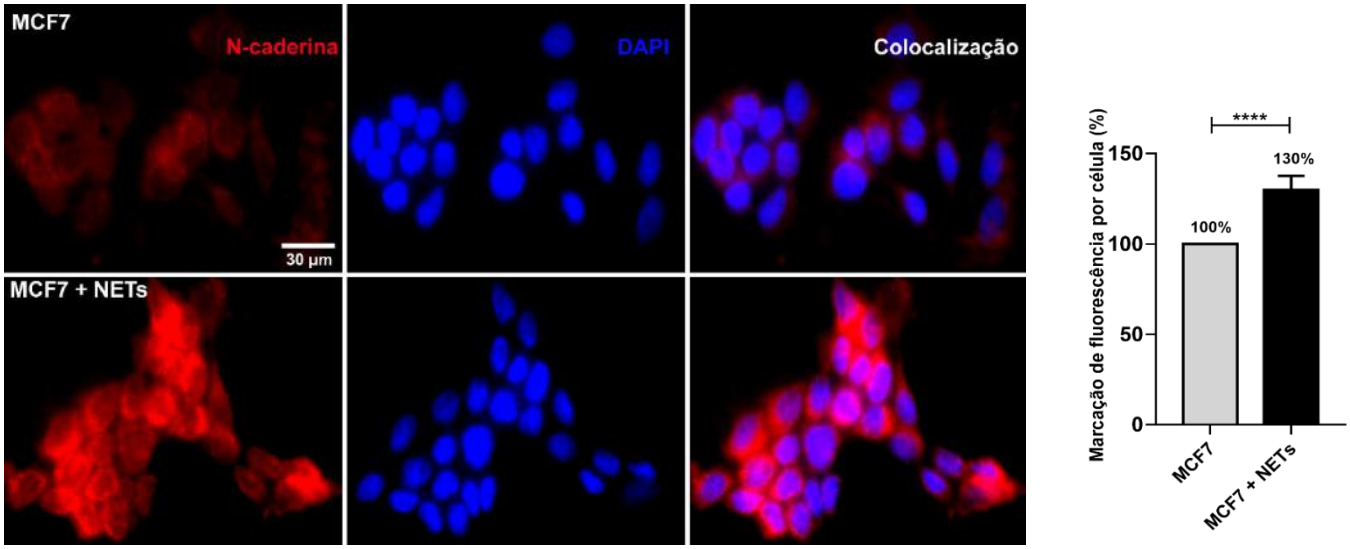

FIGURA 16. NETs modifica o padrão de expressão N-caderina em células MCF7. A. Imunocitoquímica de N-caderina (vermelho) de células MCF7 cultivadas por 16 horas na ausência (acima) ou a presença (abaixo) de NETs (500 ng/mL). Os núcleos foram corados com DAPI (azul) e as imagens mescladas são mostradas nos painéis à direita. Ampliação da imagem: 630 ×, barras da escala 30 µm. B. Ao lado, o gráfico mostra a quantificação da fluorescência (n=2). Test *T* foi aplicado para análise estatística. *** $p < 0.001$.

Por fim, analisamos os níveis de vimentina, outro marcador mesenquimal clássico adquirido no processo de TEM. Como visto na **Figura 17**, as células da linhagem MCF7 possuem níveis basais de vimentina extremamente baixos, ao contrário das células MDA-MB-231, de subtipo basal, que apresentam altos níveis de vimentina. Curiosamente, não foi observado nenhum efeito da incubação de NETs sobre a expressão de vimentina pelas células MCF7, através da técnica de Western Blotting.

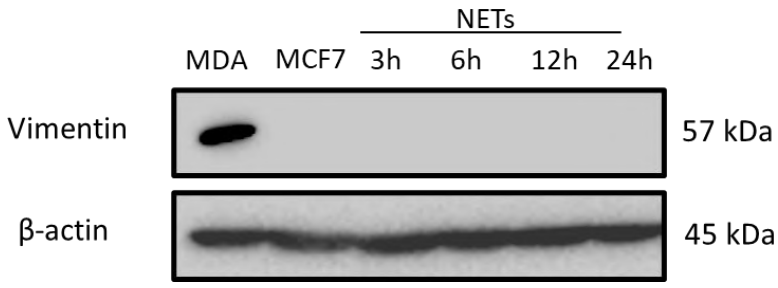

FIGURA 17. NETs não altera o padrão de expressão de vimentina em células MCF7. Níveis proteicos de vimentina, marcador de célula mesenquimal, analisados por Western Blotting. Células MCF7 (1×10^6) tratadas com NETs (500 ng / mL) por 3 a 24 h. β-actina foi usada como um controle de carregamento e MDA-MB-231 (MDA) foi usada como modelo de uma célula mesenquimal. Imagem representativa de dois experimentos independentes.

A partir das análises realizadas com a proteína E-caderina, buscou-se investigar a translocação e expressão de β-catenina. São proteínas que em homeostase interagem na membrana plasmática formando um complexo de adesão (ORSULIC et al., 1999). Quando a via de Wnt é ativada, esse complexo se rompe e a β-catenina funciona como um transdutor de sinal intracelular, translocando-se até o núcleo e promovendo a transcrição de vários genes pró-tumorais (SHANG et al., 2017; BASU et al., 2018). Utilizando a ferramenta de imunofluorescência, observou-se um maior sinal de marcação de β-catenina (146%) nas células MCF7 tratadas por 16 horas com NETs em relação às células não tratadas, como visto na **Figura 18**.

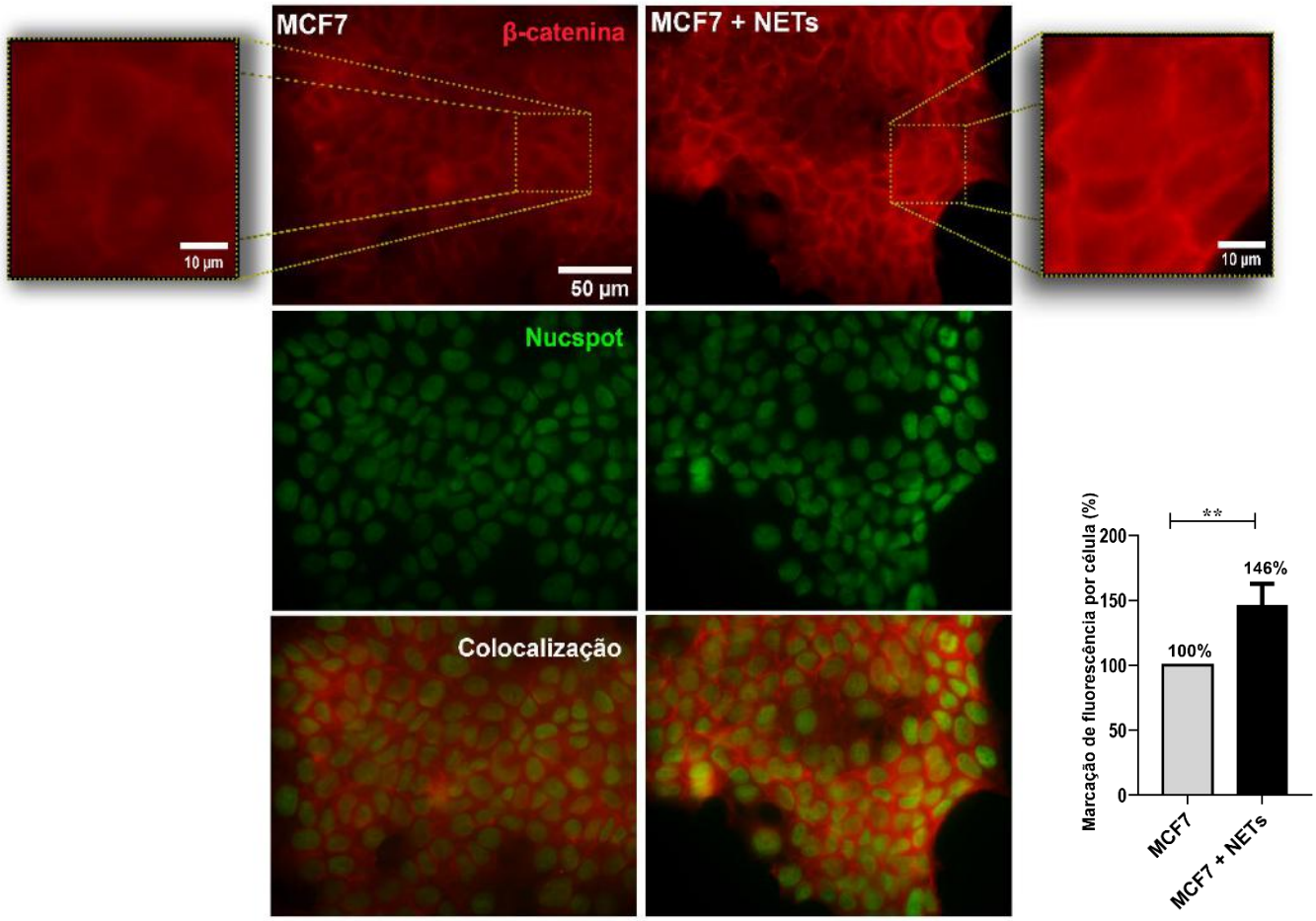

FIGURA 18. NETs modifica o padrão de expressão de β-catenina em células MCF7. Análise de β-catenina (vermelho) por imunocitoquímica em células MCF7 que foram Os núcleos foram corados com NucSpot (verde) e as imagens mescladas são mostradas logo abaixo. Imagens representativas. Ampliação 630 ×, barras de escala de 50 µm). Ao lado, o gráfico mostra a quantificação da fluorescência (n=2). Test T foi aplicado para análise estatística. ** $p < 0.005$

4.5 Expressão de marcadores de células-tronco tumorais é modulada pelas NETs

Recentes evidências vêm associando a transição epitélio-mesenquimal com a aquisição de propriedades de células-tronco tumorais no contexto do câncer (MANI et al., 2008; WEIDENFELD & BARKAN, 2018). Para avaliar se as células MCF7, de caráter epitelial, sofreram alterações na expressão de marcadores de células-tronco tumorais, analisou-se por RT-PCR e por citometria de fluxo a expressão de marcadores CD24/CD44. Estudos prévios já apontaram a típica diferença do perfil de expressão destes marcadores entre células do subtipo basal e luminal. Na figura 19, as células MCF7 (A1) possuem marcação positiva tanto para CD24 quanto para CD44. MDA-MB-231 (B2) apresenta marcação positiva para CD44 e negativa para CD24. Nota-se que a marcação de CD44 em células MCF7 é menor em relação às células MDA-MB-231. Em células que adquirem caráter mesenquimal, espera-se a perda da marcação para CD24 e aumento da expressão de CD44.

Durante este estudo, observou-se uma queda na expressão gênica de *CD24,* cerca de 35%, ao tratar as células MCF7 com NETs por 16 horas (Figura 20a). Os níveis proteicos do marcador também acompanharam a tendência de queda (aproximadamente 30%), embora não tenha sido estatisticamente relevante (Figura 20 b,c). Em contrapartida, constatou-se o aumento significativo do transcrito *CD44* (7 vezes maior no grupo tratado com NETs), bem como sua expressão de proteína na membrana das células após 16 horas de tratamento (aproximadamente 7 vezes maior), conforme Figura 20d-f.

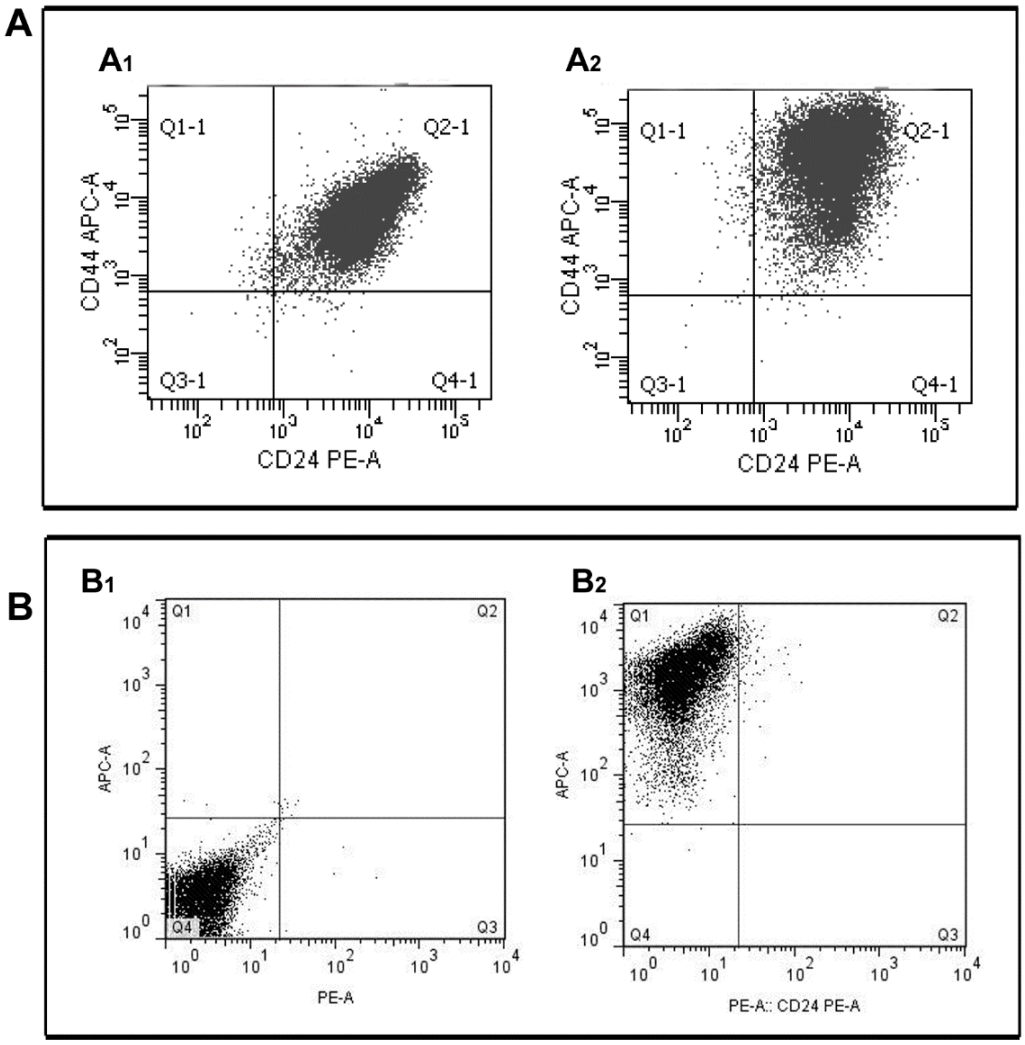

FIGURA 19. Análise comparativa dos marcadores de células-tronco tumoral entre os subtipos tipo basal e luminal de células de câncer de mama. Os painéis mostram gráficos obtidos de experimentos independentes da expressão de CD24 e CD44 em linhagens celulares MCF7 (Painel A) e MDA-MB-231 (Painel B). O painel A1, apresenta a expressão de CD44 e CD24 em células MCF7 sem tratamento e A2, células MCF7 cultivadas com NETs por 16 horas, mostrando um aumento de sinal de CD44. No painel B1, as células MDA-MB-231 não contém nenhuma marcação, enquanto no gráfico B2, observa-se o perfil de expressão basal de CD24/CD44 nas células MDA-MB-231. As células foram incubadas com anti-CD24 humano de camundongo conjugado com PE e anti-CD44 de rato conjugado com APC.

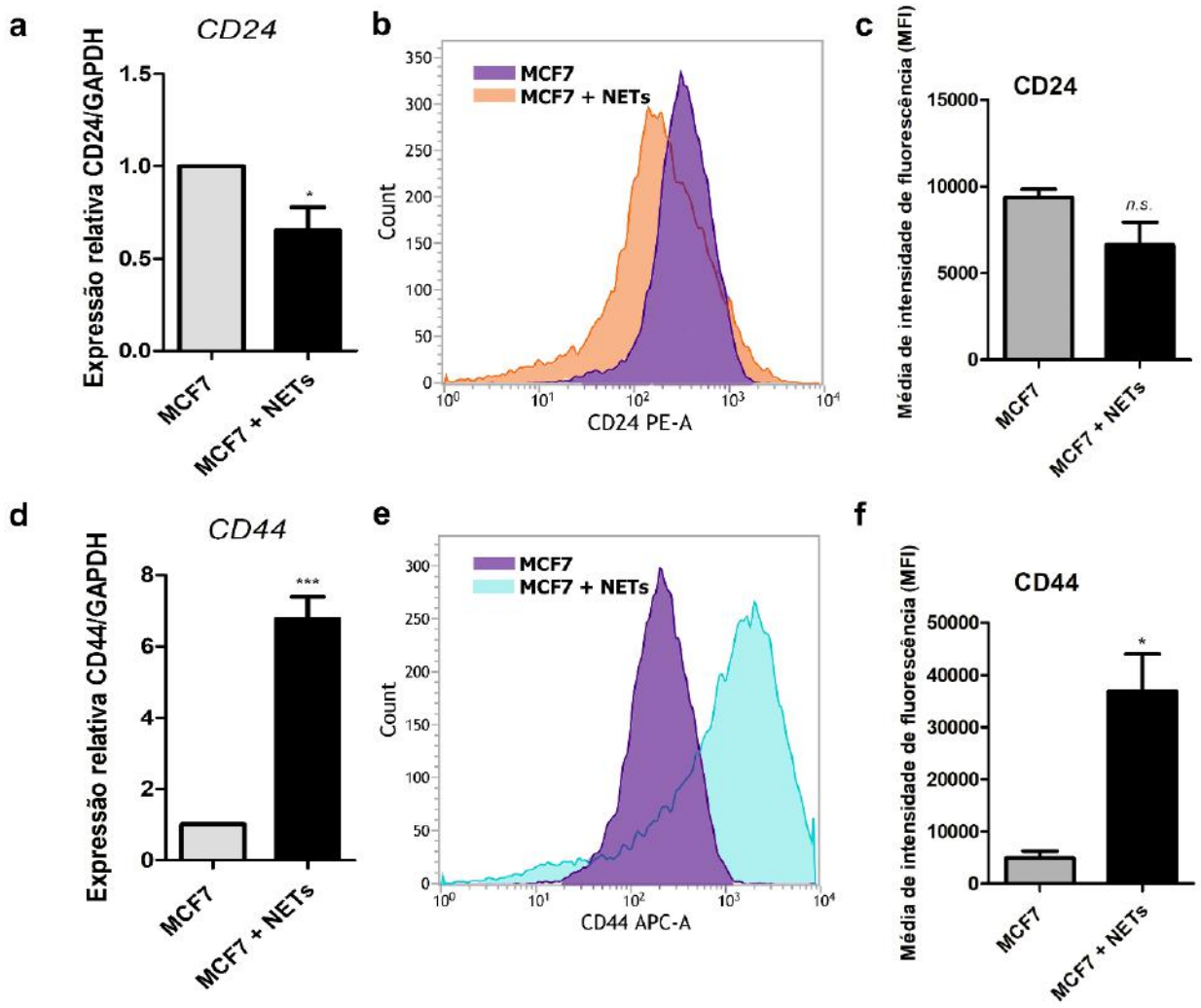

FIGURA 20. Marcadores de células-tronco tumorais são modulados pelas NETs. Expressão gênica de CD24 (A) e CD44 (D) foi analisado por RT-PCR quantitativo em células MCF7 cultivadas por 16 horas com NETs (500 ng/mL). Histogramas representativos de análise de citometria de fluxo de CD24 (B) e CD44 (E). Representação gráfica da média relativa das intensidades de fluorescência (MFI) de anticorpo CD24 marcado com ficoeritrina (PE) (C) e anticorpo CD44 marcado com aloficocianina (APC) (F). Os dados mostrados são de dois experimentos independentes. Teste *t* não pareado foi aplicado para análise estatística. A significância foi assumida para * p <0,05, *** p <0,001*; n.s.,* sem significância.

4.6 Análise de expressão gênica de fatores pró-tumorais moduladas pelas NETs

Para avaliar o efeito das NETs sobre a resposta inflamatória das células de câncer de mama, testou-se através de RT-PCR, mRNA de genes que codificam citocinas pró-inflamatórias. As NETs induziram um significativo aumento de aproximadamente 15 vezes nos níveis de mRNA para IL-1β (*IL1B*), cerca de 10 vezes para a expressão de *IL6* e 18 vezes para a expressão de IL8 (*CXCL8*) em relação às células não tratadas. Observou-se também o aumento da expressão gênica do receptor de IL8, *CXCR1* (cerca de 2 vezes), Figura 21.

Num contexto da progressão tumoral, buscou-se avaliar se as NETs também atuavam sobre as metaloproteinases, enzimas envolvidas no processo de remodelamento da matriz extracelular, culminando na migração e invasão das células tumorais aos tecidos adjacentes. Por RT-PCR, constatou-se um expressivo aumento gênico de MMP2 e MMP9 nas células MCF7 tratadas por 16 horas com NETs, ambos em torno de 120 vezes maior em comparação com as células não tratadas **(Figura 21)**.

Para confirmar o efeito das NETs, avaliou-se alguns genes pro-inflamatórios e pró-tumorais em outras linhagens de câncer de mama. Em MDA-MB-231, observou-se um aumento de cerca de 20 vezes na expressão de IL-1β (*IL1B)* nas células tratadas com NETs. Além disso, as NETs induziram um aumento em torno de 60 vezes do mRNA de *CXCL8*. Nas células HCC1954, linhagem do subtipo HER2+, o nível de expressão gênica de MMP9 foi cerca de 10 vezes maior no grupo tratado com NETs **(Figura 22)**.

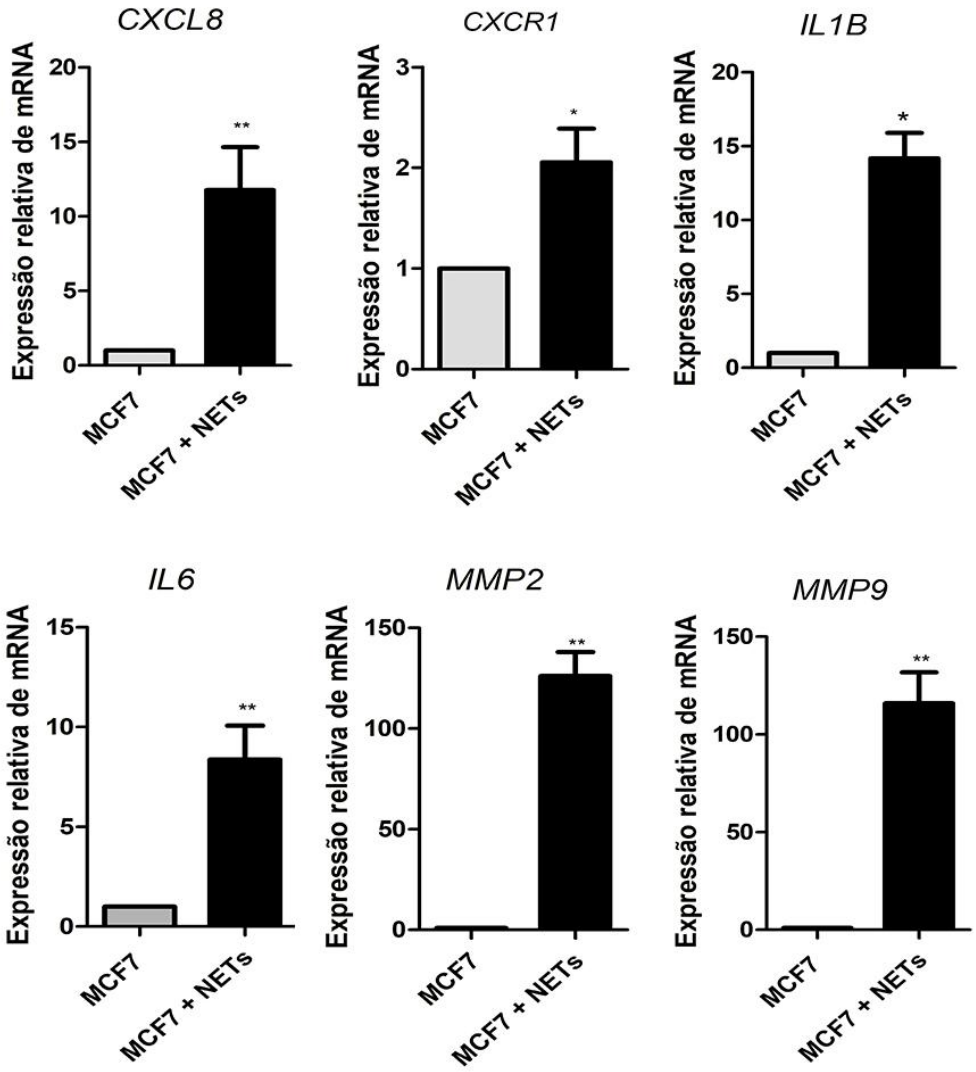

FIGURA 21. NETs promove superexpressão de genes pró-inflamatórios e pró-tumorais em células MCF7. Expressão do gene foi avaliada por RT-PCR quantitativo. Células MCF7 (5 × 10^5) mantidas em starving, foram cultivadas por 16 horas na ausência ou na presença de NETs (500 ng/mL). GAPDH foi usado como o gene de referência. E a expressão foi normalizada pelo método ΔΔCt. As colunas representam médias ± desvio padrão de três experimentos independentes. A análise estatística foi realizada usando o teste *t* não pareado. * p <0,05 e ** p <0,01.

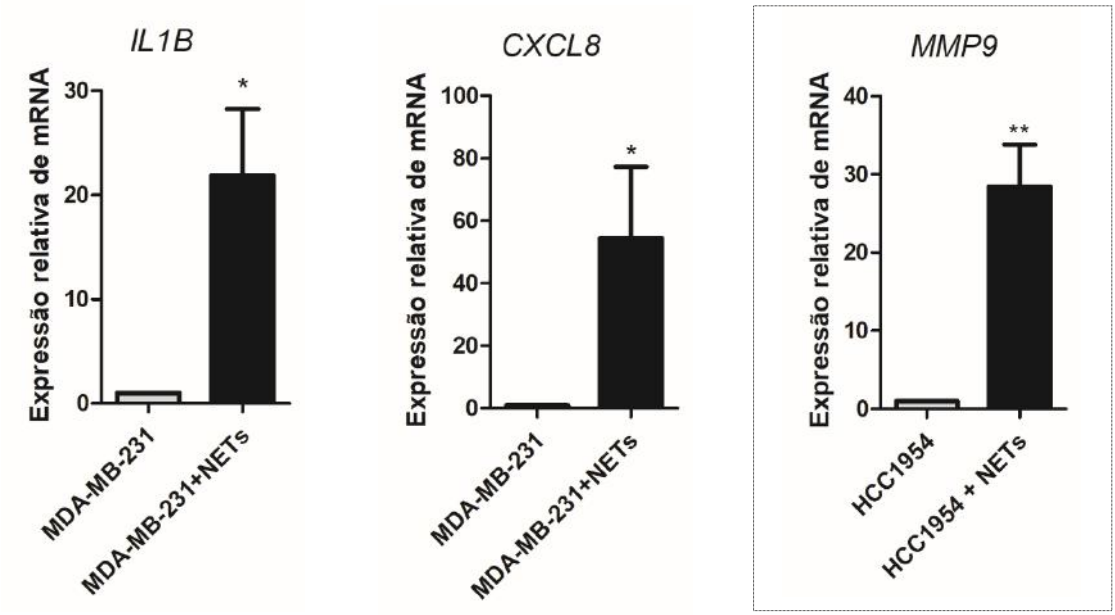

FIGURA 22. NETs promove superexpressão de genes pró-inflamatórios e pró-tumorais em outras linhagens celulares. Expressão do gene foi avaliada por RT-PCR quantitativo. 5 x 10^5 Células das linhagens MDA-MB-231 e HCC1954 foram cultivadas por 3 e 16 horas, respectivamente, na ausência (barra cinza) ou na presença (barra preta) de NETs (500 ng/mL). GAPDH foi usado como o gene de referência e a expressão foi normalizada pelo método ΔΔCt. As colunas representam médias ± desvio padrão de três experimentos independentes. Teste *t* não pareado foi aplicado para análise estatística. * p <0,05 e ** p

4.7 A integridade das NETs não altera seus efeitos pró-tumorais

Considerando a composição das redes extracelulares de neutrófilos, a cromatina compõe parte significativa desse material e pode ser reconhecida por receptores do tipo Toll expostos na membrana celular, ativando cascatas de vias inflamatórias (TAKESHITA et al., 2001). A partir daí, decidiu-se investigar a importância da integridade do DNA dessas redes para ativação da resposta pró-tumoral das células MCF7. Primeiramente, avaliou-se a eficiência da DNase I sobre as NETs, através da migração em gel de agarose. A partir de 5 minutos de incubação, já se observava a perda da banda de DNA íntegro e o aparecimento das bandas de DNA degradado ao final do gel. Portanto, concluímos que a quantidade de 5U de DNase I era suficiente para degradar o DNA das NETs em todos os tempos testados, com uma eficiência crescente com o passar do tempo (**Figura 23a**). Então, utilizou-se NETs incubadas com 5U de DNase I por 30 minutos, para

avaliar o efeito das NETs com DNA degradado sobre o comportamento migratório das células MCF7 **(Figura 23b)**.

Ensaios de migração realizados na ausência de quimioatraente na porção inferior da câmara de Boyden, demonstraram que as NETs degradadas com DNase I apresentaram um efeito similar ao visto para as NETs sobre o comportamento migratório das células. Por outro lado, quando se utilizou 2% ou 10% de soro fetal como quimioatraente, a digestão com DNAse I perceptivelmente reduziu o efeito pro-migratório promovido pelas NETs nas células MCF7. Em geral, os resultados sugerem que o efeito das NETs sobre a migração das células tumorais depende parcialmente da integridade de suas fibras de cromatina.

Em seguida, investigamos o papel da integridade do DNA na indução do perfil de expressão de moléculas pró-tumorais (**Figura 23 c,d)**. Por meio de RT-PCR, quantitativo, testou-se a expressão gênica de *CXCL8* e *MMP9*, já demonstrados como positivamente modulados pelas NETs nas células MCF7. Assim como visto no tratamento com NETs íntegras, as NETs degradas por DNase I também induziram a expressão de *CXCL8* (aproximadamente 12 vezes em relação as células sem tratamento) e de *MMP9* (em média 96 vezes maior do que visto nas células sem tratamento). Diante disso, conclui-se que a integridade do DNA não tem influência significativa no efeito pró-inflamatório promovido pelas NETs nas células de câncer de mama da linhagem MCF7.

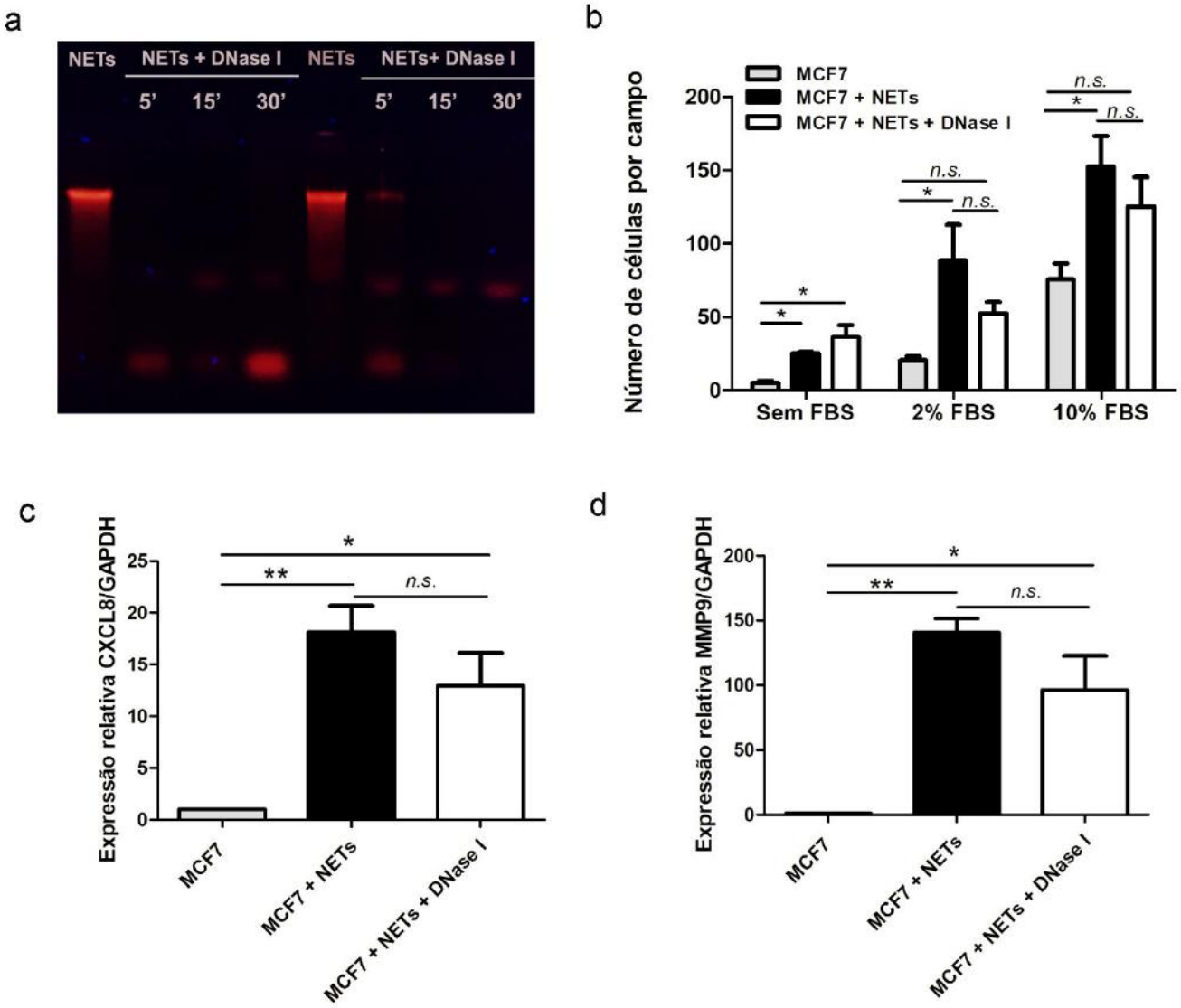

FIGURA 23. Efeitos das NETs degradas por DNasesobre as células tumorais MCF7. (A) Imagem do gel de agarose mostrando NETs de distintos doadores previamente tratados com 5 U DNase I a 37º C por diferentes momentos. (B) Ensaio de migração realizado na câmara de Boyden com NETs. Dnase I foi incubada previamente com NETs por 30 minutos. Em seguida, células MCF7 mantidas em meio sem soro, foram incubadas com NETs ou NETs com DNA degradado por 16 h para o ensaio de migração. (C-D) RT-PCR quantitativo de células MCF7 mantidas em meio sem soro e tratadas com NETs ou NETs degradadas com DNase I por 16h ONE-ANOVA e pós-teste de Tukey foram aplicados para análise estatística. A significância foi assumida para * p <0,05, ** p <0,01; *n.s.*, sem significância.

4.8 Análise *in silico* de marcadores gênicos de neutrófilos, TEM e genes pró-tumorais

Para investigar a relevância clínica da relação das NETs e a progressão tumoral promovida por TEM, utilizou-se os transcriptomas de pacientes com câncer de mama depositados no The Cancer Genome Atlas – TCGA (www.cancer.gov). Primeiramente, buscou-se analisar os níveis de expressão dos genes de assinatura neutrofílica em diferentes subtipos de câncer de mama. Os genes relacionados a neutrófilos foram pré-identificados a partir de um estudo com pacientes portadores de lúpus eritematoso sistêmico com nefrite ativa (WITHER et al., 2018). São eles: *MPO*, *DEFA1B*, *MMP8*, *CEACAM8*, *LTF* e *DEFA4*. Conforme a figura 24, a análise pelos dados de RNAseq mostrou que os genes *MPO*, *DEFA1B*, *MMP8* e *CEACAM8* foram significativamente mais expressos no subtipo basal em relação aos subtipos luminais A e B. Os genes *LTF* e *DEFA4* são mais expressos significativamente no subtipo basal do que no subtipo luminal B, mas sua expressão não é estatisticamente diferente do luminal A. Comparado ao subtipo HER2, apenas os genes *MPO* e *DEFA1B* são mais expressos no subtipo basal.

Sob um olhar clínico, o subtipo basal é mais agressivo e metastático em relação aos subtipos luminais. Os resultados apontam uma maior expressão dos genes de assinatura neutrofílica no subtipo basal em relação aos subtipos luminais, sugerindo uma infiltração maior de neutrófilos nos subtipos mais agressivos.

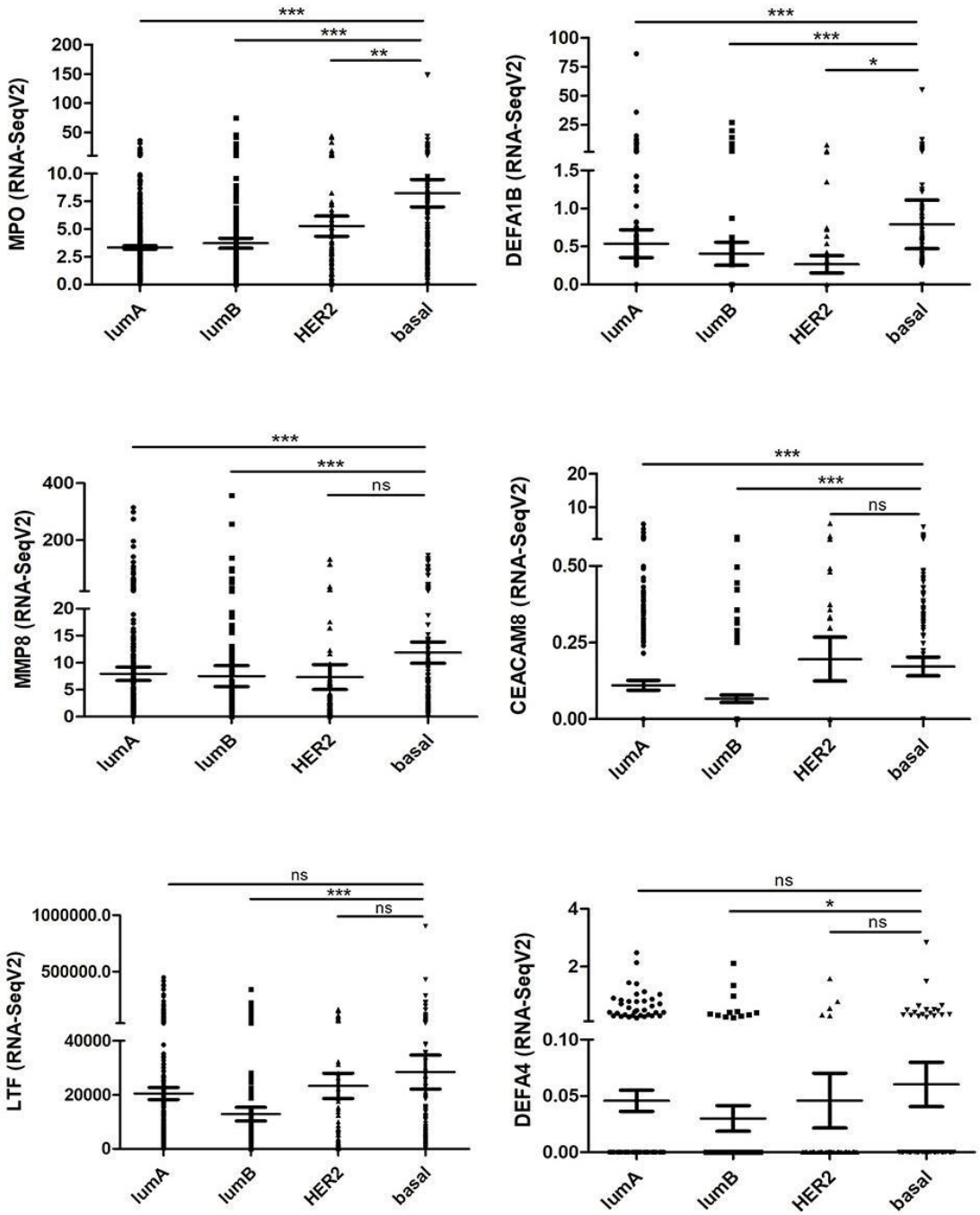

FIGURA 24. Análise de genes de assinatura relacionados a neutrófilos nos diferentes subtipos de câncer de mama. Valores de seq de RNA (fragmentos por quilobase de milhões, FPKM) de 1100 amostras de câncer de mama, depositados no banco de dados TCGA, foram estratificados em Luminal A (lumA), Luminal B (lumB), HER2 + (HER2) e subtipos basais. Cada gráfico representa um gene relacionado à neutrófilo. O teste de Mann-Whitney foi usado para testar a significância estatística. **p* <0,05, ***p* <0,01, ****p* <0,001 e *n.s.*: sem significância

Para tentar estabelecer uma relação entre a presença de neutrófilos no microambiente tumoral e a progressão tumoral, utilizamos a plataforma cBioPortal, baseada nas amostras de RNAseq de pacientes de câncer de mama, para analisar a correlação entre expressão de cada gene de neutrófilos e genes pró-tumorais avaliada anteriormente nos ensaios *in vitro.* As análises mostraram uma correlação positiva entre os genes pró-tumorais *CXCL8, CXCR1, IL1B, IL6 e MMP9 com pelo menos 4* genes relacionados a neutrófilos. Apenas MMP2 apresentou correlação com 3 genes de neutrófilos (tabela 4).

Tabela 4: Análise de correlação entre genes de assinatura neutrofílica e genes pró-tumorais em amostras de pacientes com câncer de mama depositadas no TCGA

Genes	*CEACAM8*	*DEFA1B*	*DEFA4*	*LTF*	*MMP8*	*MPO*
MMP2 *(MMP2)*	r = -0.00765 *P* = 0.800	r = 0.0114 *P* = 0.705	r = 0.0351 *P* = 0.245	r = 0.173 *P* < 0.0001	r = 0.286 *P* < 0.0001	r = 0.154 *P* < 0.0001
MMP9 *(MMP9)*	r = 0.012 *P* = 0.692	r = 0.114 *P* = 0.0002	r = 0.120 *P* < 0.0001	r = 0.0315 *P* = 0.297	r = 0.408 *P* < 0.0001	r = 0.21 *P* < 0.0001
Interleucina 6 *(IL6)*	r = 0.0983 *P* = 0.0011	r = 0.197 *P* < 0.0001	r = 0.124 *P* < 0.0001	r = 0.232 *P* < 0.0001	r = 0.208 *P* < 0.0001	r = 0.314 *P* < 0.0001
Interleucina 1β (*IL1B*)	r = 0.0767 *P* = 0.0109	r = 0.116 *P* = 0.0001	r = 0.0655 *P* = 0.0297	r = 0.255 *P* < 0.0001	r = 0.225 *P* < 0.0001	r = 0.183 *P* < 0.0001
CXCL8 (*CXCL8*)	r = 0.0445 *P* = 0.14	r = 0.141 *P* < 0.0001	r = -0.0277 *P* = 0.359	r = 0.0963 *P* = 0.0014	r = 0.39 *P* < 0.0001	r = 0.156 *P* < 0.0001
CXCR1 *(CXCR1)*	r = 0.0242 *P* = 0.422	r = 0.117 *P* < 0.0001	r = 0.0879 *P* = 0.0035	r = 0.131 *P* < 0.0001	r = 0.0677 *P* = 0.0248	r = - 0.008 *P* = 0.788

Sem correlação Correlação positiva

Subsequentemente, analisou-se os genes relacionados à transição epitélio-mesenquimal e sua correlação com genes de neutrófilos (tabela 5). Apenas o gene *SNAI1* (Snail) obteve correlação positiva significante em 5 dos 6 genes de neutrófilos analisados. A β-catenina (*CTNNB1*) apresentou correlação positiva com 3 genes relacionados à neutrófilos. Conforme o esperado, observou-se uma significativa correlação negativa entre o gene que codifica E-caderina e 4 genes relacionados a neutrófilos.

Tabela 5: Análise de correlação entre genes relacionados a neutrófilos e genes relacionados com TEM em amostras de pacientes com câncer de mama depositadas no TCGA através do cBioPortal.

Genes	*CEACAM8*	*DEFA1B*	*DEFA4*	*LTF*	*MMP8*	*MPO*
CD24 *(CD24)*	r = 0.030 *P* = 0.317	r = 0.0319 *P* = 0.291	r = -0.00795 *P* = 0.792	r = -0.0114 *P* = 0.706	r = 0.0796 *P* = 0.0083	r = 0.0605 *P* = 0.0447
CD44 *(CD44)*	r = -0.0254 *P* = 0.399	r = 0.0458 *P* = 0.129	r = 0.0443 *P* = 0.142	r = 0.014 *P* = 0.642	r = 0.0157 *P* = 0.602	r = 0.0578 *P* = 0.0555
Snail (*SNAI1*)	r = 0.0959 *P* = 0.0014	r = 0.162 *P* < 0.0001	r = 0.0522 *P* = 0.0834	r = 0.179 *P* < 0.0001	r = 0.281 *P* < 0.0001	r = 0.211 *P* < 0.0001
ZEB1 *(ZEB1)*	r = -0.0491 *P* = 0.103	r = - 0.0773 *P* = 0.0103	r = 0.0183 *P* = 0.544	r = 0.0921 *P* = 0,0022	r = 0.132 *P* < 0.0001	r = 0.0499 *P* = 0.0982
Fibronectina (*FN1*)	r = -0.0507 *P* = 0.0927	r = - 0.0792 *P* = 0.0086	r = - 0.0464 *P* = 0.124	r = - 0.0149 *P* = 0.621	r = 0.384 *P* < 0.0001	r = - 0.0309 *P* = 0.307
N-Caderina (*CDH2*)	r = 0.0134 *P* = 0.657	r = - 0.0217 *P* = 0.472	r = -0.045 *P* = 0.136	r = - 0.102 *P* = 0.0007	r = 0.275 *P* < 0.0001	r = 0.0302 *P* = 0.316
β-Catenina (*CTNNB1*)	r = -0.0022 *P* =0.941	r = - 0.0476 *P* = 0.115	r = - 0.0004 *P* = 0.99	r = 0.196 *P* < 0.0001	r = 0.176 *P* < 0.0001	r = 0.0633 *P* = 0.0359
E-Caderina (*CDH1*)	r = - 0.041 *P* = 0.174	r = -0.0728 *P* = 0.0157	r = - 0.0796 *P* = 0.0083	r = - 0.194 *P* < 0.0001	r = -0.0473 *P* = 0.117	r = - 0.144 *P* < 0.0001

Sem correlação Correlação positiva Correlação negativa

Como um facilitador dessa análise de correlação, utilizou-se uma outra plataforma de análise, Gepia 2 (http://gepia2.cancer-pku.cn/), a fim de reunir todos os genes relacionados a neutrófilos em uma única análise simultânea e correlacionar com os genes-alvo (Tabela 6). Para isso, determinou-se o total de 8 genes como genes de assinatura neutrofílica. São eles: *DEFA4, DEFA1B, MMP8, CEACAM8, LTF, MPO, CEACAM6 e ARG1*. Esses dois últimos genes foram adicionados à esta nova análise. Através da correlação de Spearman, observamos que todos os genes pró-tumorais apresentam correlação positiva com os genes de neutrófilos. Os genes *CD24* e *CD44* não apresentaram correlação com a assinatura gênica de neutrófilos, corroborando com resultado da análise anterior. Dos demais genes relacionados à TEM analisados pela plataforma cBioPortal, os genes *SNAI1* (Snail). *ZEB1*, *FN1* (Fibronectina) e *CTNNB1* (β-catenina) apresentaram correlação positiva com os genes de assinatura neutrofílica.

Tabela 6: Análise de correlação entre genes de assinatura neutrofílica em amostras de pacientes com câncer de mama depositadas no TCGA através do GEPIA 2.

Genes	Correlação *R*
MMP2 (*MMP2*)	0.2
MMP9 (*MMP9*)	0.03
Interleucina 6 *(IL6*)	0.13
Interlucina 1β (*IL1B*)	0.2
CXCL8 (*CXCL8*)	0.11
CXCR1 (*CXCR1*)	0.25
CD24 (*CD24*)	−0.024
CD44 (*CD44*)	0.015
Snail (*SNAI1*)	0.086
Zeb1 (*ZEB1*)	0.2
Fibronectina (*FN1*)	0.11
N-caderina (*CDH2*)	0.019
β-catenina (*CTNNB1*)	0.22
E-caderina (CDH1)	0.019

Sem correlação Correlação positiva

Com base nessas análises de bioinformática, observou-se uma importante correlação entre a expressão de genes de assinatura neutrofílica e genes envolvidos na progressão tumoral além de genes relacionados com a transição epitélio-mesenquimal. De forma geral, as análises *in silico* concordam com os achados observados nos ensaios *in vitro.*

Cada vez mais, os neutrófilos têm sido apontados como atores coadjuvantes na progressão tumoral. A possível relação entre NETs e a ativação do programa de TEM, levando ao aumento da agressividade tumoral e um pior prognóstico ao paciente, aponta para uma maior relevância deste estudo e um avanço na compreensão sobre os mecanismos de ação das NETs sobre as células tumorais.

5. DISCUSSÃO

A Inflamação vem sendo reconhecida como uma das características essenciais na progressão tumoral promovida pela ação do microambiente tumoral, independentemente de qualquer foco infeccioso. A vasta variedade de células imunes infiltradas no microambiente tumoral tem sido aceita como componentes do tumor. Diversos estudos apontam o efeito da inflamação crônica no desenvolvimento do tumor, desde a sua formação, proliferação e aumento da sobrevida celular, migração, aumento da angiogênese e metástase. Isso se dá pela presença de mediadores no microambiente tumoral como por exemplo, fatores de crescimento, citocinas pró-inflamatórias e outros fatores pro-tumorais (MANTOVANI et al., 2008; KORNILUK et al., 2017).

Dentre as células imunes, destaca-se os neutrófilos, que junto com os macrófagos e células NK, podem totalizar 80% das células inflamatórias no ambiente tumoral. Os neutrófilos presentes no tumor podem transitar entre diferentes fenótipos, conhecidos como N1 e N2. De acordo com o estímulo recebido, os neutrófilos podem polarizar para um fenótipo anti-inflamatório e com o potencial de inibir a progressão tumoral e a metástase (LAMBERT & PATTABIRAMAN, 2017). Neutrófilos com ação antitumoral são associados ao perfil N1. Entretanto, nos trabalhos científicos recentes, os neutrófilos têm sido apontados como coadjuvantes no ganho de agressividade tumoral. Os neutrófilos ao serem ativados, podem sofrer um processo denominado NETose, cujo processo envolve a secreção de redes de cromatina decoradas com diferentes proteínas. Essas estruturas são chamadas de redes extracelulares de neutrófilos, mais conhecidas como NETs. Ainda há muita investigação ocorrendo sobre a categorização do mecanismo de NETose de acordo com o fenótipo dos neutrófilos no microambiente tumoral. Estudos mostrando a ação das NETs na progressão do tumor, teoriza o enquadramento dos neutrófilos que sofrem netose no perfil N2 (ERPENBECK & SCHÖN, 2017), embora estudos posteriores já tenham mostrado que ambos os neutrófilos N1/N2 podem produzir NETs (HONDA & KUBES, 2018).

Assim como neutrófilos com atividade pró-tumoral de perfil N2, as NETs já foram associadas a diversas etapas da progressão tumoral (POWELL & HUTTENLOCHER, 2016). Fatores pro-tumorais secretados pelas NETs, incluindo

catepsina G, elastase neutrofílica e metaloproteinase 9, podem justificar o potencial tumorigênico das NETs, como já sugerido em alguns estudos. Sua participação vai desde o seu papel no sequestro de células tumorais circulantes, crescimento do tumor primário, interação direta com as células tumorais até várias etapas da metástase. No entanto, são necessários estudos adicionais para caracterizar melhor o perfil dos neutrófilos geradores de NETs e suas principais funções no microambiente tumoral.

No processo de metástase, a transição epitélio-mesenquimal (TEM) é um dos principais mecanismos requeridos para a transformação de perfil de agressividade tumoral, contribuindo para aquisição de um comportamento celular migratório e invasivo. Esse processo é dinâmico e transiente, que envolve a perda de clássicas características epiteliais, como por exemplo a proteína de membrana E-caderina, enquanto adquire diversos marcadores mesenquimais: N-caderina, Fibronectina e Vimentina. Essas características são moduladas pela ativação de vários fatores transcricionais: as famílias ZEB1/2, SNAIL1/2 e TWIST1/2. Além disso, o processo de desdiferenciação, envolve uma mudança drástica na morfologia da célula, uma das primeiras alterações notificadas neste trabalho observadas em células essencialmente epiteliais tratadas com NETs. Além da perda de aderência das células, soltando muito facilmente dos frascos de cultura. Isso pode ser justificado pela perda de polaridade apical-basal na fase inicial da TEM e remodelamento citoplasmático de certas proteínas de junção (YANG et al., 2020). Outra característica chave do processo é a capacidade das células romperem a matriz extracelular e migrarem para um tecido distante da sua origem. Neste trabalho, a habilidade migratória foi induzida nas células MCF7 tratadas com NETs, observando-se maior migração – apesar de não ser uma característica exclusiva de células alteradas pelo processo de TEM. No entanto, esse processo não é uniforme e podem existir diferentes etapas intermediárias, onde as células encontram-se num estágio híbrido, exibindo a co-expressão de marcadores epiteliais e mesenquimais (NIETO et al., 2016; BRABLETZ et al., 2018). Estudos demonstraram que a indução ou repressão de qualquer um dos fatores transcricionais que modulam TEM é capaz de ativar parcialmente o processo. A ativação parcial da TEM pode ser transiente, retornando ao estado de origem da célula (BRABLETZ et al., 2018). Por isso, discute-se o papel não redundante dos fatores transcricionais, agindo

diferentemente em cada tecido e tipo tumoral (STEMMLER et al., 2019). Alguns fatores transcricionais por exemplo, podem ser fortes repressores epiteliais mas são fracos promotores mesenquimais (NIETO et al., 2016). Como é o caso de ZEB1 e SNAI1, que estão mais ativados nos estágios intermediários de TEM. Neste estudo observou-se uma significativa indução dos fatores transcricionais promotores da transição epitélio-mesenquimal, ZEB1 e Snail (*SNAI1*) gerada pelas NETs, mas não de Sip1 (*ZEB2*), Slug (*SNAI2*) e Twist (*TWIST1*). Juntamente com essas observações, as NETs promoveram uma drástica perda da proteína E-caderina nas células MCF7 e HCC1954. As famílias do fatores Zeb e Snail são capazes de se ligar à sequência E-box do promotor do gene de E-caderina, reprimindo diretamente sua transcrição (YEUNG & YANG, 2017). No processo de metástase, essa proposta da plasticidade celular é bem aceita entre a comunidade científica por acreditar ser necessária para ganho de motilidade da célula tumoral e habilidade de invadir tecidos e depois aderir e se instalar em órgãos distantes do tumor primário, iniciando um sítio metastático (GOETZ et al., 2020).

Neste trabalho, marcadores mesenquimais como fibronectina e N-caderina foram positivamente modulados. No entanto, vimentina não passou a ser expressa nas células MCF7 tratadas com NETs, mantendo uma baixa expressão basal dessa proteína. A vimentina contribui para a ativação do fator transcricional Slug, induzindo TEM através organização da adesão focal e do citoesqueleto (LIU et al., 2015). Estudos *in vitro* de carcinoma ovariano mostraram células em estágio intermediário de TEM com baixa expressão de E-caderina e alta expressão de vimentina (HUANG et al., 2013). Em alguns modelos de câncer, Twist1 é capaz de regular positivamente a expressão de vimentina (LIAO & YANG, 2017). Diferentemente da nossa observação, indutores clássicos de TEM, como EGF e TGFβ, foram capazes de aumentar a expressão de vimentina nas células MCF7 (ZHANG et al. 2013; KIM et al., 2016). É possível que o tratamento com NETs por 16 horas com NETs tenha levado à uma ativação parcial da TEM, justificando a não indução de todos os fatores transcricionais e a proteína de fenótipo mesenquimal, vimentina. Além disso, a regulação epigenética tem se mostrado um importante fator para justificar a plasticidade de TEM e a existência de diferentes fenótipos celulares. Acredita-se que o desenvolvimento completo de perfil celular, mantendo o processo de TEM estável,

precisa ser suportado pelas modificações epigenéticas apropriadas (TAM & WEINBERG, 2013).

A ativação da via de Wnt/β-catenina leva à indução de *SNAI1* e consequentemente a diminuição da expressão de E-caderina. Esta via encontra-se frequentemente subregulada no câncer, mas sob diversos estímulos do microambiente tumoral ela pode ser ativada e está associada com diversos aspectos do câncer: da tumorigênese até a metástase. Quando a via de Wnt/β-catenina é ativada, ocorre um acúmulo de β-catenina no citoplasma e transientemente no interior do núcleo, onde atua como fator transcricional de diferentes oncogenes. β-catenina também é uma proteína que participa da interação entre as células e da estrutura do citoesqueleto. Em condições de homeostase, β-catenina está ligada a um complexo transmembrana formado por GSK3β (glicogênio sintase quinase-3β), AXIN (axina) e APC que regula sua atividade. Este complexo se encontra conectado a proteína de superfície E-caderina. Quando ocorre a disrupção do complexo pela perda da E-caderina há um aumento dos níveis de β-catenina livre no citoplasma que pode translocar até o núcleo e promover a transcrição gênica. β-catenina livre no citoplasma também é capaz de favorecer a migração celular e metástase. Além disso, acumulação de β-catenina no núcleo leva a um aumento de expressão do marcador CD44 em câncer colorretal (BASU, CHERIYAMUNDATH, BEN-ZE'EV, 2018). Aqui, observou-se através de imunocitoquímica o aumento dos níveis proteicos de β-catenina nas células MCF7 tratadas com NETs dispersos no seu interior. Entretanto, nas células MCF7, a localização de β-catenina é difícil de ser visualizada devido à ausência de um mecanismo de retenção e acumulação do fator transcricional β-catenina no núcleo mediada pelos fatores transcricionais LEF-1/TCF ou até pela rápida degradação proteolítica desses cofatores (JAMIESON et al., 2016; SERGIO et al., 2020).

Um dos fatores indutores de células-tronco tumorais é ativação do programa de TEM (MANI et al., 2008; MOREL et al., 2008; WEIDENFELD & BARKAN, 2018). CSCs e TEM estão associados ao ganho de resistência contra morte celular, resistência à quimioterapia, recorrência do tumor primário e metástase (TANABE et al., 2020). Para seleção das CSCs, biomarcadores têm sido definidos na literatura e se diferenciam por tipo tumoral. No câncer de mama, os biomarcadores de CSCs frequentemente utilizados são CD44, a perda de sinal de CD24 e a alta atividade de

ALDH1. Subpopulações celulares com perfil $CD44^{+}CD24^{Lo/-}$ geralmente apresentam propriedades tumorigênicas e maior agressividade tumoral (FILLMORE & KUPERWASSER, 2008; RICARDO et al., 2011). Neste estudo, utilizou-se células MCF7, de subtipo luminal, que tipicamente apresenta perfil $CD44^{+}/CD24^{+}$. Com o tratamento com as NETs, observou-se maior expressão gênica e proteica do marcador CD44. Estudos prévios utilizando TGFβ para induzir TEM em células tumorais de mama mostrou que a transcrição de ZEB1 aumenta a subpopulação de células $CD44^{high}$ juntamente com propriedades de CSCs (PRASETYANTI & MEDEMA, 2017). Em nosso estudo, também se observou uma queda significativa na expressão de mRNA de CD24, mas não dos níveis proteicos. Acredita-se que isso se deve ao tempo de *turnover* da proteína presente na membrana celular, o que justifica os níveis da imunomarcação de CD24 não reduzirem após 16 horas de tratamento com NETs. Sob outro aspecto, a marcação positiva de CD24 pode ser associada a um pior prognóstico (MOON et al., 2018). Estudos mostraram que células HEK, embrionárias de rim, $CD24^{+}$ não tinham propriedade tumorigênica como as $CD24^{-,}$ mas apresentavam perfil mais mesenquimal, o programa de TEM mais bem estabelecido e um perfil pró-inflamatório (ORTIZ-MONTERO et al., 2018). Portanto, os efeitos das NETs sobre aquisição de características de CSCs, como tumorigênese, quimiorresistência e proliferação ainda necessitam ser alisados.

TEM é capaz de estimular a produção de fatores pro-tumorais, como TGFβ, IL-6, IL-1β, IL-8, pelas células presentes no microambiente tumoral (SUAREZ-CARMONA et al., 2017). A secreção desses fatores no tumor tem sido relacionada com a agressividade tumoral e pior prognóstico em pacientes com câncer de mama (FERNANDEZ-GARCIA et al., 2016). A inflamação pode ser regulada pelos próprios fatores transcricionais relacionados à TEM. Através de análises de bioinformática e ensaios de imunoprecipitação foram identificados inúmeros sítios de ligação para o fator NFκB na região promotora de Snail (*SNAI1*), Slug (*SNAI2*), Sip1 (*ZEB2*) e Twist (*TWIST1*) (PIRES et al., 2017). A atividade de NFκB é essencial na migração celular, angiogênese, e metástase em diferentes tipos tumorais (HUBER et al., 2004; KALTSCHMIDT et al., 2019). Estudos prévios mostraram que o silenciamento de ZEB1 em células tumorais de mama MDA-MB-231 diminuiu a produção de IL-6 e IL-8 (KATSURA et al., 2017). Além disso, citocinas pró-inflamatórias secretadas no sítio primário do tumor, especificamente IL-6 e IL-8, podem induzir TEM (DOMINGUEZ,

DAVID, PALENA, 2017). Neste trabalho, observou-se um significativo aumento de citocinas pró-inflamatórias IL-6, IL-8 e lL1β juntamente com a expressão aumentada de ZEB1 e SNAI1 em células tratadas com NETs. Juntamente com o aumento da expressão de IL-8, a expressão de CXCR1, receptor da citocina IL-8, foi aumentada nas células tratadas com NETs, sugerindo uma retroalimentação do sinal inflamatório nas células MCF7, amplificando a resposta inflamatória e consequentemente, levando à progressão tumoral. Esses resultados podem sugerir uma relação entre TEM e inflamação em células de câncer de mama. TOHME e colaboradores (2016) mostraram que NETs promovem metástase hepática em modelo murino através da ativação do eixo TRL9/NFκB. Mais recentemente, Yang e colaboradores (2020) descreveram o efeito das NETs sobre células hepáticas, promovendo metástase através da resposta inflamatória induzida através da ativação de TLR4/9, via NFκB. Os receptores do tipo TLR reconhecem padrões moleculares associados a danos, como DNA contendo sequências CpG que é reconhecido por TRL9 (TAKESHITA et al., 2001) e histonas e elastase neutrofílica que podem ser reconhecidas por TLR4 (DEVANEY et al., 2003; XU et al., 2011). Novas evidências apontam para um receptor transmembrana, identificado como ccdc25 que reconhece o DNA das NETs, ativando a via de sinalização ILKβ/Parvin, e consequentemente, aumentando a motilidade celular (YANG et al., 2020). A expressão deste receptor em pacientes é associada a um pior prognóstico. No entanto, ainda há pouco entendimento sobre as vias de sinalização ativadas pelas NETs em células tumorais de mama culminando à progressão tumoral.

A integridade das fibras de DNA que compõem as NETs é uma condição essencial para algumas das atividades biológicas que exercem. Ensaios utilizando tratamento com DNase mostraram inibição da progressão tumoral. Em modelo murino de câncer de colorretal, o tratamento com DNase atenuou os efeitos pro-tumorigênicos, diminuindo o crescimento do foco metastático (TOHME et al., 2016). Efeitos antimetastáticos semelhantes foram observados em modelos de carcinoma hepatocelular e de câncer de mama (Park et al., 2016; L. Y. Yang et al., 2020). Além disso, a degradação das NETs reduz substancialmente a trombose associada ao câncer em modelos de câncer de mama e pâncreas relacionados à neutrofilia. (HISADA et al., 2018; SNODERLY, BOONE, BENNEWITZ, 2019; GOMES et al., 2019). A enzima DNase passou a ser utilizada para terapia clínica em pacientes com

fibrose cística desde os anos 90 (HONDA & KUBES, 2018). Por isso, o uso da DNase para opções terapêuticas em outras doenças tornou-se muito mais viável (SORVILLO et al., 2019). Embora a enzima seja capaz de desmontar a estrutura de cromatina das NETs, a DNase não é capaz de remover os demais componentes, como histonas e elastase neutrofílica e outras proteases, que são considerados componentes causadores de dano tecidual (ERPENBECK & SCHÖN, 2017; SORVILLO et al., 2019). Estudos com pacientes com lúpus eritematoso sistêmico observaram que a maioria dos pacientes com alta atividade da DNase apresentou recidiva da doença (SKILJEVIC et al., 2013).

Essas limitações podem justificar a necessária combinação de drogas para tratamento de doenças potencializadas pelas NETs. Outros inibidores de NETs, como inibidor de PAD4 e elastase neutrofílica têm se mostrado relevante nos ensaios *in vitro* e modelo murino por evitar a formação das NETs e não só a degradação das NETs preexistentes (ERPENBECK & SCHÖN, 2017). Apesar disso, a DNase tem apresentado ótimos resultados na redução da metástase em diferentes modelos tumorais (ALEKSEEVA et al., 2020). Neste trabalho, observamos que a degradação das NETs com o tratamento com DNase teve uma redução parcial sobre seu efeito na migração de células tumorais, bem como na expressão dos genes CXCL8 e MMP9. Portanto, acreditamos que, em nossas condições experimentais, a integridade do DNA não é essencial para a efetividade das NETs sobre as células tumorais MCF7, pois o efeito das NETs não é completamente revertido quando o DNA é degradado. Outro fator considerável é a metodologia de tratamento utilizada. Comparado com os estudos já publicados, a concentração da DNAse I utilizada em nosso trabalho é inferior (5 U/mL). YANG e colaboradores (2020) utilizaram 100 U/mL nos ensaios *in vitro*. Nossa escolha se baseou num ensaio prévio para analisar a partir de um gel de agarose a eficácia da DNAse sobre a degradação das NETs. Além disso, os ensaios utilizam a DNAse para degradar as NETs durante o estímulo dos neutrófilos com PMA e utilizam o meio condicionado para estimular as células tumorais (TOHME et al., 2016). Futuramente, pretendemos realizar análises mais aprofundadas do papel dos componentes das NETs, como elastase neutrofílica e HMGB1, sobre a indução da TEM em células de câncer de mama.

Altos níveis de neutrófilos infiltrados no sítio do tumor primário foram associados à menor sobrevida e recorrência em vários tipos de câncer, como carcinoma hepatocelular, câncer de pulmão de células não pequenas, câncer cervical, entre outros (SHEN et al., 2014). Mais recentemente, um estudo relacionou o acúmulo de neutrófilos em diferentes subtipos de câncer de mama, sugerindo haver uma quantidade maior de neutrófilos em subtipos mais agressivos (SOTO-PEREZ-DE-CELIS et al., 2017). Utilizando modelo murino, PARK et al (2016) demonstrou que células de tumor de mama mais metastáticas recrutam mais neutrófilos para o microambiente tumoral e, consequentemente, formam mais NETs. Para avaliarmos a relevância clínica deste modelo, utilizamos dados de transcriptoma de pacientes com câncer de mama depositados no TCGA e demonstramos uma correlação positiva entre genes relacionados à neutrófilos e vários genes que codificam para fatores pró-tumorais que foram regulados positivamente *in vitro* após o tratamento com NETs, incluindo fatores pró-inflamatórios e relacionados à TEM analisados previamente neste estudo. Numa primeira análise utilizando a ferramenta do cBioPortal, analisamos os genes individualmente para avaliar a co-expressão desses genes. Para refinar nossa análise, utilizamos posteriormente uma outra ferramenta, GEPIA 2, capaz de analisar a co-expressão dos genes-alvo e um *subset* de genes de assinatura neutrofílica. Esse tipo de análise foi inspirado em estudos de sequenciamento *single-cell* que é capaz de clusterizar tipos celulares de acordo com o grupo de genes mais expressos (TANG et al., 2019). Os resultados obtidos corroboram com a primeira análise, sendo a ferramenta de escolha para futuras análises de correlação gênica. Nossos resultados mostrando o efeito das NETs na aquisição de um perfil pró-metastático em células de carcinoma mamário reforçam a contribuição dos neutrófilos para ativação do processo de TEM sugerida anteriormente em diferentes tipos de câncer, como câncer de ovário e adenocarcinoma de pulmão. (HU et al., 2015; Mayer et al., 2016). Com base nessas análises, os genes de assinatura neutrofílica poderiam ser utilizados como marcadores de agressividade tumoral. Diante disso, é imprescindível buscar alternativas terapêuticas para controle da resposta inflamatória dos neutrófilos no microambiente tumoral e a secreção exacerbada das NETs impedindo a sua atividade na progressão do tumor.

6. CONCLUSÃO

As redes extracelulares de neutrófilos em tumores sólidos têm sido associadas a um pior prognóstico. Os mecanismos de atuação das NETs sobre a progressão tumoral ainda são pouco compreendidos. Este estudo propôs avaliar a atuação das NETs isoladas na indução da transição epitélio-mesenquimal em células tumorais MCF7 em cultura e definir a correlação entre a presença de neutrófilos e a expressão de genes de TEM e genes pró-tumorais em pacientes com tumor de mama. Com base em nossos temresultados, conclui-se que:

- NETs modificam a morfologia de células tumorais da linhagem de carcinoma mamário MCF7 promovendo alterações celulares típicas de TEM;

- O comportamento migratório das células MCF7 foi aumentado mediante o tratamento com NETs;

- NETs foram capazes de induzir a expressão dos fatores transcricionais Snail e Zeb e modular marcadores da transição epitélio-mesenquimal E-caderina, Fibronectina, N-caderina e β-catenina;

- Marcadores de células-tronco tumoral foram diferencialmente modulados pelas NETs, reduzindo os níveis de CD24 e aumentando a expressão de CD44, apontado para um fenótipo mais agressivo das células MCF7;

- NETs induziram uma resposta pró-inflamatória nas células de tumor de mama com a superexpressão de citocinas IL1β, IL-6 e IL-8 e genes pró-tumorais MMP2/9;

- Genes pró-tumorais e pró-inflamatórios correlacionam positivamente com genes de assinatura neutrofílica em pacientes com câncer de mama, sugerindo a medição de genes relacionados à neutrófilos como possíveis biomarcadores no câncer de mama.

7. REFERÊNCIAS

ADES, F. et al. Luminal B Breast Cancer: Molecular Characterization, Clinical Management, and Future Perspectives. **Journal of Clinical Oncology**, v. 32, n. 25, p. 2794-2803, jul. de 2014.

AL SALEH, S.; AL MULLA, F.; LUQMANI, Y. A. Estrogen Receptor Silencing Induces Epithelial to Mesenchymal Transition in Human Breast Cancer Cells. **Plos One,** v. 6, n. 6, p. e20610, jun. de 2011.

ALBRENGUES, J. et al. Neutrophil extracellular traps produced during inflammation awaken dormant cancer cells in mice. **Science**, v. 361, n. 6409, out. de 2018.

ALEKSEEVA, L. A. et al. Targeting Circulating SINEs and LINEs with DNase I Provides Metastases Inhibition in Experimental Tumor Models. **Molecular Therapy - Nucleic Acids**, v. 20, p. 50–61, jun. de 2020.

ALGRA, A. M.; ROTHWELL, P. M. Effects of regular aspirin on long-term cancer incidence and metastasis: A systematic comparison of evidence from observational studies versus randomised trials. **The Lancet Oncology**, v. 13, n. 5, p. 518–527, mai. de 2012.

AMULIC, B. et al. Cell-Cycle Proteins Control Production of Neutrophil Extracellular Traps. **Developmental Cell**, v. 43, n. 4, p. 449-462.e5, nov. de 2017.

APEL, F.; ZYCHLINSKY, A.; KENNY, E. F. The role of neutrophil extracellular traps in rheumatic diseases. **Nature Reviews Rheumatology**, v. 14, p. 467–475, jun. de 2018.

APONTE, P. M.; CAICEDO, A. Stemness in cancer: Stem cells, cancer stem cells, and their microenvironment. **Stem Cells International**, v. 2017:5619472, abr. de 2017.

ARTHUR W. LAMBERT, DIWAKAR R. PATTABIRAMAN, and R. A. W. Emerging biological principles of metastasis. **Cell**, v. 168, n. 4, p. 670–691, fev. de 2017.

BASU, S.; CHERIYAMUNDATH, S.; BEN-ZE'EV, A. Cell–cell adhesion: Linking wnt/β-catenin signaling with partial emt and stemness traits in tumorigenesis. **F1000 Research** Ltd, F100, set. de 2018.

BATLLE, E.; CLEVERS, H. Cancer stem cells revisited. **Nature Medicine**, v. 23, n. 10, p. 1124–1134, out. de 2017.

BAUMANN, M.; KRAUSE, M.; HILL, R. Clonogens and cancer stem cells. **Nature Reviews Cancer**, v. 8, n. 12, p. 990, dez. de 2008.

BERGER-ACHITUV, S. et al. A proposed role for neutrophil extracellular traps in cancer immunoediting. **Frontiers in Immunology**, v. 4, p. 1–5, mar. de 2013.

BERNARD, W. S.; CHRISTOPHER, P. W. World cancer report: Cancer Research for Cancer Prevention. **International Agency for Research on Cancer**. p. 630, 2020.

BIZZARRI, M.; CUCINA, A. Tumor and the microenvironment: A chance to reframe the paradigm of carcinogenesis? **Biomed Research International,** 2014:934038, p.9, jun. de 2014.

BOELTZ, S. et al. To NET or not to NET:current opinions and state of the science regarding the formation of neutrophil extracellular traps. **Cell Death and Differentiation**, v. 26, n. 3, p. 395–408, jan. de 2019.

BRABLETZ, T. et al. EMT in cancer. **Nature Reviews Cancer**, v. 18, p. 128–134, jan. de 2018.

BRAY, F. et al. Global cancer statistics 2018: GLOBOCAN estimates of incidence and mortality worldwide for 36 cancers in 185 countries. **CA: A Cancer Journal for Clinicians**, v. 68, n. 6, p. 394–424, set. de 2018.

BRINKMANN, V. et al. Neutrophil Extracellular Traps Kill Bacteria. **Science**, v. 303, n. 5663, p. 1532–1535, mar. de 2004.

BRINKMANN, V. Neutrophil Extracellular Traps in the Second Decade. **Journal of Innate Immunity**, v. 10, n. 5–6, p. 414–421, dez. de 2018.

BURGER, G. A.; DANEN, E. H. J.; BELTMAN, J. B. Deciphering epithelial–mesenchymal transition regulatory networks in cancer through computational approaches. **Frontiers Oncology**, 7: 162, ago. de 2017.

CAHILOG, Z. et al. The Role of Neutrophil NETosis in Organ Injury: Novel Inflammatory Cell Death Mechanisms. **Inflammation,** 43, p. 2021–2032, ago. de 2020.

CERAMI, E. et al. The cBio Cancer Genomics Portal: An open platform for exploring multidimensional cancer genomics data. **Cancer Discovery**, v. 2, n. 5, p. 401–404, mai. de 2012.

CLARKE, M. F.; HASS, A. T. Cancer Stem Cells Keywords. **Encyclopedia of Molecular Cell Biology and Molecular Medicine**, 2nd ed, p. 221–242, 2004.

COFFELT, S. B.; WELLENSTEIN, M. D.; DE VISSER, K. E. Neutrophils in cancer: Neutral no more. **Nature Reviews Cancer**, v. 16, n. 7, p. 431–446, jun. de 2016.

COOLS-LARTIGUE, J. et al. Neutrophil extracellular traps sequester circulating tumor cells and promote metastasis. **Journal of Clinical Investigation**, v. 123, n. 8,

p. 3446–3458, ago. de 2013.

COOLS-LARTIGUE, J. et al. Neutrophil extracellular traps in cancer progression. **Cellular and Molecular Life Sciences**, v. 71, n. 21, p. 4179–4194, nov. de 2014.

DAI, X. et al. Breast cancer intrinsic subtype classification, clinical use and future trends. **American Journal of Cancer Research**, v. 5, n. 10, p. 2929–2943, set. de 2015.

Daniel, C. et al. Extracellular DNA traps in inflammation, injury and healing. **Nature Reviews Nephrology, v. 15, p.** 559–575, jun de 2019.

DEMERS, M. et al. Cancers predispose neutrophils to release extracellular DNA traps that contribute to cancer-associated thrombosis. **Proceedings of the National Academy of Sciences of the United States of America**, v. 109, n. 32, p. 13076–13081, ago. de 2012.

DEMERS, M. et al. Priming of neutrophils toward NETosis promotes tumor growth. **OncoImmunology**, v. 5, n. 5, p. 1–9, fev. de 2016.

DEVANEY, J. M. et al. Neutrophil elastase up-regulates interleukin-8 via toll-like receptor 4. **FEBS Letters**, v. 544, n. 1–3, p. 129–132, jun. de 2003.

DITTMER, J. Breast cancer stem cells: Features, key drivers and treatment options. **Seminars in Cancer Biology**, v. 53, p. 59–74, dez. de 2018.

DOMINGUEZ, C.; DAVID, J. M.; PALENA, C. Epithelial-mesenchymal transition and inflammation at the site of the primary tumor. **Seminars in Cancer Biology**, v. 47, p. 177–184, dez. de 2017.

DONGRE, A.; WEINBERG, R. A. New insights into the mechanisms of epithelial–mesenchymal transition and implications for cancer. **Nature Reviews Molecular Cell Biology**, v. 20, n. 2, p. 69–84, fev. de 2019.

DVORAK, H. F. Tumors: wounds that do not heal. Similarities between tumor stroma generation and wound healing. **The New England journal of medicine**, v. 315, n. 26, p. 1650–9, dez. de 1986.

ERPENBECK, L.; SCHÖN, M. P. Neutrophil extracellular traps: Protagonists of cancer progression? **Oncogene**, v. 36, n. 18, p. 2483–2490, mai de 2017.

ESTEVA, F. J. et al. Immunotherapy and targeted therapy combinations in metastatic breast cancer. **The Lancet Oncology**, v.20, n.3, p.175-186, mar. de 2019.

FELIPE LIMA, J. et al. EMT in Breast Carcinoma - A Review. **Journal of Clinical Medicine**, v. 5, n. 7, p. 65, jul. de 2016.

FERLAY, J. et al. Estimating the global cancer incidence and mortality in 2018: GLOBOCAN sources and methods. **International Journal of cancer**, v. 144: 8, p. 1941–1953, abr. de 2019.

FERNANDEZ-GARCIA, B. et al. Prognostic significance of inflammatory factors expression by stroma from breast carcinomas. **Carcinogenesis**, v. 37, n. 8, p. 768–776, ago. de 2016.

FILLMORE, C. M.; KUPERWASSER, C. Human breast cancer cell lines contain stem-like cells that self-renew, give rise to phenotypically diverse progeny and survive chemotherapy. **Breast Cancer Research**, v. 10, n. 2, p. 1–13, mar. de 2008.

FRAGOMENI, S. M.; SCIALLIS, A.; JERUSS, J. S. Molecular Subtypes and Local-Regional Control of Breast Cancer. **Surgical clinics of North America**, v. 27, n. 1, p. 95-120, jan. de 2018

GALDIERO, M. R.; MARONE, G.; MANTOVANI, A. Cancer inflammation and cytokines. **Cold Spring Harbor Perspectives in Biology**, v. 10, n. 8, p. 1–18, ago. de 2018.

GAO, J. et al. Integrative analysis of complex cancer genomics and clinical profiles using the cBioPortal. **Science Signaling**, v. 6, n. 269, abr. de 2013.

GARRIDO-CASTRO, A. C.; LIN, N.U.; POLYAK, K. Insights into Molecular Classifications of Triple-Negative Breast Cancer: Improving Patient Selection for Treatment. Cancer Discovery, v.9 n.2, 176-198, fev. de 2019.

GOETZ, H. et al. A plausible accelerating function of intermediate states in cancer metastasis. **PLoS Computational Biology**, v. 16, n. 3, p. 1–22, mar. de 2020.

GOMES, T. et al. IL-1β Blockade Attenuates Thrombosis in a Neutrophil Extracellular Trap-Dependent Breast Cancer Model. **Frontiers in Immunology**, v. 10, p. 2088, set. de 2019.

GRANGER, V. et al. Neutrophil Extracellular Traps in Autoimmunity and Allergy: Immune Complexes at Work. **Frontiers in Immunology**, v. 10: 2824, dez. de 2019.

GRANOT, Z. et al. Tumor entrained neutrophils inhibit seeding in the premetastatic lung. **Cancer Cell**, v. 20, n. 3, p. 300–314, set. de 2011.

GRETEN, F. R.; GRIVENNIKOV, S. I. Inflammation and Cancer: Triggers, Mechanisms, and Consequences. **Immunity**, v. 51, n. 1, p. 27–41, 2019.

GRIVENNIKOV, S. I.; GRETEN, F. R.; KARIN, M. Immunity, Inflammation, and Cancer. **Cell**, v. 140, n. 6, p. 883–899, mar. de 2010.

HANAHAN, D.; WEINBERG, R. A. Hallmarks of cancer: The next generation. **Cell**, v.

144, n. 5, p. 646–674, mar. de 2011.

HARBECK, N.; GNANT, M. Breast cancer. **The Lancet**, v. 389, n. 10074, p. 1134–1150, mar. de 2017.

HAY, E. D. An overview of epithelio-mesenchymal transformation. **Acta anatomica**, v. 154, n.1, p. 8–20, 1995.

HENG, B. et al. Understanding the role of the kynurenine pathway in human breast cancer immunobiology. **Oncotarget**, v. 7, n. 6, p. 6506–6520, fev. de 2016.

HENNESSY, B. T. et al. Characterization of a naturally occurring breast cancer subset enriched in epithelial-to-mesenchymal transition and stem cell characteristics. **Cancer Research**, v. 69, n. 10, p. 4116–4124, mai. de 2009.

HISADA, Y. et al. Neutrophil Extracellular Traps Enhance Venous Thrombosis in Mice Bearing Human Pancreatic Tumors. **Arteriosclerosis, Thrombosis, and Vascular Biology**, v. 38, n. 1, mai. de 2018.

HO-TIN-NOÉ, B. et al. Innate immune cells induce hemorrhage in tumors during thrombocytopenia. **American Journal of Pathology**, v. 175, n. 4, p. 1699–1708, out. de 2009.

HONDA, M.; KUBES, P. Neutrophils and neutrophil extracellular traps in the liver and gastrointestinal system. **Nature Reviews Gastroenterology & Hepatology**, v. 15, n.4 p. 206–221, jan de 2018.

HUANG, R. Y. J. et al. An EMT spectrum defines an anoikis-resistant and spheroidogenic intermediate mesenchymal state that is sensitive to e-cadherin restoration by a src-kinase inhibitor, saracatinib (AZD0530). **Cell Death and Disease**, v. 4, n. 11, nov. de 2013.

HUANG, W. et al. MFG-E8 accelerates wound healing in diabetes by regulating “NLRP3 inflammasome-neutrophil extracellular traps” axis. **Cell Death Discovery**, v. 6, n. 1, p. 84, dez. de 2020.

HUBER, M. A. et al. NF-κB is essential for epithelial-mesenchymal transition and metastasis in a model of breast cancer progression. **Journal of Clinical Investigation**, v. 114, n. 4, p. 569–581, ago. de 2004.

IACOVIELLO, L. et al. Epidemiology of breast cancer, a paradigm of the “common soil” hypothesis. **Seminars in Cancer Biology**, n. February, v. 20, p. 0–1, fev. de 2020.

INCA - Instituto nacional do câncer José Gomes Alencar Silva. **Estimativa 2020: incidência de câncer no Brasil**. Rio de Janeiro: Ministério da Saúde, 2019. 120p.

INCA - Instituto Nacional de Câncer José Alencar Gomes da Silva / Ministério da Saúde, A situação do câncer de mama no brasil: síntese de dados dos sistemas de informação. Rio de Janeiro: Ministério da Saúde, 2019. 85p.

JAMIESON, C. et al. Characterization of a beta-catenin nuclear localization defect in MCF-7 breast cancer cells. **Experimental Cell Research**, v. 341, n. 2, p. 196–206, fev. de 2016.

JAYASEKERA, J. & MANDELBLATT, J. S. Systematic Review of the Cost Effectiveness of Breast Cancer Prevention, Screening, and Treatment Interventions. **Journal of Clinical Oncology**, v. 38, n. 4, p. 332 – 350, dez. de 2019.

JIA, D. et al. OVOL guides the epithelial-hybrid-mesenchymal transition. **Oncotarget**, v. 6, n. 17, p. 15436–15448, jun. de 2015.

JIN, W. Role of JAK/STAT3 Signaling in the Regulation of Metastasis, the Transition of Cancer Stem Cells, and Chemoresistance of Cancer by Epithelial–Mesenchymal Transition. **Cells**, v. 9, n. 1, p. 217, jan. de 2020.

JUNG, H. S. et al. Cancer cell–induced neutrophil extracellular traps promote both hypercoagulability and cancer progression. **PLoS ONE**, v. 14, n. 4, p. 1–16, abr. de 2019.

KALTSCHMIDT, C. et al. A role for NF-κB in organ specific cancer and cancer stem cells. **Cancers**, v. 11, p. 655, mai. de 2019.

KATSURA, A. et al. ZEB1-regulated inflammatory phenotype in breast cancer cells. **Molecular Oncology**, v. 11, n. 9, p. 1241–1262, set. de 2017.

KIM, J. et al. EGF induces epithelial-mesenchymal transition through phospho-Smad2/3-Snail signaling pathway in breast cancer cells. **Oncotarget,** v. *7*, p. 85021–85032, nov. de 2016.

KORNILUK, A. et al. From inflammation to cancer. **Irish Journal of Medical Science**, v. 186, n. 1, p. 57–62, fev. de 2017.

KREBS, A. M. et al. The EMT-activator Zeb1 is a key factor for cell plasticity and promotes metastasis in pancreatic cancer. **Nature Cell Biology**, v. 19, n. 5, p. 518–529, mai. de 2017.

KRESO, A.; DICK, J. E. Evolution of the cancer stem cell model. **Cell Press**, v. 14, n.3, p. 275–291, mar. de 2014.

LAPIDOT, T. et al. A cell initiating human acute myeloid leukaemia after transplantation into SCID mice. **Nature**, v. 367, n. 6464, p. 645–648, fev. de 1994.

LEAL, A. C. et al. Tumor-Derived Exosomes Induce the Formation of Neutrophil

Extracellular Traps: Implications For The Establishment of Cancer-Associated Thrombosis. **Scientific Reports**, v. 7, n. 1, p. 1–12, dez. de 2017.

LEE, K. H. et al. Neutrophil extracellular traps (NETs) in autoimmune diseases: A comprehensive review. **Autoimmunity Reviews**, v. 16, n. 11, p. 1160–1173, nov. de 2017.

LEGGETT, S. E. et al. Morphological single cell profiling of the epithelial–mesenchymal transition. **Integrative Biology**, v. 8, n. 11, p. 1133–1144, nov. de 2016.

LI, B. et al. Neutrophil extracellular traps enhance procoagulant activity in patients with oral squamous cell carcinoma. **Journal of Cancer Research and Clinical Oncology**, v. 145, n. 7, p. 1695–1707, jul. de 2019.

LIAO, T. T.; YANG, M. H. Revisiting epithelial-mesenchymal transition in cancer metastasis: the connection between epithelial plasticity and stemness. **Molecular Oncology**, v. 11, n. 7, p. 792–804, jul. de 2017.

LIU, C. Y. et al. Vimentin contributes to epithelial-mesenchymal transition ancer cell mechanics by mediating cytoskeletal organization and focal adhesion maturation. **Oncotarget**, v. 6, n. 18, p. 15966–15983, jun. de 2015.

LOOD, C. et al. Neutrophil extracellular traps enriched in oxidized mitochondrial DNA are interferogenic and contribute to lupus-like disease. **Nature Medicine**, v. 22, n. 2, p. 146–153, fev. de 2016.

LOIBL, S. Breast cancer. **The Lancet**, v. 397, n. 10286, p. 1750-1769, mai. de 2021.

LÓPEZ-LAGO, M. A. et al. Neutrophil chemokines secreted by tumor cells mount a lung antimetastatic response during renal cell carcinoma progression. **Oncogene**, v. 32, n. 14, p. 1752–1760, abr. de 2013.

LU, M. et al. MicroRNA-based regulation of epithelial-hybrid-mesenchymal fate determination. **Proceedings of the National Academy of Sciences of the United States of America**, v. 110, n. 45, p. 18144–18149, nov. de 2013.

LU, W.; KANG, Y. Epithelial-Mesenchymal Plasticity in Cancer Progression and Metastasis. **Developmental Cell**, v. 49, n. 3, p. 361–374, mai. de 2019.

LURIE, R. H. et al. Guidelines Version 6.2020 Breast Cancer. **NCCN**, set. de 2020.

MAGÁN-FERNÁNDEZ, A. et al. Neutrophil Extracellular Traps in Periodontitis. **Cells**, v. 9, n. 8, p. 1494, jun. de 2020.

MANI, S. A. et al. The Epithelial-Mesenchymal Transition Generates Cells with Properties of Stem Cells. **Cell**, v. 133, n. 4, p. 704–715, mai. de 2008.

MANTOVANI, A. et al. Cancer-related inflammation. **Nature**, v. 454, n. 7203, p. 436–444, jul. de 2008.

MAO, Y. et al. Stromal cells in tumor microenvironment and breast cancer. **Cancer and Metastasis Reviews**, v. 32, n. 1–2, p. 303–315, jun. de 2013.

MARELLI, G. et al. Inflammation as target in cancer therapy. **Current Opinion in Pharmacology**, v. 35, p. 57–65, jun. de 2017.

MARTÍNEZ-ALEMÁN, S. R. et al. Understanding the entanglement: Neutrophil extracellular traps (NETs) in cystic fibrosis. **Frontiers in Cellular and Infection Microbiology**, v. 7, n. APR, p. 104, abr. de 2017.

MASOUD, V.; PAGÈS, G. Targeted therapies in breast cancer: New challenges to fight against resistance. **World Journal of Clinical Oncology**, v. 8, n. 2, p. 120–134, abr. de 2017.

MASUCCI, M. T. et al. The Emerging Role of Neutrophil Extracellular Traps (NETs) in Tumor Progression and Metastasis. **Frontiers in Immunology**, v. 11, p. 1749, set. de 2020.

MASUCCI, M. T.; MINOPOLI, M.; CARRIERO, M. V. Tumor Associated Neutrophils. Their Role in Tumorigenesis, Metastasis, Prognosis and Therapy. **Frontiers in Oncology**, 9:1146, nov. de 2019.

MATTIUZZI, C.; LIPPI, G. Current Cancer Epidemiology glossary. **Journal of Epidemiology and Global Health**, v. 9, n. 4, p. 217–222, dez. de 2019.

MEISEL, C. T.; PORCHERI, C.; MITSIADIS, T. A. Cancer Stem Cells, Quo Vadis? The Notch Signaling Pathway in Tumor Initiation and Progression. **Cancers**, v. *9*: 1879, ago. de 2020.

MIDDLETON, E. A. et al. Neutrophil extracellular traps contribute to immunothrombosis in COVID-19 acute respiratory distress syndrome. **Blood**, v. 136, n. 10, p. 1169–1179, set. de 2020.

MILLER-OCUIN, J. L. et al. DNA released from neutrophil extracellular traps (NETs) activates pancreatic stellate cells and enhances pancreatic tumor growth. **OncoImmunology**, v. 8, n. 9, set. de 2019.

MITTAL, S.; BROWN, N. J.; HOLEN, I. The breast tumor microenvironment: role in cancer development, progression and response to therapy. **Expert Review of Molecular Diagnostics**, v. 18, n. 3, p. 227–243, mar. de 2018.

MITTAL, V. Epithelial Mesenchymal Transition in Tumor Metastasis. **Annual Review of Pathology: Mechanisms of Disease**, v. 13, n. 1, p. 395–412, jan. de 2018.

MOON, Y. W. et al. CD44/CD24 and aldehyde dehydrogenase 1 in estrogen receptor-positive early breast cancer treated with tamoxifen: CD24 positivity is a poor prognosticator. **Oncotarget**, v. 9, n. 2, p. 2622–2630, dez. de 2018.

MOREL, A. P. et al. Generation of breast cancer stem cells through epithelial-mesenchymal transition. **PLoS ONE**, v. 3, n. 8, p. 1–7, ago. de 2008.

NAJMEH, S. et al. Neutrophil extracellular traps sequester circulating tumor cells via β1-integrin mediated interactions. **International Journal of Cancer**, v. 140, n. 10, p. 2321–2330, mai. de 2017.

NEVE, R. M. et al. A collection of breast cancer cell lines for the study of functionally distinct cancer subtypes. **Cancer Cell**, v. 10, n. 6, p. 515–527, dez. de 2006.

NIE, M. et al. Neutrophil Extracellular Traps Induced by IL8 Promote Diffuse Large B-cell Lymphoma Progression via the TLR9 Signaling. **Clinical Cancer Research**, v. 25, n. 6, p. 1867–1879, mar. de 2019.

NIETO, M. A. et al. Emt: 2016. **Cell**, v. 166, n. 1, p. 21–45, jun. de 2016.

NOWELL, P. C. The clonal evolution of tumor cell populations. **Science**, v. 194, n. 4260, p. 23–28, out. de 1976.

NUNES, T. et al. Targeting cancer stem cells to overcome chemoresistance. **International journal of molecular sciences,** v. 19, n. 12:4036, dez de 2018.

OHMS, M.; MÖLLER, S.; LASKAY, T. An Attempt to Polarize Human Neutrophils Toward N1 and N2 Phenotypes in vitro. **Frontiers in Immunology**, v. 11, abr. de 2020.

ORSULIC, S. et al. E-cadherin binding prevents beta-catenin nuclear localization and beta-catenin/LEF-1-mediated transactivation. **Journal of cell science,** v. 112, p. 1237-45, abr. de 1999.

ORTIZ-MONTERO, P. et al. CD24 expression and stem-associated features define tumor cell heterogeneity and tumorigenic capacities in a model of carcinogenesis. **Cancer Management and Research**, v. Volume 10, p. 5767–5784, nov. de 2018.

PAPAYANNOPOULOS, V. Neutrophil extracellular traps in immunity and disease. **Nature Reviews Immunology**, v. 18, n. 2, p. 134–147, fev. de 2018.

PARK, J. et al. Cancer cells induce metastasis-supporting neutrophil extracellular DNA traps. **Science Translational Medicine**, v. 8, n. 361, out. de 2016.

PARK, S. Y.; CHOI, J. H.; NAM, J. S. Targeting cancer stem cells in triple-negative breast cancer. **Cancers**, v. 11, n. 7: 965, jul. de 2019.

PEITZSCH, C. et al. Cancer stem cells: The root of tumor recurrence and metastases. **Seminars in Cancer Biology**, v. 44, p. 10–24, jun. de 2017.

PETRETTO, A. et al. Neutrophil extracellular traps (NET) induced by different stimuli: A comparative proteomic analysis. **PLOS ONE**, v. 14, n. 7, p. e0218946, jul. de 2019.

PICCARD, H.; MUSCHEL, R. J.; OPDENAKKER, G. On the dual roles and polarized phenotypes of neutrophils in tumor development and progression. **Critical Reviews in Oncology/Hematology**, v. 82, p. 296–309, jul. de 2011.

PIRES, B. R. B. et al. NF-kappaB Is Involved in the Regulation of EMT Genes in Breast Cancer Cells. **PLOS ONE**, v. 12, n. 1, p. e0169622, jan. de 2017.

POMP, V. et al. Differential expression of epithelial–mesenchymal transition and stem cell markers in intrinsic subtypes of breast cancer. **Breast Cancer Research and Treatment**, v. 154, n. 1, p. 45–55, nov. de 2015.

POWELL, D. R.; HUTTENLOCHER, A. Neutrophils in the Tumor Microenvironment. **Trends in Immunology**, v. 37, n. 1, p. 41–52, jan. de 2016.

PRAGER, B. C. et al. Cancer Stem Cells: The Architects of the Tumor Ecosystem. **Cell Press**, v. 24, n. 1, p. 41–53, jan. de 2019.

PRASETYANTI, P. R.; MEDEMA, J. P. Intra-tumor heterogeneity from a cancer stem cell perspective. **Molecular Cancer**, v. 16, n. 41, fev. de 2017.

REYA, T.; CLEVERS, H. Wnt signalling in stem cells and cancer. **Nature**, v. 434**,** p. 843–850, abr. de 2005.

RICARDO, S. et al. Breast cancer stem cell markers CD44, CD24 and ALDH1: Expression distribution within intrinsic molecular subtype. **Journal of Clinical Pathology**, v. 64, n. 11, p. 937–944, jun. de 2011.

ROTHWELL, P. M. et al. Effect of daily aspirin on risk of cancer metastasis: A study of incident cancers during randomised controlled trials. **The Lancet**, v. 379, n. 9826, p. 1591–1601, mar. de 2012.

ROTHWELL, P. M. et al. Short-term effects of daily aspirin on cancer incidence, mortality, and non-vascular death: Analysis of the time course of risks and benefits in 51 randomised controlled trials. **The Lancet**, v. 379, n. 9826, p. 1602–1612, abr. de 2012.

SALEMME, R. et al. The Role of NETosis in Systemic Lupus Erythematosus. **Journal of Cellular Immunology**, v. 1, n. 2, p. 33, dez. de 2019.

SARI, I. N. et al. Hedgehog Signaling in Cancer: A Prospective Therapeutic Target for Eradicating Cancer Stem Cells. **Cells**, v. 7, n. 11, p. 208, nov. de 2018.

SCIOLI, M. G. et al. The role of breast cancer stem cells as a prognostic marker and a target to improve the efficacy of breast cancer therapy. **Cancers**, v. 11, n. 7, jul. de 2019.

SENGUPTA, S.; SUBRAMANIAN, B. C.; PARENT, C. A. Getting TANned: How the tumor microenvironment drives neutrophil recruitment. **Journal of Leukocyte Biology**, v. 105, n. 3, p. 449–462, mar. de 2019.

SERGIO, S. et al. 3D-microenvironments initiate TCF4 expression rescuing nuclear β-catenin activity in MCF-7 breast cancer cells. **Acta Biomaterialia**, v. 103, p. 153–164, 2020.

SHANG, S.; HUA, F.; HU, Z. W. The regulation of β-catenin activity and function in cancer: Therapeutic opportunities. **Oncotarget**, v. 8, n. 20, p. 33972–33989, mai. de 2017.

SHAUL, M. E. et al. Tumor-associated neutrophils display a distinct N1 profile following TGFβ modulation: A transcriptomics analysis of pro- vs. antitumor TANs. **OncoImmunology**, v. 5, n. 11, p. 1–14, set. de 2016.

SHAUL, M. E.; FRIDLENDER, Z. G. Neutrophils as active regulators of the immune system in the tumor microenvironment. **Journal of Leukocyte Biology**, v. 102, n. 2, p. 343–349, ago. de 2017.

SHAUL, M. E.; FRIDLENDER, Z. G. Tumour-associated neutrophils in patients with cancer. **Nature Reviews Clinical Oncology**, v. 16, n. 10, p. 601–620, out. de 2019.

SINGH, S.; CHAKRABARTI, R. Consequences of EMT-driven changes in the immune microenvironment of breast cancer and therapeutic response of cancer cells. **Journal of Clinical Medicine**, v. 8, n. 5, p. 642, mai. de 2019.

SKILJEVIC, D. et al. Serum DNase i activity in systemic lupus erythematosus: Correlation with immunoserological markers, the disease activity and organ involvement. **Clinical Chemistry and Laboratory Medicine**, v. 51, n. 5, p. 1083–1091, mai. de 2013.

SNODERLY, H. T.; BOONE, B. A.; BENNEWITZ, M. F. Neutrophil extracellular traps in breast cancer and beyond: Current perspectives on NET stimuli, thrombosis and metastasis, and clinical utility for diagnosis and treatment. **Breast Cancer Research**, v. 21, n. 1, p. 1–13, dez. de 2019.

SOLLBERGER, G.; TILLEY, D. O.; ZYCHLINSKY, A. Neutrophil Extracellular Traps: The Biology of Chromatin Externalization. **Developmental Cell**, v. 44, n. 5, p. 542–553, mar. de 2018.

SØRENSEN, O. E.; BORREGAARD, N. Neutrophil extracellular traps - The dark side

of neutrophils. **Journal of Clinical Investigation**, v. 126, n. 5, p. 1612–1620, 2016.

SORVILLO, N. et al. Extracellular DNA net-works with dire consequences for health. **Circulation Research**, v. 125, n. 4, p. 470-488, ago. de 2019.

SOTO-PEREZ-DE-CELIS, E. et al. Tumor-associated neutrophils in breast cancer subtypes. **Asian Pacific Journal of Cancer Prevention**, v. 18, n. 10, p. 2689–2693, out. de 2017.

SOYSAL, S. D.; TZANKOV, A.; MUENST, S. E. Role of the Tumor Microenvironment in Breast Cancer. **Pathobiology**, v. 82, n. 3–4, p. 142–152, set. de 2015.

STEMMLER, M. P. et al. Non-redundant functions of EMT transcription factors. **Nature Cell Biology**, v. 21, p. 102-112, jan. de 2019.

SUAREZ-CARMONA, M. et al. EMT and inflammation: inseparable actors of cancer progression. **Molecular Oncology**, v. 11, n. 7, p. 805–823, jan. de 2017.

TAKESHITA, F. et al. Cutting Edge: Role of Toll-Like Receptor 9 in CpG DNA-Induced Activation of Human Cells. **The Journal of Immunology**, v. 167, n. 7, p. 3555–3558, out. de 2001.

TAM, W. L.; WEINBERG, R. A. The epigenetics of epithelial-mesenchymal plasticity in cancer. **Nature Medicine**, v. 19, n. 11, p. 1438–1449, 2013.

TANABE, S. et al. Interplay of EMT and CSC in Cancer and the Potential Therapeutic Strategies. Frontiers in Pharmacology, v. 11, n. 904, jun. de 2020.

TANG, Z. et al. GEPIA2: an enhanced web server for large-scale expression profiling and interactive analysis. **Nucleic Acids Research**, v. 47, p. W556–W560, jul. de 2019.

TANIGUCHI, K.; KARIN, M. NF-B, inflammation, immunity and cancer: Coming of age. **Nature Reviews Immunology**, v. 18, p. 309-324, jan. de 2018.

THÅLIN, C. et al. Neutrophil Extracellular Traps: Villains and Targets in Arterial, Venous, and Cancer-Associated Thrombosis. **Arteriosclerosis, Throbosis and Vascular biology**, v. 39, n. 9, p. 1724 - 1738, jul. de 2018.

TOHME, S. et al. Neutrophil extracellular traps promote the development and progression of liver metastases after surgical stress. **Cancer Research**, v. 76, n. 6, p. 1367–1380, mai. de 2016.

TREFFERS, L. W. et al. Neutrophils in cancer. **Immunological Reviews**, v. 273, p. 312–328, set. de 2016.

TURDO, A. et al. Meeting the challenge of targeting cancer stem cells. **Frontiers in**

Cell and Developmental Biology, v. 7, p. 16, fev. de 2019.

VAN AVONDT, K.; HARTL, D. Mechanisms and disease relevance of neutrophil extracellular trap formation. **European Journal of Clinical Investigation**, v. 48, p. e12919, nov. de 2018.

VAN DER WINDT, D. J. et al. Neutrophil extracellular traps promote inflammation and development of hepatocellular carcinoma in nonalcoholic steatohepatitis. **Hepatology**, v. 68, n. 4, p. 1347–1360, jul. de 2018.

VAN STAALDUINEN, J. et al. Epithelial–mesenchymal-transition-inducing transcription factors: new targets for tackling chemoresistance in cancer? **Oncogene**, v. 37, n. 48, p. 6195–6211, jul. de 2018.

WALCHER, L. et al. Cancer Stem Cells—Origins and Biomarkers: Perspectives for Targeted Personalized Therapies. **Frontiers in Immunology**, v. 11, n. 1280, ago. de 2020.

WANG, L. et al. Hyperglycemia induces neutrophil extracellular traps formation through an NADPH oxidase-dependent pathway in diabetic retinopathy. **Frontiers in Immunology**, v. 9, n. 3076, jan. de 2019.

WEIDENFELD, K.; BARKAN, D. EMT and Stemness in Tumor Dormancy and Outgrowth: Are They Intertwined Processes? **Frontiers in Oncology**, v. 8, p. 381, set. de 2018.

WINTERS, S. et al. Breast Cancer Epidemiology, Prevention, and Screening. **Progress in Molecular BiologyandTranslational Science,** v. 151, p. 1–32, out. de 2017.

WITHER, J. E. et al. Identification of a neutrophil-related gene expression signature that is enriched in adult systemic lupus erythematosus patients with active nephritis: Clinical/pathologic associations and etiologic mechanisms. **PLoS ONE**, v. 13, n. 5, p. 1–19, mai. de 2018.

WU, L. et al. Tumor-associated neutrophils in cancer: Going pro. **Cancers**, v. 11, n. 564, abr. de 2019.

XU, J. et al. Extracellular Histones Are Mediators of Death through TLR2 and TLR4 in Mouse Fatal Liver Injury. **The Journal of Immunology**, v. 187, n. 5, p. 2626–2631, set. de 2011.

XU, X. C. COX-2 inhibitors in cancer treatment and prevention, a recent development. **Anticancer Drugs,** v. 13, n. 2, p. 127–137, fev. de 2002.

YANG, J. et al. Guidelines and definitions for research on epithelial–mesenchymal

transition. **Nature Reviews Molecular Cell Biology**, v. 21, n. 6, p. 341–352, abr. de 2020.

YANG, L. et al. DNA of neutrophil extracellular traps promotes cancer metastasis via CCDC25. **Nature**, v. 583, n. 7814, p. 133–138, jul. de 2020.

YANG, L. et al. Targeting cancer stem cell pathways for cancer therapy. **Signal Transdution and Targeted Therapy**, v. 5, n. 8, fev. de 2020.

YANG, L. Y. et al. Increased neutrophil extracellular traps promote metastasis potential of hepatocellular carcinoma via provoking tumorous inflammatory response. **Journal of Hematology and Oncology**, v. 13, n. 1, p. 1–15, jan. de 2020.

YAZDANI, H. O. et al. Neutrophil Extracellular Traps Drive Mitochondrial Homeostasis in Tumors to Augment Growth. Cancer Research, v. 79, n. 21, p. 5626-5639, nov. de 2019.

YEO, S. K.; GUAN, J. Breast Cancer: Multiple Subtypes within a Tumor? Breast cancer stratification and its role in guiding therapeutic decisions. **Trends cancer**, v. 3, n. 11, p. 753–760, nov. de 2018.

YEUNG, K. T.; YANG, J. Epithelial-mesenchymal transition in tumor metastasis. **Molecular oncology**, v. 11, n. 1, p. 28–39, jan. de 2017.

YIN, L. et al. Triple-negative breast cancer molecular subtyping and treatment progress. **Breast Cancer Research**, v. 22, n.61, jun. de 2020.

YIP, N. C. et al. Disulfiram modulated ROS-MAPK and NFB pathways and targeted breast cancer cells with cancer stem cell-like properties. **British Journal of Cancer**, v. 104, n. 10, p. 1564–1574, mai. de 2011.

YOUSEFI, S. et al. Viable neutrophils release mitochondrial DNA to form neutrophil extracellular traps. **Cell Death and Differentiation**, v. 16, n. 11, p. 1438–1444, nov. de 2009.

YOUSEFI, S. et al. In vivo evidence for extracellular DNA trap formation. **Cell Death and Disease**, v. 11, n. , abr. de 2020.

ZHANG, X et al. Beta-Elemene Blocks Epithelial-Mesenchymal Transition in Human Breast Cancer Cell Line MCF-7 through Smad3-Mediated Down-Regulation of Nuclear Transcription Factors. ***PLoS ONE***, v. 8: e58719, mar. de 2013.

ZHANG, J. et al. TGF-β-induced epithelial-to-mesenchymal transition proceeds through stepwise activation of multiple feedback loops. **Science Signaling**, v. 7, n. 345, p. 91, out. de 2014.

ZHOU, J. et al. Stem cells and cellular origins of breast cancer: Updates in the

rationale, controversies, and therapeutic implications. **Frontiers in Oncology,** v. 9, n. 820, ago. de 2019.

8 ANEXOS

ARTIGOS PUBLICADOS DURANTE O DOUTORADO

A **MARTINS-CARDOSO, K**.; ALMEIDA, V.H.; BAGRI, K.M.; ROSSI, M.I.D.; MERMELSTEIN, C.S.; KÖNIG, S.; MONTEIRO, R.Q. NEUTROPHIL EXTRACELLULAR TRAPS (NETS) PROMOTE PRO-METASTATIC PHENOTYPE IN HUMAN BREAST CANCER CELLS THROUGH EPITHELIAL–MESENCHYMAL TRANSITION. *CANCERS* 2020, *12*, 1542. DOI: 10.3390/CANCERS12061542

B GOMES, G.A*; **MARTINS-CARDOSO, K**.*; SANTOS, F.R.; FLORENCIO, M.; ROSA, D.; ZUMA, A.A.; SANTIAGO, G.M.P.; MOTTA, C.; CARVALHO, M.G.; FAMPA, P. ANTILEISHMANIAL ACTIVITY OF THE ESSENTIAL OILS OF *MYRCIA OVATA* CAMBESS. AND *EREMANTHUS ERYTHROPAPPUS* (DC) MCLEISCH LEADS TO PARASITE MITOCHONDRIAL DAMAGE, NATURAL PRODUCT RESEARCH, 2020 DOI: 10.1080/14786419.2020.1827402

C DE MORAES, D.C.; **CARDOSO K.M.;** DOMINGOS, L.T.S.; DO CARMO, M.C.F.R.; MONTEIRO, R.Q., FERREIRA-PEREIRA, A. B-LAPACHONE ENHANCES THE ANTIFUNGAL ACTIVITY OF FLUCONAZOLE AGAINST A PDR5P-MEDIATED RESISTANT *SACCHAROMYCES CEREVISIAE* STRAIN. BRAZILIAN JOURNAL OF MICROBIOLOGY. 2020 SEP;51(3):1051-1060. DOI: 10.1007/S42770-020-00254-9.

ARTIGOS ACEITOS PARA PUBLICAÇÃO

A JULIANA L. SOUZA, J.L.; **MARTINS-CARDOSO, K**.; GUIMARÃES, I.S.; MELO, A.C.; LOPES, A.H.; MONTEIRO, R.Q.; ALMEIDA, V.H. INTERPLAY BETWEEN EGFR AND THE PLATELET-ACTIVATING FACTOR (PAF)/PAF RECEPTOR SIGNALING AXIS MEDIATES AGGRESSIVE BEHAVIOR OF CERVICAL CANCER. FRONTIERS IN ONCOLOGY. DOI: 10.3389/FONC.2020.557280

B FAUSTO G. GOMES, F.G; ALMEIDA, V.H; **MARTINS-CARDOSO**, K.; MARTINS-DINIS, M.M; RONDON, A.M; MELO, A.C; TILLI, T.M.; MONTEIRO, R.Q. EPIDERMAL GROWTH FACTOR RECEPTOR REGULATES FIBRINOLYTIC PATHWAY ELEMENTS IN CERVICAL CANCER: FUNCTIONAL AND PROGNOSTIC IMPLICATIONS. BRAZILIAN JOURNAL OF MEDICAL AND BIOLOGICAL RESEARCH.

cancers

MDPI

Article

Neutrophil Extracellular Traps (NETs) Promote Pro-Metastatic Phenotype in Human Breast Cancer Cells through Epithelial–Mesenchymal Transition

Karina Martins-Cardoso [1], Vitor H. Almeida [1], Kayo M. Bagri [2], Maria Isabel Doria Rossi [2,3], Claudia S. Mermelstein [2], Sandra König [2] and Robson Q. Monteiro [1,*]

1 Institute of Medical Biochemistry Leopoldo de Meis, Federal University of Rio de Janeiro, Rio de Janeiro 21941 590, Brazil; kmcardoso@bioqmed.ufrj.br (K.M.-C.); vhluna@bioqmed.ufrj.br (V.H.A.)
2 Institute of Biomedical Sciences, Federal University of Rio de Janeiro, Rio de Janeiro 21941 590, Brazil; kayobiomed14@histo.ufrj.br (K.M.B.); idrossi@hucff.ufrj.br (M.I.D.R.); mermelstein@ufrj.br (C.S.M.); sandra@icb.ufrj.br (S.K.)
3 Clementino Fraga Filho University Hospital, Federal University of Rio de Janeiro, Rio de Janeiro 21941 913, Brazil
* Correspondence: robsonqm@bioqmed.ufrj.br

Received: 4 May 2020; Accepted: 9 June 2020; Published: 11 June 2020

Abstract: Neutrophil extracellular traps (NETs) have been associated with several steps of tumor progression, including primary growth and metastasis. One of the key features for the acquisition of the metastatic ability is the epithelial–mesenchymal transition (EMT), a complex cellular program. In this study, we evaluated the ability of isolated NETs in modulating the pro-metastatic phenotype of human breast cancer cells. Tumor cells were treated with isolated NETs and then samples were generated for cell migration, quantitative RT-PCR, western blotting, immunofluorescence, and flow cytometry assays. RNA-seq data from The Cancer Genome Atlas (TCGA) database were assessed. NETs changed the typical epithelial morphology of MCF7 cells into a mesenchymal phenotype, a process that was accompanied by enhanced migratory properties. Additional EMT traits were observed: increased expression of N-cadherin and fibronectin, while the E-cadherin expression was repressed. Notably, NETs positively regulated the gene expression of several factors linked to the pro-inflammatory and pro-metastatic properties. Analyses of TCGA data showed that samples from breast cancer patients exhibit a significant correlation between pro-tumoral and neutrophil signature gene expression, including several EMT and pro-metastatic factors. Therefore, NETs drive pro-metastatic phenotype in human breast cancer cells through the activation of the EMT program.

Keywords: epithelial–mesenchymal transition; neutrophil extracellular traps; breast cancer; metastasis

1. Introduction

Breast cancer is the most prevalent with the highest mortality rate in women worldwide [1]. Immunohistochemical markers, as well as genomic data, allow classifying breast cancer into subtypes that are biologically distinct and behave differently concerning therapeutic response and clinical outcome [2,3]. Breast cancer subtypes include luminal A, luminal B, human epidermal growth factor receptor-2 positive/estrogen receptor-negative (HER2+/ER−), and triple-negative (which includes basal-like). These subtypes are associated with distinct patterns of metastatic spread with significant differences in survival after relapse, in which luminal A and triple-negative represent the less and the more aggressive subtypes, respectively [4,5].

The ability of cancer cells to disseminate from primary tumors to form new tumor colonies in distant tissues is defined as metastasis, one of the hallmarks of cancer [6]. Acquisition of the metastatic capacity

is a complex process that may involve an intricate cellular program named epithelial–mesenchymal transition (EMT). EMT is driven by a set of transcriptional factors, including Snail (also known as SNAI1), Slug (also known as SNAI2), Twist-related protein 1 (TWIST1), zinc-finger E-box-binding homeobox 1 (ZEB1) and ZEB2, that regulate gene expression alterations which culminate with enhanced tumor cell migration, invasion, and metastatic properties [7,8]. EMT program is strongly influenced by stromal cells in the tumor microenvironment, which include endothelial cells, fibroblasts, inflammatory, immune cells, and others [9–11].

Among the immune cells, neutrophils are the most abundant and the first inflammatory cells recruited to the sites of tissue damage and infection [11,12]. Several lines of evidence indicate that tumor-associated neutrophils are important players in cancer progression [12,13]. More recently, it has been proposed that neutrophils may influence the tumor properties through the release of neutrophil extracellular traps (NETs) [14–17]. Primarily described as an antimicrobial mechanism, NETs are composed of a double-stranded DNA decorated with neutrophil nuclear and granular proteins, such as citrullinated histones, myeloperoxidase, metalloproteinases, and elastase [18]. Subsequent studies have demonstrated that NETs have several pro-tumoral capabilities, including the ability to sequester circulating tumor cells and contribute to metastasis [19,20], to support primary tumor growth [21,22], to modulate the pro-inflammatory tumor microenvironment [23,24] and to establish the cancer-associated prothrombotic state [25–27]. It is unclear, however, whether NETs may influence EMT to support tumor progression.

In the present study, we evaluated the ability of isolated NETs in modulating the pro-metastatic phenotype of human breast cancer cells. Incubation of isolated NETs with the luminal cell line, MCF7, altered the epithelial morphology into a mesenchymal phenotype. In accordance with the acquisition of the mesenchymal phenotype, MCF7-treated cells showed enhanced migratory properties. Morphological changes were accompanied by enhanced gene expression of the EMT-related transcriptional factors, *ZEB1* and Snail (*SNAI1*). Notably, the treatment of MCF7 cells with NETs increased the expression of N-cadherin and fibronectin, while the E-cadherin expression was repressed. NETs positively regulated gene expression of several factors linked to the pro-inflammatory and pro-metastatic properties of breast cancer cells, including interleukin-1β (IL-1β/*IL1B*), interleukin-6 (IL-6/*IL6*), interleukin-8 (IL-8/*CXCL8*), *CXCR1*, matrix metalloprotease-2 (MMP-2/*MMP2*), *MMP9*, and *CD44*. Further analyses of data from The Cancer Genome Atlas (TCGA) showed that samples from breast cancer patients exhibit a significant correlation between neutrophil signature and pro-tumoral genes, including several EMT and pro-metastatic factors. Our results suggest that NETs released in the primary tumor may contribute to the acquisition of metastatic properties during breast cancer progression. Taken together, the modulation of NETs formation during tumor progression might represent an attractive therapeutic target to decrease the metastatic spread.

2. Results

2.1. NETs Alter the Morphology and Enhance the Migratory Pattern in MCF7 Cells

The MCF7 cell line, which has been classified as a luminal subtype [28], displays an epithelial phenotype, with polyhedral form, and can form islets in vitro. Incubation of MCF7 cells with NETs for 16 h promoted drastic morphological changes (Figure 1a).

After 8 h of treatment with NETs, MCF7 cells began to acquire a more elongated fibroblast-like shape, presenting an expressive amount of membrane protrusions. We also noticed the loss of cell adhesion to the cell culture flasks after treatment with NETs. Previous findings showed that NETs increase the migratory pattern of tumor cells including colorectal, lung carcinoma, and lymphoma [15,19,29]. Then, we sought to evaluate the effect of NETs on the migratory behavior of MCF7 cells. Treatment of MCF7 cells with NETs enhanced the tumor cell migration either in the absence or in the presence of 2 or 10% fetal bovine serum (FBS) used as a chemoattractant (Figure 1b). Thus, isolated NETs promoted MCF7 migration in all conditions tested in this study.

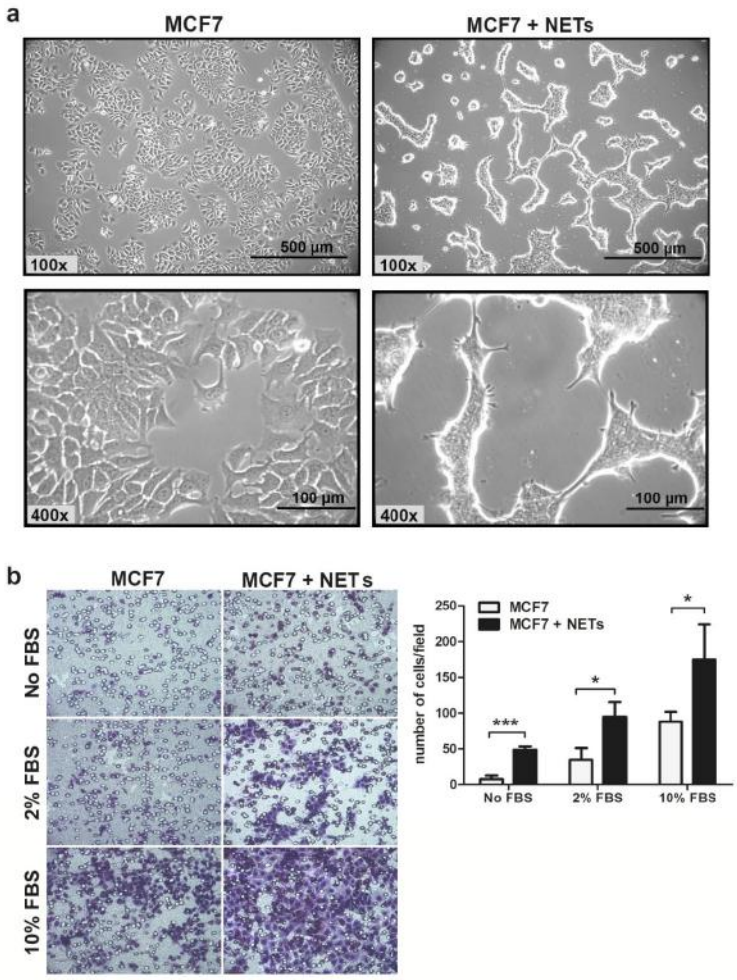

Figure 1. Neutrophil extracellular traps (NETs) alter cell morphology and enhance MCF7 migration in vitro. (**a**) Representative images of MCF7 cells that were cultured for 16 h in the absence (left) or the presence (right) of NETs (500 ng/mL). Magnification 100× and 400×, scale bar 500 µm and 100 µm, respectively. (**b**) Tumor cell migration was evaluated employing the Boyden chamber assay. MCF7 cells that were cultured for 16 h in the absence or the presence of NETs (500 ng/mL) were seeded in the upper chamber (5×10^4 cells/well) and further allowed to migrate for 20 h. As chemoattractant, medium supplemented with fetal bovine serum (FBS) (2% or 10%) was used in lower chambers. Representative images of the migration assay are shown on the left panel (200× magnification). Migrated cells were quantified, and results are shown on the right panel. Data are presented as mean ± SD from three independent experiments. Statistical analysis of each condition was evaluated by unpaired *t*-test. Significance was assumed for * $p < 0.05$, *** $p < 0.001$.

2.2. NETs Promote EMT in Breast Cancer Cells

Changes in cell morphology induced by NETs seemed a typical EMT process [30]. To investigate the possibility of a transition from epithelial to mesenchymal features induced by NETs in MCF7 cells, we next evaluated the expression of transcriptional factors known to regulate the EMT process. Quantitative RT-PCR analyses showed a significant increase in the expression of ZEB1 (*ZEB1)* and Snail (*SNAI1*) genes upon treatment of MCF7 cells with NETs (Figure 2a). No changes in the expression pattern of *ZEB2*, Slug (*SNAI2*), or Twist1 (*TWIST1)* were observed. The EMT process is marked by the loss of epithelial markers, such as E-cadherin, along with the enhancement of expression of mesenchymal markers, such as N-cadherin, fibronectin, and vimentin [7]. We further employed western blotting to evaluate the protein levels of E-cadherin, fibronectin, and vimentin. As expected, luminal-like MCF7 cells express E-cadherin and failed to express fibronectin and vimentin while basal-like MDA-MB-231

cells present a mesenchymal profile with no E-cadherin and high fibronectin and vimentin expression patterns (Figure 2b and Figure S1a–d). Interestingly, E-cadherin levels gradually reduced over time in MCF7 cells upon treatment with NETs (Figure 2b and Figure S1a,d). A similar result was observed upon treatment of the HER2+ breast cancer cell line, HCC 1954 (Figures S1e and S2), both at the protein and gene expression levels. On the other hand, fibronectin levels were progressively increased in MCF7 cells over the incubation time (Figure 2b and Figure S1b,d). Vimentin expression, which is usually not observed in MCF7 cells, appeared to be not modulated upon incubation with NETs (Figure 2b and Figure S1c,d).

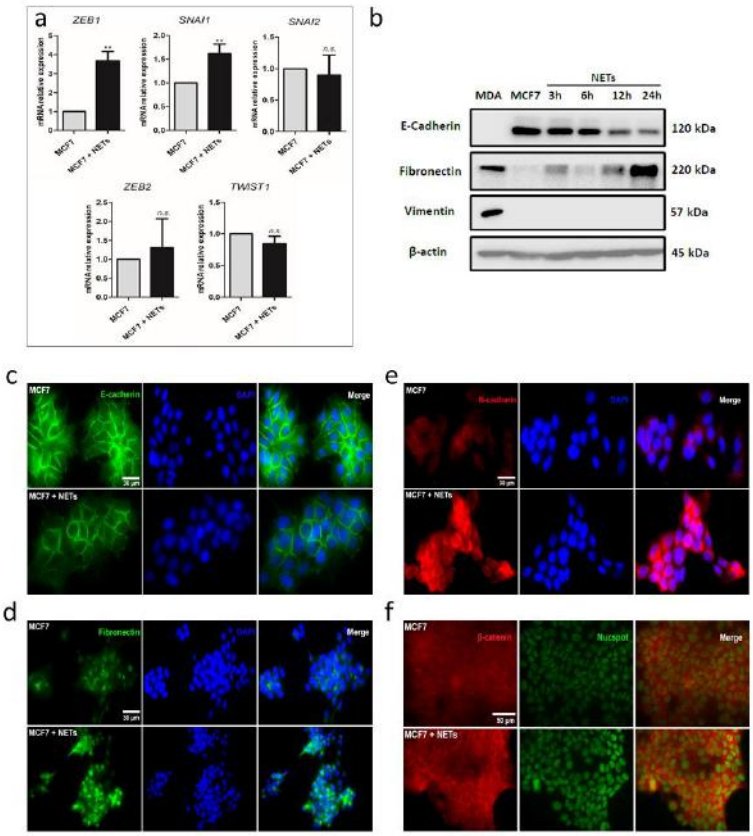

Figure 2. NETs promote epithelial–mesenchymal transition (EMT) in MCF7 cells. (**a**) Gene expression of EMT transcription factors was analyzed by quantitative RT-PCR. *GAPDH* was used as the reference gene. Relative expression of mRNA was calculated using the ΔΔCT method. Columns represent means ± SD of a minimum of three independent experiments. Unpaired *t*-test was applied for statistical analysis. ** $p < 0.01$ and *n.s.*, no significance. (**b**) Western blot analysis of the EMT markers protein levels (E-cadherin, fibronectin, and vimentin) in MCF7 cells (1×10^6) treated with NETs (500 ng/mL) for 3 to 24 h. β-actin was used as a loading control and MDA-MB-231 (MDA) was used as a mesenchymal cell model. Representative image from two independent experiments. Immunocytochemistry analysis of (**c**) E-cadherin (green, magnification 630×, scale bars 30 μm); (**d**) fibronectin (green, magnification 400×, scale bars 30 μm); (**e**) N-cadherin (red, magnification 630×, scale bars 30 μm); and (**f**) β-catenin (red, magnification 630×, scale bars 50 μm) in MCF7 cells that were cultured for 16 h in the absence (above) or the presence (below) of NETs (500 ng/mL). Nuclei were stained with 4′,6-Diamidino-2-Phenylindole (DAPI) (blue) or NucSpot (green) and merged images are shown on the right panels.

Changes in the expression pattern of E-cadherin and fibronectin were confirmed by immunofluorescence assays (Figure 2c,d and Figure S3). The typical E-cadherin downregulation observed in the EMT process is usually accompanied by an increase in the N-cadherin expression, a process known as "cadherin switching". Here, we also employed immunofluorescence to demonstrate

an increase in the N-cadherin expression pattern in MCF7 cells cultured in the presence of NETs (Figure 2e and Figure S3).

E-cadherin is a cell surface protein that may associate with the multifunctional protein, β-catenin, at the cell membrane. β-catenin commonly acts as a signal transducer of the canonical Wnt pathway, also related to EMT [31,32]. Earlier works suggest that E-cadherin can physically sequester β-catenin at the cell membrane. Thus, E-cadherin-associated β-catenin represents a reserve pool of β-catenin that can potentially feed into Wnt signaling activity [33]. In this context, immunofluorescence assays revealed higher expression of β-catenin in MCF7 cells treated with NETs, as compared to untreated cells (Figure 2f and Figure S3). Together, these results support the capacity of NETs to promote EMT in the breast cancer cell line, MCF7.

2.3. Stem Cell Markers are Modulated by NETs

There is strong evidence that the EMT program is associated with the maintenance of cancer stem cells (CSCs) in solid tumors [34]. In breast cancer, the combined expression of CD44 and CD24, commonly reveals enrichment of the $CD44^{-}CD24^{+}$ and $CD44^{+}CD24^{Lo/-}$ cell phenotypes in luminal and basal-like breast cancer cell lines, respectively [35,36]. We then investigated if isolated NETs could interfere with stem cell features of MCF7 cells by analyzing the expression of the cell surface markers, CD44 and CD24. As seen in Figure 3, NETs promoted a significant reduction in *CD24* gene expression as well as a trend to decreased cell surface protein expression in MCF7 cells, according to flow-cytometric analysis (Figure 3a–c).

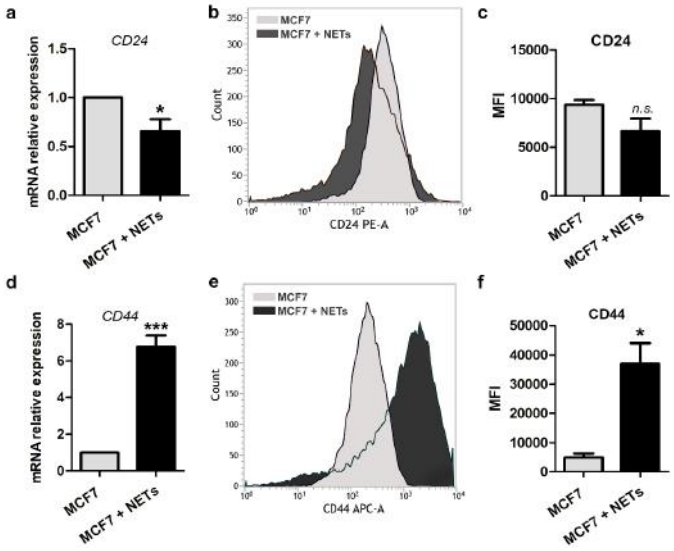

Figure 3. Cancer stem cell markers are regulated by NETs. Gene expression of *CD24* (**a**) and *CD44* (**d**) was analyzed by quantitative RT-PCR in MCF7 cells that were cultured for 16 h in the absence (gray bar) or the presence (black bar) of NETs (500 ng/mL). *GAPDH* was used as the reference gene. The relative expression level of the mRNA was calculated using the ΔΔCT method. Values represent means ± SD of three independent experiments. Representative histograms of flow cytometry analysis of CD24 (**b**) and CD44 (**e**). Graphic representation of relative mean of fluorescence intensities (MFI) of phycoerythrin (PE)-labeled CD24 antibody (**c**) and allophycocyanin (APC)-labeled CD44 antibody (**f**). Data shown are from two independent experiments. Unpaired *t*-test was applied for statistical analysis. Significance was assumed for * $p < 0.05$, *** $p < 0.001$; *n.s.*, no significance.

On the other hand, MCF7 cells treated with NETs showed significant enrichment in the CD44 marker, as evaluated by quantitative RT-PCR and flow cytometry (Figure 3d–f). Changes in the expression pattern of CD24 and CD44 markers in NETs-treated MCF7 cells lead us to suggest that along with EMT activation, NETs may promote enrichment in cells with CSC-like features.

2.4. NETs Induce a Pro-Inflammatory Response in Breast Cancer Cells

The activity of the EMT-related transcriptional factors has been linked with the production of pro-inflammatory cytokines that play key roles in the metastatic process [37]. In this context, we next evaluated the ability of NETs in modulating the expression of a set of cytokines described to be crucial for breast cancer development. As shown in Figure 4, quantitative RT-PCR analysis revealed a significant increase in the gene expression of IL-1β/*IL1B* (~15-fold), *IL6* (~10-fold), and IL-8/*CXCL8* (~10-fold). The upregulation of *CXCL8* expression in MCF7 cells was accompanied by the induction of *CXCR1* expression (~2-fold increase), which encodes for a major IL-8 receptor (Figure 4). We further evaluated the impact of NETs on MMPs gene expression, since these enzymes regulate the remodeling of the extracellular matrix, thus favoring invasion and metastasis [9,38]. Remarkably, the expression of *MMP2* and *MMP9* was ~100-fold higher in NETs-treated MCF7 cells as compared to the untreated cells (Figure 4). As seen with MCF7 cells, incubation of HCC 1954 with NETs enhanced *MMP9* expression (Figure S2b). We also employed isolated NETs to treat the basal-like MDA-MB-231 cell line, known to secrete high levels of IL-1β and IL-8. Treatment of MDA-MB-231 cells upregulated *IL1B* and *CXCL8* gene expression, as well as cyclooxygenase-2 (COX-2/*PTGS2)* (Figure 4). Together, these results indicate that NETs induce a pro-inflammatory response in breast cancer cells.

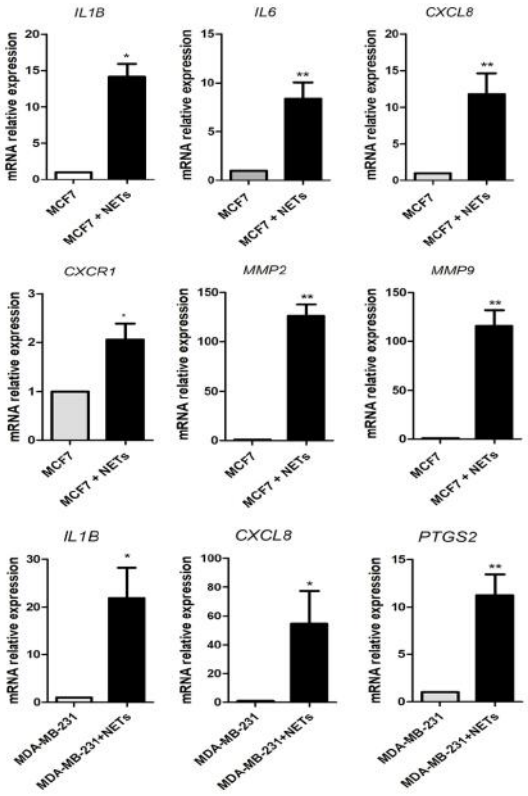

Figure 4. Pro-tumoral and pro-inflammatory mediators are regulated by NETs. MCF7 cells (5×10^5) were starved and further cultured for 16 h in the absence (grey bar) or the presence (black bar) of NETs (500 ng/mL). Genes analyzed: interleukin-1β (IL-1β/*IL1B*), interleukin-6 (IL-6/*IL6*), interleukin-8 (IL-8/*CXCL8*), *CXCR1*, matrix metalloprotease-2 (MMP-2/*MMP2*), and *MMP9*. MDA-MB-231 cells (5×10^5) were cultured for 3 h in the absence or the presence of NETs (500 ng/mL). Genes analyzed: *IL1B*, *CXCL8*, and cyclooxygenase-2 (COX-2/*PTGS2*). Gene expression was evaluated by quantitative RT-PCR using the ΔΔCT method. *GAPDH* was used as the reference gene. Columns represent means ± SD of three independent experiments. Statistical analysis was performed using unpaired *t*-test. * $p < 0.05$ and ** $p < 0.01$.

2.5. Neutrophil-Related Genes Correlate with Pro-Tumoral and EMT Genes in Breast Cancer Patients

To investigate the relevance of our in vitro findings for cancer patients, we used transcriptome data deposited in TCGA database. For this purpose, we first analyzed a set of genes defined as a neutrophil-related signature in the different breast cancer subtypes. These neutrophil-related genes (*MPO*, *DEFA1B*, *MMP8*, *CEACAM8*, *LTF*, and *DEFA4*) were identified and evaluated in a previous study [39]. The *MPO* gene encodes myeloperoxidase, an abundant enzyme in the neutrophil azurophilic granules, which has microbicidal activity through the generation of hypochlorous acid [40]. *DEFA1B* and *DEFA4* encode α-defensins found in azurophil granules of neutrophils. These defensins are small cationic peptides that promote the permeabilization and disruption of cell membranes, killing pathogens [41]. Matrix metalloproteinase-8 (*MMP8*) is an endopeptidase mainly produced by neutrophils. When neutrophils are activated, MMP-8 is released from intracellular granules and cleaves some extracellular matrix proteins, such as collagen, as well as other substrates [42]. CEACAM8, also known as CD66b, is a glycoprotein that plays a role in cell adhesion. CD66b is exclusively expressed on human granulocytes and is recognized as a granulocyte activation marker [43]. *LTF* gene is a member of the transferrin gene family and its protein product, lactotransferrin, is found in the secondary granules of neutrophils. Lactotransferrin released by neutrophils acts as a first-line defense against pathogens through the chelation of iron [44]. As seen in Figure 5, most of the neutrophil-related genes were increasingly expressed from luminal A to basal breast cancer subtypes. This observation agrees with an enhanced neutrophil accumulation in more aggressive breast cancer subtypes [45].

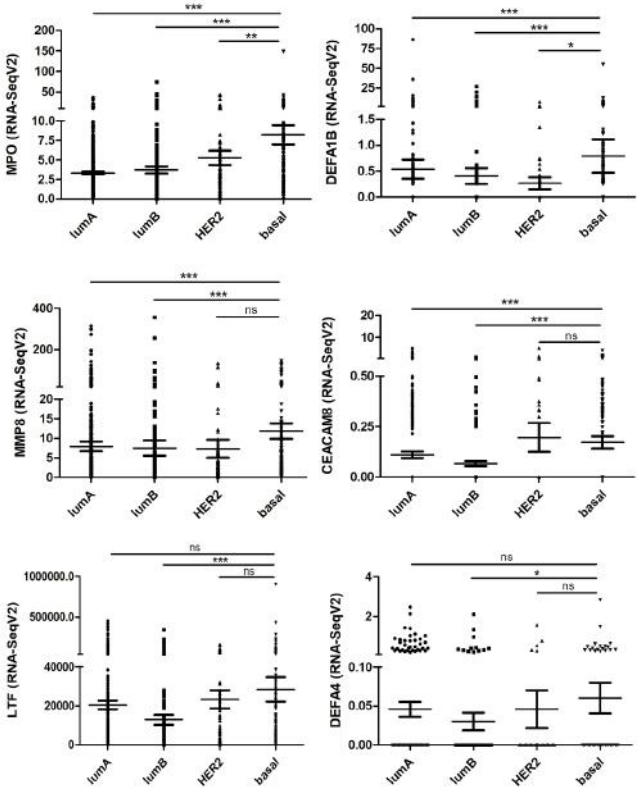

Figure 5. Analysis of neutrophil-related signature genes in the different breast cancer subtypes. RNA seq values (Fragments Per Kilobase Million, FPKM) of 1100 breast cancer samples, deposited in The Cancer Genome Atlas (TCGA) database, were stratified into Luminal A (lumA), Luminal B (lumB), HER2+ (HER2), and Basal subtypes. Genes analyzed: *MPO* (myeloperoxidase), *DEFA1B* (a-defensin 1B), *MMP8* (MMP8), *CEACAM8* (CD66b), *LTF* (lactotransferrin), and *DEFA4* (a-defensin 4). The Mann–Whitney U test was used to test for statistical significance. * $p < 0.05$, ** $p < 0.01$, *** $p < 0.001$, and n.s.: no significance.

Next, we analyzed the neutrophil-related signature gene expression versus genes encoding pro-inflammatory and pro-metastatic factors (Table 1). We found a positive correlation between neutrophil genes and several pro-tumoral factors that were upregulated in vitro. *CXCL8*, *CXCR1*, *IL1B*, *IL6*, *MMP2*, and *MMP9* showed a positive correlation with at least 3 out of 6 neutrophil signature genes. We have also analyzed EMT-related genes with the neutrophil signature genes (Table 1). We noticed a positive correlation between the neutrophil signature genes with Snail (*SNAI1)* and β-catenin *(CTNNB1)* genes. As expected, the E-cadherin *(CDH1)* gene expression showed a negative correlation with the neutrophil signature genes, since NETs decreased E-cadherin expression in MCF7 cells. *ZEB1*, fibronectin (*FN1*) and N-cadherin *(CDH2)* correlations were inconclusive. No correlation between the expression of *CD24* and *CD44* genes with the neutrophil signature genes was observed, possibly reflecting the heterogeneity of CSC markers in the primary tumors.

Table 1. Correlation analysis between neutrophil signature genes and pro-tumoral genes in human breast cancer samples from The Cancer Genome Atlas (TCGA).

Genes	*CEACAM8*	*DEFA1B*	*DEFA4*	*LTF*	*MMP8*	*MPO*
Interleukin-1β (*IL1B*)	r = 0.0767 p = 0.0109	r = 0.116 p = 0.0001	r = 0.0655 p = 0.0297	r = 0.255 p < 0.0001	r = 0.225 p < 0.0001	r = 0.183 p < 0.0001
Interleukin-6 *(IL6)*	r = 0.0983 p = 0.0011	r = 0.197 p < 0.0001	r = 0.124 p < 0.0001	r = 0.232 p < 0.0001	r = 0.208 p < 0.0001	r = 0.314 p < 0.0001
Interleukin-8 (*CXCL8*)	r = 0.0445 p = 0.14	r = 0.141 p < 0.0001	r = −0.0277 p = 0.359	r = 0.0963 p = 0.0014	r = 0.39 p < 0.0001	r = 0.156 p < 0.0001
CXCR1 *(CXCR1)*	r = 0.0242 p = 0.422	r = 0.117 p < 0.0001	r = 0.0879 p = 0.0035	r = 0.131 p < 0.0001	r = 0.0677 p = 0.0248	r = −0.008 p = 0.788
MMP-2 *(MMP2)*	r = −0.00765 p = 0.800	r = 0.0114 p = 0.705	r = 0.0351 p = 0.245	r = 0.173 p < 0.0001	r = 0.286 p < 0.0001	r = 0.154 p < 0.0001
MMP-9 *(MMP9)*	r = 0.012 p = 0.692	r = 0.114 p = 0.0002	r = 0.120 p < 0.0001	r = 0.0315 p = 0.297	r = 0.408 p < 0.0001	r = 0.21 p < 0.0001
Snail (*SNAI1*)	r = 0.0959 p = 0.0014	r = 0.162 p < 0.0001	r = 0.0522 p = 0.0834	r = 0.179 p < 0.0001	r = 0.281 p < 0.0001	r = 0.211 p < 0.0001
ZEB1 *(ZEB1)*	r = −0.0491 p = 0.103	r = −0.0773 p = 0.0103	r = 0.0183 p = 0.544	r = 0.0921 p = 0.0022	r = 0.132 p < 0.0001	r = 0.0499 p = 0.0982
E-cadherin (*CDH1*)	r = −0.041 p = 0.174	r = −0.0728 p = 0.0157	r = −0.0796 p = 0.0083	r = −0.194 p < 0.0001	r = −0.0473 p = 0.117	r = −0.144 p < 0.0001
Fibronectin (*FN1*)	r = −0.0507 p = 0.0927	r = −0.0792 p = 0.0086	r = −0.0464 p = 0.124	r = −0.0149 p = 0.621	r = 0.384 p < 0.0001	r = −0.0309 p = 0.307
N-cadherin (*CDH2*)	r = 0.0134 p = 0.657	r = −0.0217 p = 0.472	r = −0.045 p = 0.136	r = −0.102 p = 0.0007	r = 0.275 p < 0.0001	r = 0.0302 p = 0.316
β-catenin (*CTNNB1*)	r = −0.0022 p = 0.941	r = −0.0476 p = 0.115	r = −0.0004 p = 0.99	r = 0.196 p < 0.0001	r = 0.176 p < 0.0001	r = 0.0633 p = 0.0359
CD24 *(CD24)*	r = 0.030 p = 0.317	r = 0.0319 p = 0.291	r = −0.00795 p = 0.792	r = −0.0114 p = 0.706	r = 0.0796 p = 0.0083	r = 0.0605 p = 0.0447
CD44 *(CD44)*	r = −0.0254 p = 0.399	r = 0.0458 p = 0.129	r = 0.0443 p = 0.142	r = 0.014 p = 0.642	r = 0.0157 p = 0.602	r = 0.0578 p = 0.0555

Grey: No correlation; green: Positive correlation; red: Negative correlation. r = coefficient of correlation.

3. Discussion

Inflammation is one of the hallmarks of cancer [6]. The presence of leukocytes in the tumor microenvironment is well described and is extremely dynamic during the disease progression. Several lines of evidence support a role for the sustained chronic inflammation in promoting the tumor aggressiveness, including the metastatic potential. Among the immune cells found in the tumor microenvironment, neutrophils have been pointed out as important mediators of tumor progression [12,13,46]. More recently, neutrophil extracellular traps (NETs) have been associated with several steps of tumor progression, including primary growth and metastasis [19–22].

One of the key mechanisms supported by the immune/inflammatory microenvironment is the epithelial–mesenchymal transition (EMT) [37]. Key features during the EMT process include the loss of epithelial markers, such as E-cadherin, along with the enhancement of expression of

mesenchymal markers, such as N-cadherin, fibronectin, and vimentin. This process has been pointed as a dynamic gradient of loss and gain of cellular features and there are several pieces of evidence for the existence of intermediate stages, wherein both mesenchymal and epithelial markers might be co-expressed [7,8] This is in part explained by the concerted action of different transcription factors that modulate the EMT features, in which Snail and ZEB1, which are strong epithelial repressors, seem to be more activated in the intermediate EMT stages [7]. Herein, we observed that NETs promote a significant decrease in the E-cadherin expression by MCF7 cells, with minor changes in the vimentin expression pattern. This was accompanied by increased ZEB1 (*ZEB1)* and Snail *(SNAI1)* gene expression, while no changes in the expression pattern of ZEB2 (*ZEB2*), Slug (*SNAI2*) or Twist1 (*TWIST1)* were observed. In this context, vimentin expression is regulated by Slug in breast cancer models [47]. On the other hand, Huang and co-workers [48] have shown that some ovarian carcinoma cell lines exhibit intermediate EMT states presenting low E-cadherin and high vimentin expression patterns [48]. Interestingly, other EMT inducers, such as epidermal growth factor (EGF) and transforming growth factor-beta (TGF-β), were able to induce vimentin expression in MCF7 cells within 24 h of treatment [49,50]. These data suggest that the mechanism triggered by NETs seems to be slightly different from the other inducers and/or that the NET-evoked EMT occurs in a partial way. The chronic effect of NETs on EMT induction after prolonged treatments deserves further investigation.

Aberrant activation of the Wnt/β-catenin signaling pathway has been associated with several aspects of cancer biology, including tumor initiation, EMT, and metastasis [31]. As a result of the excessive Wnt/β-catenin signaling, β-catenin accumulates in the cytoplasm or within the nucleus of tumor cells, serving as a transcriptional factor, along with other partners, of pro-tumoral genes [31]. Moreover, Kim and colleagues [51] provided data showing that cell membrane-bound β-catenin evokes pro-tumoral responses by enhancing the signaling of growth factor receptors such as the epidermal growth factor receptor (EGFR) [51]. Therefore, β-catenin may exhibit pro-tumoral functions regardless of its subcellular location. Herein it was observed that treatment of MCF7 cells with NETs significantly enhanced β-catenin expression although showing a minor impact on the subcellular location of this protein. Whether NETs-induced changes in the β-catenin expression pattern accounts for the upregulation of pro-tumoral factors have yet to be evaluated.

The EMT program has been correlated with cancer stem cell (CSC) traits, including the expression of stem cell-associated antigens, enhanced chemotherapy resistance, and self-renewal properties [34,52,53]. Among the CSC surface markers, CD44 and CD24 phenotype have been widely employed in breast cancer research [35,36]. CD44 is a cell-surface glycoprotein receptor that recognizes several ligands including extracellular matrix components, such as hyaluronic acid, osteopontin, metalloproteinases, and others [54]. CD44 has been associated with migration and metastasis, being upregulated in the triple-negative breast cancer subtype [54]. Remarkably, CSC subpopulations that exhibit the $CD44^{+}CD24^{Lo/-}$ phenotype usually display increased tumorigenic properties and a higher capacity to metastasize [55]. Here, we show that the treatment of MCF7 cells, which typically exhibits the $CD44^{Lo/-}CD24^{+}$ phenotype, upregulates the gene and protein expression levels of CD44. It remains to be determined whether these changes parallel with the acquisition of additional CSC features, including additional CSC markers, enhanced tumorigenic properties, and drug resistance.

The major components of NETs (histone, DNA, and granule proteins) are recognized as damage-associated molecular patterns (DAMPs). DAMPS can be recognized through the Toll-like receptors (TLRs). For example, extracellular histones can activate TLR2 and TLR4, while TLR9 is a cell surface receptor of CpG motifs in DNA [56,57]. All TLR signaling pathways culminate in the activation of the transcription factor nuclear factor-kappa B (NF-κB), which controls the expression of several inflammatory cytokine genes [58]. Herein, we observed that the treatment of breast cancer cell lines with NETs upregulates the expression of several pro-inflammatory genes, including IL-8 (*CXCL8*), *IL6*, IL-1β (*IL1B*), and *CXCR1*. Furthermore, bioinformatics tools and chromatin immunoprecipitation assays identified many NF-κB binding sites along with the promoters of SNAI1, SNAI2, ZEB2, and TWIST1 genes [59]. Indeed, NF-κB is essential for EMT and metastasis in a model of breast cancer [60]. In this

same line, inflammatory factors in the tumor microenvironment, including TGF-β, IL-6, IL-1β, IL-8, and others can induce EMT [61–63]. On the other hand, EMT-transcription factors can modulate inflammation during the EMT process. For example, Katsura and colleagues [64] have shown that knockdown of *ZEB1* in MDA-MB-231 cells decreases the in vitro production of IL-6 and IL-8 [64]. Interestingly, we observed a significant increase in ZEB1 (*ZEB1*) and Snail (*SNAI1*) gene expression by MCF7 cells that were treated with NETs. Together, these data suggest an important linkage between inflammation and EMT signaling in breast cancer cells. Indeed, pro-inflammatory cytokine expression has also been associated with malignant progression and poor prognosis in breast carcinomas [65].

The DNA integrity of NETs has been pointed out as an essential condition for promoting some of their biological activities. Therefore, treatment with DNase, which efficiently degrades NETs, attenuates the development and progression of liver metastases in a murine model of colorectal cancer [15]. Similar antimetastatic effects have been observed in hepatocellular carcinoma and breast cancer models [20,23]. Moreover, the degradation of NETs substantially reduces cancer-associated thrombosis in neutrophilia-related breast and pancreas cancer models [26,66]. Interestingly, we observed that the digestion of NETs with DNase had a minor impact on tumor cell migration as well as in the *CXCL8* and *MMP9* gene expression (Figure S4). Therefore, we believe that, under our experimental conditions, DNA integrity is dispensable for the effect of NETs towards MCF7 cells.

The presence of neutrophils in primary tumors has been correlated with poor prognosis in human cancer [67]. Thus, increased infiltration of intratumoral neutrophils was associated with unfavorable survival and recurrence in several cancer types, including hepatocellular carcinoma, non-small-cell lung cancer, cervical cancer, and others [67]. More recently, it was reported an enhanced neutrophil accumulation in more aggressive breast cancer subtypes [45]. Here, we analyzed transcriptome data from breast cancer patients and showed a positive correlation between neutrophil signature genes and several pro-tumoral factors that were upregulated in vitro upon treatment with NETs, including pro-inflammatory and EMT-related factors. Remarkably, the contribution of neutrophil for the EMT process has been previously suggested in different cancer types, including lung adenocarcinoma and ovarian cancer [68,69].

4. Materials and Methods

4.1. Cell Culture

Breast cancer cell lines (MCF7, HCC 1954, and MDA-MB-231) were from the Rio de Janeiro Cell Bank (Rio de Janeiro, RJ, Brazil). Cells were maintained in DMEM (Dulbecco's Modified Eagle Medium, Thermo Fisher Scientific, Waltham, MA, USA) supplemented with 10% fetal bovine serum (FBS) (Cultilab, Campinas, Brazil) and 1% penicillin/streptomycin (Thermo Fisher Scientific) at 37 °C in 5% CO_2 atmosphere. For all experiments, after seeding, cells were starved for 10 h before treatment with NETs.

4.2. Neutrophils Isolation and NETs Obtention

Venous blood from healthy donors was collected in sodium citrate tubes. Neutrophils were purified from whole blood using Histopaque-1077 based (Merck, Darmstadt, Germany) density gradient centrifugation. Isolated neutrophils were stimulated with 500 nM Phorbol 12-myristate 13-acetate (Merck, Darmstadt, Germany) for 4 h. NETs were isolated following a previously described procedure [70], resuspended in sterile phosphate-buffered saline (PBS), and quantified using NanoDrop Lite Spectrophotometer (Thermo Fisher Scientific). Isolated NETs were kept at 4 °C for no more than 24 h. This protocol followed ethical standards and was approved by an institutional committee (Clementino Fraga Filho University Hospital, Federal University of Rio de Janeiro) under registry 82933518.0.0000.525.

4.3. Migration Assay

Boyden chamber assay was used to evaluate tumor cell migration employing 8 μm pore polycarbonate membranes (Neuro Probe, Gaithersburg, MD, USA). MCF7 cells (5×10^4) were cultured in the absence or the presence of NETs (500 ng/mL) for 16 h. Cells were further resuspended and seeded to the upper chambers into 50 μL serum-free medium. DMEM medium in the absence or the presence of 2 or 10% FBS was added in the lower compartment. After 20 h of incubation at 37 °C in 5% CO_2, non-migrated cells on the upper surface of the membrane were removed and the membrane was fixed and stained using Fast Panoptic Staining (Laborclin, Nova Iguacu, Brazil). The average number of migrated cells was calculated from ten random fields counted per condition.

4.4. Quantitative RT-PCR

5×10^5 cells were washed twice with PBS and starved in serum-free medium for 10 h followed by treatment with NETs (500 ng/mL). After 16 h, cultured cells were washed twice with PBS to remove NETs, and total RNA was extracted using TRIzol Reagent (Thermo Fisher Scientific, Waltham, MA, USA). From each sample, 1 μg of RNA was submitted to DNase I treatment and reverse transcription PCR. Next, real-time PCR was performed on cDNA with SYBR Green Real-Time PCR Master Mix (Thermo Fisher Scientific, Waltham, MA, USA), using the StepOnePlus Real-Time PCR System (Thermo Fisher Scientific). All reagents and primers were purchased from Thermo Fisher Scientific and showed reaction efficiencies between 90–110%. The primer sequences are shown in the Table S1. Gene expression was normalized using *GAPDH* as the reference gene. To analyze the relative fold change, we employed the $2^{-\Delta\Delta CT}$ method.

4.5. Western Blot

1×10^6 cells were starved in serum-free medium and treated with NETs (500 ng/mL) for 3, 6, 12, or 24 h. After the treatment, cells were washed, lysed and proteins were quantified using the Lowry method (DC protein assay, Bio-Rad, Hercules, CA, USA). Protein lysates (30 μg) were run on 6–10% polyacrylamide gel electrophoresis under denaturing conditions in the presence of sodium dodecyl sulfate and transferred onto PVDF membranes (GE Healthcare, Sao Paulo, Brazil). Membranes were blocked and incubated overnight, at 4 °C, with the following primary antibodies against: E-cadherin (1:10,000; #61082; BD Biosciences, San Jose, CA, USA), fibronectin (1:750; #F3648; Merck, Darmstadt, Germany), vimentin (1:500; #M0725; DakoCytomation, Glostrup, Denmark) or β-actin (1:1000; #8457; Cell Signaling Technology, Danvers, MA, USA). Then, the membranes were incubated with HRP-conjugated secondary antibodies (DakoCytomation) for 1 h, at room temperature, and immunoblots were detected using the ECL reagent (GE Healthcare, Sao Paulo, Brazil).

4.6. Immunofluorescence Microscopy

MCF7 cells (2.5×10^5) were seeded on 22 mm-Aclar plastic coverslips (Pro-Plastics Inc., Linden, NJ, USA) previously coated with rat-tail collagen. After treatment with NETs (500 ng/mL) for 16 h, cells were fixed with 4% paraformaldehyde diluted in PBS (pH 7.4), permeabilized with PBS containing 0.5% Triton X-100 and incubated with primary antibodies against: β-catenin (1:50, #C-2206, Sigma Chemical Co, Saint Louis, MO, USA), E-cadherin (1:50, #04-1103, Millipore, Burlington, MA, USA), fibronectin (1:50, #F-6140, Sigma Chemical Co, Saint Louis, MO, USA) or N-cadherin (1:50, #C-3865, Sigma Chemical Co, Saint Louis, MO, USA) for 1 h at 37 °C. Cells were washed and incubated for 1 h at 37 °C with secondary antibodies Alexa Fluor 546 or Alexa Fluor 488 (1:100), all purchased from Thermo Fischer Scientific. Nuclei were labeled with 0.1 μg/mL DAPI (Thermo Fisher Scientific) or NucSpot (1:500, Biotium, Hayward, CA, USA) for 5 min. Slides were mounted in ProLong Gold antifade reagent (Molecular Probes, Eugene, OR, USA) and examined in an Axiovert 100 inverted microscope (Carl Zeiss, Oberkochen, Germany). Images were acquired with an Olympus DP71 digital camera (Olympus, Shinjuku City, Japan). The overall fluorescence intensity was quantified using the ImageJ

software (NIH, Bethesda, MD, USA), and results were expressed as a percentage, considering untreated cells as 100%.

4.7. Flow Cytometry Analysis

After treatment with NETs (500 ng/mL) for 16 h, cells were harvested and counted. A suspension with 1×10^6 cells/mL in serum-free medium was washed twice with flow cytometry buffer (PBS containing 0.01% sodium azide and 3% FBS). Next, conjugated antibodies were added, and cells were incubated for 30 min on ice. For this assay, mouse anti-human CD24 antibody conjugated with phycoerythrin (Clone ML5; Thermo Fisher Scientific) and rat anti-CD44 conjugated with allophycocyanin (Clone IM7; Thermo Fisher Scientific) were used. Flow cytometry acquisition was performed using a FACSCanto II with FACSDiva software (BD Biosciences, San Jose, CA, USA). The analysis was done using FlowJo software (BD Biosciences, San Jose, CA, USA) and the mean fluorescence intensity (MFI) of CD24 and CD44 was evaluated.

4.8. Gene Expression Correlation Analysis

Transcriptome data from 1100 breast cancer samples available at The Cancer Genome Atlas (TCGA, Firehose Legacy Study) were accessed using the cBioPortal [71,72]. The cBioPortal platform provided visualization, analysis, and the ability to download large-scale cancer genomics data sets. In our study, we analyzed the correlation between the expression of a previously defined set of neutrophil-related genes (*DEFA4*, *DEFA1B*, *MMP8*, *CEACAM8*, *LTF*, and *MPO*) [39] and the expression of genes involved in inflammation, metastasis, EMT, and stemness in this database.

4.9. Statistical Analysis

For statistical analysis was applied the GraphPad Prism 5 (GraphPad Software, San Diego, CA, USA). Data are shown as mean ± standard deviation. The unpaired *t*-test was used to determine a significant difference between MCF7 cells and MCF7 cells treated with NETs in quantitative RT-PCR, flow cytometry, and migration assay. The details of the statistics are indicated in the figure legends. The correlation of the RNA-seq values (FPKM) was statistically analyzed by the non-parametric Spearman test. Results were considered statistically significant when p-value ≤ 0.05.

5. Conclusions

Together, the present study shows, for the first time, that isolated NETs promote epithelial–mesenchymal transition (EMT) in cultured breast cancer cells. Our findings suggest that NETs released in the primary tumor may influence the acquisition of metastatic properties during breast cancer progression. Overall, the modulation of NETs formation in the tumor microenvironment might represent an attractive therapeutic target to decrease or even prevent the metastatic spread.

Supplementary Materials: The following are available online at http://www.mdpi.com/2072-6694/12/6/1542/s1, Figure S1: Uncropped blots for analysis of EMT markers, Figure S2: Effects of NETs on HER2+ breast cancer cells, Figure S3: Quantitative analysis of immunocytochemistry assays for EMT markers in NETs-treated MCF7 cells, Figure S4: The pro-tumoral effects of NETs are independent of DNA integrity, Table S1: qRT-PCR primer sequences.

Author Contributions: Conceptualization, R.Q.M.; Methodology, K.M.-C., V.H.A., K.M.B., M.I.D.R. and S.K.; Formal analysis, K.M.-C., V.H.A., K.M.B., M.I.D.R., C.S.M. and S.K.; Investigation, K.M.-C., V.H.A., S.K. and R.Q.M.; Resources, R.Q.M.; Writing—original draft preparation, K.M.-C., V.H.A., S.K. and R.Q.M.; Writing—review and editing, K.M.-C., V.H.A. and R.Q.M.; Visualization, K.M.-C., V.H.A., K.M.B., M.I.D.R., C.S.M., S.K., R.Q.M.; Supervision, R.Q.M.; Project administration, R.Q.M.; Funding acquisition, R.Q.M. All authors have read and agreed to the published version of the manuscript.

Funding: This investigation was supported by grants from the Brazilian National Council for Scientific and Technological Development (CNPq) Grant 309946/2018-2; The State of Rio de Janeiro Research Foundation (FAPERJ) Grants E-26/010.001830/2015, E-26/202.871/2018, and E-26/010.101035/2018; and the Coordination for the Improvement of Higher Education Personnel (CAPES) grant 23038.008921/2019-15.

Acknowledgments: We would like to thank Rosangela Rosa de Araújo for her technical assistance, and T.M. Tilli (Plataforma de Oncologia Translacional, Centro de Desenvolvimento Tecnológico em Saúde/Fundação Oswaldo Cruz, RJ, Brazil) for sharing access to TCGA data.

Conflicts of Interest: The authors declare no conflicts of interests.

References

1. Bray, F.; Ferlay, J.; Soerjomataram, I.; Siegel, R.L.; Torre, L.A.; Jemal, A. Global cancer statistics 2018: GLOBOCAN estimates of incidence and mortality worldwide for 36 cancers in 185 countries. *CA A Cancer J. Clin.* **2018**, *68*, 394–424. [CrossRef]
2. Network, C.G.A.; Network, T.C.G.A.; Koboldt, D.C.; Fulton, R.S.; McLellan, M.; Schmidt, H.; Kalicki-Veizer, J.; McMichael, J.F.; Fulton, L.L.; Dooling, D.J.; et al. Comprehensive molecular portraits of human breast tumours. *Nature* **2012**, *490*, 61–70. [CrossRef]
3. Blows, F.M.; Driver, K.E.; Schmidt, M.K.; Broeks, A.; Van Leeuwen, F.E.; Wesseling, J.; Cheang, M.C.; Gelmon, K.; Nielsen, T.O.; Blomqvist, C.; et al. Subtyping of Breast Cancer by Immunohistochemistry to Investigate a Relationship between Subtype and Short and Long Term Survival: A Collaborative Analysis of Data for 10,159 Cases from 12 Studies. *PLoS Med.* **2010**, *7*, e1000279. [CrossRef]
4. Foulkes, W.D.; Smith, I.E.; Reis-Filho, J.S. Triple-Negative Breast Cancer. *New Engl. J. Med.* **2010**, *363*, 1938–1948. [CrossRef]
5. Kennecke, H.; Yerushalmi, R.; Woods, R.; Cheang, M.C.; Voduc, D.; Speers, C.H.; Nielsen, T.O.; Gelmon, K. Metastatic Behavior of Breast Cancer Subtypes. *J. Clin. Oncol.* **2010**, *28*, 3271–3277. [CrossRef]
6. Hanahan, D.; Coussens, L.M. Accessories to the Crime: Functions of Cells Recruited to the Tumor Microenvironment. *Cancer Cell* **2012**, *21*, 309–322. [CrossRef]
7. Nieto, M.A.; Huang, R.Y.-J.; Jackson, R.A.; Thiery, J.P. EMT: 2016. *Cell* **2016**, *166*, 21–45. [CrossRef]
8. Ye, X.; Weinberg, R.A. Epithelial-Mesenchymal Plasticity: A Central Regulator of Cancer Progression. *Trends Cell Biol.* **2015**, *25*, 675–686. [CrossRef]
9. Mao, Y.; Keller, E.T.; Garfield, D.H.; Shen, K.; Wang, J. Stromal cells in tumor microenvironment and breast cancer. *Cancer Metastasis Rev.* **2013**, *32*, 303–315. [CrossRef]
10. Yang, L.; Zhang, Y. Tumor-associated macrophages: From basic research to clinical application. *J. Hematol. Oncol.* **2017**, *10*, 58. [CrossRef]
11. Powell, D.R.; Huttenlocher, A. Neutrophils in the Tumor Microenvironment. *Trends Immunol.* **2015**, *37*, 41–52. [CrossRef] [PubMed]
12. Sionov, R.V.; Fridlender, Z.G.; Granot, Z. The Multifaceted Roles Neutrophils Play in the Tumor Microenvironment. *Cancer Microenviron.* **2014**, *8*, 125–158. [CrossRef]
13. Coffelt, S.B.; Wellenstein, M.D.; De Visser, K.E. Neutrophils in cancer: Neutral no more. *Nat. Rev. Cancer* **2016**, *16*, 431–446. [CrossRef] [PubMed]
14. Cools-Lartigue, J.; Spicer, J.; Najmeh, S.; Ferri, L. Neutrophil extracellular traps in cancer progression. *Cell. Mol. Life Sci.* **2014**, *71*, 4179–4194. [CrossRef] [PubMed]
15. Tohme, S.; Yazdani, H.O.; Al-Khafaji, A.B.; Chidi, A.P.; Loughran, P.; Mowen, K.; Wang, Y.; Simmons, R.L.; Huang, H.; Tsung, A. Neutrophil Extracellular Traps Promote the Development and Progression of Liver Metastases after Surgical Stress. *Cancer Res.* **2016**, *76*, 1367–1380. [CrossRef]
16. Albrengues, J.; Shields, M.A.; Ng, D.; Park, C.G.; Ambrico, A.; Poindexter, M.E.; Upadhyay, P.; Uyeminami, D.L.; Pommier, A.; Küttner, V.; et al. Neutrophil extracellular traps produced during inflammation awaken dormant cancer cells in mice. *Science* **2018**, *361*, eaao4227. [CrossRef]
17. Dwivedi, N.; Chang, H.-H.; Ho, I.-C. Citrullination and Neutrophil Extracellular Traps. *Protein Deimination in Human Health Dis.* **2017**, *36*, 137–159. [CrossRef]
18. Brinkmann, V.; Zychlinsky, A. Neutrophil extracellular traps: Is immunity the second function of chromatin? *J. Cell Boil.* **2012**, *198*, 773–783. [CrossRef]
19. Cools-Lartigue, J.; Spicer, J.; McDonald, B.; Gowing, S.; Chow, S.; Giannias, B.; Bourdeau, F.; Kubes, P.; Ferri, L. Neutrophil extracellular traps sequester circulating tumor cells and promote metastasis. *J. Clin. Investig.* **2013**, *123*, 3446–3458. [CrossRef]

20. Park, J.; Wysocki, R.; Amoozgar, Z.; Maiorino, L.; Fein, M.R.; Jorns, J.; Schott, A.F.; Kinugasa-Katayama, Y.; Lee, Y.; Won, N.H.; et al. Cancer cells induce metastasis-supporting neutrophil extracellular DNA traps. *Sci. Transl. Med.* **2016**, *8*, 361ra138. [CrossRef]
21. Yazdani, H.O.; Roy, E.; Comerci, A.J.; Van Der Windt, D.J.; Zhang, H.; Huang, H.; Loughran, P.; Shiva, S.; Geller, D.A.; Bartlett, D.L.; et al. Neutrophil Extracellular Traps Drive Mitochondrial Homeostasis in Tumors to Augment Growth. *Cancer Res.* **2019**, *79*, 5626–5639. [CrossRef]
22. Demers, M.; Wong, S.L.; Martinod, K.; Gallant, M.; Cabral, J.E.; Wang, Y.; Wagner, D.D. Priming of neutrophils toward NETosis promotes tumor growth. *OncoImmunology* **2016**, *5*, e1134073. [CrossRef]
23. Yang, L.-Y.; Luo, Q.; Lu, L.; Zhu, W.-W.; Sun, H.-T.; Wei, R.; Lin, Z.-F.; Wang, X.-Y.; Wang, C.-Q.; Lu, M.; et al. Increased neutrophil extracellular traps promote metastasis potential of hepatocellular carcinoma via provoking tumorous inflammatory response. *J. Hematol. Oncol.* **2020**, *13*, 3–15. [CrossRef]
24. Zha, C.; Meng, X.; Li, L.; Mi, S.; Qian, D.; Li, Z.; Wu, P.; Hu, S.; Zhao, S.; Cai, J.; et al. Neutrophil extracellular traps mediate the crosstalk between glioma progression and the tumor microenvironment via the HMGB1/RAGE/IL-8 axis. *Cancer Biol. Med.* **2020**, *17*, 154–168.
25. Leal, A.C.; Mizurini, D.M.; Gomes, T.; Rochael, N.C.; Saraiva, E.M.; Dias, M.S.; Werneck, C.; Sielski, M.S.; Vicente, C.P.; Monteiro, R.Q. Tumor-Derived Exosomes Induce the Formation of Neutrophil Extracellular Traps: Implications For The Establishment of Cancer-Associated Thrombosis. *Sci. Rep.* **2017**, *7*, 6438. [CrossRef]
26. Gomes, T.; Várady, C.B.S.; Lourenço, A.L.; Mizurini, D.M.; Rondon, A.M.R.; Leal, A.C.; Gonçalves, B.S.; Bou-Habib, D.C.; Medei, E.; Monteiro, R.Q. IL-1β Blockade Attenuates Thrombosis in a Neutrophil Extracellular Trap-Dependent Breast Cancer Model. *Front. Immunol.* **2019**, *10*, 2088. [CrossRef]
27. Demers, M.; Krause, D.S.; Schatzberg, D.; Martinod, K.; Voorhees, J.R.; Fuchs, T.A.; Scadden, D.T.; Wagner, D.D. Cancers predispose neutrophils to release extracellular DNA traps that contribute to cancer-associated thrombosis. *Proc. Natl. Acad. Sci. USA* **2012**, *109*, 13076–13081.
28. Neve, R.M.; Chin, K.; Fridlyand, J.; Yeh, J.; Baehner, F.L.; Fevr, T.; Clark, L.; Bayani, N.; Coppé, J.-P.; Tong, F.; et al. A collection of breast cancer cell lines for the study of functionally distinct cancer subtypes. *Cancer Cell* **2006**, *10*, 515–527. [CrossRef]
29. Nie, M.; Yang, L.; Bi, X.; Wang, Y.; Sun, P.; Yang, H.; Liu, P.; Li, Z.; Xia, Y.; Jiang, W.-Q. Neutrophil Extracellular Traps Induced by IL8 Promote Diffuse Large B-cell Lymphoma Progression via the TLR9 Signaling. *Clin. Cancer Res.* **2018**, *25*, 1867–1879. [CrossRef]
30. Leggett, S.; Sim, J.Y.; Rubins, J.E.; Neronha, Z.; Williams, E.K.; Wong, I.Y. Morphological single cell profiling of the epithelial-mesenchymal transition. *Integr. Boil.* **2016**, *8*, 1133–1144. [CrossRef]
31. Shang, S.; Hua, F.; Hu, Z. The regulation of β-catenin activity and function in cancer: Therapeutic opportunities. *Oncotarget* **2017**, *8*, 33972–33989. [CrossRef]
32. Basu, S.; Cheriyamundath, S.; Ben-Ze'Ev, A. Cell–cell adhesion: Linking Wnt/β-catenin signaling with partial EMT and stemness traits in tumorigenesis. *F1000Research* **2018**, *7*, 1488. [CrossRef]
33. Orsulic, S.; Huber, O.; Aberle, H.; Arnold, S.; Kemler, R. E-cadherin binding prevents beta-catenin nuclear localization and beta-catenin/LEF-1-mediated transactivation. *J. Cell Sci.* **1999**, *112*, 1237–1245.
34. Mani, S.A.; Guo, W.; Liao, M.-J.; Eaton, E.N.; Ayyanan, A.; Zhou, A.Y.; Brooks, M.; Reinhard, F.; Zhang, C.C.; Shipitsin, M.; et al. The Epithelial-Mesenchymal Transition Generates Cells with Properties of Stem Cells. *Cell* **2008**, *133*, 704–715. [CrossRef]
35. Ricardo, S.; Vieira, A.F.; Gerhard, R.; Leitão, D.; Pinto, R.; Cameselle-Teijeiro, J.F.; Milanezi, F.; Schmitt, F.C.; Paredes, J. Breast cancer stem cell markers CD44, CD24 and ALDH1: Expression distribution within intrinsic molecular subtype. *J. Clin. Pathol.* **2011**, *64*, 937–946. [CrossRef] [PubMed]
36. Fillmore, C.M.; Kuperwasser, C. Human breast cancer cell lines contain stem-like cells that self-renew, give rise to phenotypically diverse progeny and survive chemotherapy. *Breast Cancer Res.* **2008**, *10*, R25. [CrossRef]
37. Suarez-Carmona, M.; Lesage, J.; Cataldo, D.; Gilles, C. EMT and inflammation: Inseparable actors of cancer progression. *Mol. Oncol.* **2017**, *11*, 805–823. [CrossRef]
38. Yeung, K.T.; Yang, J. Epithelial-mesenchymal transition in tumor metastasis. *Mol. Oncol.* **2016**, *11*, 28–39. [CrossRef]

39. Wither, J.; Prokopec, S.D.; Noamani, B.; Chang, N.-H.; Bonilla, D.; Touma, Z.; Ávila-Casado, C.; Reich, H.N.; Scholey, J.; Fortin, P.R.; et al. Identification of a neutrophil-related gene expression signature that is enriched in adult systemic lupus erythematosus patients with active nephritis: Clinical/pathologic associations and etiologic mechanisms. *PLoS ONE* **2018**, *13*, e0196117. [CrossRef] [PubMed]
40. Aratani, Y. Myeloperoxidase: Its role for host defense, inflammation, and neutrophil function. *Arch. Biochem. Biophys.* **2018**, *640*, 47–52. [CrossRef]
41. Kagan, B.L.; Selsted, M.E.; Ganz, T.; Lehrer, R.I. Antimicrobial defensin peptides form voltage-dependent ion-permeable channels in planar lipid bilayer membranes. *Proc. Natl. Acad. Sci. USA* **1990**, *87*, 210–214.
42. Van Lint, P.; Libert, C. Matrix metalloproteinase-8: Cleavage can be decisive. *Cytokine Growth Factor Rev.* **2006**, *17*, 217–223. [CrossRef]
43. Torsteinsdottir, I.; Arvidson, N.-G.; Hallgren, R.; Hakansson, L. Enhanced Expression of Integrins and CD66b on Peripheral Blood Neutrophils and Eosinophils in Patients with Rheumatoid Arthritis, and the Effect of Glucocorticoids. *Scand. J. Immunol.* **1999**, *50*, 433–439. [CrossRef] [PubMed]
44. Baggiolini, M.; De Duve, C.; Masson, P.L.; Heremans, J.F. Association of Lactoferrin with Specific Granules in Rabbit Heterophil Leukocytes. *J. Exp. Med.* **1970**, *131*, 559–570. [CrossRef]
45. Soto-Perez-De-Celis, E.; Chavarri-Guerra, Y.; Leon-Rodriguez, E.; Gamboa-Dominguez, A. Tumor-Associated Neutrophils in Breast Cancer Subtypes. *Asian Pac. J. Cancer Prev.* **2017**, *18*, 2689–2694. [PubMed]
46. Wu, L.; Saxena, S.; Awaji, M.; Singh, R.K. Tumor-Associated Neutrophils in Cancer: Going Pro. *Cancers* **2019**, *11*, 564. [CrossRef]
47. Liu, C.-Y.; Lin, H.-H.; Tang, M.; Wang, Y.-K. Vimentin contributes to epithelial-mesenchymal transition cancer cell mechanics by mediating cytoskeletal organization and focal adhesion maturation. *Oncotarget* **2015**, *6*, 15966–15983. [CrossRef] [PubMed]
48. Huang, R.Y.-J.; Wong, M.K.; Tan, T.Z.; Kuay, K.T.; Ng, A.H.C.; Chung, V.Y.; Chu, Y.-S.; Matsumura, N.; Lai, H.-C.; Lee, Y.F.; et al. An EMT spectrum defines an anoikis-resistant and spheroidogenic intermediate mesenchymal state that is sensitive to e-cadherin restoration by a src-kinase inhibitor, saracatinib (AZD0530). *Cell Death Dis.* **2013**, *4*, e915. [CrossRef]
49. Kim, J.; Kong, J.; Chang, H.; Kim, H.; Kim, A. EGF induces epithelial-mesenchymal transition through phospho-Smad2/3-Snail signaling pathway in breast cancer cells. *Oncotarget* **2016**, *7*, 85021–85032. [CrossRef]
50. Zhang, X.; Li, Y.; Zhang, Y.; Song, J.; Wang, Q.; Zheng, L.; Liu, D. Beta-Elemene Blocks Epithelial-Mesenchymal Transition in Human Breast Cancer Cell Line MCF-7 through Smad3-Mediated Down-Regulation of Nuclear Transcription Factors. *PLoS ONE* **2013**, *8*, e58719. [CrossRef] [PubMed]
51. Kim, E.; Lisby, A.; Ma, C.; Lo, N.; Ehmer, U.; Hayer, K.E.; Furth, E.E.; Viatour, P. Promotion of growth factor signaling as a critical function of β-catenin during HCC progression. *Nat. Commun.* **2019**, *10*, 1909. [CrossRef]
52. May, C.D.; Sphyris, N.; Evans, K.W.; Werden, S.J.; Guo, W.; Mani, S.A. Epithelial-mesenchymal transition and cancer stem cells: A dangerously dynamic duo in breast cancer progression. *Breast Cancer Res.* **2011**, *13*, 202. [CrossRef] [PubMed]
53. Morel, A.-P.; Lièvre, M.; Thomas, C.; Hinkal, G.; Ansieau, S.; Puisieux, A. Generation of Breast Cancer Stem Cells through Epithelial-Mesenchymal Transition. *PLoS ONE* **2008**, *3*, e2888. [CrossRef]
54. Senbanjo, L.T.; Chellaiah, M.A. CD44: A Multifunctional Cell Surface Adhesion Receptor Is a Regulator of Progression and Metastasis of Cancer Cells. *Front. Cell Dev. Boil.* **2017**, *5*, 811. [CrossRef] [PubMed]
55. Al-Hajj, M.; Wicha, M.S.; Benito-Hernandez, A.; Morrison, S.J.; Clarke, M.F. Prospective identification of tumorigenic breast cancer cells. *Proc. Natl. Acad. Sci. USA* **2003**, *100*, 3983–3988. [CrossRef] [PubMed]
56. Takeshita, F.; Leifer, C.A.; Gursel, I.; Ishii, K.J.; Takeshita, S.; Gursel, M.; Klinman, D.M. Cutting edge: Role of Toll-like receptor 9 in CpG DNA-induced activation of human cells. *J. Immunol.* **2001**, *167*, 3555–3558. [CrossRef] [PubMed]
57. Xu, J.; Zhang, X.; Monestier, M.; Esmon, N.L.; Esmon, C.T. Extracellular histones are mediators of death through TLR2 and TLR4 in mouse fatal liver injury. *J. Immunol.* **2011**, *187*, 2626–2631. [CrossRef]
58. Kawai, T.; Akira, S. Signaling to NF-κB by Toll-like receptors. *Trends Mol. Med.* **2007**, *13*, 460–469. [CrossRef]
59. Pires, B.R.B.; Mencalha, A.L.; Ferreira, G.M.; De Souza, W.F.; Morgado-Diaz, J.A.; Maia, A.M.; Corrêa, S.; Abdelhay, E.S.F.W. NF-kappaB Is Involved in the Regulation of EMT Genes in Breast Cancer Cells. *PLoS ONE* **2017**, *12*, e0169622. [CrossRef]

60. Huber, M.A.; Azoitei, N.; Baumann, B.; Grünert, S.; Sommer, A.; Pehamberger, H.; Kraut, N.; Beug, H.; Thomas, H.; Gruenert, S. NF-κB is essential for epithelial-mesenchymal transition and metastasis in a model of breast cancer progression. *J. Clin. Investig.* **2004**, *114*, 569–581. [CrossRef]
61. Fernando, R.I.; Castillo, M.D.; Litzinger, M.; Hamilton, D.H.; Palena, C. IL-8 signaling plays a critical role in the epithelial-mesenchymal transition of human carcinoma cells. *Cancer Res.* **2011**, *71*, 5296–5306. [CrossRef]
62. Miao, J.-W.; Liu, L.-J.; Huang, J. Interleukin-6-induced epithelial-mesenchymal transition through signal transducer and activator of transcription 3 in human cervical carcinoma. *Int. J. Oncol.* **2014**, *45*, 165–176. [CrossRef]
63. Li, Y.; Wang, L.; Pappan, L.; Galliher-Beckley, A.; Shi, J. IL-1β promotes stemness and invasiveness of colon cancer cells through Zeb1 activation. *Mol. Cancer* **2012**, *11*, 87. [CrossRef] [PubMed]
64. Katsura, A.; Tamura, Y.; Hokari, S.; Harada, M.; Morikawa, M.; Sakurai, T.; Takahashi, K.; Mizutani, A.; Nishida, J.; Yokoyama, Y.; et al. ZEB1-regulated inflammatory phenotype in breast cancer cells. *Mol. Oncol.* **2017**, *11*, 1241–1262. [CrossRef] [PubMed]
65. Fernández-García, B.; Eiro, N.; Miranda, M.-A.; Cid, S.; Gonzalez, L.O.; Dominguez, F.; Vizoso, F.J. Prognostic significance of inflammatory factors expression by stroma from breast carcinomas. *Carcinog.* **2016**, *37*, 768–776. [CrossRef] [PubMed]
66. Hisada, Y.; Houston, R.; Maqsood, A.; Thalin, C.; Noubouossie, D.F.; Wallen, H.; Kolev, K.; Cooley, B.C.; Key, N.S.; Mackman, N. Abstract 041: Neutrophil Extracellular Traps Enhance Venous Thrombosis in Mice Bearing Human Pancreatic Tumors. *Arter. Thromb. Vasc. Boil.* **2018**, *38*, 218–225. [CrossRef]
67. Shen, M.; Hu, P.; Donskov, F.; Wang, G.; Liu, Q.; Du, J. Tumor-Associated Neutrophils as a New Prognostic Factor in Cancer: A Systematic Review and Meta-Analysis. *PLoS ONE* **2014**, *9*, e98259. [CrossRef]
68. Hu, P.; Shen, M.; Zhang, P.; Zheng, C.; Pang, Z.; Zhu, L.; Du, J. Intratumoral neutrophil granulocytes contribute to epithelial-mesenchymal transition in lung adenocarcinoma cells. *Tumor Boil.* **2015**, *36*, 7789–7796. [CrossRef]
69. Mayer, C.; Darb-Esfahani, S.; Meyer, A.-S.; Hübner, K.; Rom, J.; Sohn, C.; Braicu, I.; Sehouli, J.; Hänsch, G.M.; Gaida, M.M. Neutrophil Granulocytes in Ovarian Cancer—Induction of Epithelial-To-Mesenchymal-Transition and Tumor Cell Migration. *J. Cancer* **2016**, *7*, 546–554. [CrossRef]
70. Najmeh, S.; Cools-Lartigue, J.; Giannias, B.; Spicer, J.; Ferri, L.E. Simplified Human Neutrophil Extracellular Traps (NETs) Isolation and Handling. *J. Vis. Exp.* **2015**, *98*, 52687. [CrossRef]
71. Cerami, E.; Gao, J.; Dogrusoz, U.; Gross, B.E.; Sumer, S.O.; Aksoy, B.A.; Skanderup, A.J.; Byrne, C.J.; Heuer, M.L.; Larsson, E.; et al. The cBio cancer genomics portal: An open platform for exploring multidimensional cancer genomics data. *Cancer Discov.* **2012**, *2*, 401–404. [CrossRef]
72. Gao, J.; Aksoy, B.A.; Dogrusoz, U.; Dresdner, G.; Gross, B.; Sumer, S.O.; Sun, Y.; Skanderup, A.J.; Sinha, R.; Larsson, E.; et al. Integrative Analysis of Complex Cancer Genomics and Clinical Profiles Using the cBioPortal. *Sci. Signal.* **2013**, *6*, pl1. [CrossRef]

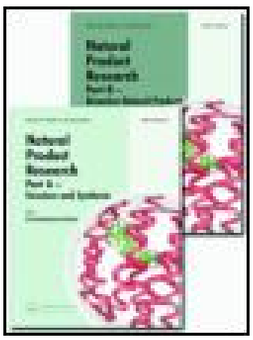

Natural Product Research

Formerly Natural Product Letters

ISSN: (Print) (Online) Journal homepage: https://www.tandfonline.com/loi/gnpl20

Antileishmanial activity of the essential oils of *Myrcia ovata* Cambess. and *Eremanthus erythropappus* (DC) McLeisch leads to parasite mitochondrial damage

Geovany Amorim Gomes , Karina Martins-Cardoso , Frances Regiane dos Santos , Melissa Florencio , Dayana Rosa , Aline Araujo Zuma , Gilvandete Maria Pinheiro Santiago , Maria Cristina M. Motta , Mario Geraldo de Carvalho & Patrícia Fampa

To cite this article: Geovany Amorim Gomes , Karina Martins-Cardoso , Frances Regiane dos Santos , Melissa Florencio , Dayana Rosa , Aline Araujo Zuma , Gilvandete Maria Pinheiro Santiago , Maria Cristina M. Motta , Mario Geraldo de Carvalho & Patrícia Fampa (2020): Antileishmanial activity of the essential oils of *Myrcia ovata* Cambess. and *Eremanthus erythropappus* (DC) McLeisch leads to parasite mitochondrial damage, Natural Product Research, DOI: 10.1080/14786419.2020.1827402

To link to this article: https://doi.org/10.1080/14786419.2020.1827402

NATURAL PRODUCT RESEARCH
https://doi.org/10.1080/14786419.2020.1827402

Taylor & Francis
Taylor & Francis Group

SHORT COMMUNICATION

Antileishmanial activity of the essential oils of *Myrcia ovata* Cambess. and *Eremanthus erythropappus* (DC) McLeisch leads to parasite mitochondrial damage

Geovany Amorim Gomes[a]*, Karina Martins-Cardoso[b,c]*, Frances Regiane dos Santos[d], Melissa Florencio[b,e], Dayana Rosa[b,e], Aline Araujo Zuma[f], Gilvandete Maria Pinheiro Santiago[g], Maria Cristina M. Motta[f], Mario Geraldo de Carvalho[d] and Patrícia Fampa[b]

[a]Centro de Ciências Exatas e Tecnologia, Universidade Estadual Vale do Acaraú, Sobral, CE, Brazil; [b]Departamento de Ciências Farmacêuticas, Instituto de Ciências Biológicas e da Saúde, Universidade Federal Rural do Rio de Janeiro, Seropédica, RJ, Brazil; [c]Instituto de Bioquímica Médica Leopoldo de Meis, Universidade Federal do Rio de Janeiro, Rio de Janeiro, RJ, Brazil; [d]Departamento de Química Orgânica, Instituto de Química, Universidade Federal Rural do Rio de Janeiro, Seropédica, RJ, Brazil; [e]Programa de Pós-Graduação em Ciências Veterinárias, Universidade Federal Rural do Rio de Janeiro, Seropédica, RJ, Brazil; [f]Instituto de Biofísica Carlos Chagas Filho, Universidade Federal do Rio de Janeiro, Rio de Janeiro, RJ, Brazil; [g]Departamento de Farmácia, Universidade Federal do Ceará, Fortaleza, CE, Brazil

ABSTRACT

Leishmania amazonensis is a species causative of cutaneous and anergic diffuse cutaneous leishmaniasis, treatment-resistant form, in the New World. Plants essential oils exhibit great potential as microbicide agents. We described the composition of the essential oils of two plants native from Brazil, *Myrcia ovata*, with geranial and neral as major constituents, and *Eremanthus erythropappus,* with α-bisabolol. *In vitro* effects of these essential oils on *L. amazonensis* promastigotes growth and ultrastructure were analysed as well as their cytotoxicity to murine macrophages. Both oils were highly active with IC_{50}/96 h of 8.69 and 9.53 μg/mL for *M. ovata* and *E. erythropappus* against promastigotes and caused ultrastructural alterations including mitochondrial enlargement. Cytotoxicity for murine macrophages varied with the oil concentrations. The IC_{50} low values of both *M. ovata* and *E. erythropappus* oils against *L. amazonensis* and their relative low cytotoxicity to mammal host cells support their potential use against cutaneous leishmaniasis.

ARTICLE HISTORY
Received 11 June 2020
Accepted 5 September 2020

KEYWORDS
Leishmania amazonensis; promastigote forms; essential oils; Myrcia ovata; Eremanthus erythropappus; chemotherapy

CONTACT Patrícia Fampa pfampa@ufrrj.br
*G.A.G and K.M.C. contributed equally to this work

Supplemental data for this article can be accessed at https://doi.org/10.1080/14786419.2020.1827402.

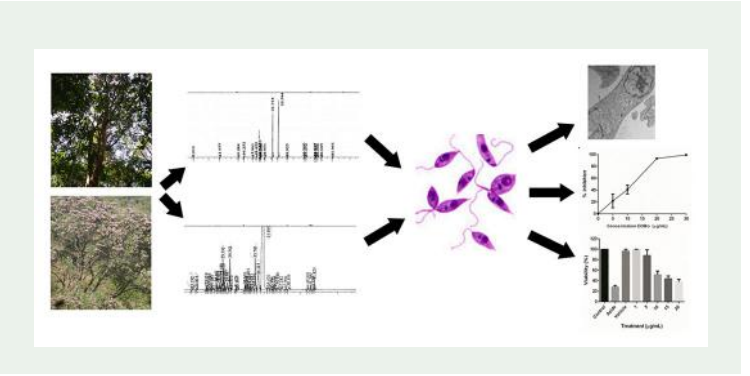

1. Introduction

Leishmaniasis consists of a group of neglected diseases, among other 17 recognized by World Health Organization, caused by protozoan parasites belonging to the genus *Leishmania* (Trypanosomatidae family) and transmitted by dipteran insect vectors, sandflies. Brazil is endemic for the three clinical forms of the disease: visceral, cutaneous, and mucocutaneous (Anversa et al. 2018). The treatment has been mainly based on pentavalent antimonials (Glucantime®) for decades and more recently amphotericin B and pentamidine. However, due to toxic effects on multiple organs, resistant parasite lineages development and drugs high costs, treatment alternatives, vaccines, diagnostics and vector control agents strategies must be supported (Hotez et al. 2016; Burza et al. 2018). Plant derivatives such as extracts, essential oils, or isolated components present antileishmanial potential effects (Rodrigues et al. 2015; Hamarsheh et al. 2017, Mathlouthi et al. 2018). Leaves of *Myrcia ovata* Cambess (Myrtaceae), native plant and popularly known as "laranjinha-do-mato" in Brazil, are frequently used as an infusion in folk medicine. Its EO presents several activities, such as insecticide, antibacterial, antibiofilm, fungicide (Sampaio et al. 2016) and anti-inflammatory (Dos Santos et al. 2014). *Eremanthus erythropappus* (DC) McLeisch (Asteraceae), also known as *Vanillosmopsis erythropappa* Schultz-Bip, popularly called "candeia-da-serra", is found at South, Southeast, West Central and Northeast regions of Brazil. It is used as a healing agent and in the treatment of infections and stomach ulcers (Silvério et al., 2013). The EO isolated from the stem exhibits antiphlogistic, antimycotic, healing, antibacterial, antioxidant, antiulcerogenic, and antispasmodic properties (Sousa et al. 2008). In the present work, essential oils of *Myrcia ovata* leaves (EoMo) and *Eremanthus erythropappus* stem (EoEE) were extracted and their compositions were characterized. Then, essential oils effects against *Leishmania amazonensis* promastigotes were evaluated.

2. Results and discussion

The components of EOMo and EOEe were identified and are listed in Supplementary Table 1 with their correspondent compositions percentage and retention indexes. GC-MS and GC-FID analyses of EOMo led to the identification and quantification of seven

different components, representing 93.55% of oil total composition. The chemical composition of EOMo found in this work (Figure S1A, B, Table S1, supplementary material) was similar to that previously reported (Lima et al. 2011), once the isolated oil presented geranial and neral monoterpenes as major components with percentages of 50.4 and 35.8%, respectively. The analysis of EOEe revealed the presence of thirteen constituents, corresponding to 94.22% of oil composition with α-bisabolol as the major constituent (Figure S1A,C, Table S1, supplementary material) and varying when compared to previously described for this plant in Minas Gerais, Brazil (Dos Santos et al., 2015). EOMo caused *L. amazonensis* growth inhibition at the tested concentrations in a dose-dependent manner with a considerable difference at 20 and 30 μg/mL compared to untreated control. Both higher concentrations caused 100% of growth inhibition since day zero of treatment. The calculated IC_{50}/96 h was of 8.69 μg/mL for EOMo (Figure S2A,C). EOEe at 5 and 10 μg/mL caused around 35% of parasite growth inhibition, but also presented a more significant effect against *L. amazonensis* promastigotes at 20 and 30 μg/mL with almost 100% of growth inhibition after 96 h treatment. The calculated IC_{50}/96 h was of 9.53 μg/mL for EOEe (Figure S2B, D, supplementary material). Comparing both oils, the inhibition effect of EOMo started earlier at promastigotes (48 and 72 h) than EOEe, as demonstrated for concentrations of 5 and 10 μg/mL (Figure S2, supplementary material). Essential oils of different plants have been tested for their anti-*L. amazonensis* promastigote forms properties. *Chenopodium ambrosioides* EO led to an IC_{50}/72 h of 3.7 μg/mL (Bosquiroli et al. 2017), *Lippia sidoides* caused inhibition with IC_{50}/48 h of 44.38 μg/mL and *Ferula galbaniflua* with IC_{50}/48 h of 95.7 μg/mL (Sampaio et al., 2016). The effectiveness varies enormously within distinct oils composition and proportion of the different constituents. The treatment of *L. amazonensis* promastigotes with EOMo and EOEe led to morphological alterations (Figure S3C, D, E, supplementary material), when compared to untreated controls (Figure S3A, B, supplementary material). After three-day incubation with 10 μg/mL EOEe, parasites presented lipid bodies' accumulation (Figure S3C, supplementary material). EOMo at 5 μg/mL caused mitochondrial swelling after four days of treatment (Figure S3E, supplementary material) and at the higher concentration of 10 μg/mL for three days, EOMo caused nucleolus disorganization and the appearance of autophagosome suggestive structures (Figure S3D, supplementary material). Santin et al. (2009) tested the effect of citral, major component of *Cymbopogon citratus* EO and which is the mixture of geranial and neral isomers and also the major constituent of EOMo, on *L. amazonensis*. Ultrastructural alterations included mitochondrial damage and parasites with two or more flagella among other effects. Balb/c mice peritoneal macrophages were incubated with different concentrations of EOMo and EOEe (1 to 20 μg/mL) for 48 h when XTT viability assay was performed. For EOMo, the lowest concentrations of 1 and 5 μg/mL maintained 100% of the viability compared to non-treated control, nevertheless the concentrations of 10, 15 and 20 μg/mL reduced the viability around 50% (Figure S4A, supplementary material). For all tested concentrations of EOEe, the viability remained around 60% of the non-treated control (Figure S4B, supplementary material). Nevertheless, the results concerning cytotoxicity of EOEe on mice macrophages were not fully conclusive, requiring further analyses. As perspective, it is worth analysing the action of the oils constituents alone or their combined potential synergic

effect on *Leishmania* and therefore identifying the more efficient chemotherapy as well as achieving less toxicity on host cells. Furthermore, additional studies are needed to evaluate the activity of these compounds against amastigote forms.

Acknowledgments

To Professors Lucia Helena Pinto-da-Silva, Debora Decote Ricardo de Lima and Maria das Graças Miranda Danelli of Laboratório de Imunologia e Virologia Veterinária (Instituto de Veterinária/ UFRRJ) for making their laboratory facilities available for some experiments. Financial support by Coordenação de Aperfeiçoamento de Pessoal de Nível Superior (CAPES), Conselho Nacional de Desenvolvimento Científico e Tecnológico (CNPq) and Fundação de Amparo à Pesquisa do Estado do Rio de Janeiro (FAPERJ).

Disclosure statement

The authors declare no conflict of interest.

ORCID

Geovany Amorim Gomes http://orcid.org/0000-0002-8659-7703
Karina Martins-Cardoso http://orcid.org/0000-0002-0986-4193
Melissa Florencio http://orcid.org/0000-0002-3037-5909
Dayana Rosa http://orcid.org/0000-0001-8150-964X
Aline Araujo Zuma http://orcid.org/0000-0002-1286-7045
Gilvandete Maria Pinheiro Santiago http://orcid.org/0000-0002-6832-8374
Maria Cristina M. Motta http://orcid.org/0000-0002-0947-4830
Mario Geraldo de Carvalho http://orcid.org/0000-0001-5805-734X
Patrícia Fampa http://orcid.org/0000-0003-3440-1622

References

Adams RP. 2007. Identification of essential oils components by gas chromatography/mass spectrometry. IL, USA: Allured Pub. Corp: Carol Stream.

Anversa L, Tiburcio MGS, Richini-Pereira VB, Ramirez LE. 2018. Human leishmaniasis in Brazil: a general review. Rev Assoc Med Bras (1992)). 64(3):281–289.

Bosquiroli LSS, dos Ferreira ACS, Farias KS, da Costa EC, de Matos MFC, Kadri MCT, Rizk YS, Alves FM, Perdomo RT, Carollo CA, et al. 2017. In vitro antileishmania activity of sesquiterpene-rich essential oils from nectandra species. Pharm Biol. 55(1):2285–2291.

Burza S, Croft SL, Boelaert M. 2018. Leishmaniasis. The Lancet. 392(10151):951–970.

Dos Santos GCM, Gomes GA, Gonçalves GM, de Sousa LM, Santiago GMP, de Carvalho MG, Marinho BG. 2014. Essential oil from *Myrcia ovata*: chemical composition, antinociceptive and anti-inflammatory properties in mice. Planta Med. 80(17):1588–1596.

Santos NOD, Mariane B, Lago JHG, Sartorelli P, Rosa W, Soares MG, da Silva AM, Lorenzi H, Vallim MA, Pascon RC, et al. 2015. Assessing the chemical composition and antimicrobial activity of essential oils from Brazilian Plants-Eremanthus erythropappus (Asteraceae), *Plectrantuns barbatus*, and *P. amboinicus* (Lamiaceae)). Molecules. 20(5):8440–8452.

Hamarsheh O, Azmi K, Amro A, Schultheis MAZ, et al. 2017. Antileishmanial potential of crude plant extracts derived from medicinal plants in Palestine. Ann Clin Cytol Pathol. 3(4):1065.

Hotez PJ, Pecoul B, Rijal S, Boehme C, Aksoy S, Malecela M, Tapia-Conyer R, Reeder JC. 2016. Eliminating the neglected tropical diseases: translational science and new technologies. PLoS Negl Trop Dis. 10(3):e0003895

Lima MAA, Oliveira FFM, de Gomes GA, Lavor PL, Santiago GMP, et al. 2011. Evaluation of larvicidal activity of the essential oils of plants species from Brazil against *Aedes aegypti* (Diptera: Culicidae). Afr J. 10(55):11716–11720.

Mathlouthi A, Belkessam M, Sdiri M, Diouani MF, Souli A, El-Bok S, Ben-Attia M. 2018. Chemical composition and antileishmania major activity of essential oils from *Artemesia* spp. grown in Central Tunisia. J. Essent. Oil-Bear Plants. 21(5):1186–1198.

Rodrigues KADF, Amorim LV, Dias CN, Moraes DFC, Carneiro SMP, Carvalho FADA. 2015. *Syzygium cumini* (L.) Skeels essential oil and its major constituent α-pinene exhibit anti-Leishmania activity through immunomodulation in vitro. J Ethnopharmacol. 160:32–40.

Sampaio TS, de Castro Nizio D. A., White LAS, Melo JO, Almeida CS, Alves MF, Gagliardi PR, Arrigoni-Blank M. d F, Wisniewski Junior A, Sobral MEG, et al. 2016. Chemical diversity of a wild population of *Myrcia ovata* Cambessedes and antifungal activity against *Fusarium solani*. Ind Crops Prod. 86:196–209.

Santin MR, dos Santos AO, Nakamura CV, Dias Filho BP, Ferreira ICP, Ueda-Nakamura T. 2009. In vitro activity of the essential oil of *Cymbopogon citratus* and its major component (citral) on *Leishmania amazonensis*. Parasitol Res. 105(6):1489–1496.

Silvério MS, Del-Vechio-Vieira G, Pinto MAO, Alves MS, Sousa OV. 2013. Chemical composition and biological activities of essential oils of *Eremanthus erythropappus* (DC) McLeisch (Asteraceae). Molecules. 18(8):9785–9796.

Sousa OV, de Dutra RC, Yamamoto CH, Pimenta DS. 2008. Estudo comparativo da composição química e da atividade biológica dos óleos essenciais das folhas de *Eremanthus erythropappus* (DC) McLeisch. [Comparative study of the chemical composition and biological activity of *Eremanthus erythropappus* (DC) McLeisch Leaves Essential Oils]. Rev Bras de Farm. 89(2): 113–116.

Van Den Dool H, Kratz PD. 1963. A generalization of the retention index system including linear temperature programmed gas liquid partition chromatography. J. Chromat A. 11(1):463–471.

Brazilian Journal of Microbiology
https://doi.org/10.1007/s42770-020-00254-9

CLINICAL MICROBIOLOGY - RESEARCH PAPER

β-Lapachone enhances the antifungal activity of fluconazole against a Pdr5p-mediated resistant *Saccharomyces cerevisiae* strain

Daniel Clemente de Moraes[1] · Karina Martins Cardoso[2] · Levy Tenório Sousa Domingos[1] · Maria do Carmo Freire Ribeiro Pinto[3] · Robson Q. Monteiro[2] · Antônio Ferreira-Pereira[1]

Received: 23 September 2019 / Accepted: 28 February 2020

Abstract

Objectives The aim of this study was to evaluate the ability of lapachones in disrupting the fungal multidrug resistance (MDR) phenotype, using a model of study which an azole-resistant *Saccharomyces cerevisiae* mutant strain that overexpresses the ATP-binding cassette (ABC) transporter Pdr5p.

Methods The evaluation of the antifungal activity of lapachones and their possible synergism with fluconazole against the mutant *S. cerevisiae* strain was performed through broth microdilution and spot assays. Reactive oxygen species (ROS) and efflux pump activity were assessed by fluorometry. ATPase activity was evaluated by the Fiske and Subbarow method. The effect of β-lapachone on *PDR5* mRNA expression was assessed by RT-PCR. The release of hemoglobin was measured to evaluate the hemolytic activity of β-lapachone.

Results α-nor-Lapachone and β-lapachone inhibited *S. cerevisiae* growth at 100 μg/ml. Only β-lapachone enhanced the antifungal activity of fluconazole, and this combined action was inhibited by ascorbic acid. β-Lapachone induced the production of ROS, inhibited Pdr5p-mediated efflux, and impaired Pdr5p ATPase activity. Also, β-lapachone neither affected the expression of *PDR5* nor exerted hemolytic activity.

Conclusions Data obtained indicate that β-lapachone is able to inhibit the *S. cerevisiae* efflux pump Pdr5p. Since this transporter is homologous to fungal ABC transporters, further studies employing clinical isolates that overexpress these proteins will be conducted to evaluate the effect of β-lapachone on pathogenic fungi.

Keywords Fluconazole · Lapachone · Multidrug resistance · Yeast

Introduction

Infections caused by azole-resistant fungi are a matter of extreme concern to public health, due to the high mortality associated with them, mainly in immunocompromised individuals [1]. Nevertheless, a low number of drugs is available to treat fungal infections, and there are several disadvantages related to their use, such as the increasing incidence of resistance to azole and echinocandin drugs, and the toxicity induced by amphotericin B [2].

The multidrug resistance (MDR) phenotype is majorly responsible for the failure of antifungal treatments. It confers to the microorganism a high degree of resistance to structurally and functionally unrelated compounds [3]. In fungi, the main

Responsible Editor: Luis Henrique Souza Guimaraes

✉ Antônio Ferreira-Pereira
apereira@micro.ufrj.br

[1] Laboratório de Bioquímica Microbiana, Instituto de Microbiologia Paulo de Góes, Centro de Ciências da Saúde, Universidade Federal do Rio de Janeiro, Avenida Carlos Chagas Filho 373, Cidade Universitária, Rio de Janeiro, RJ CEP: 21941-590, Brazil

[2] Instituto de Bioquímica Médica Leopoldo de Meis, Centro de Ciências da Saúde, Universidade Federal do Rio de Janeiro, Avenida Carlos Chagas Filho 373, Cidade Universitária, Rio de Janeiro, RJ CEP: 21941-590, Brazil

[3] Laboratório de Química Heterocíclica, Instituto de Pesquisas de Produtos Naturais, Centro de Ciências da Saúde, Universidade Federal do Rio de Janeiro, Avenida Carlos Chagas Filho 373, Cidade Universitária, Rio de Janeiro, RJ CEP: 21941-590, Brazil

Published online: 10 March 2020

MDR mechanism relies on the overexpression of efflux transporters within the plasma membrane [4]. These proteins, also called efflux pumps, extrude the drugs from the cell, avoiding them to reach the intracellular concentration required to a successful antifungal activity [5]. The co-administration of an antifungal agent, such as fluconazole, and a substance capable of inhibiting efflux pumps would preclude antifungal resistance, therefore ensuring the proper outcome of the treatment [6].

MDR transporters related to antifungal resistance belong mainly to the ATP-binding cassette (ABC) superfamily, which consists of primary active transporters that use ATP hydrolysis as an energy source for the transport of substances against a concentration gradient [7]. Besides *Candida* spp., *Cryptococcus* spp., and *Aspergillus* spp., MDR transporters are also found in *Saccharomyces cerevisiae* [8]. Moreover, *S. cerevisiae* MDR transporters are homologous to efflux pumps of pathogenic fungi. For example, the ABC pumps CaCdr1p [9] and CaCdr2p [10], the major *Candida albicans* MDR transporters, are homologous to *S. cerevisiae* Pdr5p, Snq2p, and Yor1p. The high similarity shared by these proteins enables the use of *S. cerevisiae* as a model of study of antifungal resistance in pathogenic fungi [11].

Lapachones are natural naphthoquinones that possess several pharmacological activities [12, 13]. In a previous work, our group aimed to study the effect of lapachones on *C. albicans* virulence factors. It was observed that β-lapachone and α-nor-lapachone were able to inhibit *C. albicans* growth, yeast-to-hyphae transition, biofilm formation, and cell wall mannoprotein expression [14].

Considering the relevance of fungal infections caused by resistant strains, the urgent need of discovering new therapeutic options, and the in vitro effectiveness of lapachones against *C. albicans* growth and virulence factors, the aim of this study was to evaluate the ability of lapachones in inhibiting Pdr5p-mediated antifungal resistance, using a model of study which an azole-resistant *Saccharomyces cerevisiae* mutant strain that overexpresses this transporter.

Materials and methods

Strains and culture conditions

In this study, two mutant strains of *S. cerevisiae* were used. The first strain, namely, AD124567 (Pdr5p+), overexpresses Pdr5p, while the genes encoding the Pdr3p regulator and the other five ABC transporters (Yor1p, Snq2p, Pdr10p, Pdr11p, and Ycf1p) have been deleted. The second one, namely, AD1234567 (Pdr5p−), had all the six genes related to ABC transporters deleted, and also the gene that encodes the Pdr5p transporter [15]. Consequently, Pdr5p+ strain shows fluconazole resistance, while Pdr5p− strain is sensitive to this antifungal agent. Both strains were grown in yeast peptone dextrose (YPD) medium (2% glucose, 1% yeast extract, 2% peptone) at 30 °C with agitation and were harvested in the exponential phase of growth whenever experiments were about to be performed. At growth experiments, cells were incubated in the presence of β-lap for 48 h. In previous studies, it was observed that 90 min is a suitable incubation time considering the functioning of Pdr5p, and then, it was chosen to be used at the subsequent assays using intact cells. At experiments employing purified membranes and erythrocytes, 60 min of incubation time was chosen because it is optimal to observe Pdr5p ATPase activity and hemolytic effects, respectively. Cellular concentrations were evaluated by optical density measurements (600 nm) and expressed as "cells/ml".

Chemicals

Fluconazole was obtained commercially from the university pharmacy (UFJF, Juiz de Fora—MG, Brazil). Fluconazole stock solutions were prepared in distilled water, sterilized by filtration (0.22 μm), and maintained at − 20 °C. α-Lapachone (α-lap), α-nor-lapachone (α-nor), β-lapachone (β-lap), and β-nor-lapachone (β-nor) (Fig. 1) were synthesized by the Laboratory of Heterocyclic Chemistry from the Institute of Natural Products Research (IPPN/UFRJ) and dissolved in dimethyl sulfoxide (DMSO) (Sigma-Aldrich®, St. Louis, USA, D4540) to a final concentration of 10 mg/ml [16]. 2′,7′-Dichlorodihydrofluorescein diacetate (DCFH-DA) (D6883), Nile red (19193), ascorbic acid (200.06), JumpStart Taq DNA Polymerase (D9307), SYBR Green (S9430), PCR Reference dye (R4526), and dNTP set (GE-28-4065) were also purchased from Sigma-Aldrich®, and stock solutions were prepared in distilled water and stored at 2–8 °C.

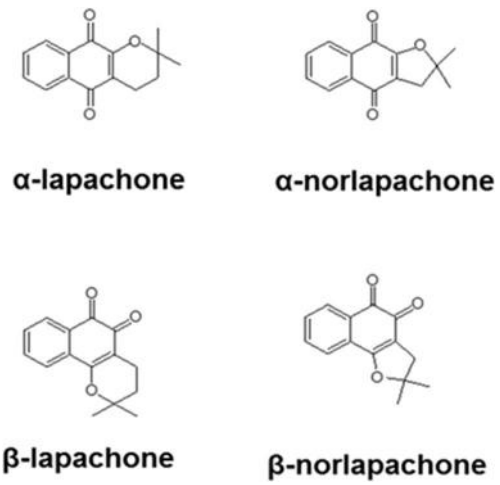

Fig. 1 Structure of the compounds tested in this study: α-lapachone; α-nor-lapachone; β-lapachone; β-nor-lapachone

Antifungal susceptibility test

The minimal inhibitory concentration (MIC) was determined according to the M27-A3 methodology for broth microdilution from CLSI [17] with slight modifications. Briefly, 2×10^4 cells/ml of Pdr5p+ strain were inoculated into YPD medium and incubated at 30 °C for 48 h with agitation (75 rpm), in the presence of serial concentrations (100–6.25 μg/ml) of lapachones. Cell growth was measured using a microplate reader at 600 nm (Fluostar Optima, BMG Labtech, Offenburg, Germany).

Checkerboard assay

The ability of lapachones to enhance fluconazole activity was evaluated through the checkerboard assay as described elsewhere [18] with slight modifications. Briefly, 2×10^4 cells/ml of Pdr5p+ strain were inoculated into YPD medium and incubated at 30 °C for 48 h with agitation (75 rpm), in the presence of combinations of serial concentrations of lapachones (100–6.25 μg/ml) and fluconazole (500–31.25 μg/ml). Cell growth was measured using a microplate reader at 600 nm (Fluostar Optima, BMG Labtech, Offenburg, Germany). The interaction between lapachones and fluconazole was evaluated by the fractional inhibitory concentration index (FICI) model. The FICI is defined as the sum of the FIC of each drug, while FIC is the ratio MIC in combination/MIC alone. Synergistic, additive, indifferent, and antagonistic interactions were defined by a FICI < 0.5, 0.5–1.0, 1.0–4.0, or > 4.0, respectively.

Spot assay

The spot assay was performed as described elsewhere [19]. Briefly, 5-fold serial dilutions of 6×10^5 cells/ml of Pdr5p+ were spotted onto YPD agar plates in the presence or absence of 125 μg/ml fluconazole, 12.5 μg/ml β-lap, and 25 mM ascorbic acid. Then, plates were incubated at 30 °C for 48 h and photographed.

Reactive species oxygen measurement

The fluorescent probe DCFH-DA was used in order to assess the production of reactive species oxygen (ROS) induced by β-lap and the combination of β-lap/fluconazole [20]. Briefly, 10^7 cells/ml of Pdr5p+ strain were incubated at 30 °C for 90 min in the presence of 100 μg/ml β-lap, 125 μg/ml fluconazole, 100 μg/ml β-lap + 125 μg/ml fluconazole, and 100 μg/ml β-lap + 125 μg/ml fluconazole + 25 mM ascorbic acid. Untreated cells were used as the negative control. Cells were harvested by centrifugation at 5000*g* for 3 min and pellets were resuspended in PBS containing 10 μM DCFH-DA and incubated for 15 min in darkness. Fluorescence was measured at 485/538 nm (excitation/emission) (Fluostar Optima, BMG Labtech, Offenburg, Germany), and results were expressed as mean intensity fluorescence.

Nile red accumulation assay

The effect of β-lap on the efflux activity of Pdr5p was assessed as described elsewhere [21], with slight modifications. Briefly, Pdr5p+ cells (10^7 cells/ml) were harvested by centrifugation at 5000*g* for 3 min and washed twice with cold PBS 10 mM at pH 7.2. Afterward, cells were incubated in a 96-well black polystyrene microplate for 60 min at 30 °C in the presence of 100 μg/ml β-lap, followed by the addition of 7 μM of Nile red and incubation at 30 °C for 30 min. Lastly, cells were resuspended in PBS containing 0.2% glucose and incubated for 30 min at 30 °C. The Pdr5p− strain was used as a blank control. Fluorescence was measured at 485/538 nm (excitation/emission) (Fluostar Optima, BMG Labtech, Offenburg, Germany), fluorescence of the blank systems was discounted, and results were expressed in comparison to the untreated system.

Preparation of plasma membranes

S. cerevisiae plasma membranes were obtained from mutant strain Pdrp5+ and from the null mutant Pdr5p− as previously described elsewhere [22]. Briefly, cells in the exponential phase of growth were harvested and washed with 10 mM sodium azide. Then, yeast cell wall was digested and differential centrifugation was performed in order to remove contaminants (4500*g* for 10 min, 12,000*g* for 12 min, and 20,000*g* for 40 min, respectively). Plasma membrane preparations were stored in liquid nitrogen and thawed immediately prior to use in the Pdr5p ATPase activity assays.

ATPase activity

The effect of β-lap on the ATPase activity of Pdr5p was evaluated by incubating membranes containing Pdr5p (0.013 mg/mL final concentration) in a 96-well plate at 37 °C for 60 min in a reaction medium containing 100 mM Tris-HCl (pH 7.5), 4 mM $MgCl_2$, 75 mM KNO_3, 7.5 mM NaN_3, 0.3 mM ammonium molybdate, and ATP (1 mM, 2 mM, or 3 mM) in the presence of different concentrations of the compound (100–6.25 μg/ml). After incubation, the reaction was stopped by the addition of 1% SDS [23], and the amount of released inorganic phosphate (Pi) was measured through the Fiske and Subbarow method [24]. Briefly, 100 μL of ammonium molybdate was added to the wells, and inorganic phosphate released from ATP hydrolysis was measured spectrophotometrically at 660 nm (Fluostar Optima, BMG Labtech, Offenburg, Germany). Preparations containing plasma membranes obtained from the null mutant strain AD1234567 (Pdr5p− membranes) were used as controls, and the difference between the

ATPase activity of the Pdr5p+ and Pdr5p− membranes represents the ATPase activity that is mediated by Pdr5p. A Lineweaver-Burk plot was designed in order to assess the type of inhibition promoted by β-lap.

Mitochondrial membrane potential measurement

The effect of β-lapachone on the mitochondrial membrane potential of Pdr5p+ strain was evaluated as described by Hwang et al. [25], with slight modifications. Briefly, 10^7 cells/ml of Pdr5p+ strain were incubated at 30 °C for 90 min in the presence of 100 μg/ml β-lap and 10 μM sodium azide. Untreated cells were used as negative control. Cells were harvested by centrifugation at 5000*g* for 3 min and pellets were resuspended in PBS containing 2.5 μg/ml JC-1 and incubated for 15 min in darkness. Fluorescence was measured at 485/530 nm (excitation/emission) and at 485/590 nm (SpectraMax i3x, Molecular Devices, CA, USA), and results were expressed as the JC-1 fluorescence ratio (590 nm/530 nm).

RT-PCR

Quantification of mRNA expression levels was performed as previously described [26]. Briefly, Pdr5p+ cells (10^7 cells/ml) were incubated in the presence or absence (calibrator system) of 100 μg/ml β-lap, 125 μg/ml fluconazole, and 100 μg/ml β-lap + 125 μg/ml fluconazole for 90 min at 30 °C. Then, cells were harvested by centrifugation at 5000*g* for 3 min and washed twice with PBS 10 mM pH 7.2. The pellet was resuspended in an RNA lysis buffer (10 mM Tris-HCl pH 8.0; 0.5 M EDTA; 0.5% SDS; 1% 2-mercaptoethanol), mixed for 30 s and incubated at 65 °C for 1 h. Afterwards, RNA was extracted using a homemade TRIzol Reagent (38% phenol pH 4.3, 0.8 M guanidine thiocyanate, 0.4 M ammonium thiocyanate, 0.1 M sodium acetate pH 5.0, 5% glycerol) [27]. From each sample, 1.0 μg of total RNA was subjected to RNase-free DNase I (Thermo Fisher Scientific, MA, USA) treatment, and complementary DNA was synthesized using the high-capacity cDNA reverse. Quantitative PCR was performed using a SYBR Mix, consisting of 20 mM Tris, 50 mM potassium chloride, 5 mM magnesium chloride, 5 μL JumpStart Taq DNA polymerase, 0.5× SYBR Green, and 200 nM dNTP. Gene expression profile was evaluated using the StepOnePlus™ Real-Time PCR System (Thermo Fisher Scientific, MA, USA) under default parameters. The $2^{-\Delta\Delta CT}$ method was adopted to calculate the relative abundance of the samples employing TFC1 as a housekeeping gene to normalize the expression of *PDR5* gene. The following real-time PCR primers (0.4 μM) were used: *PDR5F*: 5′-CCCA AGTGCCATGCCTAGAT-3′; *PDR5R*: 5′-CGTT AGCAACACCAACAGCC-3′; *TFC1F*: TGGATGAC GTTGATGCAGAT-3′; *TFC1R*: 5′-GCTCGCTTTTCATT GTTTCC-3′.

Human erythrocyte viability

The effect of β-lap on human erythrocyte viability was assessed as described elsewhere [18]. Cells were washed three times and resuspended in PBS to a final of concentration of 2% v/v. Then, cells were incubated in the presence of different concentrations of β-lap (128–0.5 μg/ml) for 60 min at 37 °C. Afterward, cells were harvested by centrifugation at 3000*g* for 5 min and 100 μl of supernatant was transferred to the wells of a 96-well microplate. The absorbance of hemoglobin released from human erythrocytes was measured at 540 nm (Fluostar Optima, BMG Labtech, Offenburg, Germany). Controls of 100% and 0% hemolysis were performed by incubating the cells in PBS in the presence or absence of 1% Triton X-100, respectively.

Statistical analysis

All the experiments were performed at least three times, and the results were expressed as mean ± standard deviation. Data were analyzed by Student's *t* test, and *P* values lower than 0.05 were considered significant.

Results

Antifungal susceptibility test

While α-nor and β-lap completely inhibited *S. cerevisiae* growth at 100 μg/ml, α-lap inhibited fungal growth in 28% at 100 μg/ml. Moreover, β-nor did not present antifungal activity against Pdr5p+ cells (Fig. 2). Furthermore, Fig. 2

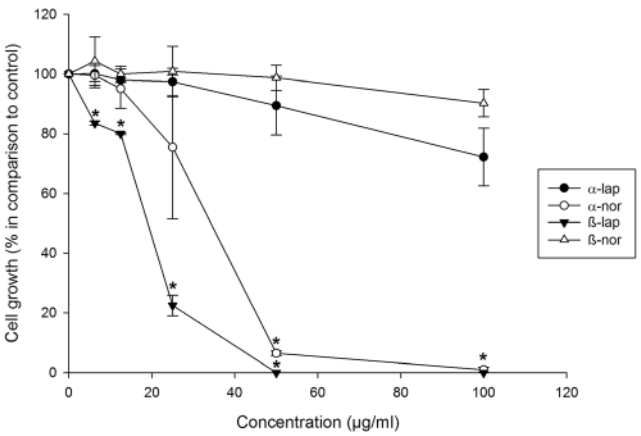

Fig. 2 Evaluation of the growth of Pdr5p+ cells in the presence of the tested compounds. Cells were grown in the presence of α-lapachone, α-nor-lapachone, β-lapachone, and β-nor-lapachone at 6.25–100 μg/ml at 37 °C for 48 h. Cell growth was measured spectrophotometrically (600 nm). Data represent mean ± standard error of three independent experiments. Black circle for α-lapachone. Whit circle for α-nor-lapachone. Inverted black triangle for β-lapachone. White triangle for β-nor-lapachone. *$p < 0.05$

shows that the inhibition of cell growth by α-lap, α-nor, and β-lap was dose-dependent.

Checkerboard assay

Data obtained by checkerboard assay are summarized in Table 1. Combining α-lap, α-nor, or β-nor with fluconazole did not enhance the antifungal activity of the compounds, and FICI values ranged from 1.5 to 2.0, indicating no interaction. Nevertheless, the association between β-lap and fluconazole promoted a 4-fold decrease in their MIC values, with a FICI of 0.5, indicating synergism.

Spot assay

The combined activity between β-lapachone and fluconazole was also evaluated through the spot assay. Results presented in Fig. 3 show that Pdr5p+ cells grew in the absence and presence of 125 μg/ml fluconazole (positive control). Cells were able to grow at all yeast concentrations tested. On the other hand, the combination of β-lap and fluconazole completely inhibited cell growth.

Reactive species oxygen measurement

Pdr5p+ cells produced a basal concentration of ROS after incubation in the absence of any substances (Fig. 4a). Treatment with 125 μg/ml fluconazole did not change significantly the fluorescence emitted by DCFH-DA, indicating that this antifungal agent did not stimulate ROS production by Pdr5p+ cells. Nonetheless, treatment with 100 μg/ml β-lap led to an approximately 2-fold increase of ROS concentration. Combining β-lap with fluconazole did not augment the ROS production in comparison with treatment with β-lap alone. Ascorbic acid significantly diminished ROS production, being used as a negative control. Moreover, combining β-lap, fluconazole and ascorbic acid promoted cell growth comparable with a positive control (Fig. 4b).

Table 1 Checkerboard assays of *S. cerevisiae* mutant strain overexpressing the multidrug efflux pump Pdr5p

	Lapachone (μg/ml)			Fluconazole (μg/ml)			FICI	Outcome
	MIC a	MIC c	FIC	MIC a	MIC c	FIC		
α-Lap	> 100	> 100	1	500	500	1	2	I
α-Nor	100	50	0.5	500	500	1	1.5	I
β-Lap	50	12.5	0.25	500	125	0.25	0.5	S
β-Nor	> 100	> 100	1	500	500	1	2	I

MIC a, MIC of compound alone; *MIC c*, MIC of compound combined; *FIC*, fractional inhibitory concentration; *FICI*, fractional inhibitory concentration index; *I*, indifferent; *S*, synergistic

In this methodology, β-lap was used at a concentration (100 μg/ml) higher than its MIC in combination with fluconazole, due to the increase in the number of yeasts used. Toxicity was not observed when 10^7 cells/ml was incubated with 100 μg/ml β-lap at 30 °C for 48 h, a period higher than the used in the present methodology (data not shown).

Nile red accumulation assay

Nile red is a highly fluorescent phenoxazine derivative and is also a substrate for MDR transporters. In a cell where efflux pumps are either blocked or low expressed, Nile red incorporates into the cytoplasm and stains it red. However, a cell that overexpresses MDR transporters extrudes Nile red from the intracellular environment, diminishing fluorescence. Treatment of Pdr5p+ cells with 100 μg/ml β-lap increased Nile red accumulation in 79.4%, in comparison with the untreated cells, as shown in Fig. 5.

ATPase activity

Since Pdr5p is an ATP-binding cassette protein, it uses ATP hydrolysis as an energy source to extrude drugs from the cell. Thus, inhibiting ATPase activity of Pdr5p would preclude its ability to transport substances. At concentrations ranging from 6.25 to 100 μg/ml, β-lap inhibited Pdr5p ATPase activity by 72.6–82.5% (Fig. 6a). The Lineweaver-Burk plot shows that the effect of β-lap on Pdr5p ATPase activity resulted from a mixed inhibition (Fig. 6b).

Mitochondrial membrane potential measurement

ATP production by mitochondria is dependent of the mitochondrial membrane potential. Since ATP is the energy source of ABC proteins, disrupting mitochondrial membrane potential (MMP) would jeopardize ATP production, avoiding the functioning of Pdr5p. At 100 μg/ml, β-lap reduced MMP by 25%, while sodium azide decreased MMP by 37% (Fig. 7).

RT-PCR

Besides the impairment of the efflux pump activity, another strategy that could be used to overcome drug resistance is the inhibition of gene transcription. In order to verify this hypothesis, the RT-PCR assay was performed. Neither β-lap and fluconazole alone nor the combination between these drugs affected the transcription of the *PDR5* gene (Fig. 8).

Human erythrocyte viability

Treatment of human erythrocytes with β-lap at 128 μg/ml produced hemolysis (3.77%) comparable with PBS (3.56%)

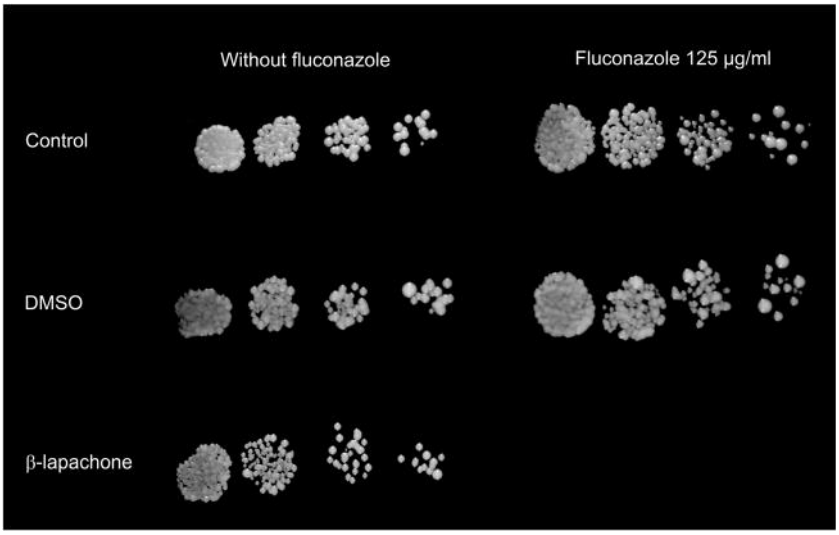

Fig. 3 Combined effect of β-lapachone and fluconazole on the growth of Pdr5p+ cells in solid media through spot assay. Serial 5-fold dilution cells were spotted onto YPD agar in the presence or absence of 125 µg/ml fluconazole, 0.125% DMSO, and 12.5 µg/ml β-lapachone. Combining fluconazole and β-lapachone resulted in the complete inhibition of Pdr5p+ cell growth

and DMSO at 1.28% (5.23%) (Fig. 9), denoting to a non-hemolytic activity of the compound.

Discussion

The research focusing on the discovery of new antifungal therapies has largely increased in the past decade, due to high mortality caused by invasive fungal infections in immunocompromised individuals [28, 29]. The present status of fungal infection epidemiology is the consequence of the remarkable ability of fungi to acquire resistance to antifungal agents. Then, overcoming fungal resistance mechanisms would be a promising approach to cope with infections caused by MDR microorganisms [30].

Since the main MDR mechanism of pathogenic fungi is related to the overexpression of efflux transporters along the plasma membrane, inhibiting these proteins could avoid the extrusion of the antifungal agent and hence allow its antifungal activity [31]. Thus, the aim of this study was to evaluate whether lapachones, natural products with known antifungal activity, are able to enhance the antifungal activity of fluconazole through the inhibition of Pdr5p, a *S. cerevisiae* MDR transporter.

Firstly, the effect of lapachones on Pdr5p+ cells growth was evaluated through a microdilution technique. A dose-dependent effect of β-lap on the growth of Pdr5p+ strain was observed, with a MIC value of 50 µg/ml. Menacho-Márquez and Murguía [32] assessed the effect of β-lap on the growth of a wild-type *S. cerevisiae* strain and have also

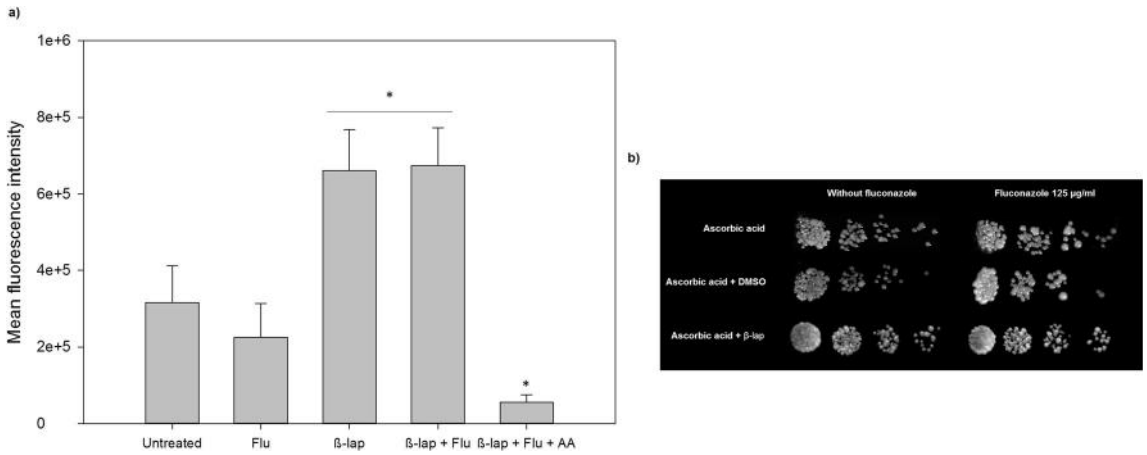

Fig. 4 Effect of β-lapachone and fluconazole alone and in combination on ROS production by Pdr5p+ cells. **a** ROS production after treatment with 125 µg/ml fluconazole was comparable with control. Treatment with 100 µg/ml β-lapachone increased ROS production. Combining β-lap with fluconazole did not enhance ROS production in comparison with treatment with β-lapachone alone. Ascorbic acid significantly diminished ROS production, being used as a negative control. $*p < 0.05$ in comparison with untreated system. **b** Combined effect of ascorbic acid, β-lapachone, and fluconazole on the growth of Pdr5p+ cells in solid media through spot assay. Serial 5-fold dilution cells were spotted onto YPD agar in the presence or absence of 125 µg/ml fluconazole, 25 mM ascorbic acid, 0.125% DMSO, and 12.5 µg/ml β-lapachone. Combining 100 µg/ml β-lapachone, 125 µg/ml fluconazole, and 25 mM ascorbic acid promoted cell growth comparable to the positive control

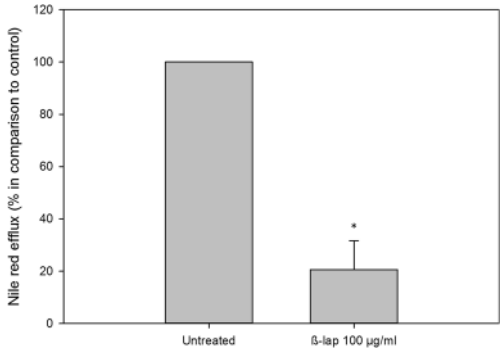

Fig. 5 Assessment of Pdr5p activity by Nile red accumulation assay. Pdr5p+ cells were incubated in the presence or absence of 100 μg/ml β-lapachone for 60 min at 30 °C. Then, cells were loaded with Nile red, and the transporter was activated by adding 0.2% glucose. Treatment of Pdr5p+ cells with β-lapachone inhibited Nile red efflux by 79.4%. *$p < 0.05$

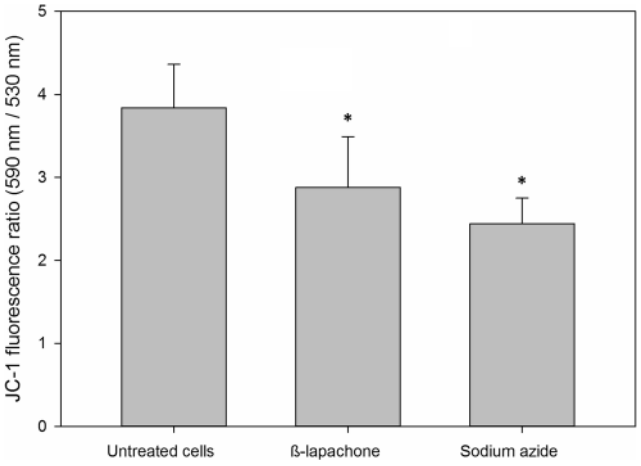

Fig. 7 Mitochondrial membrane potential in the presence of β-lapachone was assessed by JC-1 labeling. β-Lapachone at 100 μg/ml reduced MMP by 25%, while sodium azide decreased MMP by 37%. *$p < 0.05$

observed a dose-dependent profile; however, the highest concentration employed in this study was 20 μg/ml. At this concentration, a reduction of 60% on *S. cerevisiae* growth was observed, while we obtained an 80% growth reduction at 25 μg/ml.

The greater effect of α-nor and β-lap against yeast growth was reported by our group in a previous study using a fluconazole-resistant *C. albicans* strain [14]. Nevertheless, α-lap and β-nor have also shown antifungal activity against *C. albicans*, which was not observed in the present study against *S. cerevisiae* cells. Moreover, Pdr5p+ cells were less susceptible to lapachones than the aforementioned *C. albicans* strain. A study using a higher number of *C. albicans* and *S. cerevisiae* strains must be performed in order to compare the susceptibility of these two microorganisms to lapachones and confirm this finding.

In order to screen the compounds for use on the subsequent methodologies, the interaction between lapachones and fluconazole, a well-known antifungal drug, was evaluated by the checkerboard method. Only β-lap presented synergism with fluconazole against Pdr5p+ cellular growth. For this reason, this compound was selected and used in the following assays. This is the first report regarding the synergic effect between β-lap and an antifungal agent. The interaction between β-lap and antimicrobial drugs has been characterized in other organisms, such as *Mycobacterium* sp. [33] and

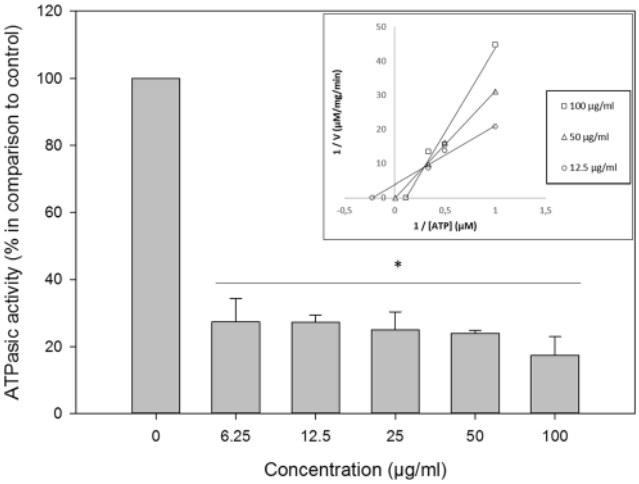

Fig. 6 The effect of β-lapachone on the ATPase activity of Pdr5p was evaluated by incubating membranes containing Pdr5p in the presence of different concentrations of the compound (100–6.25 μg/ml). β-Lapachone inhibited Pdr5p ATPase activity by 72.6–82.5%. The Lineweaver-Burk plot shows that the effect of β-lap on Pdr5p ATPase activity occurred due to a mixed inhibition (inset). *$p < 0.05$

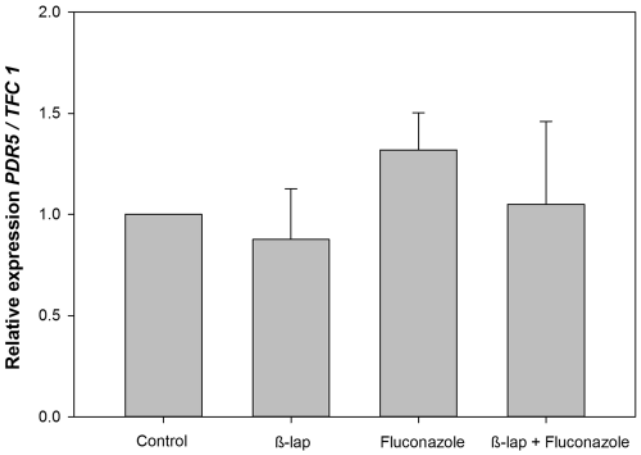

Fig. 8 The influence of β-lapachone alone or in combination with fluconazole on *PDR5* mRNA expression of Pdr5p+ cells was assessed by RT-PCR. TFC1 was used as a housekeeping gene and the untreated cells as a reference sample. The relative expression level of mRNA was calculated using the ΔΔCT method. Values represent mean + SD of three independent experiments. One hundred micrograms per milliliter of β-lapachone, 125 μg/ml fluconazole, and 100 μg/ml β-lapachone + 125 μg/ml fluconazole did not exert any significant effect on *PDR5* gene expression

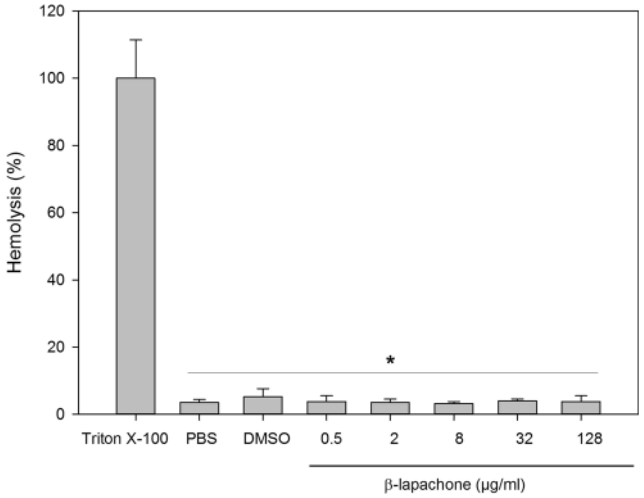

Fig. 9 Evaluation of β-lapachone toxicity against human erythrocytes. A human erythrocyte suspension (0.5% v/v) was incubated in the presence of serial concentrations of β-lapachone (128–0.5 μg/ml) for 60 min, and the absorbance of released hemoglobin was measured at 540 nm. Controls of 100% and 0% hemolysis were performed by incubating the cells in PBS in the presence or absence of 1% Triton X-100, respectively. DMSO (1.28%) was also used as control. β-Lapachone showed toxicity comparable with PBS and DMSO. *$p < 0.05$

Staphylococcus aureus [34], but the mechanisms involved were not yet clarified.

According to Ramos-Pérez et al. [35], the antifungal activity of β-lap is related to its ability to induce ROS production, since a *yap1*Δ mutant strain was hypersensitive to the quinone at 30 μM. Anaissi-Afonso et al. [36] have also observed that β-lap and derivatives at 10–100 μM exert their antifungal activity through oxidative stress and mitochondrial disfunction. On the other hand, Menacho-Márquez et al. [37] observed that pre-incubation with dicoumarol did not affect the antifungal toxicity of β-lap, indicating that ROS production is not the mechanism responsible for the toxicity of β-lap against *S. cerevisiae*. In this study, it was observed that combining β-lap and fluconazole did not enhance ROS production. Nonetheless, ascorbic acid prevented the inhibitory effect of the combination β-lap and fluconazole on *S. cerevisiae* growth, pointing to the essential role of ROS on the synergism between β-lap and fluconazole. Li et al. [38] observed that osthole, a prenylated coumarin obtained from the Chinese herb *Cnidii fructus*, presented a synergistic effect with fluconazole against the growth of fluconazole-resistant *Candida albicans* strains. The mechanism involved in this action may be related to ROS production, since combining these substances led to the upregulation of oxidation-reduction genes. Interestingly, unlike β-lap, osthole combined with fluconazole promoted a threefold increase of intracellular ROS production (in comparison with osthole alone), reinforcing the participation of ROS on the synergistic interaction between these compounds.

Pdr5p+ strain was used in this study because its azole resistance is a consequence of the overexpression of Pdr5p, an ABC transporter related to the MDR phenotype. In order to unveil whether the combined activity of β-lap and fluconazole occurs due to the inhibition of Pdr5p function, a methodology using Nile red was employed [39]. In this study, it was observed that β-lap significantly increased Nile red fluorescence within the cells, meaning that the efflux of this dye was inhibited. Then, it may be concluded that β-lap affects the functioning of Pdr5p transporter, which explains the results obtained on the checkerboard assay. The inhibition of Pdr5p by β-lap allows fluconazole to reach the intracellular concentration needed to perform its antifungal activity. Consequently, a synergic activity between β-lap and fluconazole was achieved.

In order to evaluate whether the inhibition of Pdr5p is related to a decrease in its ATPase activity, purified plasma membranes with a high concentration of Pdr5p were used. Results show that β-lap significantly impaired Pdr5p ATPase activity through a mixed inhibition. In previous studies, our group reported the inhibition of Pdr5p ATPase activity by several distinct substances, such as organic compounds containing tellurium [19]. Nonetheless, the inhibition of ATPase activity is not required for the impairment of efflux pump activity. Farnesol, a natural sesquiterpene compound, inhibits efflux promoted by *Candida albicans* CaCdr1p without affecting ATPase activity [40]. Interestingly, Loo and Clarke [41] showed that tariquidar, a quinoline compound known as a potent inhibitor of P-glycoprotein, stimulates the ATPase activity of this efflux transporter by changing the nucleotide-binding domain (NBD) conformation.

In addition to a direct action on Pdr5p ATPase activity, β-lap could decrease ATP production by perturbing mitochondrial function. In order to evaluate if the compound is capable of change, the mitochondrial membrane potential (MMP), the potentiometric probe JC-1 was used. JC-1 accumulation in mitochondria depends on its potential. Mitochondrial polarization promotes the generation of red J-aggregates, capable of emitting fluorescence at 590 nm. On the other hand, green monomers that possess an emission fluorescence at 530 nm are formed when mitochondria is depolarized. Then, the ratio between the fluorescence intensity at 590 nm/530 nm is directly related to MMP [42]. It was observed that β-lap decreased MMP, indicating an indirect impairment of ATPase activity of Pdr5p, since mitochondrial polarization is essential to ATP production. Previous studies have shown that mitochondria is an important target of β-lap both in fungi [36] and other organisms such as *Trypanosoma cruzi* [43] and cancer cells [44].

As well as inhibiting the transporter activity, a substance may preclude the efflux process by downregulating the transcription of *PDR5* gene. Data obtained showed that β-lap, fluconazole, and the combination β-lap + fluconazole did not change mRNA levels. The inhibition of a fungal MDR transporter by a natural product without alteration in transcript levels has already been reported. Geraniol, a monoterpene

found in essential oils of several plants, competitively inhibits CaCdr1p (a *C. albicans* ABC transporter) through binding to its active site. However, geraniol affects neither the transcription nor the translation of the transporter [6]. Then, we may conclude that the capability of inhibiting ABC transporters gene transcription is not essential for a substance to be used as an efflux pump inhibitor.

Lack of toxicity is an essential requirement for a substance be considered suitable for clinical usage. Thus, the ability of β-lap to disrupt erythrocytes was assessed, by measuring the release of hemoglobin after treatment with the compound. Results show that β-lap did not possess hemolytic activity, and it is fundamental considering a clinical situation where an intravenous administration is mandatory. Furthermore, the majority of drugs taken orally reach the bloodstream to be distributed to the target tissue. Then, using drugs with hemolytic activity would also be harmful considering oral administration.

Besides antifungal activity, β-lap showed synergistic activity with fluconazole against the growth of the *S. cerevisiae* strain used in this study. Moreover, data obtained indicates that this synergism is related to ROS production, inhibition of Pdr5p ATPase activity, and mitochondrial disfunction, leading to the impairment of efflux mediated by this transporter. In addition, β-lap did not exert toxic effects upon human erythrocytes. Considering our results and the homology between *S. cerevisiae* Pdr5p and pathogenic fungi MDR transporters, we may suggest that β-lap is a potential candidate to be used in association to fluconazole in the treatment of fluconazole-resistant fungal infections. Further studies employing pathogenic fungi clinical isolates that overexpress these proteins will be conducted to evaluate the effect of β-lapachone on pathogenic fungi.

Acknowledgments This research was supported by the Conselho Nacional de Desenvolvimento Científico e Tecnológico (CNPq) (Brazil) and Fundação de Amparo a Pesquisa do Estado do Rio de Janeiro (FAPERJ). The authors would like to thank Geralda Rodrigues Almeida for the technical support.

Funding information This study was financed by the Coordenação de Aperfeiçoamento de Pessoal de Nível Superior—Brazil (CAPES)—Finance Code 001.

Compliance with ethical standards

Conflict of interest The authors declare that they have no conflict of interest.

References

1. Dudoignon E, Alanio A, Anstey J, Coutrot M, Fratani A, Jully M et al (2019) Outcome and potentially modifiable risk factors for candidemia in critically ill burns patients: a matched cohort study. Mycoses 62:237–246
2. Ben-Ami R (2018) Treatment of invasive candidiasis: a narrative review. J Fungi 4:97
3. Healey KR, Perlin DS (2018) Fungal resistance to Echinocandins and the MDR phenomenon in *Candida glabrata*. J Fungi 4:105
4. Sanguinetti M, Posteraro B (2015) Antifungal drug resistance among *Candida* species: mechanisms and clinical impact. Mycoses 58:2–13
5. Cardno TS, Ivnitski-steele I, Lackovic K, Cannon RD (2016) Targeting efflux pumps to overcome antifungal drug resistance. Future Med Chem 8:1485–1501
6. Singh S, Fatima Z, Ahmad K, Hameed S (2018) Fungicidal action of geraniol against *Candida albicans* is potentiated by abrogated CaCdr1p drug efflux and fluconazole synergism. PLoS One 13: e0203079
7. Cavalheiro M, Pais P, Galocha M (2018) Host-pathogen interactions mediated by MDR transporters in fungi: as pleiotropic as it gets! Genes 9:332
8. Golin J, Ambudkar SV (2015) The multidrug transporter Pdr5 on the 25th anniversary of its discovery: an important model for the study of asymmetric ABC transporters. Biochem J 467:353–363
9. Prasad R, Wergifosse PD (1995) Molecular cloning and characterization of a novel gene of *Candida albicans*, CDR1, conferring multiple resistance to drugs and antifungals. Curr Genet 27:320–329
10. Sanglard D, Ischer F, Monod M, Billel J (1997) Cloning of *Candida albicans* genes conferring resistance to azole antifungal agents: characterization of CDR2, a new multidrug ABC transporter gene. Microbiology:405–416
11. Demuyser L, Van Dijck P (2019) Can *Saccharomyces cerevisiae* keep up as a model system in fungal azole susceptibility research ? Drug Resist Updat 42:22–34
12. Oliveira D, Sousa E, Alves S, Tomaz V, Suarez S, Lima M et al (2016) Effects of a novel b-lapachone derivative on *Trypanosoma cruzi* : parasite death involving apoptosis, autophagy and necrosis. Int J Parasitol Drugs Resist 6:207–219
13. Yang Y, Zhou X, Xu M, Piao J, Zhang Y, Lin Z (2017) β-Lapachone suppresses tumour progression by inhibiting epithelial-to-mesenchymal transition in NQO1-positive breast cancers. Sci Rep 7:2681
14. Moraes DC, Curvelo JAR, Anjos CA, Moura KCG, Pinto MCFR, Portela MB (2018) β-Lapachone and α-nor-lapachone modulate *Candida albicans* viability and virulence factors. J Mycol Med 28:314–319
15. Decottignies A, Kolaczkowski M, Balzi E, Goffeau A (1994) Solubilization and characterization of the overexpressed *PDR5* multidrug resistance nucleotide triphosphatase of yeast. J Biol Chem 269:12797–12803
16. Hooker SC (1936) The constitution of lapachol and its derivatives. Part IV. Oxidation with potassium permanganate. J Am Chem Soc 58:1168–1173
17. Rex JH, Alexander BD, Andes D, Arthington-Skaggs B, Brown SD, Chaturvedi V et al (2008) Reference method for broth dilution antifungal susceptibility testing of yeasts: approved standard-third edition. Clin Lab Stand Inst:1–25
18. Niimi K, Harding DRK, Parshot R, King A, Lun DJ, Decottignies A, Niimi M, Lin S, Cannon RD, Goffeau A, Monk BC (2004) Chemosensitization of fluconazole resistance in *Saccharomyces cerevisiae* and pathogenic fungi by a D-octapeptide derivative. Antimicrob Agents Chemother 48:1256–1271
19. Figueira L, De Sá R, Toledo FT, De Sousa BA, Gonçalves AC, Tessis AC et al (2014) Synthetic organotelluride compounds induce the reversal of Pdr5p mediated fluconazole resistance in *Saccharomyces cerevisiae*. BMC Microbiol:1–9
20. Bueno I, Batista J, Rocha T, Silva M (2015) Diphenyl diselenide (PhSe)2 inhibits biofilm formation by *Candida albicans*, increasing

both ROS production and membrane permeability. J Trace Elem Med Biol 29:289–295
21. Keniya MV, Fleischer E, Klinger A, Cannon RD (2015) Inhibitors of the *Candida albicans* major facilitator superfamily transporter Mdr1p responsible for fluconazole resistance. PLoS One 10: e0126350
22. Rangel LP, Fritzen M, Yunes RA, Leal PC, Creczynski-Pasa TB, Ferreira-Pereira A (2010) Inhibitory effects of gallic acid derivatives on *Saccharomyces cerevisiae* multidrug resistance protein Pdr5p. FEMS Yeast Res 10:244–251
23. Dulley JR (1975) Determination of inorganic phosphate in the presence of detergents or protein. Anal Biochem 67:91–96
24. Fiske CH, Subbarow Y (1925) The colorimetric determination of phosphorus. J Biol Chem 66-375:400
25. Hwang JH, Choi H, Kim AR, Yun JW, Yu R, Woo ER, Lee DG (2014) Hibicuslide C-induced cell death in Candida albicans involves apoptosis mechanism. J Appl Microbiol 117:1400–1411
26. Ricardo E, Costa-de-oliveira S, Dias AS (2009) Ibuprofen reverts antifungal resistance on *Candida albicans* showing overexpression of CDR genes. FEMS Yeast Res 9:618–625
27. Valach M (2016) RNA extraction using the "home-made" TRIzol substitute. protocols.io. http://www.protocols.io/view/RNA-extraction-using-the-home-made-Trizol-substitu-eiebcbe. Accessed 10 July 2019
28. De Oliveira HC, Monteiro MC, Rossi AS (2019) Identification of off-patent compounds that present antifungal activity against the emerging fungal pathogen *Candida auris*. Front Cell Infect Microbiol 9:1–10
29. Wang C, Zhang Y, Zhang W, Yuan S, Ng T, Ye X (2019) Purification of an antifungal peptide from seeds of *Brassica oleracea* var gongylodes and investigation of its antifungal activity and mechanism of action. Molecules 24:1337
30. Spitzer M, Robbins N, Wright GD (2017) Combinatorial strategies for combating invasive fungal infections. Virulence 8:169–185
31. Prasad R, Rawal MK (2014) Efflux pump proteins in antifungal resistance. Front Pharmacol 5:1–13
32. Menacho-Márquez M, Murguia JR (2006) β-Lapachone activates a Mre11p-Tel1p G1/S checkpoint in budding yeast. Cell Cycle 5: 2509–2516
33. Silva JL, Mesquita ARC, Ximenes EA (2009) In vitro synergic effect of β -lapachone and isoniazid on the growth of *Mycobacterium fortuitum* and *Mycobacterium smegmatis*. Mem Inst Oswaldo Cruz 104:580–582
34. Macedo L, Fernandes T, Silveira L, Mesquita A, Franchitti AA, Ximenes EA (2013) β-Lapachone activity in synergy with conventional antimicrobials against methicillin resistant *Staphylococcus aureus* strains. Phytomedicine 21:25–29
35. Ramos-Pérez C, Lorenzo-Castrillejo I, Quevedo O, García-Luis J, Matos-Perdomo E, Medina-Coello C, Estévez-Braun A, Machín F (2014) Yeast cytotoxic sensitivity to the antitumour agent β-lapachone depends mainly on oxidative stress and is largely independent of microtubule or topoisomerase-mediated DNA damage. Biochem Pharmacol 92:206–219
36. Anaissi-Afonso L, Oramas-Royo S, Ayra-Plasencia J, Martín-Rodríguez P, García-Luis J, Lorenzo-Castrillejo I et al (2018) Lawsone, juglone, and β-lapachone derivatives with enhanced mitochondrial-based toxicity. ACS Chem Biol 13:1950–1957
37. Menacho-Márquez M, Rodríguez-Hernández CJ, Villarong MÁ, Pérez-Valle J, Gadea J, Belandia B et al (2015) EIF2 kinases mediate β-lapachone toxicity in yeast and human cancer cells. Cell Cycle 14:630–640
38. Li DD, Chai D, Huang XW, Guan SX, Du J, Zhang HY et al (2017) Potent in vitro synergism of fluconazole and osthole against fluconazole-resistant *Candida albicans*. Antimicrob Agents Chemother 61:e00436–e00417
39. Ivnitski-steele I, Holmes AR, Lamping E, Monk BC, Richard D, Sklar LA (2009) Identification of Nile red as a fluorescent substrate of the *Candida albicans* ABC transporters Cdr1p and Cdr2p and the MFS transporter Mdr1p. Anal Biochem 394:87–91
40. Sharma M, Prasad R (2011) The quorum-sensing molecule farnesol is a modulator of drug efflux mediated by ABC multidrug transporters and synergizes with drugs in *Candida albicans*. Antimicrob Agents Chemother 55:4834–4843
41. Loo TW, Clarke DM (2014) Tariquidar inhibits P-glycoprotein drug efflux but activates ATPase activity by blocking transition to an open conformation. Biochem Pharmacol 92:558–566
42. Chazotte B (2011) Labeling mitochondria with JC-1. Cold Spring Harb Protoc 6:1103–1104
43. Menna-Barreto RFS, Corrêa JR, Pinto AV, Soares MJ, De Castro SL (2007) Mitochondrial disruption and DNA fragmentation in *Trypanosoma cruzi* induced by naphthoimidazoles synthesized from β-lapachone. Parasitol Res 101:895–905
44. Li YZ, Li CJ, Pinto AV, Pardee AB (1999) Release of mitochondrial cytochrome C in both apoptosis and necrosis induced by β-lapachone in human carcinoma cells. Mol Med 5:232–239

frontiers in Oncology

ORIGINAL RESEARCH
published: 17 December 2020
doi: 10.3389/fonc.2020.557280

Interplay Between EGFR and the Platelet-Activating Factor/PAF Receptor Signaling Axis Mediates Aggressive Behavior of Cervical Cancer

Juliana L. Souza[1], Karina Martins-Cardoso[1], Isabella S. Guimarães[2], Andréia C. de Melo[2], Angela H. Lopes[3], Robson Q. Monteiro[1] and Vitor H. Almeida[1]**

[1] Instituto de Bioquímica Médica Leopoldo de Meis, Universidade Federal do Rio de Janeiro, Rio de Janeiro, Brazil, [2] Divisão de Pesquisa Clínica e Desenvolvimento Tecnológico, Instituto Nacional de Câncer, Rio de Janeiro, Brazil, [3] Instituto de Microbiologia Paulo de Góes, Universidade Federal do Rio de Janeiro, Rio de Janeiro, Brazil

OPEN ACCESS

Edited by:
Matiullah Khan,
AIMST University, Malaysia

Reviewed by:
Simone Anfossi,
University of Texas MD Anderson Cancer Center, United States
Marilia Seelaender,
University of São Paulo, Brazil

***Correspondence:**
Vitor H. Almeida
vhluna@bioqmed.ufrj.br
Robson Q. Monteiro
robsonqm@bioqmed.ufrj.br

Specialty section:
This article was submitted to Cancer Molecular Targets and Therapeutics, a section of the journal Frontiers in Oncology

Received: 29 April 2020
Accepted: 16 November 2020
Published: 17 December 2020

Citation:
Souza JL, Martins-Cardoso K, Guimarães IS, de Melo AC, Lopes AH, Monteiro RQ and Almeida VH (2020) Interplay Between EGFR and the Platelet-Activating Factor/PAF Receptor Signaling Axis Mediates Aggressive Behavior of Cervical Cancer. Front. Oncol. 10:557280. doi: 10.3389/fonc.2020.557280

Epidermal growth factor receptor (EGFR) is a receptor tyrosine kinase widely expressed in cervical tumors, being correlated with adverse clinical outcomes. EGFR may be activated by a diversity of mechanisms, including transactivation by G-protein coupled receptors (GPCRs). Studies have also shown that platelet-activating factor (PAF), a pro-inflammatory phospholipid mediator, plays an important role in the cancer progression either by modulating the cancer cells or the tumor microenvironment. Most of the PAF effects seem to be mediated by the interaction with its receptor (PAFR), a member of the GPCRs family. PAFR- and EGFR-evoked signaling pathways contribute to tumor biology; however, the interplay between them remains uninvestigated in cervical cancer. In this study, we employed The Cancer Genome Atlas (TCGA) and cancer cell lines to evaluate possible cooperation between EGFR, PAFR, and lysophosphatidylcholine acyltransferases (LPCATs), enzymes involved in the PAF biosynthesis, in the context of cervical cancer. It was observed a strong positive correlation between the expression of EGFR × PAFR and EGFR × LPCAT2 in 306 cervical cancer samples. The increased expression of LPCAT2 was significantly correlated with poor overall survival. Activation of EGFR upregulated the expression of PAFR and LPCAT2 in a MAPK-dependent fashion. At the same time, PAF showed the ability to transactivate EGFR leading to ERK/MAPK activation, cyclooxygenase-2 (COX-2) induction, and cell migration. The positive crosstalk between the PAF-PAFR axis and EGFR demonstrates a relevant linkage between inflammatory and growth factor signaling in cervical cancer cells. Finally, combined PAFR and EGFR targeting treatment impaired clonogenic capacity and viability of aggressive cervical cancer cells more strongly than each treatment separately. Collectively, we proposed that EGFR, LPCAT2, and PAFR emerge as novel targets for cervical cancer therapy.

Keywords: cervical cancer, epidermal growth factor receptor, platelet-activating factor, platelet-activating factor receptor, lysophosphatidylcholine acyltransferase 2, signaling pathways

INTRODUCTION

Cervical cancer is the fourth most common tumor and the fourth leading cause of cancer death in women worldwide, with 570,000 cases and 311,000 deaths in 2018. Most cases of this neoplasia occur in low- and middle-income countries and the human papillomavirus (HPV) infection is the virtually necessary factor for cervical cancer development (1). Patients with advanced-stage tumors have 5-year survival rates lower than 50% (2), and novel therapeutic strategies are needed to improve these women's prognosis.

Membrane proteins, such as receptor tyrosine kinases (RTKs) and G protein-coupled receptors (GPCRs), are critical in the intercellular communication and signal transduction, modulating gene expression and cell responses to the extracellular stimuli. Alterations in these receptors and their regulated signaling pathways are commonly observed in cell transformation and tumor progression, making them useful as biomarkers, prognostic factors, and pharmacological targets (3).

The human epidermal growth factor receptor (EGFR/HER-1) belongs to the HER (Human EGF Receptor) receptor tyrosine kinase family. EGFR activation by ligands leads to its dimerization, phosphorylation, and activation of signaling pathways, such as PI3K (phosphoinositide 3-kinase) - Akt, MAPK (mitogen-activated protein kinase)/ERK (extracellular signal-regulated kinase), STATs (signal transducer and activator of transcription), and PLC (phospholipase C) - PKC (protein kinase C), which promote cell proliferation, angiogenesis, apoptosis evasion and cell invasion (4, 5). The literature has shown that EGFR is expressed in about 80% of cervical carcinomas and is correlated with disease progression (6–8). In addition, previous reports demonstrated that EGFR can be transactivated by various agonists unrelated to EGFR ligands, such as GPCR ligands, in models that include cervical cancer cells (9–11).

Chronic inflammatory microenvironment has been suggested as an enabling characteristic of cell transformation and oncogenesis (12). Platelet-activating factor (PAF, 1-O-alkyl-2-acetyl-sn-glycero-3-phosphocholine) is a biologically active phospholipid mediator with potent pro-inflammatory activity. Although PAF has been named for its ability to induce platelet activation at nanomolar concentrations, several studies have revealed other PAF's biological actions in a wide variety of cell types and tissues (13).

Functionally, there are two pathways for PAF biosynthesis: the *de novo* pathway and the remodeling pathway. The remodeling route is triggered by inflammation and is the main source of PAF under pathological situations. The initiation of the remodeling pathway requires hydrolysis of phosphatidylcholine (PC) by phospholipase A2 (PLA2), which generates a free fatty acid, such as arachidonic acid, and lyso-PC, a precursor of PAF. Lyso-PC acetyltransferases (LPCATs) then convert lyso-PC into PAF through acetylation in the sn-2 position. Finally, PAF activates the PAF receptor (PAFR), which belongs to the superfamily of GPCRs (14, 15). Inappropriate activation of the PAF-PAFR axis is thought to play an important role in cancer biology, tumor radioresistance, and modulation of the tumor microenvironment (16, 17).

Some studies have demonstrated the participation of EGFR-evoked signaling pathways as positive modulators of two key enzymes, cytosolic PLA2 (18) and LPCAT2 (15), involved in the remodeling route of PAF biosynthesis. Indeed, EGFR activation increases PAF production in ovarian cancer cell lines in a PLA2-dependent mechanism (19). PAF also transactivates EGFR and downstream pathways in ovarian cancer cells, diversifying the GPCR-mediated signal (20, 21). However, the role of the crosstalk between EGFR and the PAF-PAFR axis in other types of cancer has yet to be investigated.

Herein, we identified EGFR, LPCAT2, and PAFR as targets for cervical cancer therapy, using TCGA-based *in silico* analyzes. The bidirectional interaction between EGFR signaling pathway and the LPCAT-PAF-PAFR axis, and the functional impact of inhibiting both pathways with target drugs were investigated *in vitro*. The experimental design of the study is shown in **Figure 1**.

MATERIALS AND METHODS

Correlation Analysis of Gene Expression

Transcriptome data were collected from The Cancer Genome Atlas (TCGA[1]). The subset of TCGA data included the RNA sequencing of 306 samples of cervical squamous cell carcinoma and cervical adenocarcinoma. RNA-seq values (*EGFR* × *LPCAT1/2/3/4*, *EGFR* × *PTAFR*, and *EGFR* × *PLA2G4A*) were correlated and statistically analyzed by the non-parametric Spearman test.

Overall Survival Study

Overall survival analyzes were performed using the open-access platform named cBioPortal for Cancer Genomics (22, 23). To observe the relationship between the upregulation of PAFR (*PTAFR* gene), cPLA2 (*PLA2G4A* gene) and the four enzymes of the LPCAT family (*LPCAT1/2/3/4*) with the overall survival of cervical cancer patients, the Firehose Legacy study (TCGA, n = 304) was selected. A cut-off of 2.0 standard deviations above the median of expression (z-score) was established to separate the groups: "upregulated expression" and "cases without alteration".

Cell Lines and Chemicals

CASKI and C33A cells were grown in RPMI 1640 medium (Thermo Fisher Scientific, MA, USA) supplemented with 10% fetal bovine serum (FBS), 1% penicillin/streptomycin (Thermo Fisher Scientific), and incubated at 37°C in a 5% CO_2

Abbreviations: COX-2, cyclooxygenase 2; cPLA2, cytosolic phospholipase A2; EGF, epidermal growth factor; EGFR, epidermal growth factor receptor; ERK, extracellular signal-regulated kinase; GAPDH, glyceraldehyde 3-phosphate dehydrogenase; GPCR, G protein-coupled receptor; HPV, human papillomavirus; LPCAT, lysophosphatidylcholine acyltransferase; MAPK, mitogen-activated protein kinase; PAF, platelet-activating factor; PAFR, platelet-activating factor receptor; PC, phosphatidylcholine; PGE2, prostaglandin E2; TCGA, The Cancer Genome Atlas.

[1] https://cancergenome.nih.gov/

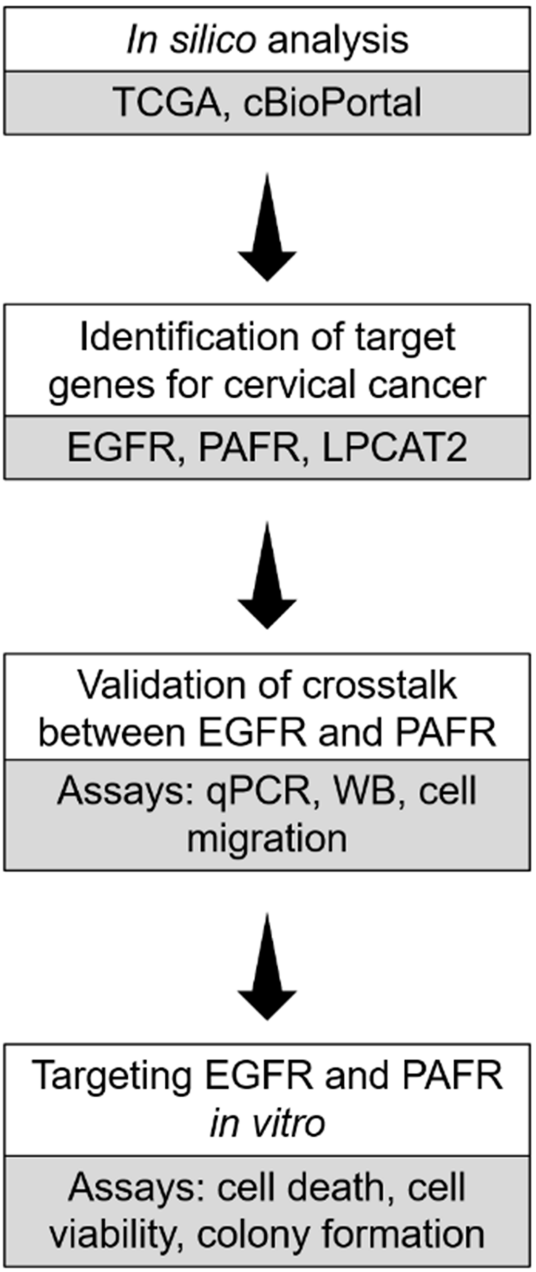

FIGURE 1 | Experimental design of the study. *In silico* analysis were employed to identify genes that could potentially serve as targets in cervical cancer. *In vitro* assays were further utilized to validate the crosstalk between epidermal growth factor receptor (EGFR) and platelet-activating factor receptor (PAFR). In addition, EGFR and PAFR were tested as targets using *in vitro* assays.

atmosphere. Unless otherwise stated, cell lines were seeded at 1×10^6 cells in 25 cm^2 culture flasks and left to adhere overnight.

Cetuximab (anti-EGFR monoclonal antibody, Erbitux®) was provided by the Brazilian National Cancer Institute (Rio de Janeiro, Brazil). WEB2086 (PAFR competitive antagonist), β-Acetyl-γ-O-alkyl-L-α-phosphatidylcholine (PAF), PD98059 (MEK inhibitor), LY294002 (PI3K inhibitor) and human epidermal growth factor (EGF) were purchased from Merck, Germany.

Gene Expression Analysis by Quantitative PCR

After 16 h of starving in serum-free medium, cells were treated with cetuximab (100 μg/ml) or PD98059 (50 μM) or LY294002 (25 μM) for 90 min, when indicated. After treatment, cells were stimulated with PAF (100 nM) or EGF (50 ng/ml or 100 ng/ml) for 90 min. TRIzol Reagent was used to extract total RNA. From each sample generated, 1 μg of RNA was submitted to DNase I treatment and RT-PCR. Next, real-time PCR was performed on cDNA aliquots with Taqman Fast Real-Time PCR Master Mix, using the StepOnePlus Real-Time PCR System (Thermo Fisher Scientific). References regarding Taqman gene expression assays were 4326317E (*GAPDH*), Hs00153133_m1 (COX-2, *PTGS2* gene), Hs00265399_s1 (PAFR, *PTAFR* gene) and Hs01044164_m1 (*LPCAT2*). All reagents and probes were purchased from Thermo Fisher Scientific. Gene expression was normalized by *GAPDH* as a reference gene. To analyze the relative fold change, we employed the $2^{-\Delta\Delta CT}$ method.

Western Blotting

In experiments analyzing the signaling pathways, cells were starved for 16h and treated with cetuximab (100 μg/ml) for 90 min, when indicated. Afterward, cells were stimulated with PAF (100 nM) for 5 to 20 min. In experiments to evaluate COX-2 protein expression, the same protocol was used. However, treatment with PAF lasted 3 h. In experiments analyzing PAFR downregulation, CASKI cells were simultaneously starved and treated with cetuximab (100 μg/ml) for 24 h and 48 h. Following treatment completion, cells were lysed, and proteins were quantified using the Lowry method (DC protein assay, Bio-Rad, CA, USA). Protein lysates (20–30 μg) from each condition were subjected to 8%–10% SDS–PAGE and transferred onto a PVDF Hybond-P membrane (GE Healthcare, Brazil). Membranes were blocked and incubated overnight with p-ERK1/2 (Cell Signaling Technology, MA, USA), ERK1/2 (Cell Signaling Technology), COX-2 (Cell Signaling Technology, MA, USA), PAFR (Abcam, MA, USA) and β-actin (Cell Signaling Technology) primary antibodies. Subsequently, membranes were incubated with HRP-conjugated secondary antibodies (DakoCytomation, Denmark) for 1 h at room temperature, and immunoblots were detected using the ECL reagent (GE Healthcare, Brazil).

Cell Migration Assay

The cell migration assay was performed in the Boyden chamber using 8 μm pore polycarbonate membranes (Neuro Probe, MD, USA). CASKI cells were seeded at 4×10^5 cells per well in 6-well cell culture plates and allowed to adhere overnight. On the next day, after 10 h of starving in serum-free medium, cells were treated with cetuximab (100 μg/ml) for 90 min and then stimulated with PAF (100 nM) for approximately 16 h. After that, cells were washed and harvested in serum-free medium. To the upper chambers, 5×10^4 cells were added, while the lower

chambers were filled with RPMI containing 5% FBS to stimulate migration. After 20 h of incubation, non-migrated cells on the upper membrane surface were scraped, and the membranes were fixed and stained using fast staining (Panoptic, Laborclin, Brazil). Finally, the membrane was photographed at 100x magnification. Ten fields were counted, and each sample was performed in triplicate.

Flow Cytometry-Based Cell Death Detection

CASKI cell line was seeded at 4×10^5 cells per well in 6-well cell culture plates and allowed to adhere overnight. Next, cells were treated with cetuximab (100 μg/ml) and/or WEB 2086 (50 μM) for 24 h. After treatment, the supernatant was collected, and adherent cells were trypsinized. The material collected was centrifuged and washed twice with cold PBS (phosphate-buffered saline). Nicoletti buffer (0.1% sodium citrate, 0.1% NP-40, 200 μg/ml RNase and 50 μg/ml propidium iodide) was used to stain the DNA of the cells. Analysis of the DNA content was observed by collecting 20,000 events using the BD FACSCalibur flow cytometer (BD Biosciences, EUA). Doublets and debris were identified and excluded. Events with DNA hypodiploid (sub-G0/G1 peak) were considered as dead cells.

Cell Viability Assay

CASKI was seeded at a density of 2,500 cells/well in 96-well cell culture plates. After overnight incubation, cells were treated with cetuximab (100 μg/ml) and/or WEB 2086 (100 μM) for 72 h in medium supplemented with 2% FBS. After treatment, cells were incubated with a solution of MTT (3-(4,5-dimethythiazol-2-yl)-2,5-diphenyl-tetrazolium bromide) (Merck, Germany) for 3.5 h. The formazan crystals formed were solubilized in DMSO, and the optical density was measured at a wavelength of 538 nm using Spectra Max ABS Plus (Molecular Devices, CA, EUA). Cell viability was expressed as a percentage of the control.

Colony Formation Assay

CASKI cells were seeded at a low density of 300 cells per well in 6-well cell culture plates. On the next day, cells were treated with cetuximab (100 μg/ml) and/or WEB 2086 (50 μM) and allowed to grow for 13 days. After the incubation time, colonies were stained with 0.1% crystal violet (Merck, Germany) for 30 min under slight agitation. Each well was washed with PBS, and the plates were photographed. Finally, crystal violet was eluted in 200 μl of methanol, and absorbance at the wavelength of 595 nm was measured using Spectra Max ABS Plus (Molecular Devices, CA, EUA).

Statistical Analysis

All experiments were performed at least three times and data were expressed as the mean ± SD. GraphPad Prism 5 (GraphPad Software, CA, USA) was used to perform all statistical analyses. When comparing only two groups, the unpaired Student's t-test was performed, while for comparison between multiple test groups, One-way analysis of variance (ANOVA) followed by Tukey's post-test was applied. Spearman's rank correlation was used for gene expression correlation analyzes. The statistical significance of the overall survival study was determined using the log-rank test. The differences were considered significant whenever $P \leq 0.05$.

RESULTS

EGFR Expression Positively Correlates With the Expression of Elements of the PAF Pathway in Cervical Cancer Samples

To initiate the current study, transcriptome data from cervical cancer patients deposited in TCGA were used to observe possible correlations between the mRNA expression levels of EGFR, cPLA2, PAFR and the components of the LPCAT family. A strong positive correlation was observed between EGFR × PAFR (Spearman's r = 0.4848, P < 0.0001, **Figure 2A**), and EGFR × LPCAT2 (Spearman's r = 0.3844, P < 0.0001, **Figure 2B**). No correlation between the expression of EGFR and LPCAT1, LPCAT4 or cPLA2 (**Supplementary Figures 1A, C, D**) was found. Albeit a slight correlation between the expression of EGFR and LPCAT3 was found (Spearman's r = 0.1160, P = 0.0416, **Supplementary Figure 1B**), PAFR and LPCAT2 were chosen for the subsequent studies due to the strength of the correlation with EGFR, which suggests a possible mechanism of transcriptional regulation.

LPCAT2 Upregulation Is Associated With Unfavorable Clinical Outcome in Cervical Cancer Patients

Recent studies, including ours, have demonstrated that the overexpression of EGFR negatively impacts the overall survival of cervical cancer patients and the response to chemoradiation (6, 11). For this reason, we decided to analyze if the upregulation of elements of the PAF pathway would also negatively affect the overall survival of those patients. Data from 304 patients are available in the cBioPortal platform (TCGA, Firehose Legacy). In the selected criteria, mRNA upregulation of *EGFR*, PAFR (*PTAFR* gene), *LPCAT1*, *LPCAT2*, *LPCAT3*, *LPCAT4*, and cPLA2 (*PLA2G4A* gene) was found in 7.9%, 4.3%, 4.3%, 2.6%, 5.6%, 4.9%, and 3% of the cases, respectively, as shown in **Table 1**. No significant impact on overall survival was observed with increased expression of PAFR (**Figure 3A**), LPCAT1 (**Supplementary Figure 2A**), LPCAT3 (**Supplementary Figure 2B**), and LPCAT4 (**Supplementary Figure 2C**). However, the upregulation of LPCAT2 (P = 0.0239, **Figure 3B**), the same enzyme that positively correlates with the expression of EGFR, showed negative prognostic value for cervical cancer patients, as well as cPLA2 (P = 0.0052, **Supplementary Figure 2D**). The median survival for the group with LPCAT2 overexpressed was 40.9 months vs. 101.7 months for the group without alteration in this gene, thus solidifying the importance of the present study. The prognostic impact of LPCAT2 and cPLA2 must be confirmed in other cohorts of cervical cancer patients since the increased expression of these genes was observed in a small number of cases (8/304 and 9/304, respectively).

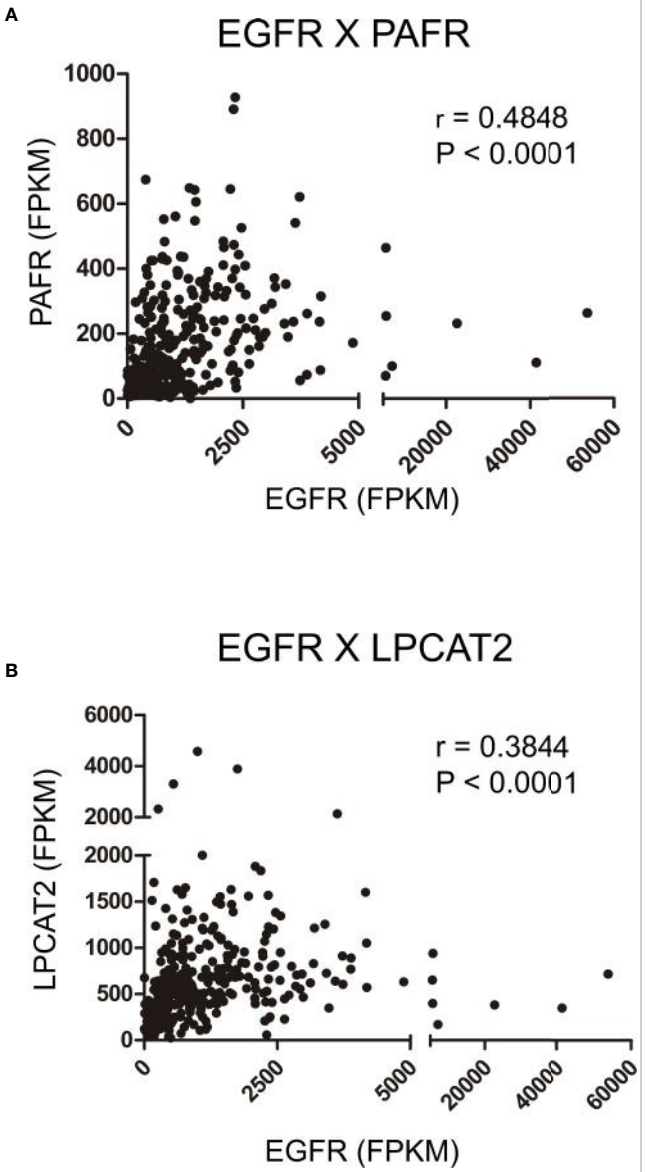

FIGURE 2 | Epidermal growth factor receptor (EGFR) expression correlates with the expression of platelet-activating factor receptor (PAFR) and lysophosphatidylcholine acyltransferase 2 (LPCAT2) in cervical cancer samples. Analyzes of the correlations between EGFR × PAFR **(A)**, and EGFR × LPCAT2 **(B)** in 306 cervical cancer samples. The Cancer Genome Atlas (TCGA) database was used to obtain RNA-seq data, and Spearman's test was performed to evaluate the coefficient of correlation (r) between the gene expression levels.

EGFR Activation Upregulates the mRNA Expression of Components of the PAF Pathway in Cervical Cancer Cells

For this study, two cervical carcinoma cell lines were used. While the C33A cell line does not exhibit the HPV infection, the CASKI cell line – derived from an epidermoid carcinoma of the cervix metastatic to the small bowel mesentery – shows multiple copies of HPV-16 integrated into its genome. Also, CASKI cells are more resistant to chemoradiation than C33A cells (24). Thus, the CASKI cell line presents a more aggressive behavior than C33A cells, representing a useful and straightforward dichotomic model.

TABLE 1 | Cases of cervical cancer patients with increased expression of the genes listed (TCGA, Firehose Legacy study, n = 304).

	Cases with mRNA upregulated (%)
EGFR	24/304 (7.9%)
PAFR	13/304 (4.3%)
LPCAT1	13/304 (4.3%)
LPCAT2	8/304 (2.6%)
LPCAT3	17/304 (5.6%)
LPCAT4	15/304 (4.9%)
cPLA2	9/304 (3%)

A previous study from our group showed that CASKI cells express about 80 times more EGFR than the C33A cell line. This difference is also reflected at the protein level since C33A cells showed undetectable levels of EGFR by western blotting (11). To observe if this pattern is maintained for the expression of PAFR and LPCAT2, quantitative PCR was performed. As seen for EGFR, CASKI cells present higher basal mRNA expression levels of PAFR (**Figure 4A**) and LPCAT2 (**Figure 4E**) than C33A cells.

Stimulation of EGFR has been associated with the activation of the PAFR pathway (19). In this context, we examined whether the treatment with EGF would stimulate the expression of PAFR and LPCAT2. CASKI cells were incubated with EGF (50 ng/ml or 100 ng/ml) and mRNA levels of PAFR (**Figure 4B**) and LPCAT2 (**Figure 4F**) were again measured by qPCR. Stimulation with the highest concentration of EGF was able to increase the expression of both elements of the PAF pathway. Moreover, pre-incubation with cetuximab, a potent monoclonal antibody against EGFR, was able to block the effects of EGF over the cells. Not surprisingly, stimulation of C33A with the highest concentration of EGF was not able to elevate mRNA levels of either PAFR (**Figure 4C**) or LPCAT2 (**Figure 4G**). These results indicate that the activation of EGFR can positively modulate the expression of the PAF receptor and the LPCAT2 enzyme, possibly elevating PAF production in aggressive cervical cancer cells. Then, we decided to identify the contribution of EGFR-activated classically signaling pathways in the upregulation of PAFR and LPCAT2. The Ras-Raf-MEK-ERK and PI3K-Akt-mTOR signaling pathways were inhibited with PD98059 (MEK inhibitor) and LY294002 (PI3K inhibitor), respectively. Interestingly, PD98059 completely reversed EGF-mediated PAFR (**Figure 4D**) and LPCAT2 (**Figure 4H**) induction in CASKI cells, unlike LY294002. These results suggest that the ERK/MAPK pathway is responsible for modulating the expression of these genes after EGFR activation.

PAF Induces the Transactivation of the EGFR and the Downstream Signaling Pathways

In ovarian cancer models, it has been shown that the stimulation of PAFR transactivates EGFR (20, 21). In this context, we examined if the same was true for the cervical cancer model. CASKI cells were incubated with PAF, for different periods of time, and the ERK1/2 phosphorylation was further assessed since

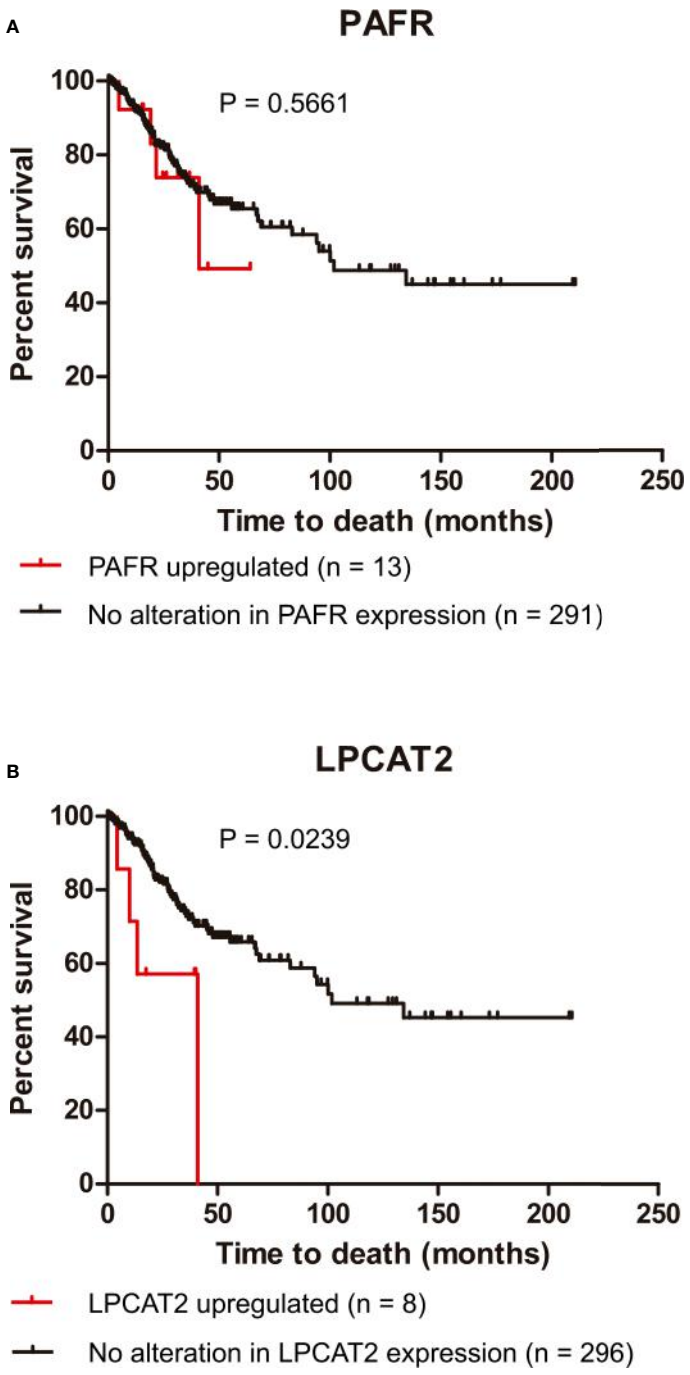

FIGURE 3 | Lysophosphatidylcholine acyltransferase 2 (LPCAT2) upregulation is associated with poor overall survival in cervical cancer patients. Through the cBioPortal platform, were performed overall survival analyzes to evaluate the relation between the upregulations of platelet-activating factor receptor (PAFR) **(A)** and LPCAT2 **(B)**, and prognosis in cervical cancer [The Cancer Genome Atlas (TCGA), Firehose Legacy study; n = 304]. Kaplan-Meier method was implemented to generate survival curves and statistical significance among these curves was determined using the log-rank test.

the MAPK pathway is a known downstream route of the EGFR. The activation of PAFR caused a significant increase in ERK phosphorylation that was completely blocked by pre-incubation with cetuximab (**Figure 5A**). As already shown by our group, C33A cells have higher basal levels of p-ERK1/2 than the CASKI cell line (24), probably due to a loss-of-function mutation in the *PTEN* gene (25). Interestingly, PAF failed to induce ERK activation in C33A (**Figure 5A**).

This same pattern of biological response was observed in the expression of cyclooxygenase-2 (COX-2), a downstream gene of the

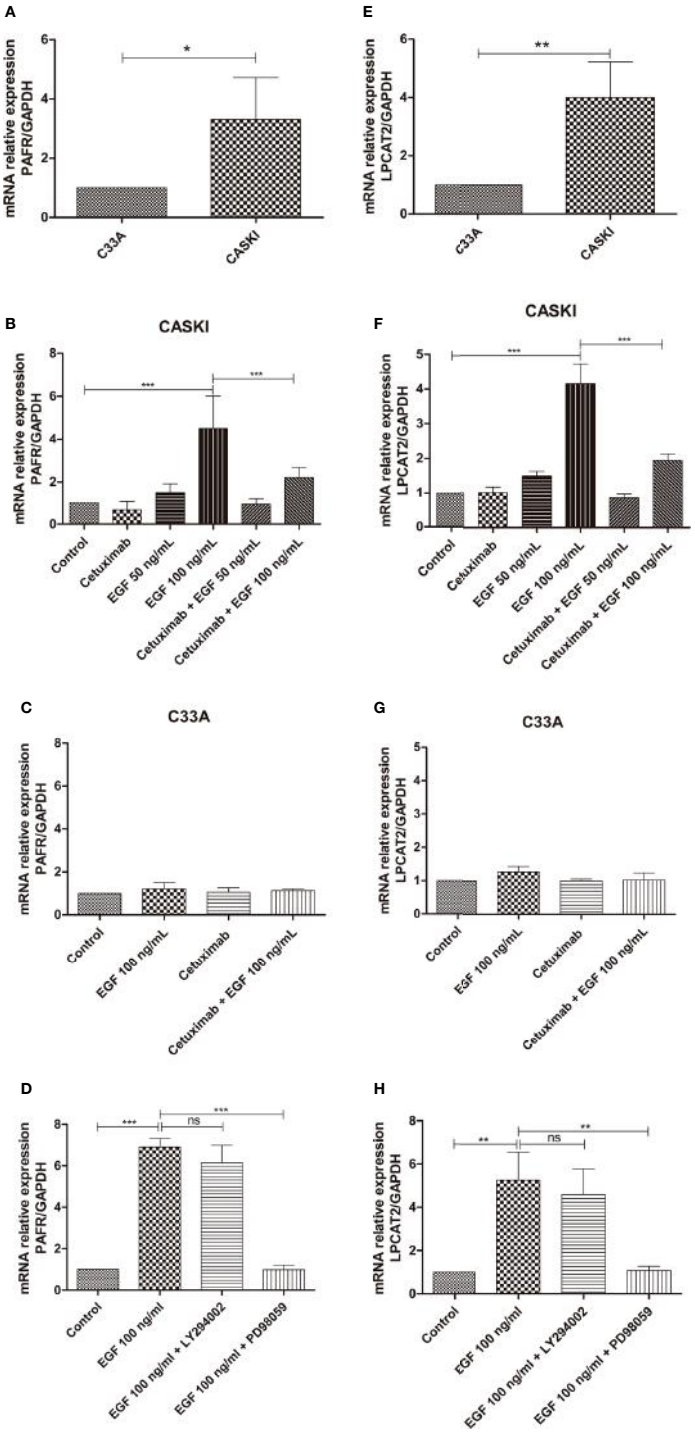

FIGURE 4 | Epidermal growth factor receptor (EGFR) activation upregulates the mRNA expression of lysophosphatidylcholine acyltransferase 2 (LPCAT2) and platelet-activating factor receptor (PAFR) in cervical cancer cells. For the basal expression analysis, qPCR was performed to analyze the relative gene expression of PAFR **(A)** and LPCAT2 **(E)**. To analyze if the activation of EGFR modulates components of the PAF pathway, cells were starved for 16 h, and then treated with cetuximab (100 μg/ml). One hour and a half later, cells were stimulated with EGF (50 or 100 ng/ml) for 1.5 h. After treatment, mRNA was extracted and converted into cDNA. Gene expression assays for PAFR in CASKI cells **(B)** and C33A cells **(C)**; and for LPCAT2 in CASKI cells **(F)** and C33A **(G)** were performed. Alternatively, CASKI cells were starved and pretreated with PD98059 (50 μM) or LY294002 (25 μM) for 1.5 h. Then, cells were stimulated with EGF (100 ng/ml) for 1.5 h. Gene expression assays for PAFR **(D)** and LPCAT2 **(H)** were performed. The comparative CT method (ΔΔCT) was utilized to calculate relative mRNA expression and GAPDH was used as the reference gene. Values represent mean + SD of at least three independent experiments. For multiple comparisons, one-way ANOVA and Tukey's post-test were used; while for comparisons of only two conditions, Student's t-test was performed. ns, not significant, *P < 0.05, **P < 0.01, ***P < 0.001.

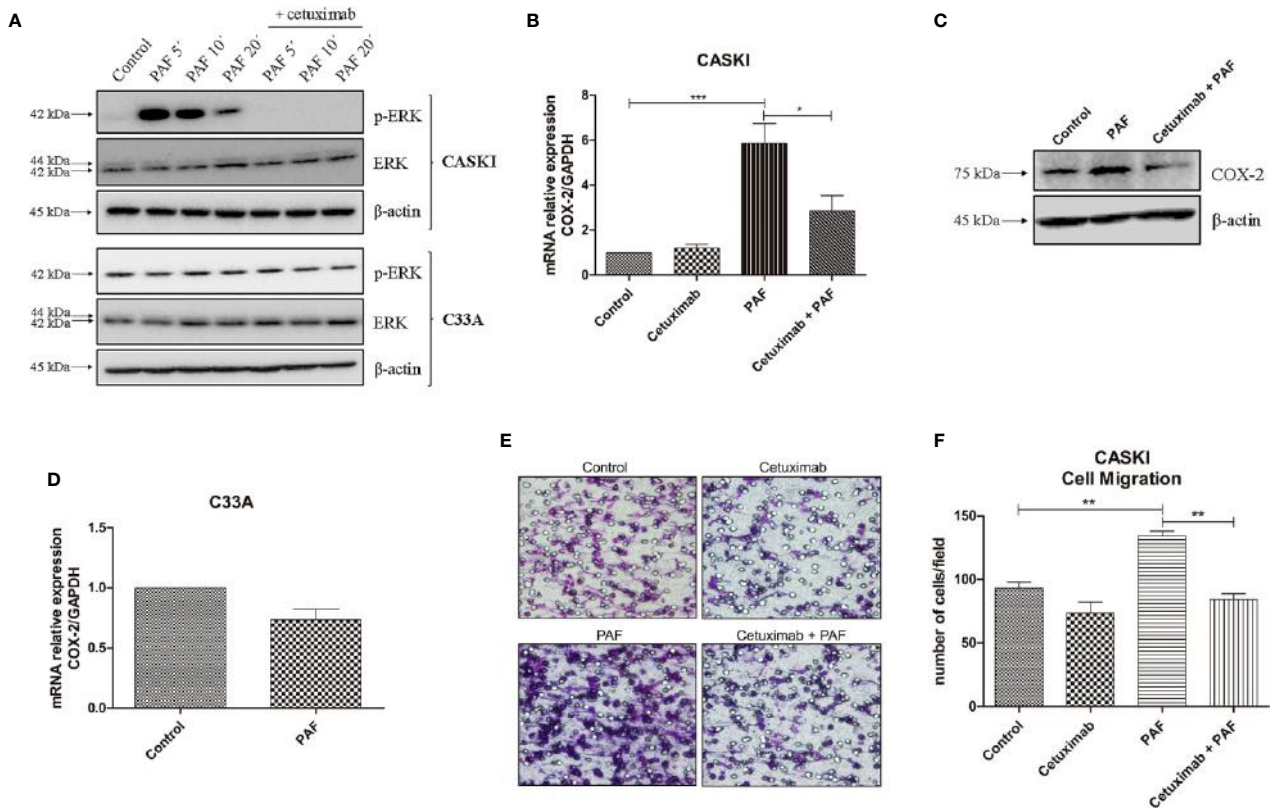

FIGURE 5 | Platelet-activating factor (PAF) transactivates epidermal growth factor receptor (EGFR), modulating MAPK activation, COX-2 upregulation, and cell migration. **(A)** CASKI and C33A cells were starved for 16 h and treated with cetuximab (100 μg/ml). One and a half-hour later, cells were stimulated with PAF (100 nM) for 5–20 min. Afterward, cells were lysed and levels of p-ERK, total ERK and beta-actin (loading control) were determined by Western blotting. Representative image of two experiments. **(B)** After starving, CASKI cells were treated with cetuximab (100 μg/ml) for 1.5 h, and subsequently treated with PAF (100 nM) also for 1.5 h. Then, mRNA was extracted and converted into cDNA. Gene expression assays for COX-2 and GAPDH (reference gene) were performed by qPCR. Values represent mean + SD of five independent experiments. **(C)** CASKI cell line was starved and treated with cetuximab (100 μg/ml) for 1.5 h, and subsequently stimulated with PAF (100 nM) for 3 h, when cells were lysed and the levels of COX-2 and β-actin (loading control) were determined by Western blotting. Representative image of two experiments. **(D)** C33A cells were starved and stimulated with PAF (100 nM) for 1.5h. Gene expression assays for COX-2 and GAPDH were also performed. Values represent mean + SD of five independent experiments. **(E, F)** For the cell migration assay, after starving, CASKI cells were treated with cetuximab (100 μg/ml) for 1.5 h followed by 16 h stimulation with PAF (100 nM). Then, cells were added to a Boyden chamber, using 8 μm pore polycarbonate membranes, and left to migrate toward RPMI containing 5% SFB for 20 h. **(E)** Representative images of the migration assay are shown on the panel (100× magnification). **(F)** Values represent mean of the number of cells migrated counted per field + SD of three independent experiments. For multiple comparisons, one-way ANOVA and Tukey's post-test were used; while for comparisons of only two conditions, Student´s t-test was performed. *P < 0.05, **P < 0.01, ***P < 0.001.

EGFR signaling (26, **Supplementary Figure 3**). COX-2 is an inflammatory enzyme overexpressed in cervical tumors (26), with negative prognostic value in this type of cancer (11, 27). PAFR activation increased COX-2 expression in CASKI cells, and pre-incubation with cetuximab blocked this phenomenon, both at the mRNA (**Figure 5B**) and protein levels (**Figure 5C**). In C33A cells, COX-2 expression is not modulated by PAF stimuli (**Figure 5D**), as well MAPK activation, possibly due to its lower levels of PAFR (mRNA and protein) as compared to CASKI cells (**Figure 4A** and **Supplementary Figure 4A**), in addition to not expressing EGFR. These results indicate that the effects observed upon activation of the PAF-PAFR axis are mostly dependent on EGFR activity.

Interestingly, in addition to blocking PAF-mediated EGFR transactivation, treatment with cetuximab for 48 h downregulated PAFR expression by 35% (**Supplementary Figure 4B**). This represents another mechanism for attenuating PAF signaling, corroborating our findings that EGFR positively regulates PAFR expression (**Figure 4B**).

Beyond the analysis of the impact of the EGFR transactivation by PAF in signaling cascades and gene expression modulation, we analyzed its effect on CASKI cells' ability to migrate. PAF promoted an increase of the motility of this cell line, a phenomenon that was completely reversed by EGFR inhibition with cetuximab (**Figures 5E, F**). Since treatment with cetuximab alone showed no difference from the control and that the pre-incubation with cetuximab reversed the PAF effects, our results again suggest that EGFR is the downstream effector of PAFR in CASKI cells.

Combined Inhibition of PAFR and EGFR Impairs the Clonogenic Capacity of Aggressive Cervical Cancer Cells

Since a positive feedback loop appears to occur in CASKI cells, where EGFR induces the expression of components of the LPCAT-PAF-PAFR axis and PAF can transactivate EGFR, we assessed the biological impact of the combined inhibition of EGFR and PAFR in this cell line. Cetuximab was used to inhibit EGFR, while WEB 2086 was used to inhibit PAFR. WEB 2086 is a very potent, safe, tolerable, and selective PAF antagonist (28).

CASKI cell line was treated with cetuximab and/or WEB 2086 for 24 h, when cell death was evaluated, using propidium iodide staining. DNA fragmentation was measured since it is a key feature of cell death (29). Cells treated with cetuximab or WEB2086 exhibited 10-14% of its events within sub-G1 DNA content, as shown by flow cytometry, indicating cells undergoing DNA fragmentation. However, combined treatment did not present an additive/synergistic effect in cell death, showing 12% of the events with hypodiploid DNA content (**Figure 6A**).

In addition to cell death, we evaluated the effect of combining cetuximab with WEB2086 on the viability of CASKI cells after 72 h of treatment. Isolated treatment with WEB2086 or cetuximab decreased cell viability by approximately 18% and 25%, respectively. Interestingly, the combination of WEB2086 + cetuximab compromised CASKI cells' viability by about 37% (**Figure 6B**).

Ultimately, the prolonged treatment of CASKI cells (13 days), measured by colony formation assay, revealed an interesting

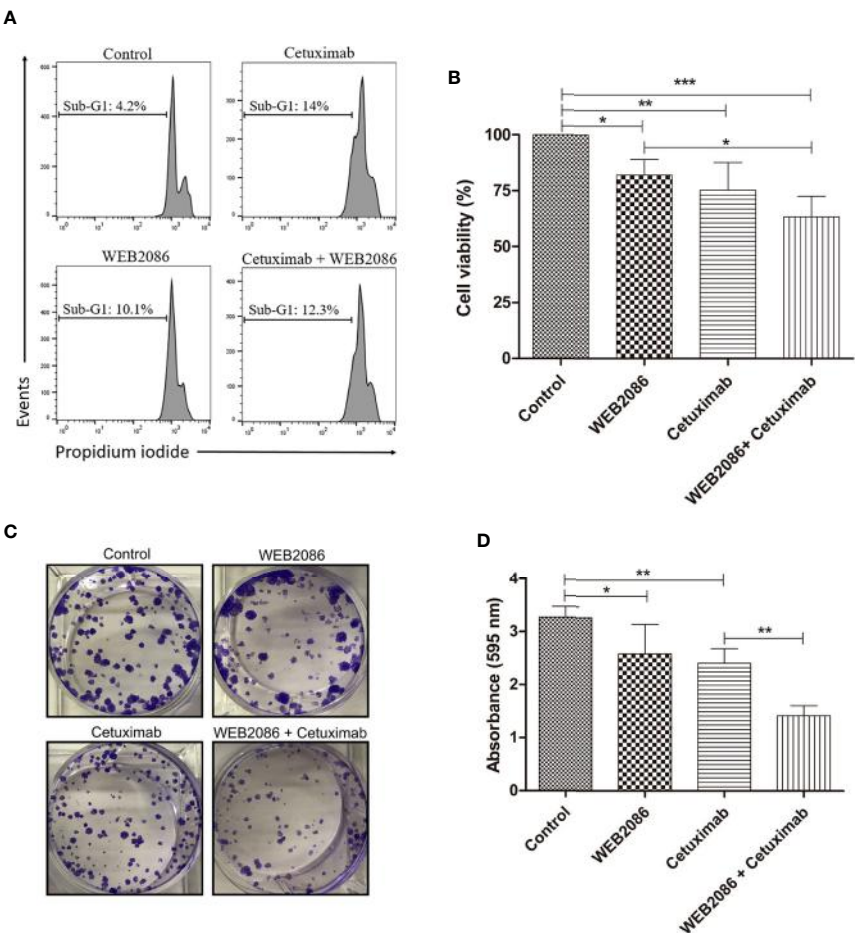

FIGURE 6 | Effects of the combined platelet-activating factor receptor (PAFR) and epidermal growth factor receptor (EGFR) inhibition in CASKI cells. **(A)** CASKI cells were treated with cetuximab (100 μg/ml) and/or WEB 2086 (50 μM) for 24 h. Cell death was evaluated by propidium iodide staining, followed by flow cytometry. Cells with hypodiploid DNA content (sub-G1 peak) were considered apoptotic cells. Representative histograms of three independent experiments. **(B)** For the MTT assay, CASKI cells were seeded at 2,500 cells/well in 96-well cell culture plates. Then, cells were treated with cetuximab (100 μg/ml) and/or WEB 2086 (100 μM) for 72 h in medium supplemented with 2% fetal bovine serum (FBS). After treatment, cells were incubated with a solution of MTT. The formazan crystals generated were solubilized in DMSO and the optical density was measured at a wavelength of 538 nm. Cell viability was expressed as a percentage of the control. Values represent mean + SD of four independent experiments. **(C, D)** For the clonogenic assay, CASKI cells were seeded at low density and treated for 13 days with cetuximab (100 μg/ml) and/or WEB 2086 (50 μM). Then, colonies were stained with crystal violet and photographed. **(C)** Representative image of the colonies of the CASKI cell line after targeted therapies against EGFR and PAFR. **(D)** Crystal violet was eluted in methanol and absorbance at 595 nm was measured. Values represent mean + SD of five independent experiments. One-way ANOVA and Tukey's post-test were used. *P < 0.05, **P < 0.01, ***P < 0.001.

pharmacologic strategy. Combined treatment significantly reduced the size and number of colonies in relation to control and to isolated treatments with cetuximab or WEB2086 (**Figure 6C**), causing reduced staining of the colonies with crystal violet, as evidenced in the absorbance of the eluted dye (**Figure 6D**). These findings indicate that the combined targeting treatment using anti-PAFR and anti-EGFR may have significant therapeutic potential for cervical cancer cells.

DISCUSSION

In the current study, strong positive correlations between EGFR × PAFR, and EGFR × LPCAT2 in cervical cancer samples were shown, which led to the hypothesis that EGFR can regulate the expression of these genes involved in the biosynthesis and signaling of PAF. Indeed, EGFR activation upregulated the expression of PAFR and LPCAT2 in cervical cancer cells through a MAPK-dependent mechanism.

The PAF-PAFR axis is largely associated with cancer progression (30), neoangiogenesis (31), modulation of the tumor microenvironment with downregulation of the anti-cancer immune response (32), and evasion of the chemoradiation-induced cell death (16, 33). To our knowledge, there is only one study that investigated the role of PAFR in cervical cancer, where increased expression of this receptor was observed in tumor samples as compared to normal cervical tissues (33). In this same study, authors observed higher PAFR expression in cervical tumors from patients who underwent irradiation compared with biopsies taken before radiotherapy. Moreover, radiotherapy increased PAFR expression *in vitro* and induced the production of PAF-like molecules in cervical cancer cells. Finally, the PAFR blockade sensitized these tumor cell lines to γ-radiation (33).

To date, few studies have investigated the function of LPCAT2 in tumor biology. The LPCAT2 expression levels were positively correlated with aggressive behavior in prostate cancer (34) and were significantly upregulated in cervical, breast, and colon cancer tissues, suggesting a role in the progression of these tumors (35). Recently, Cotte and colleagues showed that LPCAT2 drives cell-death resistance to chemotherapy through a lipid droplet accumulation-dependent mechanism, impairing caspase activation and endoplasmic reticulum stress response (36). Our results revealed that the LPCAT2 upregulation, but not PAFR, has negative prognostic value in cervical cancer patients. In accordance with our study, Deng and colleagues showed the PAF exacerbates peritonitis partly through inflammasome activation, but PAFR is dispensable for PAF-induced inflammasome activation in vivo or in vitro (37). These data, along with ours, suggest that the presence of PAF (generated by LPCAT2, for example) is more important for the aggressive behavior of some tumor types than the levels of PAFR expressed in the cancer cells.

Abnormal phosphatidylcholine (PC) metabolism is reported in cervical cancer. A recent study identified that PC and lyso-PC (also known as lyso-PAF) are down- and upregulated in plasma of cervical cancer patients, respectively, compared to patients with the benign uterine disease (38). These results suggest increased activity of the PLA2 enzyme in cervical cancer since the hydrolysis of PC by PLA2 generates both lyso-PC and free fatty acids. It remains to be determined whether lyso-PC is only a metabolic intermediate for LPCATs or has a role in cancer cell signaling. Some lyso-PC species might be an important function in Chagas disease progression (39). Interestingly, we showed that increased expression of cPLA2 is associated with poor overall survival in cervical cancer patients. However, EGFR expression did not correlate with cPLA2 expression levels in cervical cancer samples. An interesting hypothesis is that EGFR signaling pathways regulate cPLA2 at post-translational level, rather than gene expression regulation since this PLA2 isoform is activated by phosphorylation and Ca^{2+} (18).

Several studies have shown that GPCRs can transactivate EGFR in different models (9–11). However, PAFR-mediated EGFR transactivation has only been demonstrated in ovarian cancer cells so far (20, 21). In this ovarian cancer model, EGFR transactivation involves the PAFR activation, the activation of phospholipase C-β, inositol trisphosphate-induced Ca^{2+} mobilization, activation of the non-receptor tyrosine kinase Src, cleavage and secretion of heparin-binding EGF-like growth factor (HB-EGF) in a matrix metalloproteinase-dependent mechanism (21).

Alternatively, EGFR can be transactivated by GPCRs in the absence of EGF-like ligands, suggesting that the EGFR transactivation by GPCRs can also occur through intracellular signaling routes (40). In our study, we observed that the PAF-induced ERK1/2 phosphorylation was completely inhibited by the anti-EGFR monoclonal antibody, cetuximab, in CASKI cells. Cetuximab blocks EGFR activation because it binds with high affinity to the receptor's extracellular domain, preventing interaction with physiological ligands (41). Thus, our results suggest that EGFR transactivation by PAF occurs through the shedding of EGF-like ligands in the extracellular milieu.

In CASKI cells, EGFR transactivation by PAF induced the expression of the enzyme COX-2. High expression of COX-2 and increased production of its major metabolite, PGE2, have been found in the cervical carcinoma in relation to normal cervix (42). Kim and colleagues (27) showed that the coexpression of EGFR and COX-2 may be used as a potent risk factor to predict the poor survival of patients with squamous cell carcinoma of the uterine cervix. PGE2 is the most abundant prostaglandin in humans and is known as a critical mediator in inflammation. The functions of PGE2 are mainly facilitated by four specific G-protein-coupled receptors (EP1-EP4) with various signaling pathways (43). Sales and colleagues reported that, in addition to the expression of COX-2 and production of PGE2, cervical tumors express EP2 and EP4 receptors, suggesting an autocrine/paracrine regulation of the neoplastic cell function (42). Jung-Min et al. showed that HPV16 oncoproteins induce EP4 receptor expression in cervical cancer cells (44). In this same study, the authors showed an increased expression of EP4 in 52 cervical cancer tissues compared with four healthy controls by immunohistochemistry (44). EP4 plays a role in cervical cancer

progression since GW627368X (a highly selective EP4 antagonist) inhibits the proliferation and angiogenesis of cervical cancer cell lines and suppresses tumor growth in xenograft mice model (45). In addition, EP3 upregulation was associated with poor overall survival of 250 cervical cancer patients. The EP3 receptor was also significantly correlated with lymph node invasion and tumor staging (46). It remains to be determined whether COX-2-derived prostanoids have pro-tumor effects in our model and whether PAF can induce the expression of PGE2 receptors, especially EP2, EP3 and EP4.

In the hypothesized model (**Figure 7**), the EGFR activation induces the expression of the LPCAT2 enzyme, a member of the remodeling pathway of PAF biosynthesis. Besides, EGFR can induce the expression of the PAF receptor, which can be activated by the PAF produced by LPCAT2 in EGFR-expressing cancer cells, in an autocrine mechanism, or surrounding cells in the microenvironment, in a paracrine fashion. PAFR, then, can transactivate EGFR through the cleavage and release of EGF-like ligands from the plasma membrane. EGFR activation promotes LPCAT2 upregulation, and consequently PAF production and PAFR activation, suggesting a positive feedback loop. Still, the activation of both EGFR and PAFR leads to the expression of the inflammatory enzyme COX-2. COX-2 produces prostanoids such as prostaglandin E2 (PGE2), using arachidonic acid released after the enzymatic action of cytosolic PLA2 (43), the same enzyme that initiates the PAF production pathway. Therefore, in situations in which PGE2 is produced, depending on the levels of LPCATs expression, PAF is also produced. PGE2, as well as PAF, is a lipid mediator with potent pro-tumoral and pro-inflammatory activities (43). Studies have shown that PGE2 can also transactivate EGFR through EP receptors (47). This positive crosstalk between the PAF-PAFR axis and EGFR demonstrates an important linkage between inflammatory and growth factor signaling in cervical cancer cells.

We also showed that the combined inhibition of EGFR and PAFR has great therapeutic potential in cervical cancer cells that express these receptors. However, a dissonance was observed between the results of the short-term cell death assay and the long-term colony formation assay, which lasts for 13 days. It is important to highlight that the anti-cancer therapeutic agents not only induce apoptotic cell death but also trigger growth-arresting events, such as other mechanisms of cell death, quiescence, accelerated senescence and mitotic catastrophe, responses that are manifested several days after the introduction of the treatment. Thus, the colony formation

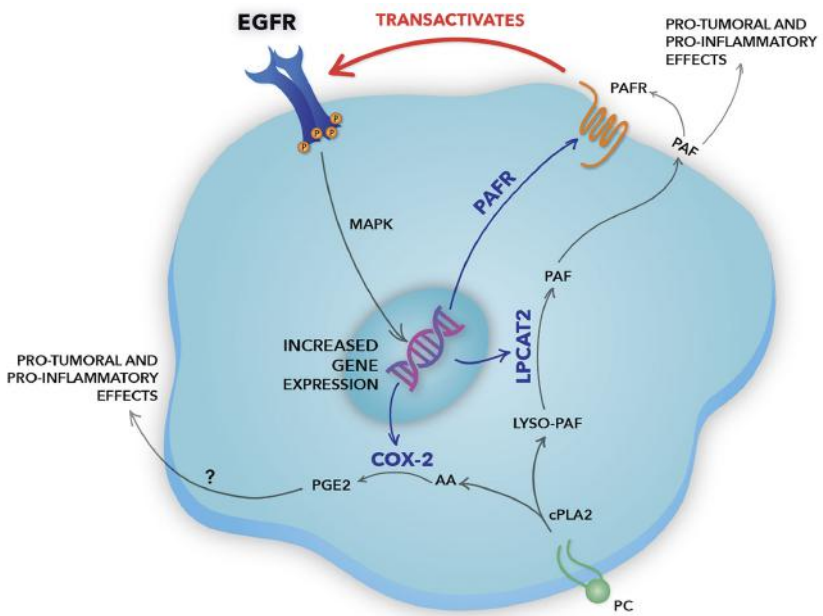

FIGURE 7 | Schematic representation of the positive crosstalk between epidermal growth factor receptor (EGFR) and the platelet-activating factor (PAF) pathway in cervical cancer cells. In our hypothesized model, EGFR activation induces gene expression of the lysophosphatidylcholine acyltransferase 2 (LPCAT2) enzyme, a member of the PAF biosynthesis pathway. EGFR can also induce the expression of PAF receptor (PAFR), which, then, can be activated by the PAF produced by LPCAT2 in EGFR-expressing cancer cells, in an autocrine fashion, or surrounding cells in a paracrine mechanism. PAFR can induce EGFR transactivation through the cleavage and release of EGF-like ligands from the plasma membrane, promoting MAPK activation and cell migration. The bidirectional interaction between the EGFR and the LPCAT-PAF-PAFR axis reveals the presence of a positive feedback loop. Still, the activation of both EGFR and PAFR leads to the expression of the inflammatory enzyme COX-2. COX-2 produces prostanoids, such as prostaglandin E2 (PGE2), using arachidonic acid released after the enzymatic action of cPLA2, the same enzyme that initiates the PAF biosynthesis pathway. Studies have shown that PGE2, like PAF, has an important pro-inflammatory and pro-tumoral effect, being able to transactivate EGFR. Genes upregulated by EGFR are indicated by blue arrows. Therefore, EGFR rises as a central pillar of the signaling pathways mediated by GPCRs, inducing a more aggressive phenotype in cervical cancer cells.

assay provides an integrated readout of all these early and late responses, being considered the gold standard for cytotoxicity evaluation (48).

Further investigation into the potential use of EGFR inhibitors, PAF antagonists and LPCAT inhibitors in the treatment of cervical cancer is needed through preclinical and clinical studies. Remarkably, we must emphasize the importance of an adequate selection of patients for a future clinical trial involving these target drugs, since only 26% of the cervical cancer patients included in TCGA (Firehose Legacy study) showed upregulation of, at least, one of the genes of these signaling pathways (*EGFR*, *PTAFR*, *LPCAT1*, *LPCAT2*, *LPCAT3*, *LPCAT4*, and *PLA2G4A*).

In the current study, we showed a significant positive correlation between EGFR and PAFR, and between EGFR and LPCAT2 in 306 cervical cancer samples deposited in TCGA database. In these patients, LPCAT2 upregulation was associated with poor prognosis. Moreover, we also reported an interplay between the EGFR signaling pathway and components of the LPCAT-PAF-PAFR axis in cervical cancer cells. Finally, combined EGFR and PAFR inhibition compromised cell viability and clonogenic capacity of aggressive cervical cancer cells. Taken together, our data suggest that EGFR, LPCAT2, and PAFR emerge as novel targets for cervical cancer therapy.

DATA AVAILABILITY STATEMENT

The datasets presented in this study can be found in online repositories. The names of the repository/repositories and accession number(s) can be found below: The 'Cervical Squamous Cell Carcinoma and Endocervical Adenocarcinoma (TCGA, Firehose Legacy)' study data from cBioPortal [https://www.cbioportal.org/study/summary?id=cesc_tcga].

AUTHOR CONTRIBUTIONS

JS performed and analyzed the experiments, wrote the manuscript. KM-C and IG performed experiments. AM and AL analyzed the data and participated in manuscript preparation. RM provided the hypothesis question, wrote the manuscript, and analyzed the data. VA performed and analyzed the experiments, wrote the manuscript, designed the study, and provided the hypothesis question. All authors contributed to the article and approved the submitted version.

FUNDING

This work was supported by the Brazilian National Council for Scientific and Technological Development (CNPq) [309946/2018-2]; the State of Rio de Janeiro Research Foundation (FAPERJ) [E-26/202.871/2018]; and the Coordination for the Improvement of Higher Education Personnel (CAPES) [23038.008921/2019-15].

ACKNOWLEDGMENTS

We would like to thank Ms. Rosângela Araújo for her technical assistance and Ms. Anna C. Pinheiro for the graphic design of the schematic representation of the crosstalk between EGFR and the LPCAT-PAF-PAFR pathway.

SUPPLEMENTARY MATERIAL

The Supplementary Material for this article can be found online at: https://www.frontiersin.org/articles/10.3389/fonc.2020.557280/full#supplementary-material

SUPPLEMENTARY FIGURE 1 | Correlation analyzes between the EGFR expression and the expression of cPLA2 and LPCAT enzymes in cervical cancer samples. Analyzes of the correlations between the expression levels of EGFR × LPCAT1 **(A)**, EGFR × LPCAT3 **(B)**, EGFR × LPCAT 4 **(C)**, and EGFR × cPLA2 **(D)** in 306 cervical cancer samples. TCGA database was used to obtain RNA-seq data, and Spearman's test was performed to evaluate the strength of the correlations.

SUPPLEMENTARY FIGURE 2 | Relation between the increased expression of cPLA2 and LPCAT enzymes with overall survival in cervical cancer patients. Through the cBioPortal platform, overall survival analyzes were performed to evaluate the association between the upregulations of LPCAT1 **(A)**, LPCAT3 **(B)**, LPCAT4 **(C)**, and cPLA2 **(D)** with prognosis in cervical cancer (TCGA, Firehose Legacy study; n = 304). Kaplan-Meier method was used to generate survival curves, and the statistical significance was determined using the log-rank test.

SUPPLEMENTARY FIGURE 3 | EGFR upregulates COX-2 expression in CASKI cells. After starving, CASKI cells were treated with cetuximab (100 μg/ml) for 1.5 h and subsequently treated with EGF (100 ng/ml) for 1.5 h. Then, mRNA was extracted and converted into cDNA. Gene expression assays for COX-2 and GAPDH (reference gene) were performed by qPCR. Values represent mean + SD of three independent experiments.

SUPPLEMENTARY FIGURE 4 | PAFR protein levels are differentially expressed in cervical cancer cell lines and regulated by EGFR. **(A)** CASKI and C33A cell lines were lysed and the levels of PAFR and β-actin (loading control) were determined by Western blotting. Representative image of three experiments. **(B)** CASKI was treated with cetuximab (100 μg/ml) for 24 h or 48 h in serum-free medium, when cells were lysed and the levels of PAFR and β-actin (loading control) were determined by Western blotting.

REFERENCES

1. Bray F, Ferlay J, Soerjomataram I, Siegel RL, Torre LA, Jemal A. Global cancer statistics 2018: GLOBOCAN estimates of incidence and mortality worldwide for 36 cancers in 185 countries. *CA Cancer J Clin* (2018) 68(6):394–424. doi: 10.3322/caac.21492
2. Tierney JF, Vale C, Symonds P. Concomitant and Neoadjuvant Chemotherapy for Cervical Cancer. *Clin Oncol* (2008) 20(6):401–16. doi: 10.1016/j.clon.2008.04.003
3. Lin CY, Lee CH, Chuang YH, Lee JY, Chiu YY, Lee YHW, et al. Membrane protein-regulated networks across human cancers. *Nat Commun* (2019) 10 (1):1–17. doi: 10.1038/s41467-019-10920-8
4. Jorissen RN, Walker F, Pouliot N, Garrett TPJ, Ward CW, Burgess AW. Epidermal growth factor receptor: Mechanisms of activation and signalling. In: G Carpenter, editor. *The EGF Receptor Family: Biologic Mechanisms and Role in Cancer*. Cambridge, MA: Academic Press (2003). p. 33–55. doi: 10.1016/B978-012160281-9/50004-9

5. Wee P, Wang Z. Epidermal Growth Factor Receptor Cell Proliferation Signaling Pathways. *Cancers* (2017) 9(5):52. doi: 10.3390/cancers9050052
6. Tian WJ, Huang ML, Qin QF, Chen Q, Fang K, Wang PL. Prognostic Impact of Epidermal Growth Factor Receptor Overexpression in Patients with Cervical Cancer: A Meta-Analysis. *PloS One* (2016) 11(7):e0158787. doi: 10.1371/journal.pone.0158787
7. Cerciello F, Riesterer O, Sherweif M, Odermatt B, Ciernik IF. Is EGFR a moving target during radiotherapy of carcinoma of the uterine cervix? *Gynecol Oncol* (2007) 106(2):394–9. doi: 10.1016/j.ygyno.2007.04.019
8. de Almeida VH, de Melo AC, Meira DD, Pires AC, Nogueira-Rodrigues A, Pimenta-Inada HK, et al. Radiotherapy modulates expression of EGFR, ERCC1 and p53 in cervical cancer. *Braz J Med Biol Res* (2018) 51(1):e6822. doi: 10.1590/1414-431x20176822
9. Daub H, Weiss FU, Wallasch C, Ullrich A. Role of transactivation of the EGF receptor in signalling by G-protein-coupled receptors. *Nature* (1996) 379:557–60. doi: 10.1038/379557a0
10. Prenzel N, Zwick E, Daub H, Leserer M, Abraham R, Wallasch C, et al. EGF receptor transactivation by G-protein-coupled receptors requires metalloproteinase cleavage of proHB-EGF. *Nature* (1999) 402:884–8. doi: 10.1038/47260
11. de Almeida VH, Guimarães IDS, Almendra LR, Rondon AMR, Tilli TM, de Melo AC, et al. Positive crosstalk between EGFR and the TF-PAR2 pathway mediates resistance to cisplatin and poor survival in cervical cancer. *Oncotarget* (2018) 9(55):30594–609. doi: 10.18632/oncotarget.25748
12. Hanahan D, Weinberg RA. Hallmarks of cancer: The next generation. *Cell* (2011) 144(5):646–74. doi: 10.1016/j.cell.2011.02.013
13. Ishii S, Nagase T, Shimizu T. Platelet-activating factor receptor. *Prostaglandins Other Lipid Mediat* (2002) 68–69:599–609. doi: 10.1016/S0090-6980(02)00058-8
14. Snyder F. Metabolism of platelet activating factor and related ether lipids: enzymatic pathways, subcellular sites, regulation, and membrane processing. *Prog Clin Biol Res* (1988) 282:57–72.
15. Morimoto R, Shindou H, Tarui M, Shimizu T. Rapid production of platelet-activating factor is induced by protein kinase Cα-mediated phosphorylation of lysophosphatidylcholine acyltransferase 2 protein. *J Biol Chem* (2014) 289 (22):15566–76. doi: 10.1074/jbc.M114.558874
16. Melnikova V, Bar-Eli M. Inflammation and melanoma growth and metastasis: The role of platelet-activating factor (PAF) and its receptor. *Cancer Metastasis Rev* (2007) 26:359. doi: 10.1007/s10555-007-9092-9
17. Chammas R, Andrade LNDS, Jancar S. Oncogenic effects of PAFR ligands produced in tumours upon chemotherapy and radiotherapy. *Nat Rev Cancer* (2017) 17:253. doi: 10.1038/nrc.2017.15
18. Xu J, Weng YI, Simoni A, Krugh BW, Liao Z, Weisman GA, et al. Role of PKC and MAPK in cytosolic PLA2 phosphorylation and arachadonic acid release in primary murine astrocytes. *J Neurochem* (2002) 83(2):259–70. doi: 10.1046/j.1471-4159.2002.01145.x
19. Yu Y, Zhang X, Hong S, Zhang M, Cai Q, Jiang W, et al. Epidermal growth factor induces platelet-activating factor production through receptors transactivation and cytosolic phospholipase A2 in ovarian cancer cells. *J Ovarian Res* (2014) 7:39. doi: 10.1186/1757-2215-7-39
20. Aponte M, Jiang W, Lakkis M, Li MJ, Edwards D, Albitar L, et al. Activation of Platelet-Activating Factor Receptor and Pleiotropic Effects on Tyrosine Phospho-EGFR/Src/FAK/Paxillin in Ovarian Cancer. *Cancer Res* (2008) 68 (14):5839–48. doi: 10.1158/0008-5472.CAN-07-5771
21. Yu Y, Zhang M, Zhang X, Cai Q, Zhu Z, Jiang W, et al. Transactivation of epidermal growth factor receptor through platelet-activating factor/receptor in ovarian cancer cells. *J Exp Clin Cancer Res* (2014) 33:85. doi: 10.1186/s13046-014-0085-6
22. Gao J, Aksoy BA, Dogrusoz U, Dresdner G, Gross B, Sumer SO, et al. Integrative analysis of complex cancer genomics and clinical profiles using the cBioPortal. *Sci Signal* (2013) 6(269):1. doi: 10.1126/scisignal.2004088
23. Cerami E, Gao J, Dogrusoz U, Gross BE, Sumer SO, Aksoy BA, et al. The cBio Cancer Genomics Portal: An Open Platform for Exploring Multidimensional Cancer Genomics Data. *Cancer Discovery* (2012) 2(5):401–4. doi: 10.1158/2159-8290.CD-12-0095
24. Meira DD, de Almeida VH, Mororó JS, Nóbrega I, Bardella L, Silva RLA, et al. Combination of cetuximab with chemoradiation, trastuzumab or MAPK inhibitors: Mechanisms of sensitisation of cervical cancer cells. *Br J Cancer* (2009) 101(5):782–91. doi: 10.1038/sj.bjc.6605216
25. Yaginuma Y, Yamashita T, Ishiya T, Morizaki A, Katoh Y, Takahashi T, et al. Abnormal structure and expression of PTEN/MMAC1 gene in human uterine cancers. *Mol Carcinog* (2000) 27(2):110–6. doi: 10.1002/(SICI)1098-2744(200002)27:2<110::AID-MC6>3.0.CO;2-E
26. Kulkarni S, Rader JS, Zhang F, Liapis H, Koki AT, Masferrer JL, et al. Cyclooxygenase-2 is overexpressed in human cervical cancer. *Clin Cancer Res* (2001) 7(2):429–34.
27. Kim GE, Kim YB, Cho NH, Chung HC, Pyo HR, Lee JD, et al. Synchronous Coexpression of Epidermal Growth Factor Receptor and Cyclooxygenase-2 in Carcinomas of the Uterine Cervix: A Potential Predictor of Poor Survival. *Clin Cancer Res* (2004) 10(4):1366–74. doi: 10.1158/1078-0432.CCR-0497-03
28. Adamus WS, Heuer H, Meade CJ, Brecht HM. Safety, tolerability, and pharmacologic activity of multiple doses of the new platelet activating factor antagonist WEB 2086 in human subjects. *Clin Pharmacol Ther* (1989) 45(3):270–6. doi: 10.1038/clpt.1989.27
29. Elmore S. Apoptosis: A Review of Programmed Cell Death. *Toxicol Pathol* (2007) 35(4):495–516. doi: 10.1080/01926230701320337
30. Chen J, Lan T, Zhang W, Dong L, Kang N, Zhang S, et al. Platelet-activating factor receptor-mediated PI3K/AKT activation contributes to the malignant development of esophageal squamous cell carcinoma. *Oncogene* (2015) 34:5114–27. doi: 10.1038/onc.2014.434
31. Biancone L, Cantaluppi V, Del Sorbo L, Russo S, Tjoelker LW, Camussi G. Platelet-activating factor inactivation by local expression of platelet-activating factor acetyl-hydrolase modifies tumor vascularization and growth. *Clin Cancer Res* (2003) 9(11):4214–20.
32. da Silva Junior IA, Stone SC, Rossetti RM, Jancar S, Lepique AP. Modulation of Tumor-Associated Macrophages (TAM) Phenotype by Platelet-Activating Factor (PAF) Receptor. *J Immunol Res* (2017) 2017:5482768. doi: 10.1155/2017/5482768
33. da Silva-Junior IA, Dalmaso B, Herbster S, Lepique AP, Jancar S. Platelet-activating factor receptor ligands protect tumor cells from radiation-induced cell death. *Front Oncol* (2018) 8:2018.00010:10. doi: 10.3389/fonc.2018.00010
34. Williams KA, Lee M, Hu Y, Andreas J, Patel SJ, Zhang S, et al. A Systems Genetics Approach Identifies CXCL14, ITGAX, and LPCAT2 as Novel Aggressive Prostate Cancer Susceptibility Genes. *PloS Genet* (2014) 10(11): e1004809. doi: 10.1371/journal.pgen.1004809
35. Agarwal AK, Garg A. Enzymatic activity of the human 1-acylglycerol-3-phosphate-O- acyltransferase isoform 11: Upregulated in breast and cervical cancers. *J Lipid Res* (2010) 51:2143–52. doi: 10.1194/jlr.M004762
36. Cotte AK, Aires V, Fredon M, Limagne E, Derangère V, Thibaudin M, et al. Lysophosphatidylcholine acyltransferase 2-mediated lipid droplet production supports colorectal cancer chemoresistance. *Nat Commun* (2018) 9(1):322. doi: 10.1038/s41467-017-02732-5
37. Deng M, Guo H, Tam JW, Johnson BM, Brickey WJ, New JS, et al. Platelet-activating factor (PAF) mediates NLRP3-NEK7 inflammasome induction independently of PAFR. *J Exp Med* (2019) 216(12):2838–53. doi: 10.1084/jem.20190111
38. Yin MZ, Tan S, Li X, Hou Y, Cao G, Li K, et al. Identification of phosphatidylcholine and lysophosphatidylcholine as novel biomarkers for cervical cancers in a prospective cohort study. *Tumor Biol* (2016) 37:5485–92. doi: 10.1007/s13277-015-4164-x
39. Gazos-Lopes F, Oliveira MM, Hoelz LVB, Vieira DP, Marques AF, Nakayasu ES, et al. Structural and Functional Analysis of a Platelet-Activating Lysophosphatidylcholine of Trypanosoma cruzi. *PloS Negl Trop Dis* (2014) 8(8):e3077. doi: 10.1371/journal.pntd.0003077
40. Fischer OM, Hart S, Gschwind A, Ullrich A. EGFR signal transactivation in cancer cells. *Biochem Soc Trans* (2003) 31:1203–8. doi: 10.1042/bst0311203
41. Li S, Schmitz KR, Jeffrey PD, Wiltzius JJW, Kussie P, Ferguson KM. Structural basis for inhibition of the epidermal growth factor receptor by cetuximab. *Cancer Cell* (2005) 7(4):301–11. doi: 10.1016/j.ccr.2005.03.003
42. Sales KJ, Katz AA, Davis M, Hinz S, Soeters RP, Hofmeyr MD, et al. Cyclooxygenase-2 expression and prostaglandin E(2) synthesis are upregulated in carcinomas of the cervix: a possible autocrine/paracrine regulation of neoplastic cell function via EP2/EP4 receptors. *J Clin Endocrinol Metab* (2001) 86(5):2243–9. doi: 10.1210/jcem.86.5.7442
43. Ye Y, Wang X, Jeschke U, von Schönfeldt V. COX-2-PGE2-EPs in gynecological cancers. *Arch Gynecol Obstet* (2020) 301(6):1365–75. doi: 10.1007/s00404-020-05559-6

44. Oh JM, Kim SH, Lee YI, Seo M, Kim SY, Song YS, et al. Human papillomavirus E5 protein induces expression of the EP4 subtype of prostaglandin E2 receptor in cyclic AMP response element-dependent pathways in cervical cancer cells. *Carcinogenesis* (2009) 30(1):141–9. doi: 10.1093/carcin/bgn236
45. Parida S, Pal I, Parekh A, Thakur B, Bharti R, Das S, et al. GW627368X inhibits proliferation and induces apoptosis in cervical cancer by interfering with EP4/EGFR interactive signaling. *Cell Death Dis* (2016) 7(3):e2154. doi: 10.1038/cddis.2016.61
46. Heidegger H, Dietlmeier S, Ye Y, Kuhn C, Vattai A, Aberl C, et al. The Prostaglandin EP3 Receptor Is an Independent Negative Prognostic Factor for Cervical Cancer Patients. *Int J Mol Sci* (2017) 18(7):1571. doi: 10.3390/ijms18071571
47. Pai R, Soreghan B, Szabo IL, Pavelka M, Baatar D, Tarnawski AS. Prostaglandin E2 transactivates EGF receptor: A novel mechanism for promoting colon cancer growth and gastrointestinal hypertrophy. *Nat Med* (2002) 8:289–93. doi: 10.1038/nm0302-289
48. Mirzayans R, Andrais B, Scott A, Tessier A, Murray D. A sensitive assay for the evaluation of cytotoxicity and its pharmacologic modulation in human solid tumor-derived cell lines exposed to cancer-therapeutic agents. *J Pharm Pharm Sci* (2007) 10(2):298s–311s.

Conflict of Interest: The authors declare that the research was conducted in the absence of any commercial or financial relationships that could be construed as a potential conflict of interest.

Brazilian Journal of Medical and Biological Research (2021) 54(6): e10754, http://dx.doi.org/10.1590/1414-431X202010754
ISSN 1414-431X Research Article

Epidermal growth factor receptor regulates fibrinolytic pathway elements in cervical cancer: functional and prognostic implications

F.G. Gomes[1], V.H. Almeida[1], K. Martins-Cardoso[1], M.M.D.C. Martins-Dinis[1,2], A.M.R. Rondon[1], A.C. de Melo[3], T.M. Tilli[4], and R.Q. Monteiro[1]

[1]Instituto de Bioquímica Médica Leopoldo de Meis, Universidade Federal do Rio de Janeiro, Rio de Janeiro, RJ, Brasil
[2]Instituto Nacional de Ciência e Tecnologia de Biologia Estrutural e Bioimagem, Universidade Federal do Rio de Janeiro, Rio de Janeiro, RJ, Brasil
[3]Clinical Research Division, Instituto Nacional de Câncer, Rio de Janeiro, RJ, Brasil
[4]Plataforma de Oncologia Translacional, Centro de Desenvolvimento Tecnológico em Saúde, Fundação Oswaldo Cruz, Rio de Janeiro, RJ, Brasil

Abstract

Epidermal growth factor receptor (EGFR) signaling and components of the fibrinolytic system, including urokinase-type plasminogen activator (uPA) and thrombomodulin (TM), have been implicated in tumor progression. In the present study, we employed cBioPortal platform (http://www.cbioportal.org/), cancer cell lines, and an *in vivo* model of immunocompromised mice to evaluate a possible cooperation between EGFR signaling, uPA, and TM expression/function in the context of cervical cancer. cBioPortal analysis revealed that EGFR, uPA, and TM are positively correlated in tumor samples of cervical cancer patients, showing a negative prognostic impact. Aggressive human cervical cancer cells (CASKI) presented higher gene expression levels of EGFR, uPA, and TM compared to its less aggressive counterpart (C-33A cells). EGFR induces uPA expression in CASKI cells through both PI3K-Akt and MEK1/2-ERK1/2 downstream effectors, whereas TM expression induced by EGFR was dependent on PI3K/Akt signaling alone. uPA induced cell-morphology modifications and cell migration in an EGFR-dependent and -independent manner, respectively. Finally, treatment with cetuximab reduced *in vivo* CASKI xenografted-tumor growth in nude mice, and decreased intratumoral uPA expression, while TM expression was unaltered. In conclusion, we showed that EGFR signaling regulated expression of the fibrinolytic system component uPA in both *in vitro* and *in vivo* settings, while uPA also participated in cell-morphology modifications and migration in a human cervical cancer model.

Key words: Cervical cancer; Epidermal growth factor receptor; Urokinase-type plasminogen activator; Thrombomodulin; Fibrinolytic system

Introduction

Cervical cancer is the fourth most incident type of cancer among women, with 570,000 new estimated cases in 2018 (1), a vast majority of which occurring in developing countries. Cervical cancer is the third most common type of malignancy among Brazilian women, with a high mortality rate (2). The major risk factor for cervical cancer is human papillomavirus (HPV) infection (3).

The epidermal growth factor receptor (EGFR) has been associated with cervical cancer progression (4,5). EGFR is well described concerning its involvement in several processes such as proliferation and resistance to chemotherapy. Furthermore, EGFR expression has been correlated with poor survival among cervical cancer patients (6). HPV infection was shown to increase the amount of EGF receptors exposed on the cell membrane (by inhibiting EGFR degradation) (7) and enhance the expression of intracellular signal transducers commonly associated with EGFR signaling, such as phosphatidylinositol-3 kinase (PI3K) and extracellular signal-regulated kinase (ERK) (8). Different clinical trials have been performed employing anti-EGFR therapy for cervical cancer patients, showing ambiguous results: either with no beneficial outcomes (9), treatment-associated side effects (10), or an approximate 10% increase in overall survival (11).

A different group of receptors and secreted proteins that have been increasingly shown to participate in cancer invasion and metastasis is the fibrinolytic system.

Correspondence: R.Q. Monteiro: <robsonqm@bioqmed.ufrj.br>

Received September 17, 2020 | Accepted January 4, 2021

The fibrinolytic system is classically associated with the degradation of fibrin clots in the blood. However, the study performed by Malone and coworkers showed that cancer tissues from metastatic foci had increased fibrinolytic activity compared to primary non-metastatic tumor samples (12). The generation of plasmin, a key effector in the fibrinolytic system within the cancer microenvironment, has been demonstrated to be involved in extracellular matrix degradation, pro-ligand and pro-metalloprotease cleavage, and tumor cell invasion in different models (13–15). Plasmin is generated by cleavage of the circulating inactive plasminogen by plasminogen activators, such as urokinase-type plasminogen activator (uPA), which is the most relevant plasminogen activator within solid tissues. Furthermore, plasminogen can bind to different receptors on the cell surface, such as thrombomodulin (TM), annexin A2 (ANXA2), and S100 calcium-binding protein A10 (S100A10) (16,17). High expressions of uPA and uPA receptor (uPAR) have already been shown to correlate with cancer metastasis and worse patient prognosis (18).

EGFR signaling has been directly linked with components of the fibrinolytic system, for example, in breast cancer and glioblastoma. Jo et al. (19) showed that EGFR signaling was inhibited in breast cancer cells by silencing or inhibiting uPAR. Furthermore, in glioblastoma, EGFR was shown to induce uPA expression by proto-oncogene tyrosine-protein kinase Src (c-Src) and ERK signaling (20). A possible compensatory mechanism may also take place in glioblastoma where there is an increased expression of both uPA and uPAR in response to EGFR inhibition, favoring resistance to EGFR-targeted therapy (21,22).

It remains unanswered, however, if EGFR signaling is related somehow to components of the fibrinolytic system in cervical cancer. In the present work, we observed a positive expression correlation between EGFR and several fibrinolytic system elements, including uPA and TM on human cervical tumor samples, with prognostic significance. We also observed that EGFR signaling positively regulated expression of both uPA and TM in an aggressive cervical cancer cell line, and that uPA expression led to cell morphology alterations and increased migration. Finally, *in vivo*, we observed that treatment with an anti-EGFR antibody, cetuximab injected subcutaneously, reduced tumor growth, a process that was accompanied by a decreased intra-tumoral expression of uPA.

Material and Methods

Expression-correlation analysis

Transcriptome data from 302 patients were collected from the "TCGA, Firehouse Legacy" cohort on the platform cBioPortal (http://www.cbioportal.org/) (23,24) between May 22, 2020 and May 23, 2020. This cohort had 304 patients (as of May 23, 2020) two of which had two samples taken (totaling 306 samples from 304 patients). These two patients were excluded from the analysis, therefore the total number of samples/patients shown in the present work is 302. mRNA expression (RNA Seq V2 RSEM) in FPKM (frames per kilobase per million) data was downloaded, plotted using Graphpad Prism™ (USA), and analyzed by non-parametric Spearman correlation.

Overall survival analysis

From the cBioPortal platform, we established a cut-off of 1.5 standard deviations above the median of expression to separate groups of "overexpression" and "cases without alteration" of the cohort "TCGA, Firehouse Legacy", from the 302 patients. After the establishment of the gene expression cut-off, we analyzed overall survival at the "survival" window on cBioPortal, extracted the data, and assembled the graphs with Graphpad™. Mantel-Cox test was used for statistical analysis.

Cell lines

Human cervical cancer cells CASKI (more aggressive) and C-33A (less aggressive) were cultivated in RPMI medium supplemented with 10% fetal bovine serum (FBS), and maintained in 37°C, 5% CO_2. CASKI cell line was originated from an intestinal metastasis of an epidermoid cervical carcinoma and was infected with multiple copies of HPV-16 (ATCC, CRL-1550™). C-33A cells originated from a primary epidermoid cervical carcinoma, uninfected by HPV (ATCC, HTB-31™).

Real-time PCR

Briefly, C-33A or CASKI were seeded (4×10^5 cells/well) onto 6-well plates, in RPMI medium supplemented with 10% FBS. The next day, the wells were washed with phosphate-buffered saline (PBS) and cells were starved (FBS-free medium) for 16 h. After starving, cells were treated with anti-EGFR antibody (cetuximab, Merck, Germany, 100 μg/mL), PI3K inhibitor (LY294002, Sigma-Aldrich, USA, 25 μM), or MEK inhibitor (PD98059, Sigma-Aldrich, 50 μM), for 1h. Then, cells were treated with EGF (50 ng/mL) for 1.5 h or 3 h, 37°C, 5% CO_2. The wells were washed with PBS and 0.5–1 mL Trizol (Sigma-Aldrich) was added to each well. The extracts were transferred into microcentrifuge tubes and stored at –20°C, for posterior RNA isolation. From each sample, 1 μg of total RNA was reverse transcribed to cDNA. Next, quantitative PCR was performed on cDNA aliquots.

For TM real-time PCR, 5 μL master mix (Thermo Fisher Scientific, USA), 0.5 μL TaqMan probe for human TM (Hs00264920_s1) or human GAPDH (reference gene, 4326317E), 2 μL injection water, and 2.5 μL diluted cDNA (1:20 v/v) were added, totaling 10 μL per well of a 96-well PCR plate. Quantitative PCR was performed with a StepOnePlus™ real-time PCR system (Thermo Fisher Scientific). The cycling conditions were: 95°C (20 s), followed by 50 cycles of 95°C (1 s) and 60°C (20 s).

For uPA real-time PCR, 7.5 μL SYBR green mix, 0.6 μL forward primer (10 μM), 0.6 μL reverse primer

(10 μM) (both primers purchased from Thermo Fisher Scientific), 4.8 μL injection water, and 1.5 μL cDNA (diluted 1:20 v/v) were added, totaling 15 μL per well of a 96-well PCR plate. The cycling conditions were: 95°C (10 min), followed by 45 cycles of 95°C (15 s) and 60°C (1 min). Finally, the melting curve was 95°C (15 s), 60°C (1 min), and 95°C (15 s). In this case, 18S was used as a reference gene (25) (Table 1). The $(1 + \text{efficiency})^{-\Delta\Delta CT}$ method was used to analyze the fold increase.

Plasmin enzymatic activity assay

CASKI or C-33A cells were seeded (3×10^4/well) onto 96-well plates in RPMI medium supplemented with 10% FBS. When necessary, 100 μg/mL cetuximab was added to the wells after seeding and incubated for 30 min, 37°C, 5% CO_2. Then, EGF was added to the wells of interest at 10, 50, or 100 ng/mL and the plates were incubated for 18 h at 37°C, 5% CO_2. The wells were washed twice with FBS/phenol red-free medium and uPA inhibitor (BC-11 hydrobromide, Abcam, USA) was added at a final concentration of 50 μM for approximately 15 min at room temperature. After BC-11 incubation, lys-plasminogen was added at 0.5 μM, and 250 μM of plasmin-chromogenic substrate S2251 (Diapharma, USA) was immediately pipetted to the wells. Plates were analyzed on a Spectramax 190 plate reader (Molecular Devices, USA) for 5 h, at 37°C, during which 405 nm reads were performed at 4 min intervals. All experiments were performed in duplicate.

Flow cytometry

Flow cytometry assays were performed using an anti-TM antibody conjugated with the APC (allophycocyanin) fluorophore, which has peak excitation at 645 nm and emission at 660 nm. Briefly, 5×10^5 cells were incubated with 2.5 μL anti-TM antibody in 100 μL final volume, 12.5 μg/mL final concentration (BioLegend, clone M80, USA), for 30 min, on ice. The cells were then washed with PBS and resuspended on 400 μL of FACs buffer (PBS + 5% FBS). Basal TM expression of C-33A and CASKI cells was evaluated on a FACSVerse™ machine (BD Biosciences, USA). TM-protein expression was also evaluated after stimuli with 50 ng/mL EGF +/– cetuximab, for 6 h. The experiment was performed on an Accuri™ (BD Biosciences) flow cytometer, evaluating the percentage of positive events and mean fluorescence intensity (MFI).

Cell morphology and migration

CASKI cells (5×10^5/well) were seeded onto 6-well plates. After 24 h, cells were starved in FBS-free media for 10 h and treated with or without 0.5 μM glu-plasminogen, 100 μg/mL cetuximab, and/or 50 μM BC-11 for approximately 16 h at 37°C, 5% CO_2. Plates were photographed with a Qimaging camera (Q35443, CE, Canada), at 10× magnification. Immediately after the photographs, cells were harvested for the Boyden chamber migration assay, which was performed using 8-μm pore polycarbonate membranes (Costar, USA). The lower compartments were

Table 1. Sequence and product size for the primers used on SYBR green real-time PCR protocol.

Gene name	Primers	Product size
uPA	F: GTCACCTACGTGTGTGGAGG	147 base pairs
	R: CTTCATCTCCCCTTGCGTGT	
18S	F: AACCCGTTGAACCCCATT	149 base pairs (ref. 25)
	R: CCATCCAATCGGTAGTAGCG	

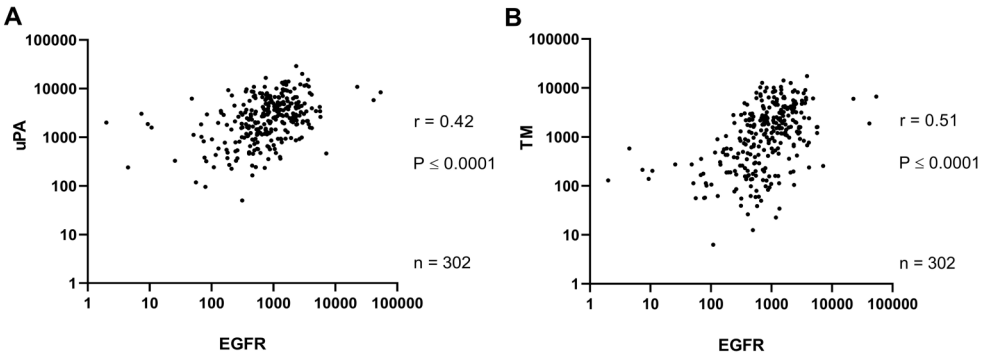

Figure 1. Epidermal growth factor receptor (EGFR), urokinase-type plasminogen activator (uPA), and thrombomodulin (TM) expressions have a positive correlation in samples from human cervical tumors. Data are reported as FPKM (frames per kilobase per million). Spearman correlation test was used for statistical analysis.

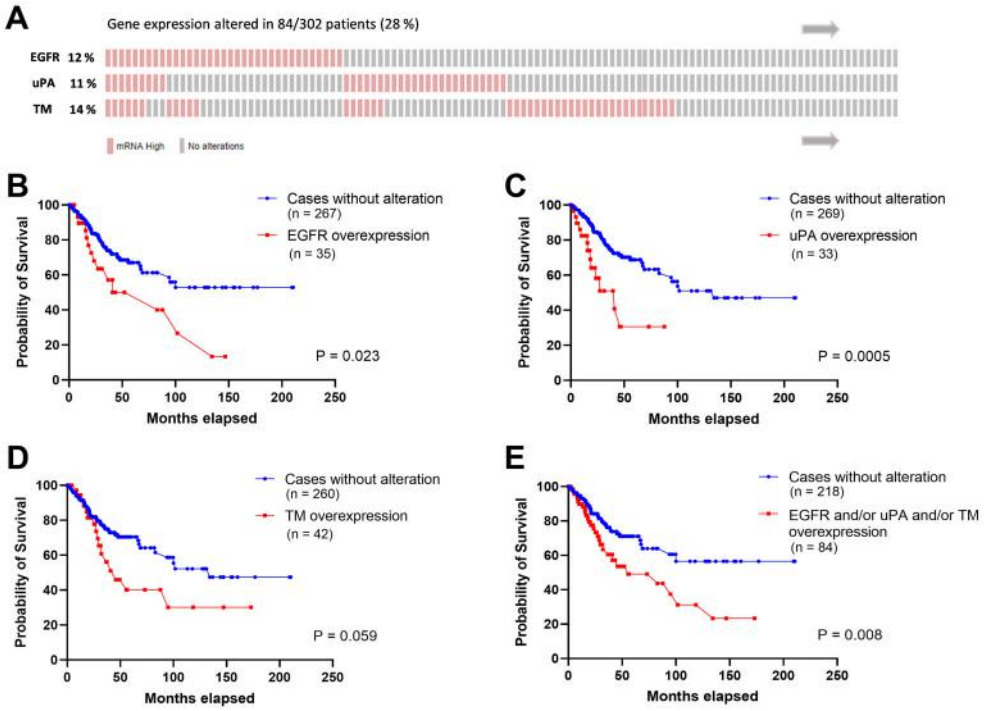

Figure 2. Overall survival analysis of cervical cancer patients concerning epidermal growth factor receptor (EGFR), urokinase-type plasminogen activator (uPA), and thrombomodulin (TM) tumor overexpression. **A**, Map of the alterations in the EGFR, TM, and uPA gene expression in tumor samples of 302 cervical cancer patients. Patients who exhibited overexpression of these genes in the tumor are indicated in red. This map was generated through cBioPortal, which is based on the clinical and molecular information provided by TCGA. Overall survival analysis of cervical cancer patients with gene expression of 1.5 standard deviations above the median for EGFR (**B**), uPA (**C**), TM (**D**), or any of the three genes, in an isolated or concomitant manner (**E**). Survival curve comparison was done through the Log-rank (Mantel-Cox) statistical test.

filled with RPMI media containing 5% FBS and 3×10^4 treated cells were seeded in 50 μL serum-free media to the upper chambers. After 20 h of incubation, at 37°C with 5% CO_2, the non-migrated cells in the upper chambers were removed and the membranes were fixed and stained using the fast Panoptic staining kit (Laborclin, Brazil). Ten image fields were evaluated for each condition. The mean number of cells per field was calculated for each condition (of each experiment) and plotted.

In vivo assays

For *in vivo* assays, 1×10^7 CASKI cells were subcutaneously injected into both flanks of immunocompromised Balb/c nude female mice. One week later, when tumors became palpable, the size of tumors was calculated using the following formula: $V = D \times d^2 / 2$, where V: tumor volume (mm^3); D: larger tumor mass diameter (mm); d: smaller tumor diameter (mm).

The measurements were made using a caliper. Day 0 was defined as the day when the cell injections were made, and then tumors were measured on days 7, 9, 12, 14, and 15. Injected animals were separated into two groups: 1) Control group: treated intraperitoneally with 200 μL PBS (4 animals); and 2) Intervention group: treated intraperitoneally with 200 μL cetuximab (1 mg/animal, 3 animals). Both tumors in each animal were analyzed as an independent experimental unit. Treatments were performed on the same day of size measurements, except for day 15. On day 15, the animals were anesthetized with ketamine/xylazine and euthanized by cervical displacement. Immediately after euthanasia, tumors were excised using scissors and scalpel and weighed on a precision scale. Finally, tumors were cut into smaller pieces with a scissor, inserted into 1.5 mL Eppendorf tubes containing Trizol, and stored at –20°C. Samples were then macerated using a Turrax homogenizer (Daigger Scientific, USA), which was washed with DEPC water, Trizol, 75% ethanol, and DEPC water, in this order, between samples. Samples were then further processed for real-time PCR. The use of animals in this work was approved by the Commission of Ethics in Animal Use of the Federal University of Rio de Janeiro, registered at the National Control Council of Animal Experimentation under the process number 01200.001568/2013-87, protocol 102/16.

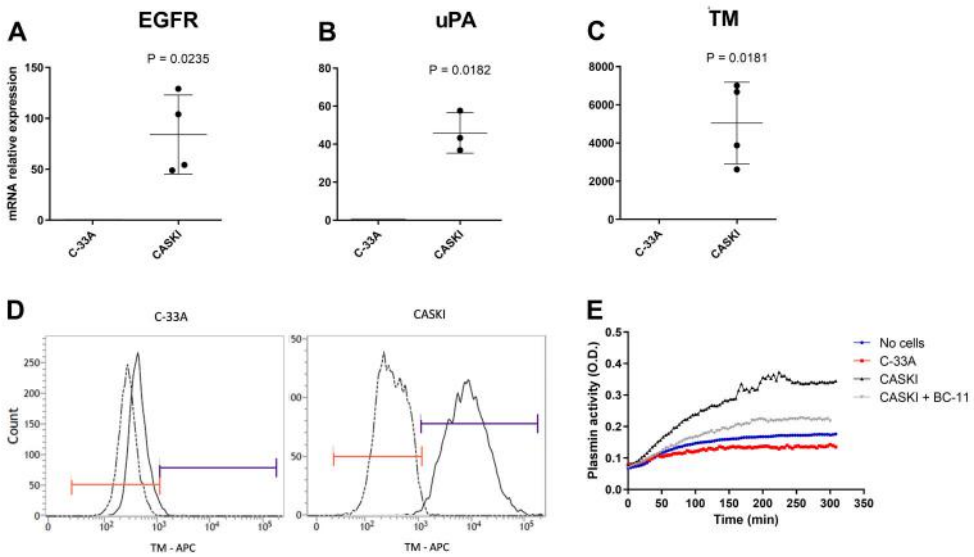

Figure 3. CASKI cells express higher levels of epidermal growth factor receptor (EGFR), urokinase-type plasminogen activator (uPA), and thrombomodulin (TM) compared to C-33A cells (**A**–**C**). Data are reported as means ± SD of 3–4 independent experiments (unpaired *t*-test). **D**, Representative histograms of the flow cytometry for TM of C-33A and CASKI cells, analyzing the percentage of positive events. **E**, Representative graph of the plasmin enzymatic activity assay of C-33A and CASKI cells (+/– uPA inhibitor, BC-11, 50 μM) followed by 0.5 μM lys-plasminogen and 250 μM chromogenic substrate S2251, analyzed over 5 h with 4 min between each read at 405 nm.

Data analysis and presentation

When comparing two groups, one-sample *t*-test (when one of the group's data had been normalized to "1") or two-sample unpaired two-tailed *t*-test was employed. For multiple comparisons, one-way ANOVA with Tukey's post-test was used. All statistical analyses were done with Graphpad Prism™. When applicable, data are reported as means ± SD (with the exception of Figure 6A, which reports means ± SE). Experimental units for *in vitro* assays were considered to be the mean result of each experiment, performed on different cell-culture passages.

Results

EGFR, uPA, and TM expressions were positively correlated in samples from human cervical cancer tumors, which correlated with poor overall survival

A positive correlation between EGFR x uPA expressions ($r=0.42$, $P<0.0001$, Figure 1A) and EGFR x TM expressions ($r=0.51$, $P<0.0001$, Figure 1B) was observed in cervical cancer samples. In the criteria established in the current study, the mRNA upregulation of EGFR, uPA, and TM was found in 12, 11, and 14% of the cases, respectively (Figure 2A). Furthermore, cervical cancer patients with increased expression of EGFR (P=0.023, Figure 2B), uPA (P=0.0005, Figure 2C), or TM (P=0.059, Figure 2D) had decreased overall survival compared to the patients with normal levels. The effect of the upregulation in one, two, or all three genes in this group of patients (n=84) was also significantly associated with poor overall survival (P=0.008, Figure 2E). A positive correlation between EGFR expression and other components of the fibrinolytic system (Table S1) was also observed, although the increased expression of each gene showed no correlation with alterations of overall survival of the cervical cancer patients (Supplementary Figure S1).

CASKI cells expressed higher levels of EGFR, uPA, and TM compared to C-33A cells

The more aggressive CASKI cells expressed higher mRNA levels of the EGFR, uPA, and TM (Figure 3A–C) genes compared to C-33A. On a protein level, C-33A cells were negative for TM, as observed by flow cytometry, whereas CASKI cells were mostly positive (Figure 3D). C-33A cells also did not generate active plasmin from added plasminogen (reaction catalyzed by cell-produced plasminogen activators, such as uPA) while, in contrast, CASKI cells had an uPA-dependent generation of active plasmin (Figure 3E). Previously published data from our group shows that CASKI cells have higher protein levels of EGFR compared to C-33A cells (26).

EGFR signaling upregulated uPA and TM expression in CASKI cells

On a protein level, the addition of the anti-EGFR monoclonal antibody cetuximab reduced basal plasmin generation, as well as reverted the EGF-mediated increase of plasmin activity (Figure 4A) in CASKI cells. EGF addition to C-33A cells did not alter uPA expression or plasmin generation (Supplementary Figure S2).

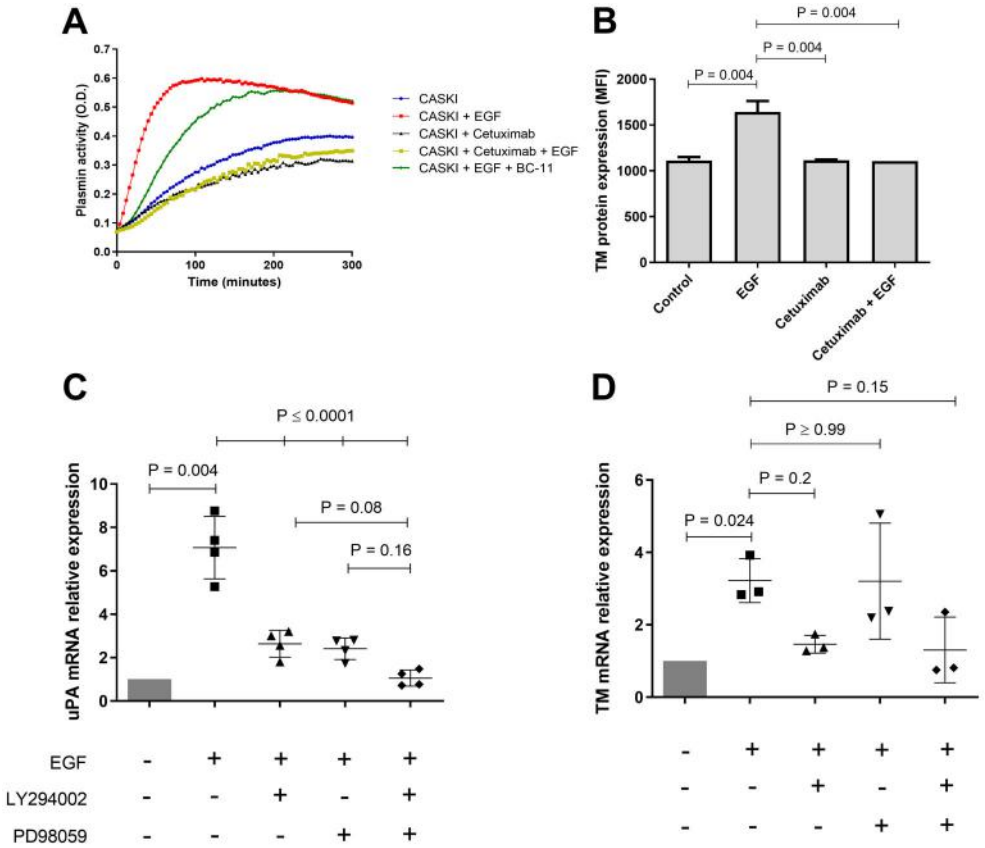

Figure 4. Epidermal growth factor receptor (EGFR) signaling upregulates urokinase-type plasminogen activator (uPA) and thrombomodulin (TM) expression in CASKI cells. **A**, Representative graph of the plasmin enzymatic activity assay performed with CASKI cells treated overnight with epidermal growth factor (EGF) alone, cetuximab alone, EGF 30 min after cetuximab treatment, or EGF overnight plus BC-11 15 min before starting measurements. **B**, Flow cytometry staining for TM in CASKI cells treated with EGF, cetuximab, or the combination of both. Data are reported as mean fluorescence intensity ± SD. One-way ANOVA with Tukey's post-test was used for statistical analysis. Real-time PCR for uPA (**C**) or TM (**D**) in CASKI cells treated with EGF +/– LY294002, +/– PD98059. A one-sample *t*-test was performed for comparisons to the normalization control "CASKI", and one-way ANOVA with Tukey's post-test was performed for the remaining comparisons. In all cases, LY294002 and PD98059 were added to the cells 1 h before EGF addition, which was then done for 15 min (western blot) or 1.5 h (real-time PCR). Final concentrations were: 50 ng/mL EGF, 25 μM LY294002, and 50 μM PD98059.

EGF-induced plasmin generation in CASKI cells was promoted by uPA (Figure 4A). TM protein expression increased with EGF addition to CASKI cells, and such effect was reverted by cetuximab (Figure 4B, Supplementary Figure S3).

In order to evaluate whether EGFR signaling had a direct impact on uPA and TM expression, CASKI cells were incubated with EGF with or without inhibitors of the downstream EGFR-signaling branches PI3K-Akt (LY294 002) and MEK1/2-ERK1/2 (PD98059) (Figure 4C and D). EGF-induced uPA expression was significantly diminished in CASKI cells by both inhibitors (Figure 4C), whereas EGF-induced TM expression was significantly diminished by PI3K inhibition (Figure 4D).

uPA participated in morphology-altering and migration phenomena in CASKI cells

To assess the possible functional impact that EGFR-dependent plasmin generation may have on CASKI cells, we evaluated the cell morphology under different treatments (Figure 5A–E). Upon plasminogen addition, cells changed their morphology into a highly connected state, assembling into "branched" structures composed of overlapping cells, as opposed to the control-monolayer cell disposition (Figure 5A and B). Both uPA and EGFR inhibition, in an isolated manner, hampered this plasminogen-induced cell-morphology alteration (Figure 5C and D) and the combination of both inhibitors seemed to reverse this effect to a state that mostly resembled the control group (Figure 5E).

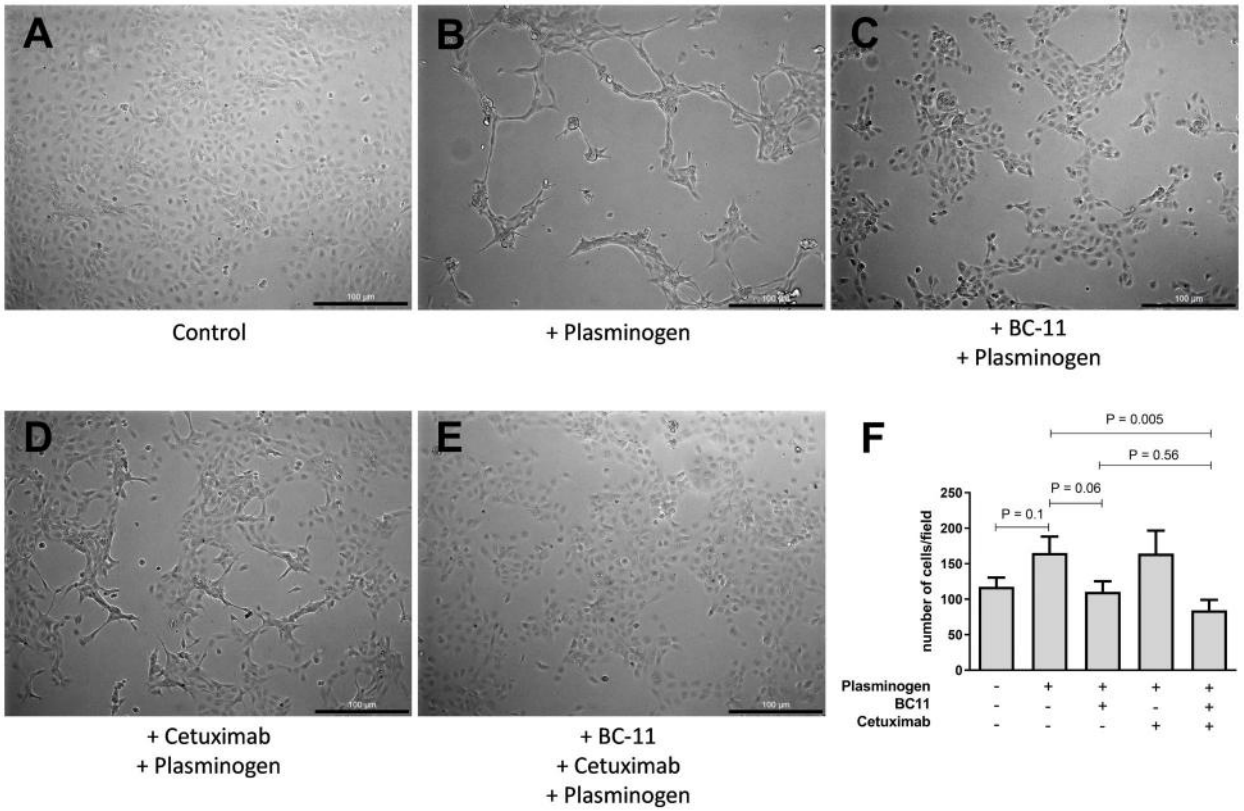

Figure 5. Epidermal growth factor receptor (EGFR)/urokinase-type plasminogen activator (uPA) participated in morphology-altering and migration phenomena in CASKI cells. **A**–**E**, Bright field light microscopy pictures (100× magnification, scale bar 100 μm) of CASKI cells treated for 16 h with plasminogen +/– uPA inhibitor (BC-11) or +/– anti-EGFR monoclonal antibody (cetuximab). **F**, Cell migration experiment in the Boyden chamber was performed on the cells treated the same as in the microscopy images. Final treatment concentrations: 0.5 μM glu-plasminogen, 50 μM BC-11, and 100 μg/mL cetuximab. Data are reported as means ± SD of three independent experiments. One-way ANOVA with Tukey's post-test was used for statistical analysis.

Cell migration experiments were performed immediately after cell-morphology images were taken and, although plasminogen addition led to a trend of increased cell migration on a Boyden chamber model, EGFR or uPA inhibition alone did not decrease plasminogen-induced cell migration, whereas the combination of both inhibitors significantly hampered this process (Figure 5F).

In vivo treatment with cetuximab decreased tumor growth/weight and intra-tumoral uPA expression

Cetuximab treatment reduced *in vivo* tumor growth and weight (Figure 6A and B) and led to a trend of uPA expression reduction within the tumor tissue (Figure 6C), whereas TM expression was unaffected by *in vivo* cetuximab treatment (Figure 6D).

Discussion

Cervical cancer is a type of malignancy that, unfortunately, still imposes a great burden on women living in low and middle income countries. Although the standard treatment consisting on surgical resection for initial disease or chemotherapy in combination with radiotherapy for locally advanced disease is of fundamental importance, there is still a great need for: 1) new therapeutic targets and 2) biomarkers for screening patients that could benefit more from certain targeted therapies. EGFR has been considered to be a receptor involved in cervical cancer progression (4,5), however, clinical trials are still not conclusive as to whether blocking EGFR is effective enough for justifying its use in the clinical setting (9–11). Furthermore, it has been described that, in other types of cancer in which anti-EGFR treatment is Food and Drug Administration-approved, it is quite common for patients to develop resistance mechanisms towards EGFR-targeted therapy (27).

In the present work, EGFR, uPA, and TM expression had a positive correlation on human cervical tumor samples, and the high expression of these genes was associated with worse patient overall survival.

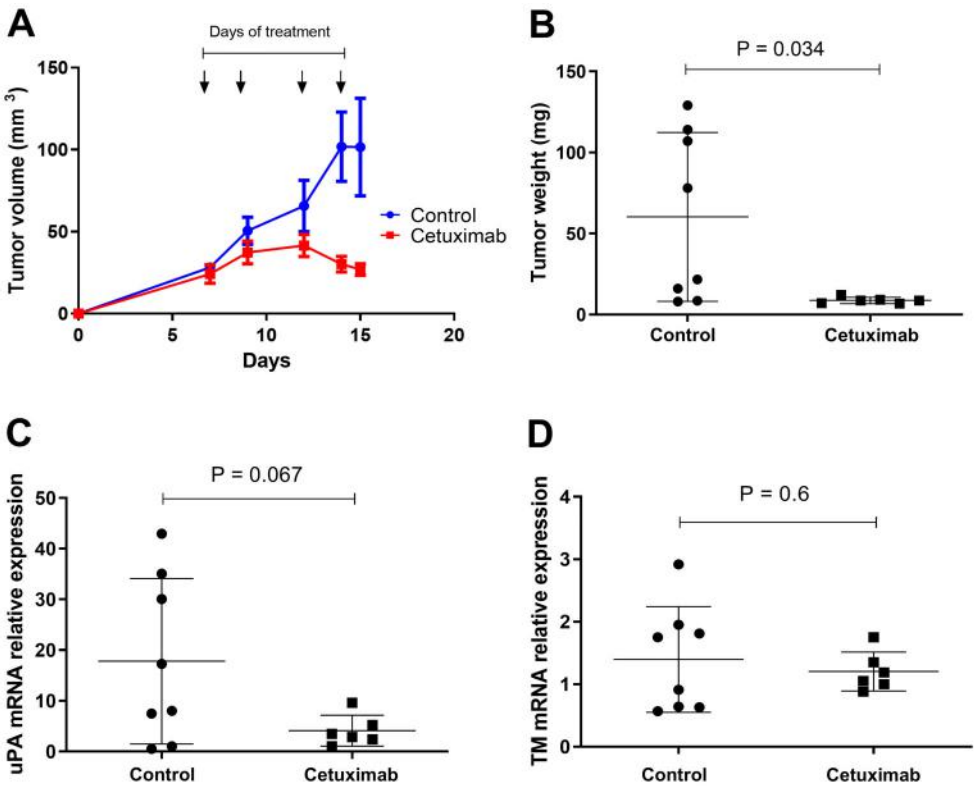

Figure 6. *In vivo* treatment with cetuximab decreased tumor growth/weight and intra-tumoral urokinase-type plasminogen activator (uPA) expression. **A**, Tumor growth of subcutaneously injected CASKI cells (1×10^7) into Balb/c nude mice. The arrows indicate the time points in which PBS or 1 mg cetuximab were administered intraperitoneally in a final volume of 200 μL per animal. After euthanasia of the animals, tumors were excised, weighed (**B**), prepared for RNA extraction, and quantitative real-time PCR was performed for uPA (**C**) and thrombomodulin (TM) (**D**). Two-sample Student's *t*-test was used for statistical analysis comparing control group (n=8) *vs* cetuximab group (n=6).

A meta-analysis published in 2002, with data from 8,377 breast cancer patients, showed that increased uPA levels correlated with worse disease-free and overall survival (28). Serum uPA levels in 252 breast cancer patients were positively correlated with worse progression-free and overall survival, as well as associated with an increase in plasma HER2 levels, a receptor of the EGFR family (29). In 2014, however, another study showed that plasma levels of uPA did not correlate with lymph node metastasis status, also in human breast cancer (30). In colorectal cancer, uPA levels in plasma or primary site *vs* normal mucosa did not correlate with alterations in patient survival (31). In cervical cancer, Sugimura et al. showed that uPA staining in primary tumor biopsies correlated positively with lymph node metastasis status (32). Another group in 2002, however, did not observe any prognostic impact of intra-tumoral uPA, also among cervical cancer patients (33).

It has been shown that the uPA receptor, uPAR, can transactivate EGFR (19) and that both uPA and uPAR participate in the resistance mechanisms towards anti-EGFR treatment in glioblastoma (21,22). One hypothesis that arises in light of these results is that, in cervical cancer, there may be a positive feedback loop, in which EGFR positively regulates uPA expression, and that its receptor, uPAR, may favor EGFR transactivation, as has been shown in glioblastoma (19). Furthermore, the silencing of uPA and uPAR in a pancreatic cancer model reduces *in vivo* tumor growth and angiogenesis (34). A clinical trial has been published using an uPA inhibitor called WX-671 in locally advanced pancreatic cancer, showing no notable difference between groups treated with chemotherapy alone or in combination with uPA inhibition (35). Another clinical trial using a competitive inhibitor of the binding between uPA and uPAR, called A6, showed minimal beneficial effects on patients with gynecological tumors such as the ovary, fallopian tube, and peritoneum (36). Perhaps finding signaling partners for either EGFR or uPA could be useful in optimizing therapeutic efficiency for these targets.

In the present work, we showed that EGFR, uPA, and TM levels of human cervical tumors correlated with worse overall patient survival and that uPA and TM were positively regulated by EGFR. Furthermore, uPA expression can have a direct impact on cervical cancer cell function, specifically EGFR-dependent cell morphology modifications and EGFR-independent cell migration. To the best of our knowledge, we are the first to show this interplay between EGFR signaling and components of the fibrinolytic system in cervical cancer. Therefore, we propose uPA as a potentially novel candidate to be studied in combination with EGFR in cervical cancer, either as a therapeutic target or as a biomarker for EGFR signaling and patient prognosis.

Supplementary Material

Click here to view [pdf].

Acknowledgments

We would like to sincerely thank PhD student Clarissa França Dias Carneiro for assistance in formatting figures and quality of reporting, Prof. Dr. Luciana Serrão and Prof. Dr. Jerson Lima for allowing the use of their facilities and equipment, and Ms. Rosangela Araujo and the team of animal care at the National Center of Structural Biology and Bioimaging (CENABIO) for technical assistance. This work was supported by the National Council for Scientific and Technological Development (CNPq, grant number 309946/2018-2), the Coordination for the Improvement of Higher Education Personnel (CAPES, grant number 23038.008921/2019-15), the Carlos Chagas Filho Foundation for Research Support of the State of Rio de Janeiro (FAPERJ, grant number E-26/202.871/2018), and The Brazilian Cancer Foundation.

References

1. WHO. *Cervical cancer.*<https://www.who.int/cancer/prevention/diagnosis-screening/cervical-cancer/en/>. Accessed on March 3, 2020.
2. Instituto Nacional de Câncer (BR) Coordenação de Prevenção e Vigilância. Estimativa 2020: incidência de câncer no Brasil. Rio de Janeiro: INCA; 2019.
3. Subramanya D, Grivas PD. HPV and cervical cancer: updates on an established relationship. *Postgrad Med* 2008; 120: 7–13, doi: 10.3810/pgm.2008.11.1928.
4. Wang Z. ErbB receptors and cancer. *Methods Mol Biol* 2017; 1652: 3–35, doi: 10.1007/978-1-4939-7219-7_1.
5. Sigismund S, Avanzato D, Lanzetti L. Emerging functions of the EGFR in cancer. *Mol Oncol* 2018; 12: 3–20, doi: 10.1002/1878-0261.12155.
6. Tian WJ, Huang ML, Qin QF, Chen Q, Fang K, Wang PL. Prognostic impact of epidermal growth factor receptor overexpression in patients with cervical cancer: a meta-analysis. *PLoS One* 2016; 11: e0158787, doi: 10.1371/journal.pone.0158787.
7. Maufort JP, Shai A, Pitot HC, Lambert PF. A role for HPV16 E5 in cervical carcinogenesis. *Cancer Res* 2010; 70: 2924–2931, doi: 10.1158/0008-5472.CAN-09-3436.
8. Manzo-Merino J, Contreras-Paredes A, Vázquez-Ulloa E, Rocha-Zavaleta L, Fuentes-Gonzalez AM, Lizano M. The role of signaling pathways in cervical cancer and molecular therapeutic targets. *Arch Med Res* 2014; 45: 525–539, doi: 10.1016/j.arcmed.2014.10.008.
9. Hertlein L, Lenhard M, Kirschenhofer A, Kahlert S, Mayr D, Burges A, et al. Cetuximab monotherapy in advanced cervical cancer: a retrospective study with five patients. *Arch Gynecol Obstet* 2011; 283: 109–113, doi: 10.1007/s00404-010-1389-1.
10. Kurtz JE, Hardy-Bessard AC, Deslandres M, Lavau-Denes S, Largillier R, Roemer-Becuwe C, et al. Cetuximab, topotecan and cisplatin for the treatment of advanced cervical cancer: a phase II GINECO trial. *Gynecol Oncol* 2009; 113: 16–20, doi: 10.1016/j.ygyno.2008.12.040.
11. Nogueira-Rodrigues A, Moralez G, Grazziotin R, Carmo CC, Small IA, Alves FV, et al. Phase 2 trial of erlotinib combined with cisplatin and radiotherapy in patients with locally advanced cervical cancer. *Cancer* 2014; 120: 1187–1193, doi: 10.1002/cncr.28471.
12. Malone JM, Wangensteen SL, Moore WS, Keown K. The fibrinolytic system. A key to tumor metastasis? *Ann Surg* 1979; 190: 342–349, doi: 10.1097/00000658-197909000-00009.
13. Heissig B, Eiamboonsert S, Salama Y, Shimazu H, Dhahri D, Munakata S, et al. Cancer therapy targeting the fibrinolytic system. *Adv Drug Deliv Rev* 2016; 99: 172–179, doi: 10.1016/j.addr.2015.11.010.
14. Lin H, Xu L, Yu S, Hong W, Huang M, Xu P. Therapeutics targeting the fibrinolytic system. *Exp Mol Med* 2020; 52: 367–379, doi: 10.1038/s12276-020-0397-x.
15. Tang L, Han X. The urokinase plasminogen activator system in breast cancer invasion and metastasis. *Biomed Pharmacother* 2013; 67: 179–182, doi: 10.1016/j.biopha.2012.10.003.
16. Didiasova M, Wujak L, Wygrecka M, Zakrzewicz D. From plasminogen to plasmin: role of plasminogen receptors in human cancer. *Int J Mol Sci* 2014; 15: 21229–21252, doi: 10.3390/ijms151121229.
17. Cheng TL, Chen PK, Huang WK, Kuo CH, Cho CF, Wang KC, et al. Plasminogen/thrombomodulin signaling enhances VEGF expression to promote cutaneous wound healing. *J Mol Med (Berl)* 2018; 96: 1333–1344, doi: 10.1007/s00109-018-1702-1.
18. Mahmood N, Mihalcioiu C, Rabbani SA. nFront multifaceted role of the urokinase-type plasminogen activator (uPA) and its receptor (uPAR): diagnostic, prognostic, and therapeutic applications. *Front Oncol* 2018; 8: 24, doi: 10.3389/fonc.2018.00024.
19. Jo M, Thomas KS, O'Donnell DM, Gonias SL. Epidermal growth factor receptor-dependent and -independent

cell-signaling pathways originating from the urokinase receptor. *J Biol Chem* 2003; 278: 1642–1646, doi: 10.1074/jbc.M210877200.
20. Amos S, Redpath GT, Dipierro CG, Carpenter JE, Hussaini IM. Epidermal growth factor receptor-mediated regulation of urokinase plasminogen activator expression and glioblastoma invasion via C-SRC/MAPK/AP-1 signaling pathways. *J Neuropathol Exp Neurol* 2010; 69: 582–592, doi: 10.1097/NEN.0b013e3181e008fe.
21. Hu J, Muller KA, Furnari FB, Cavenee WK, VandenBerg SR, Gonias SL. Neutralizing the EGF receptor in glioblastoma cells stimulates cell migration by activating uPAR-initiated cell signaling. *Oncogene* 2015; 34: 4078–4088, doi: 10.1038/onc.2014.336.
22. Wykosky J, Hu J, Gomez GG, Taylor T, Villa GR, Pizzo D, et al. A urokinase receptor-Bim signaling axis emerges during EGFR inhibitor resistance in mutant EGFR glioblastoma. *Cancer Res* 2015; 75: 394–404, doi: 10.1158/0008-5472.CAN-14-2004.
23. Gao J, Aksoy BA, Dogrusoz U, Dresdner G, Gross B, Sumer SO, et al. Integrative analysis of complex cancer genomics and clinical profiles using the cBioPortal. *Sci Signal* 2013; 6: pl1, doi: 10.1126/scisignal.2004088.
24. Cerami E, Gao J, Dogrusoz U, Gross BE, Sumer SO, Aksoy BA, et al. The cBio cancer genomics portal: an open platform for exploring multidimensional cancer genomics data. *Cancer Discov* 2012; 2: 401–404, doi: 10.1158/2159-8290.CD-12-0095.
25. Tilli TM, Castro CS, Tuszynski JA, Carels N. A strategy to identify housekeeping genes suitable for analysis in breast cancer diseases. *BMC Genomics* 2016; 17: 639, doi: 10.1186/s12864-016-2946-1.
26. de Almeida VH, Guimarães IDS, Almendra LR, Rondon AMR, Tilli TM, de Melo AC, et al. Positive crosstalk between EGFR and the TF-PAR2 pathway mediates resistance to cisplatin and poor survival in cervical cancer. *Oncotarget* 2018; 9: 30594–30609, doi: 10.18632/oncotarget.25748.
27. Chong CR, Jänne PA. The quest to overcome resistance to EGFR-targeted therapies in cancer. *Nat Med* 2013; 19: 1389–1400, doi: 10.1038/nm.3388.
28. Look MP, van Putten WL, Duffy MJ, Harbeck N, Christensen IJ, Thomssen C, et al. Pooled analysis of prognostic impact of urokinase-type plasminogen activator and its inhibitor PAI-1 in 8377 breast cancer patients. *J Natl Cancer Inst* 2002; 94: 116–128, doi: 10.1093/jnci/94.2.116.
29. Banys-Paluchowski M, Witzel I, Aktas B, Fasching PA, Hartkopf A, Janni W, et al. The prognostic relevance of urokinase-type plasminogen activator (uPA) in the blood of patients with metastatic breast cancer. *Sci Rep* 2019; 9: 2318, doi: 10.1038/s41598-018-37259-2.
30. Harms W, Malter W, Krämer S, Drebber U, Drzezga A, Schmidt M. Clinical significance of urokinase-type plasminogen activator (uPA) and its type-1 inhibitor (PAI-1) for metastatic sentinel lymph node involvement in breast cancer. *Anticancer Res* 2014; 34: 4457–4462.
31. Langenskiöld M, Holmdahl L, Angenete E, Falk P, Nordgren S, Ivarsson ML. Differential prognostic impact of uPA and PAI-1 in colon and rectal cancer. *Tumour Biol* 2009; 30: 210–220, doi: 10.1159/000239796.
32. Sugimura M, Kobayashi H, Kanayama N, Terao T. Clinical significance of urokinase-type plasminogen activator (uPA) in invasive cervical cancer of the uterus. *Gynecol Oncol* 1992; 46: 330–336, doi: 10.1016/0090-8258(92)90227-A.
33. Horn LC, Pippig S, Raptis G, Fischer U, Köhler U, Hentschel B, et al. Clinical relevance of urokinase-type plasminogen activator and its inhibitor type 1 (PAI-1) in squamous cell carcinoma of the uterine cervix. *Aust N Z J Obstet Gynaecol* 2002; 42: 383–386, doi: 10.1111/j.0004-8666.2002.00385.x.
34. Gorantla B, Asuthkar S, Rao JS, Patel J, Gondi CS. Suppression of the uPAR-uPA system retards angiogenesis, invasion, and *in vivo* tumor development in pancreatic cancer cells. *Mol Cancer Res* 2011; 9: 377–389, doi: 10.1158/1541-7786.MCR-10-0452.
35. Heinemann V, Ebert MP, Laubender RP, Bevan P, Mala C, Boeck S. Phase II randomised proof-of-concept study of the urokinase inhibitor upamostat (WX-671) in combination with gemcitabine compared with gemcitabine alone in patients with non-resectable, locally advanced pancreatic cancer.
Br J Cancer 2013; 108: 766–770, doi: 10.1038/bjc.2013.62.
36. Gold MA, Brady WE, Lankes HA, Rose PG, Kelley JL, De Geest K, et al. A phase II study of a urokinase-derived peptide (A6) in the treatment of persistent or recurrent epithelial ovarian, fallopian tube, or primary peritoneal carcinoma: a Gynecologic Oncology Group study. *Gynecol Oncol* 2012; 125: 635–639, doi: 10.1016/j.ygyno.2012.03.023.

Curriculum Vitae

- Nome: KARINA MARTINS CARDOSO
- Nascimento: 19**/08/1989**
- Naturalidade: Rio de Janeiro

Formação Acadêmica

- Graduação: Licenciatura em Ciências Biológicas, Universidade Federal Rural do Rio de Janeiro. 2008 – 2013.
- Gradução: Bacharel em Ciências Biológicas, Universidade Federal Rural do Rio de Janeiro. 2013 – 2015.
- Mestrado: Química Biológica, Universidade Federal Rural do Rio de Janeiro. 2014 – 2016.
- Doutorado: Química Biológica, Universidade Federal Rural do Rio de Janeiro. 2016 – 2020.

Orientação de Monografia

1. "Avaliação do nível de conhecimento sobre zoonoses e perfil dos alunos do curso de ciências biológicas semipresencial da UFRJ/CEDERJ", Camila de Oliveira Cordoba – Universidade Federal do Rio de Janeiro/CEDERJ.

Publicações

MARTINS-CARDOSO, K.; ALMEIDA, V.H.; BAGRI, K.M.; ROSSI, M.I.D.; MERMELSTEIN, C.S.; KÖNIG, S.; MONTEIRO, R.Q. NEUTROPHIL EXTRACELLULAR TRAPS (NETS) PROMOTE PRO-METASTATIC PHENOTYPE IN HUMAN BREAST CANCER CELLS THROUGH EPITHELIAL–MESENCHYMAL TRANSITION. *CANCERS* 2020, *12*, 1542. DOI: 10.3390/CANCERS12061542

GOMES, G.A*; **MARTINS-CARDOSO, K**.*; SANTOS, F.R.; FLORENCIO, M.; ROSA, D.; ZUMA, A.A.; SANTIAGO, G.M.P.; MOTTA, C.; CARVALHO, M.G.; FAMPA, P. ANTILEISHMANIAL ACTIVITY OF THE ESSENTIAL OILS OF *MYRCIA OVATA* CAMBESS. AND *EREMANTHUS ERYTHROPAPPUS* (DC) MCLEISCH LEADS TO PARASITE MITOCHONDRIAL DAMAGE, NATURAL PRODUCT RESEARCH, 2020 DOI: 10.1080/14786419.2020.1827402

DE MORAES, D.C.; **CARDOSO K.M.;** DOMINGOS, L.T.S.; DO CARMO, M.C.F.R.; MONTEIRO, R.Q., FERREIRA-PEREIRA, A. B-LAPACHONE ENHANCES THE ANTIFUNGAL ACTIVITY OF FLUCONAZOLE AGAINST A PDR5P-MEDIATED RESISTANT *SACCHAROMYCES CEREVISIAE* STRAIN. BRAZILIAN JOURNAL OF MICROBIOLOGY. 2020 SEP;51(3):1051-1060. DOI: 10.1007/S42770-020-00254-9.

JULIANA L. SOUZA, J.L.; **MARTINS-CARDOSO, K**.; GUIMARÃES, I.S.; MELO, A.C.; LOPES, A.H.; MONTEIRO, R.Q.; ALMEIDA, V.H. INTERPLAY BETWEEN EGFR AND THE PLATELET-ACTIVATING FACTOR (PAF)/PAF RECEPTOR SIGNALING AXIS MEDIATES AGGRESSIVE BEHAVIOR OF CERVICAL CANCER. FRONTIERS IN ONCOLOGY. DOI: 10.3389/FONC.2020.557280